Anexo I

Don Agustín Trujillo Pino, SECRETARIO DEL DEPARTAMENTO DE INFORMÁTICA Y SISTEMAS DE LA UNIVERSIDAD DE LAS PALMAS DE GRAN CANARIA,

CERTIFICA,

Que los miembros del Consejo del Departamento, reunidos en sesión extraordinaria el 10 de noviembre de 2010, tomaron el acuerdo de dar el consentimiento para su tramitación a la tesis doctoral titulada "***Contributions to Effective Protocol Design to Mitigate Continuous Multimedia Services Short Disruptions in WiFi Networks***" presentada por la doctoranda Doña Kholoud Atalah y dirigida por los Doctores Don Álvaro Suárez Sarmiento y Doña Elsa Macías López.

Y para que así conste, y a efectos de lo previsto en el Artº 73.2 del Reglamento de Estudios de Doctorado de esta Universidad, firmo la presente en Las Palmas de Gran Canaria a diez de noviembre de dos mil diez.

Anexo II

UNIVERSIDAD DE LAS PALMAS DE GRAN CANARIA

Departamento: **Informática y Sistemas**

Programa de Doctorado: **Tecnologías de la Información y sus Aplicaciones**

Título de la Tesis

Contributions to Effective Protocol Design to Mitigate Continuous Multimedia Services Short Disruptions in WiFi Networks

Tesis Doctoral presentada por Dª **Kholoud Atalah**

Dirigida por el Dr. D. **Álvaro Suárez Sarmiento**

Codirigida por la Dra. Dª. **Elsa Macias López**

El Director, **La Codirectora** **La Doctoranda,**

Las Palmas de Gran Canaria, a 27 de octubre de 2010

UNIVERSIDAD DE LAS PALMAS DE GRAN CANARIA
Departamento de Informática y Sistemas

Centro de Innovación para la Sociedad de la Información

Contributions to Effective Protocol Design to Mitigate Continuous Multimedia Services Short Disruptions in WiFi Networks

by

KHOLOUD ATALAH
Grupo de Arquitectura y Concurrencia
Departamento de Ingeniería Telemática

Being a thesis submitted for the degree of

Doctor of Philosophy

In The University of Las Palmas de Gran Canaria

Directors

Álvaro Suárez Sarmiento & Elsa Macias López

October 2010

بسم الله الرحمن الرحيم

﴿يرفع الله الذين آمنوا منكم والذين أوتوا العلم درجات﴾

صدق الله العظيم

Dedication

Most importantly I feel very grateful to my husband, my children and my family in Gaza to whom this dissertation is dedicated, for their immense love, their innumerable sacrifices, their unconditional support and their continuous encouragement throughout my life.

أهدي هذه الأطروحة إلى زوجي الحبيب الذي أشعر بالامتنان الشديد له
وإلى أطفالي الأعزاء
وإلى عائلتي الحبيبة في غزة
على محبتهم وتضحياتهم التي لا تحصى ودعمهم وتشجيعهم المستمر طوال حياتي

ACKNOWLEDGMENT

This is a great opportunity to express my utmost grateful to the “Vicerrectorado de Investigación, Desarrollo e Innovación” at the University of Las Palmas de Gran Canaria for giving me the opportunity to continue my PhD by the scholarship “Personal Investigador en Formación”.

Dr. Alvaro Suarez Sarmiento has coached, guided, and motivated me as my advisor and has made this dissertation possible. I offer my earnest and most sincere gratitude to him. He has shown confidence in me by encouraging me to work on the problems that I am interested in. I also thank him for his endless support and patience during all the anxious times of this journey.

I also thank and appreciate Dra. Elsa Macias Lopez for always being available whenever I needed.

I would like to thank Dr. Enrique Rubio Royo for giving us the opportunity to participate in the doctorate program.

I am pleased to thank Dr. Juan Manuel Afonso, Dra. Marisol Izquerdo and Alejandro Jonzales for their immense help with in taking care of the administrative details in a timely manner and for their constant support.

I have had many people who have inspired and helped me. I would like to thank Tinerfe Martin for all his valuable contribution in the experiment. Also I would like to thank Alexi and Miguel Angel for helping me in all software problems, and for Pilar, Begoña and Inmaculada. And great thanks to Rachid Ganga for helping and supporting me during the PhD years.

Finally I do not want to forget my close friends Asma Skareb, Fatima Zahra Zouhaire for their continuous encouragement and support, and Boshra Abdrahman who was as my second mother in Spain.

ABSTRACT

Real Time Multimedia Applications (*RTMAs*) provided by wireless networks, such as *Wireless Fidelity* (*WiFi*), suffer video services short disruptions, causing video streaming packets loss. *Mobile Clients* (*MC*) could experience disruptions in disconnection zones: Handover zones, out of coverage zones or through holes where sudden signal drop occurs. Up to our knowledge, the holes problem was not studied in previous works. Therefore, our objective was to develop a protocol in order to avoid video streaming packets loss during short disruptions in WiFi networks. This is the first study addressing this issue considering the presence of holes.

We proposed a protocol based on novel mathematical specifications for the *Coverage Area* (*CA*), it consists of two important techniques, the *Received Signal Strength Indicator* (*RSSI*) Gradient Predictor and Filter, and the buffer management and transmission speed control technique. The protocol was specified and verified using the *Specification and Description Language* (*SDL*), and it was simulated by a specific Java simulator derived from the SDL diagram.

The experimental test of the Gradient Predictor and Filter demonstrated its efficiency in predicting the next MC coverage level, and its ability of mitigating the holes effect. It showed the best performance in comparison with the Kalman filter and the Grey Model. The simulation results proved that the protocol is suitable for all types of disconnections caused by holes, handover, or out of coverage constituting a new advance comparing to previous available techniques. Moreover, it offered sufficient amount of video frames in *MC Buffer* (*MCB*) to be consumed during the mentioned disconnections (even for long time) resulting in continuous adequate video playing and

offering enough time to the user to move from a CA to another without interruptions. This protocol could help in overcoming disruption issues providing continuous adequate quality RTMA for users. This interesting work has been published in two international journals, and has been presented in two international conferences; one paper was awarded a certificate of merit.

Future work includes the development of the mathematical specifications of MC movements and the RSSI Gradient predictor and filter, which will support the protocol to be suitable for all movements even the non periodic patterns.

RESUMEN

Las Aplicaciones Multimedia a Tiempo Real (*RTMAs* del ingles *Real Time Multimedia Applications*) soportadas por las redes inalámbricas, tales como *Wireless Fidelity* (*WiFi*), sufren de interrupción del servicio de video durante las desconexiones cortas, causando la pérdida de paquetes de vídeo streaming. Los *Clientes Móviles* (*MCs* del inglés *Mobile Clients*) podrían experimentar interrupciones en las zonas de desconexión: handover, fuera de cobertura o los agujeros donde se pierda la señal de manera súbita e inesperada. Por lo tanto, nuestro objetivo fue desarrollar un protocolo para mitigar los problemas de interrupción del servicio de video durante las desconexiones de corta duración en redes WiFi.

Hemos propuesto un protocolo basado en novedad especificación matemática para el *Área de Cobertura* (*CA* del ingles *Coverage Area*), que consta de dos técnicas importantes: el Predictor y el Filtro del *Indicador de la potencia de la Señal Recibida* (*RSSI* del ingles *Received Signal Strength Indicator*) Gradiente, y la técnica de la gestión del buffer y del control de velocidad de transmisión. El protocolo se ha especificado y verificado con el *Lenguaje de Especificación y Descripción* (*SDL* del ingles: *Specification and Description Language*), y se simuló usando un simulador específico de Java derivado del diagrama de SDL.

La prueba experimental del Filtro y el Predictor Gradiente ha demostrado su eficacia en la predicción del próximo nivel de cobertura del MC, y su capacidad de mitigar el efecto de los agujeros. También se mostró el mejor rendimiento en comparación con el filtro de Kalman y el modelo de Grey. Los resultados de la simulación demostraron que el protocolo es adecuado para todos tipos de desconexiones

causadas por los agujeros, el handover, o fuera de cobertura que constituye un nuevo avance en comparación con anteriores técnicas disponibles. Además, ofrece la suficiente cantidad de vídeo frames en *MC Buffer* (*MCB*) para consumirlos durante las desconexiones mencionado (aunque por mucho tiempo), resultando en video jugando adecuado continúo y ofrece suficiente tiempo para el usuario para pasar de una CA a otro sin interrupciones.

Este protocolo podría ayudar a superar problemas de interrupción proporciona RTMA continua de calidad adecuada para los usuarios. Este interesante trabajo ha sido publicado en dos revistas internacionales, y ha sido presentado en dos conferencias internacionales, un artículo ha ganado el certificado de mérito.

El trabajo futuro incluye el desarrollo de las especificaciones matemáticas de los movimientos del MC y el filtro y predictor del RSSI Gradiente, que soportan el protocolo para ser conveniente para todos los movimientos, incluso los patrones no periódicos.

Table of Contents

List of Tables

List of Figures

List of Abbreviations

Ack	Acknowledgment
AP	Access Point
APP	AP Proxy
AVC	Advanced Video Coding
BE	Best effort
BS	Base Station
BSA	Basic Service Area
BSB	Base Station Buffer
BSBM	Base Station Buffer Manager
BSS	Basic Service Set
CA	Coverage Area
CBV	Control Buffered Video
CCT	Clear Channel Threshold
CID	Connection Identifier
CoAs	Care of Addresses
COS	Cosine
CSMA/CA	Carrier Sense Multiple Access with Collision Avoidance
CTS	Control Transmission Speed
DCF	Distributed Coordination Function
DiffServ	Differentiated Services
DL	Down Link
DSL	Digital Subscriber Line
DSSS	Direct Sequence Spread Spectrum
DVB-H	Digital Video Broadcasting - Handheld
DSVF	Decrease Speed of Video Frames transmission
EDCA	Enhanced Distributed Channel Access
ertPS	Extended rtPS
ESS	Extended Service Set
FBSS	Fast BS Switching
FHSS	Frequency Hopping Spread Spectrum
FIFO	First In First Out

GM	Grey Model
GoV	Groups of Video
GPC	Grant per Connection
GPS	Global Positioning System
GPSS	Grant per SS
GSM	Global System for Mobile communications
H-ARQ	Hybrid-Automatic Repeat Request
HCF	Hybrid Coordination Function
HE-AAC	High-Efficiency Advanced Audio Coding
HH	Horizontal Handover
HP	Hard Proactive
HS	Handover State
IBSS	Independent Basic Service Set
IEEE	Institute of Electrical and Electronics Engineers
IM	Irregular Movement
IntServ	Integrated Services
IP	Internet Protocol
IPTV	Internet Protocol TV
ISVF	Increase Speed of Video Frames transmission
MAC	Medium Access Control
MANJ	Moving Average of Negative Jitter
MBS	Multicast and Broadcast Service
MC	Mobile Client
MCB	Mobile Client Buffer
MCBM	Mobile Client Buffer Manager
MDHO	Macro Diversity Handover
MI	Mobile Internet
MIH	Media Independent Handover
MIMO	Multiple Input Multiple Output
MOS	Mean Opinion Score
MPEG	Moving Picture Experts Group
MSC	Message Sequence Chart
MPLS	Multi-Protocol Label Switching

NAR	New Access Router
nrtPS	Non-Real Time Polling Service
OFDMA	Orthogonal Frequency Division Multiplexing Access
PAR	Previous Access Router
PDA	Personal Digital Assistant
PDT	Predict Disconnection Time
PH	Proactive Handover
QoE	Quality of Experience
QoS	Quality of Service
RF	Radio Frequency
RH	Reactive Handover
RM	Regular Movement
RSSI	Received Signal Strength Indicator
RST	Reception Sensitivity Threshold
RT	Roaming Threshold
RTMA	Real Time Multimedia Application
RTSP	Real Time Streaming Protocol
rtPS	Real Time Polling Service
SASHA	Smooth Adaptive Soft-Handover Algorithm
SDL	Specification and Description Language
SIN	Sine
SIP	Session Initiation Protocol
SNR	Signal to Noise Ratio
SP	Soft Proactive
SS	Subscriber Station
SSID	Service Set Identifier
TCP	Transmission Control Protocol
TDD2	Time Division Duplex2
UDP	User Datagram Protocol
UGS	Unsolicited Grant Service
UL	Up Link
ULPGC	University of Las Palmas de Gran Canaria
VH	Vertical Handover

VoD	Video on Demand
VoIP	Voice over Internet Protocol
WiFi	Wireless Fidelity
WiMAX	Worldwide Interoperability for Microwave Access
WLAN	Wireless Local Area Networks
WMAN	Wireless Metropolitan Area Network
WMM	Wireless Multi-Media
WNIC	Wireless Network Interface Card

CHAPTER 1

INTRODUCTION

Real time multimedia applications provided by wireless networks suffer video services disruption during short disconnections. In wireless networks, service disruptions are due to coverage fails such as holes and handover. The disruption problem could be solved by incorporating filtering and prediction models with an effective buffer management technique.

1.1 Real Time Multimedia Applications

Real Time Multimedia Applications (*RTMA*) are applications that send and receive media streams through communication channels, the received packets must be decoded before rendering the audio and the video at receiver terminal [1]. Nowadays, RTMAs are experiencing rapid development due to the growing popularity of video applications [2]. Thus, a *Wireless Local Area Network* (*WLAN*) such as IEEE 802.11 supports RTMA, mainly *Voice over Internet Protocol* (*VoIP*) and video services [3]. Moreover, a *Wireless Metropolitan Area Network* (*WMAN*) such as IEEE 802.16 provides better capability to offer wireless services as multimedia streaming and real-time surveillance [4].

Most RTMAs types use the streaming technology to offer audio and video services via internet. *Streaming* is a technique to deliver audio and video that are distributed over telecommunications networks, and transmitted, through an *Internet Protocol* (*IP*) network, from the source host to the destination host. Many network protocols were specifically designed for streaming media [4], thus some protocols provide basic network services support in the network layer, others work in the transport layer such as: *User Datagram Protocol* (*UDP*) and *Transmission Control Protocol* (*TCP*) [5], while other protocols define messages and procedures in the application layer to control multimedia delivery such as: The *Real-Time Streaming Protocol* (*RTSP*) and the *Session Initiation Protocol* (*SIP*) [4].

VoIP is an important protocol that uses IP to transmit voice data packets, the voice is converted to a digital signal, compressed and subsequently broken down into a series of packets that are transported through the IP network; these packets are reassembled and decoded at the receiving host [6]. *Skype*, *MSN*, *Google Talk*, and *VoIPBuster* are examples of VoIP applications.

The *Multimedia Real Time Streaming* is a RTMA that includes two common distribution mechanisms over IP networks that are live streaming and on-demand streaming. In *Live Streaming*, there is a direct connection between the encoder and the server where the encoder is capturing, digitizing and compressing the received analog signal of video and audio, then passing the resulting compressed file to the server. Whereas *On-demand Streaming* has not a direct connection between the encoder and the receiver, because the compressed video must be stored, then it can be distributed by the

user. On the other hand, the server and the client communication for on-demand content is the same as live content, the main difference is that in the first mechanism the user can rewind or fast forward the video, while this option is not available in the second mechanism. Thus, real time video constitutes an example of live streaming [4], while *Video on Demand* (*VoD*) system constitutes an example of on-demand streaming. The latter is an interactive multimedia system where the client can choose a movie from a database stored in a video server. In addition, the system could provide the user with different functions including pause, fast forward, fast rewind, slow forward, slow rewind and jump to previous/future frame.

Most RTMAs need high *Quality of Service* (*QoS*) and high network demand due to the special requirements of the audio and video perception, being very sensitive to delay and jitter, and require high bandwidth [5]. This means that RTMAs require special network performance that is measured by many parameters such as packet loss, end to end delays, jitter, bandwidth, timeliness, reliability and cost [7]. For example, video conferencing requires an end-to-end delay not greater than 200 ms; as a result the possibility to retransmit lost packets is restricted [3]. However, wireless channel characteristics such as shadowing, multipath fading and interferences still limiting the available bandwidth for the deployed applications. All the users of RTMAs are looking for the continuous receiving of the real video and audio streaming. In addition, many other requirements are important such as high quality images, as imaging systems may introduce an amount of distortion or artifacts in the signal, thus the quality assessment is very important [8]. Furthermore, the user seeks to receive high quality audio (clear audio), which is difficult since it is affected by many factors as the extended delay of voice path [Web-1]. Therefore, some audio codecs were developed to improve audio quality as *High-Efficiency Advanced Audio Coding* (*HE-AAC*). The *Mean Opinion Score* (*MOS*) provides a numerical indication of the perceived quality of the received media after compression and transmission, and it is expressed as a single number in the range of 1 to 5, where 1 is the lowest perceived quality (unacceptable) and 5 is the highest perceived quality (excellent) [4].

1.2 Wireless Networks Standards

Nowadays, many technologies for wireless networks are available to support RTMA; *Wireless Fidelity* (*WiFi*) and *Worldwide Interoperability for Microwave Access* (*WiMAX*) are examples of these technologies.

1.2.1 WiFi and IEEE 802.11

WiFi is the WLAN technology based on the IEEE 802.11 standard and certified by the WiFi Alliance, it is a global non-profit association specialized in certification in order to enhance the user experience for mobile wireless devices [Web-2].

WiFi can provide high data rate at limited area up to 200 m, IEEE 802.11a provides up to 54 Mbps at 5 GHz unlicensed band [9], while IEEE 802.11b enables up to 11 Mbps at 2.4 GHz unlicensed band [10], and the IEEE 802.11g provides up to 54 Mbps at 2.4 GHz unlicensed band [11]. IEEE 802.11 Working Group-n published the new specification IEEE 802.11n which is based on *Multiple Input Multiple Output* (*MIMO*) air interface technology, it includes enhancements for performance, security and roaming, and supports operation in either the 2.4 GHz or the 5 GHz bands, and it enables data rate up to 600 Mbps operating in 20 MHz or 40 MHz bandwidth [12].

The IEEE 802.11 is the current leading standard for WLAN, it supports RTMAs like VoIP and video conferencing [3] to mobile and portable stations [13] [14], that is achieved by the two high speed IEEE 802.11g and IEEE 802.11n, and the IEEE 802.11e QoS-based *Medium Access Control* (*MAC*) layer [13]. IEEE 802.11 specifies two physical layers [15]: The *Direct Sequence Spread Spectrum* (*DSSS*) and the *Frequency Hopping Spread Spectrum* (*FHSS*).

Different WiFi enabled devices that support RTMAs are present in the market, including VoIP phones, TV, MP3 players, game consoles and other multimedia players. For example, at home, wireless devices can be used to provide wireless voice connectivity through VoIP WiFi phones, furthermore, a WLAN could be used to distribute contents from a multimedia server to any device at home [Web-3].

The IEEE 802.11 standard is characterized by being simple and robust against failures caused by the distributed approach of its MAC protocol [16]. IEEE 802.11 can operate in the mode of Ad-Hoc network where *Mobile Client* (*MC*) communicates

directly with other MC without the need of an *Access Point* (*AP*) to interconnect them, in this case they form the *Independent Basic Service set* (*IBSS*) [14] [17].

The basic IEEE 802.11 MAC protocol is the *Distributed Coordination Function* (*DCF*) [15] [16] which employs *Carrier Sense Multiple Access with Collision Avoidance* (*CSMA/CA*) as the access method [13], but IEEE 802.11e introduces the *Hybrid Coordination Function* (*HCF*) protocol for QoS support. The HCF defines two MAC mechanisms: Contention-based channel access and controlled channel access [16].

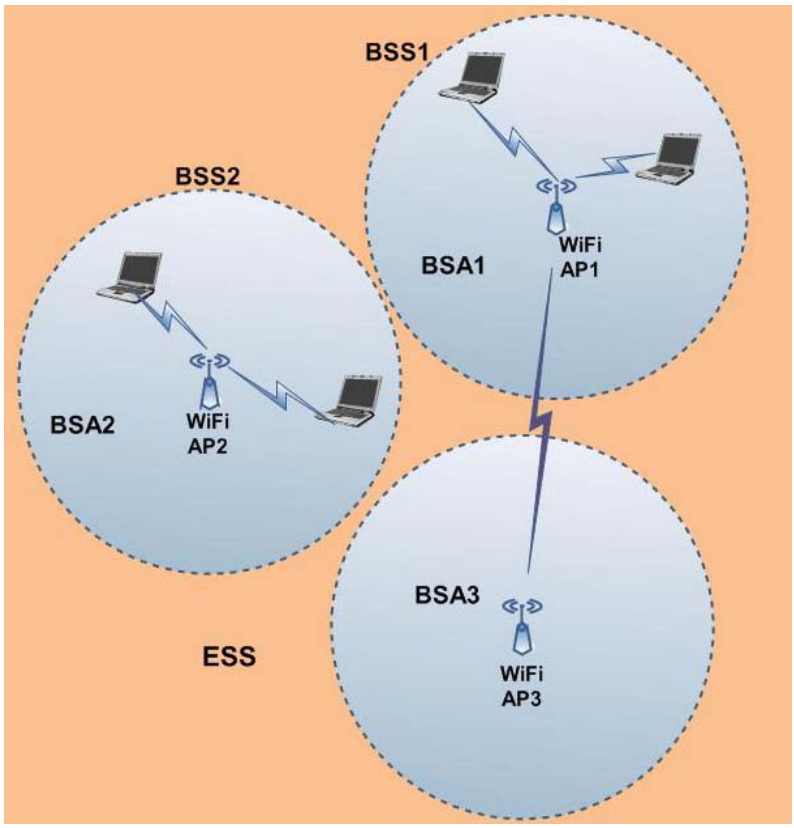

Figure 1.1: WiFi network topologies

In the infrastructure mode of IEEE 802.11 (Figure 1.1) all MCs are associated to an AP. The interconnection structure forms the *Basic Service Set* (*BSS*). The interconnection of more APs can extend a BSS into an *Extended Service Set* (*ESS*) [17]. Elsewhere, any MC could still in communication with other MCs while it is inside the *Coverage Area* (*CA*) of its BSS, which is known as *Basic Service Area* (*BSA*) [14] [18]. Moreover, there are many possible physical locations of the BSS, they could be partially overlapped, physically disjoint, physically collocated, or physically present in the same space [14].

WiFi QoS Support: IEEE 802.11e

With QoS control, WiFi AP could prioritize the traffic and optimize the network resources sharing way among different applications. Thus, all Multimedia applications in WiFi networks require QoS control, and in its absence, all applications that are running on different devices have the same priority to transmit data frames [Web-3]. Therefore, it is not possible to prioritize data packets of such applications with the default DCF approach, so the IEEE 802.11e amendments were introduced to provide features needed to prioritized RTMA packets [19] [20]. The only IEEE 802.11e feature included by WiFi Alliance in the *Wireless Multi-Media* (*WMM*) certification program is the *Enhanced Distributed Channel Access* (*EDCA*) which is supported by many devices nowadays [21].

The WMM defines four priority classes: Voice, video, background and best effort, it specifies the maximum value of the random timer for each class. More the value is smaller, more the possibility of a device to access the air interface is higher. WMM also defines the maximum time allowed for a frame of a certain class to block the air interface. The video has higher random timer than the voice, and VoIP frames should always be sent before data packets in the best effort queue. These applications use the *Differentiated Services* (*DiffServ*) field of the IP packet header to inform the protocol layer about the priority queue, while the AP or the *Digital Subscriber Line* (*DSL*) modem is responsible of the QoS on network links [21].

1.2.2 WiMAX and IEEE 802.16

WiMAX is a recent wireless access IP-based technology [Web-4]; it enables operators to provide fixed and mobile clients with multiple real time multimedia services [22]-[25] such as VoD, VoIP, Real Time Chatting, *Mobile Internet* (*MI*) [Web-4].

WiMAX system Release1 is based on IEEE 802.16e-2005 and IEEE 802.16e-2009, while Release2 is based on IEEE 802.16m that is expected to be completed soon. These versions of the IEEE 802.16 standards are the keys to the WiMAX Forum Certified Program [Web-5] [Web-6].

The IEEE 802.16d (or IEEE 802.16-2004), for Fixed WiMAX, does not support mobility, while IEEE 802.16e-2005 for Mobile WiMAX does. It operates in frequencies between 2 and 11 GHz and offers scalability in both radio access technology and

network channels from 1.25 to 20 MHz [Web-7]. Moreover, WiMAX Release 2 supports several 20 MHz channels [Web-6].

Mobile WiMAX Release1 is able to support peak *Down Link* (*DL*) sector data rate up to 46 Mbps, assuming a DL/UL (*Up Link*) ratio of 3:1 and peak *UL* sector data rate up to 14 Mbps, assuming a DL/UL ratio of 1:1, in a 10 MHz channel. Moreover, mobile WiMAX can cover a typical cell radius 2-5 km [Web-8]. The IEEE 802.16e is an *Orthogonal Frequency Division Multiple Access* (*OFDMA*) based technology, which enables WiMAX to achieve optimal throughput and capacity, and improves the indoor coverage [Web-8] [26].

WiMAX supports several key features [Web-9] such as: Tolerance to multipath and self-interference, *Time Division Duplex2* (*TDD2*), *Hybrid-Automatic Repeat Request* (*H-ARQ*), frequency selective scheduling, network-optimized hard handoff, *Multicast and Broadcast Service* (*MBS*), flexible radio resource allocation and low power consumption in mobile devices. In Mobile WiMAX technology (Figure 1.2), the *Base Station* (*BS*) is connected to a wired IP network and connects many *Subscriber Stations* (*SSs*) that can be fixed stations or moving vehicles [27], and must be supported with a WiMAX *Wireless Network Interface Card* (*WNIC*). WiMAX has the potential to replace many telecommunications infrastructures as telephone networks wires and cellular networks.

In addition, another important topic is that providing RTMAs with advanced QoS requirements is a challenging. Interestingly, WiMAX supports advanced QoS and low latency for improving RTMAs [Web-4], it also supports various frame durations [28], and its frame based MAC approach is centrally controlled offering a guaranteed multimedia QoS [20].

The IEEE 802.16 specifies the physical layer and the MAC layer, and defines a connection oriented MAC protocol, with each connection between SS and BS being identified by a 16 bit *Connection Identifier* (*CID*). WiMAX uses two methods to allocate bandwidth: *Grant per Connection* (*GPC*) where bandwidth is assigned to each connection and *Grant per SS* (*GPSS*) where SS re-distributes the transmission slots allotted by the BS to all its connections [28].

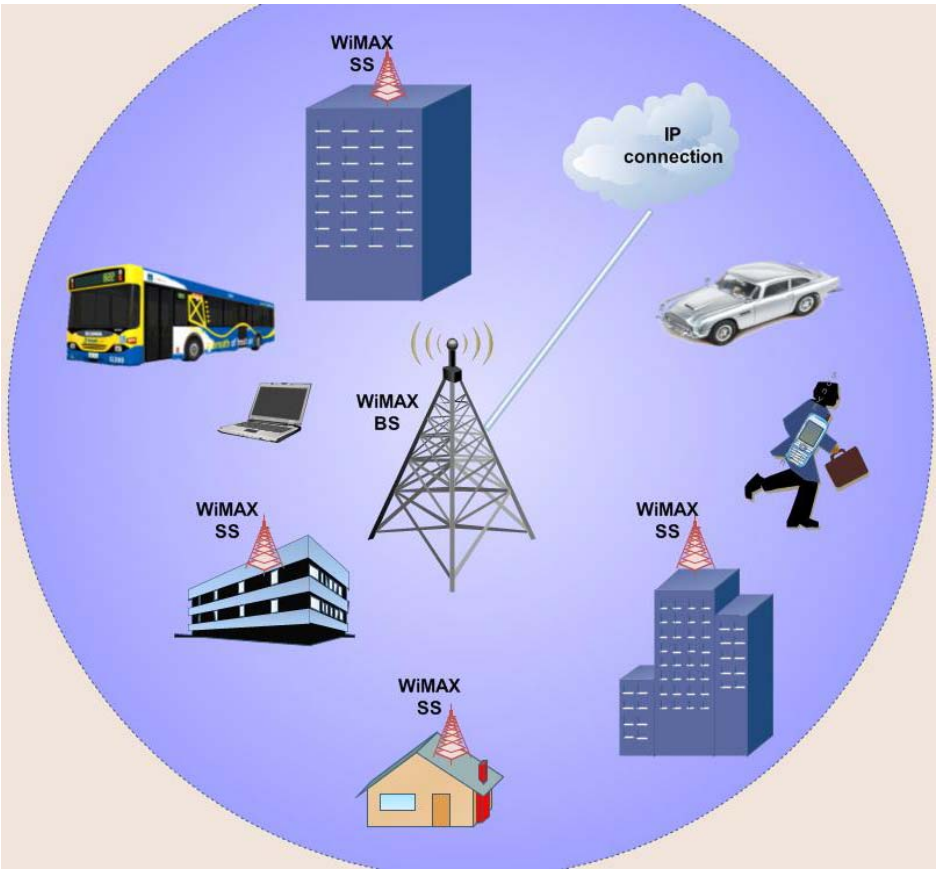

Figure 1.2: Mobile WiMAX network architecture

The IEEE 802.16e defines five classes of scheduling services [28]-[31]:

- *Unsolicited Grant Service* (*UGS*): It supports real-time service flows that generate fixed size packets such as VoIP.
- *Real Time Polling Service* (*rtPS*): It supports real-time service flows that produce variable size data packets. The user must identify the size of each packet before receiving permission to send it, such as *Moving Picture Experts Group* (*MPEG*) video [31].
- *Extended rtPS* (*ertPS*).
- *Non-real time polling service* (*nrtPS*): It supports non-real-time flows that require variable size data grants.
- *Best effort* (*BE*): It supports best effort traffic such as email.

The first three classes require guaranteed data and delay, and their applications are affected by the handover process [32]. In addition, IEEE 802.16 uses five QoS parameters to reserve resources for user traffic flows: Minimum data rate, maximum data rate, maximum delay, jitter and priority level [31].

1.3 Problems of Coverage in Wireless Networks for RTMAs

Recently a plethora of different RTMAs has been proposed to be implemented in wireless networks:

- The *mobile game* is a RTMA that is played on a mobile phone, smartphone, *Personal Digital Assistant* (*PDA*), laptop or any type of handheld or wireless devices. Actually, the mobile game in wireless environment is receiving more attention and importance, but not all the mobile phones could be used as a gaming platform. Also, most of the products currently available in the market feature one or two games within its retail version [33].
- *Internet Protocol TV* (*IPTV*) is one of the recent RTMAs, it provides the user with an interactive form of TV using existing computer networks instead of the traditional television systems. IPTV provides good level of QoS and *Quality of Experience* (*QoE*), security, interactivity, and reliability [4].
- The *Mobile TV* is another RTMA; it could be broadcasted by a mobile wireless network, or independently by a dedicated broadcasting system such as the *Digital Video Broadcasting – Handheld* (*DVB-H*), consequently the mobile devices require dedicated receiver hardware. Mobile TV is not expected to be successful until it faces the competition with the audio and video on-demand streaming, because the latter applications are preferable for mobile users as the contents could be used according to the consumer preferences, while mobile TV is live streaming requiring continuous network coverage [21].
- Video compression techniques such as MPEG-2/4 and H.264/AVC (*Advanced Video Coding*) are a critical part of RTMAs over WLAN [4] [13] [21] [34].

Moreover, in wireless networks, there are different characteristics and service requirements to support RTMAs such as high level of quality, data rate, maximum tolerable packet error rate and delay bounds [35]. In RTMAs, packets must reach the client before their play out time and with enough time to be decoded, then to be displayed [5], so RTMAs streaming packets should have higher priority than others in order to reduce the jitter [21].

1.3.1 QoS for RTMA Considering Client Movement

Nowadays, there is an increasing number of RTMAs subscribed by mobile users, making urgently convenient to guarantee QoS in wireless networks [15]. Due to the lack of built-in mechanisms to support RTMAs, and resources limitation, it is a challenge to ensure QoS for throughput and delay-sensitive RTMAs [15] [36]. Thus, the existing wireless networks provide limited QoS for RTMAs [37] and this depends on the capacity of each network [5]. In some cases, it is very difficult to guarantee QoS for RTMAs especially with wireless terminals in movement [38], where the need for location detection and possible disconnections make it difficult to determine the reason of packet loss and the interval of loss [39]. Elsewhere, when the MC moves through coverage zones where the signal drops, an interruption could occur in the audio stream [21]. There are many models to support QoS such as the *Integrated Services* (*IntServ*) and the DiffServ, while the *MultiProtocol Label Switching* (*MPLS*) is a protocol for QoS assurance [4] [34].

RTMAs depend mainly on the QoS metrics that are provided by the wireless network, and the sensitivity to each metric varies widely from one application to another. The following metrics are considered as the basic QoS metrics [34] [40] [41]:

- *Throughput*: The effective number of data units transported per time unit (e.g., bps) [40]. The maximum throughput of the transmission medium is equal to the channel capacity [4]. VoIP, video streaming and interactive gaming are multimedia applications that are highly sensitive to throughput reductions [Web-3]. Nowadays, some MCs are supported by multiple WNICs of different technologies, which enable the MC to increase the bandwidth required for the RTMA, this happens when it is possible to connect to more than one network in the overlapped areas of these different technologies [36].
- *Delay*: The interval of time between the packet delivery from the source to the destination [4] [40].
- *Jitter*: Usually referred to “delay variation” [40], it is the delay fluctuation from one packet to the next one in the same connection flow [4]. RTMAs have strict requirements in delay and jitter, which is necessary for interactive communications like VoIP and video conferencing. The one way transmission delay should be less than 150 ms. It is demonstrated that streaming audio or video is less sensitive to delay or jitter than real-time traffic [41].

- *Packet loss*: The percentage of data units that do not reach the destination in a specific interval of time [40]. Packet loss can be caused by the low bandwidth of wireless link, signal attenuation, obstruction or handoff [39]. RTMAs are not very sensitive to packet loss rate. For example a loss rate of 1% is acceptable for real-time video with rate 16-384 Kbps [41]. For IPTV, video conferencing and video telephony, packet loss due to the excessive delay is the primary factor affecting the required quality [5]. There are several techniques to recover lost packets such as packet retransmission at the transport layer, error correction at the physical layer, or using codecs at the application layer [4].

1.3.2 Definition of Coverage Area

The CA has not a perfect spherical form, because really there are some locations with no signal strength inside the CA, it is related to the radiation pattern of the antenna or the presence of holes. Furthermore, the signal fluctuations and the handover process could cause disconnections.

The CA is the radiation pattern of the antenna which has different forms depending on the design and frequency of the antenna; it represents the relative field strength (power) graphically, or simply the distribution of the *Received Signal Strength Indicator* (*RSSI*) in the space [42]. The RSSI is an indicator of the signal strength, it is affected by the natural conditions such as the weather and the presence of obstacles, and the fluctuations in the signal could produce disconnections and streaming loss inside the CA.

The Figure 1.3 shows the CA (radiation pattern) of a simple outdoor antenna that is located in the center. In the vertical plot, it is shown that the radiation has not a spherical form, it consists of many lobes: The above is called the main lobe and is the biggest, the lower is called the back lobe, and the rest of lobes are called the side lobes [43]. This form of radiation clarifies the presence of many positions without coverage, or with weak signal, the white points represent the presence of holes where no signal could be detected.

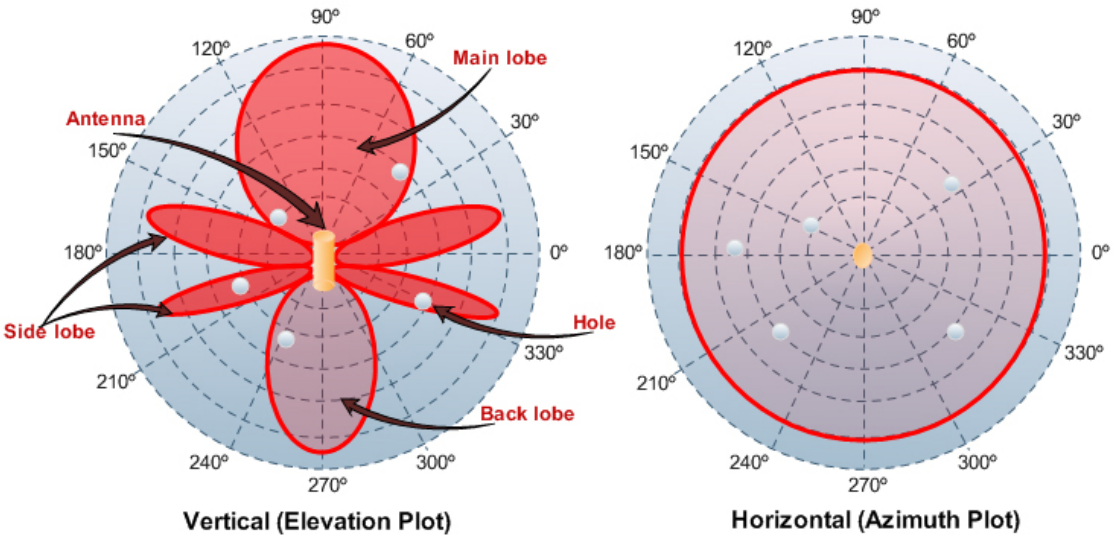

Figure 1.3: Real CA (antenna radiation)

1.3.3 Holes

In all wireless networks, where MCs receive signals from AP or BS, signals are affected by surrounding conditions such as the climate, or obstacles such as tunnels, causing signal variation and drop at some moments. Positions of signal drop (RSSI = 0) are called holes. Disconnections caused by holes could not be predicted except for some rare cases where disconnection occurs frequently in the same position; that enables the MC to memorize these positions.

For example, when a connected MC is passing through a tunnel, it will disconnect loosing video frames. In Figure 1.4 the MC with laptop is walking in a street, it has a good connection with the AP that is mounted above the building until t = 2 s, then the signal decreases gradually as it enters the tunnel, the connection is lost totally at t = 4 s which is explained in the diagram, the drop in the signal at t = 4 s is called hole. Later, the signal is enhanced when MC goes out from the tunnel, which is illustrated with the rising curve in the diagram. In this case of holes, if MC passes frequently from the same route, the hole could be predicted, while in other situations of a movable obstacle such as a train, it is very difficult to predict hole's position because it appears sporadically.

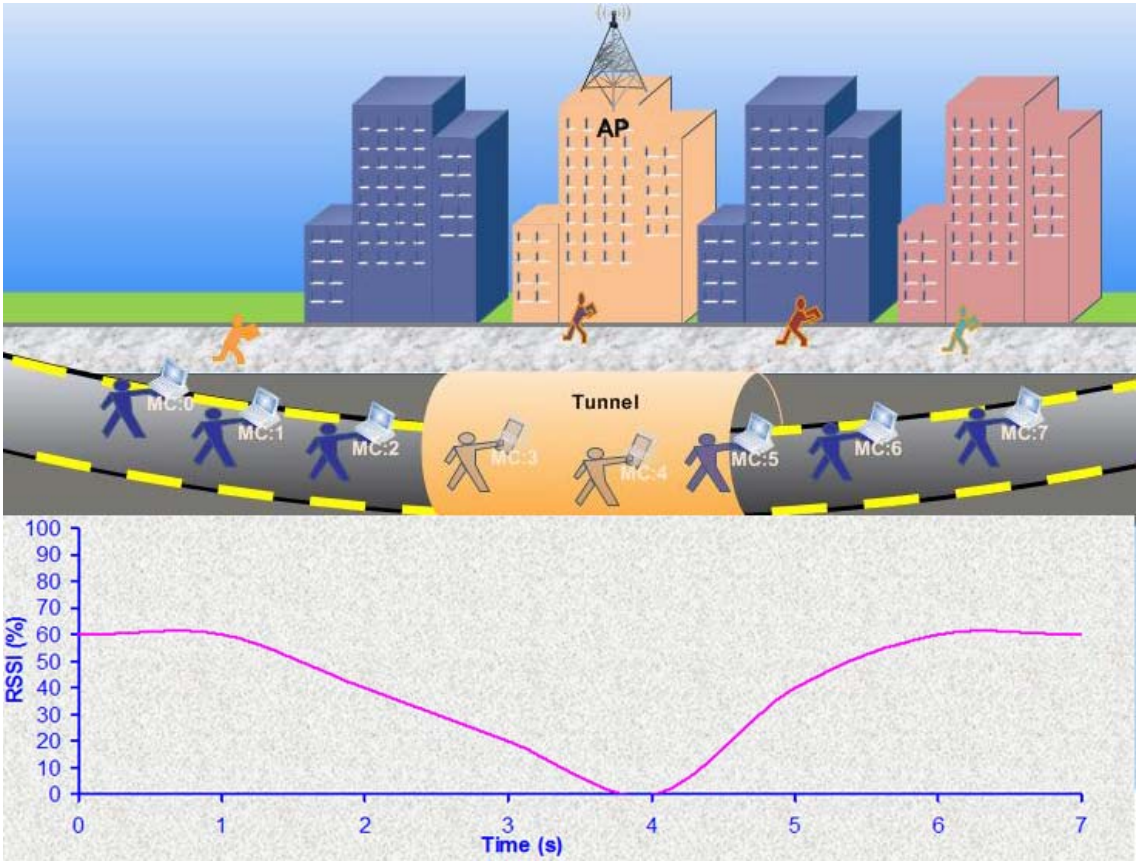

Figure 1.4: The hole in case of MC passing through a tunnel

1.3.4 Handover and Roaming

Nowadays, MCs are provided with several WNICs (Multi-homed systems that have multiple network interfaces [44]) in order to allow their access to different wireless technologies [45] and to extend the area in which they can connect. By contrast, there is no available commercial device with WiFi and WiMAX. Therefore, when MC starts loosing connection with the associated AP and stops receiving data for several seconds [38] [46], it will search for another AP to associate with. This process is named roaming or handover.

There are several definitions of the *Roaming* and *Handover*. Roaming is defined as the ability of a network operator to provide their clients with the same services available in their home network when they are using other system inside or outside the country [Web-10]. From the home carrier's perspective there are two types of roaming: *Inbound Roaming* where clients from another wireless network come into home

network and use its services, while in the *Outbound Roaming*, the home network clients visit another network and use its services.

From the region perspective, the roaming types are:

- *Regional roaming*: The possibility to move from one region to another inside national coverage of the mobile operator.
- *National roaming*: The ability to move from one mobile operator to another in the same country.
- *International roaming*: The ability to move to a network of a foreign telecommunication service provider outside the country.

Many reports agree on the definition of handover as the process occurring when MC moves its connection between different BSs or APs whether they use the same or different technologies [17] [30] [44] [47]-[49]. When this process supports service continuity by maintaining network connection channel, low latency (handover latency is the time between loosing MC connectivity with its current AP and receiving the first IP packet from the new AP [50]) and packet transmission during the movement, it is called *Seamless Handover* [45] [47] [48] [51]-[53]. The IEEE 802.16 defines the handover process in which MC migrates from the air-interface provided by one BS to the air-interface provided by another BS [54].

There are different types of handover (Figure 1.5) depending on many factors; for example basing on BS technology, we distinguish [45] [51] [55]:

- *Horizontal Handover* (*HH*) that occurs when MC moves between networks that use the same technology and the same type of WNIC. In addition, the two networks could be operated by the same network operator, where the mobile device IP address remains unchanged, and handover occurs in the wireless link layer [31].
- *Vertical Handover* (*VH*) is defined when these different networks use different technologies and different WNIC, and changing the IP address is required [31]. There are two types defined under this class [55]:
  a. *Upward vertical handover*: Handover to a mobile overlay with a larger cell size and lower bandwidth per unit area.
  b. *Downward vertical handover*: Handover to a mobile overlay with a smaller cell size and higher bandwidth per unit area.

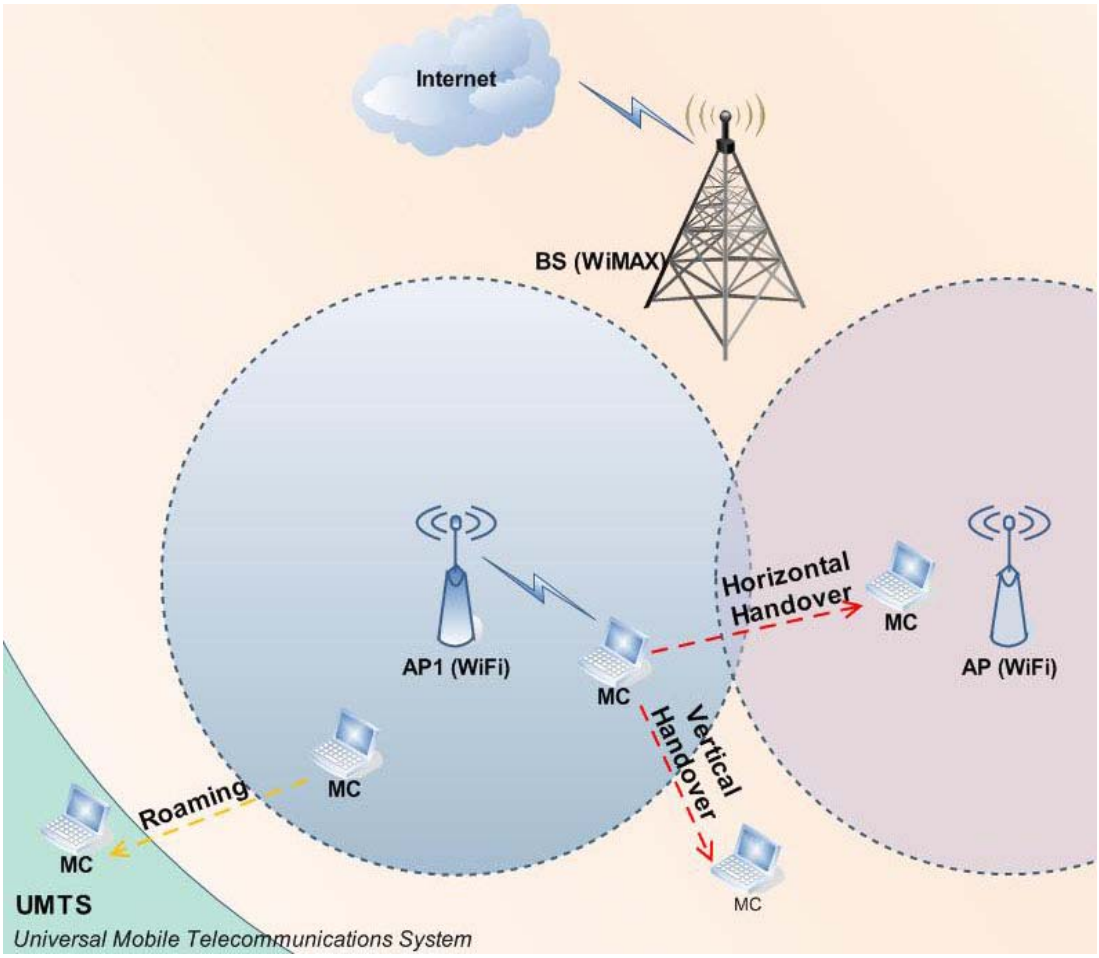

Figure 1.5: Handover types and roaming

Some reports called the HH as *Intra-Technology* handover and the VH as *Inter-Technology* handover [56]. While the Intra-system handover is defined between sectors of the same system, the inter-system handover happens between different systems [53].

Likewise, different handover types could be distinguished by their strategies [57]:

- *Reactive Handover* (*RH*) delays handover as much as possible i.e. handover starts only when MC loses completely its current AP signal [56].
- *Proactive Handover* (*PH*) that triggers handover before the complete loss of original cell signal. Two strategies are available under this type depending on the handover procedure (refers to the sequence of actions between MC and AP [17]):
  a. *Hard Proactive* (*HP*) where MC disconnects from the associated AP before connecting to the visible AP [24] [47], which permits a single connectivity

with one AP [45]. The same definition was given to the *backward handover* [49].

b. *Soft Proactive* (*SP*): In this case, MC makes a successful connection with the new AP before disconnecting from the current one [47] being connected to more than one AP at the same time [24] [45]. This definition was given to the *forward handover* [49].

It is important to recognize the *Ping-Pong* handover which is unnecessary handover processes that occur when MC makes a handover to a neighboring BS and returns to the original BS after a short time [58]. Two reasons could cause the handover:

- The MC is moving out of the current AP CA and needs to associate to new AP.
- The MC detects multiple APs within its range, and needs to switch among them to improve some aspects of communication such as reducing packet loss, improving throughput or reducing the cost [31].

Hence, the handover process requires two important things:

- Maintaining the connection as the associated AP is changed due to network change.
- Maintaining the required QoS for the applications that are active on MC device as the AP is changed.

Handover Support in WiFi

The original IEEE 802.11 did not specify any handover mechanisms [57], but the two amendments IEEE 802.11f and IEEE 802.11r provide handover capability between AP that are interconnected at the link layer, and the link layer handover takes place in three distinct phases [15] [50] [56]:

- *Discovery*: The station detects weak signal strength of the current AP and scans for other available signals to establish a new connection [50].
- *Authentication*: The station and the AP selected by the scanning phase exchange station authentication messages.
- *Association*: The station requests an association identifier from the AP to be used for data delivery [56].

Additionally, the IEEE 802.11r specifies fast handover that supports QoS [59]; it is called Fast BSS transition and aims to reduce disconnection time when station moves its connection from one BSS to another. Fast BSS transition includes protocols that can be applied only on station transition between APs inside the same mobility domains in the same ESS [59]; thereby two of them are defined:

- *Fast BSS Transition*: When resource request is not required prior to the station transition to the new AP.
- *Fast BSS Transition Resource Request*: When resource request is required prior to the station transition.

These protocols need information exchange between the AP and the station during the association phase, and this is performed by two methods [59]:

- *Over the air*: The station communicates directly with the new AP.
- *Over the distributed system*: The station communicates with the new AP via the current associated AP.

Handover Support in Mobile WiMAX

The IEEE 802.16 provides handover procedure to support mobility between BSs [27]. It defines two handover variants [54]:

- *Break-before-make handover*: Service with the target BS starts after service disconnection with the previous serving BS.
- *Make-before-break handover*: Service with the target BS starts before service disconnection with the previous serving BS.

Likewise, the IEEE 802.16e provides two handover modes [Web-4] [27]:

- *Hard handover*.
- *Soft handover*: There are two handover procedures under this mode [27] [30] [24] [54]:
  a. *Macro Diversity Handover* (*MDHO*).
  b. *Fast BS Switching* (*FBSS*).

1.4 Video Streaming Service Disruption in Wireless Networks

The later discussed problems of coverage affect directly on video streaming services, because the weak signal locations produce disruptions in video service delivery. We

now analyze the problems this disruption provoke segmenting them in three different situations:

- *Problems with Handover*: The handover has bad effect on video streaming's QoS metrics such as jitter and delay during RTMA sessions, due to the execution of several operations during handover. The handover delay is the interval of time starting when MC data receiving stops until moving its connection to the new AP [60]. To reduce latency during handover, [61] proposed fast handover technique to meet the seamless mobility for video streaming service. The main problem yields during the delay period, the connection is lost and no more video packets are buffered in the MC, thus the displayed video lacks some frames and the user could see low quality video or could loss part of it. Therefore, to overcome this issue, an effective technique is necessary to provide the user with sufficient video frames before the disconnection in order to keep the video in displaying mode with an acceptable quality.
- *Problems with holes*: It is the same problem caused by handover, but the problem of holes is its impossible prediction when it is caused by movable objects. Thus, proposed solutions of handover could not be effective in case of holes. For this reason, filtering models and techniques are better as the detected signal could be filtered to avoid any sudden disconnection and to smooth the signal curve.
- *Problems of video streaming service in WiFi and WiMAX*: The video streaming service requires high energy consumption rate, causing problems with mobile devices that depend on limited energy batteries, since it is unpractical to charge device battery during movement. In video streaming service, the energy is mainly used for computation, transmission and display. Nevertheless, in transmission, the energy is consumed to transmit and receive the *Radio Frequency* (*RF*) audio and video signals, and also in computation to encode and decode these signals.
- Moreover, the problem of Mobile IP, which is a network layer mobility management scheme; is that it allows MCs to maintain their connection with the home wireless network when moving to a new network. This is possible by tunneling the transferred packets through a home agent in the same network

[Web-10] [51] [62]. However, the disadvantage of this scheme is that the home and foreign agents could become bottlenecks, since they handle the tunneled packets for a large number of mobile hosts [51]. This scheme uses three procedures: the agent discovery, registration, routing and tunneling [7].

1.5 Objective of the Thesis

The main objective of the present thesis was to develop a protocol in order to mitigate video streaming service disruptions in WiFi networks. In order to achieve this objective we:

- Defined the ***mathematical specification of the CA*** and its relation with disconnection zones and different MC movement models.
- Developed a ***new mathematical RSSI Gradient Predictor and Filter,*** to enhance and improve the signal by mitigating the adverse effects of coverage holes, and to predict the MC disconnection states.
- Developed an effective ***buffer management and transmission speed control technique***, to maintain the *MC Buffer* (*MCB*) in its upper limit as long as possible, in order to offer sufficient video frames to be consumed during the service disruption duration. We controlled the video transmission speed depending on the MC state.
- ***Verified the protocol*** using the *Specification and Description Language* (*SDL*). We verified the possibility of exchanging signals and messages between the MC, AP and BS, in order to control the transmission speed and the buffered video.
- Implemented a ***specific Java simulator*** generated from the SDL diagram to simulate the protocol and to demonstrate its efficiency and performance.

1.6 Related Work and Motivations

The prediction is an essential step in developing techniques that solve the video streaming packets loss problem during service disruptions duration. Many filters were used as predictors in the field of wireless communications, where the RSSI value was the data for these filters in direct or indirect way (e.g. calculating it using other parameters like distance). *Grey Model* (*GM*), Kalman filter, Fourier Transform, Particle [63] and Bayesian filter [64] are filters used by many researchers.

As a prediction model, GM plays an important role to make accurate prediction in various fields [65]; we can predict next RSSI by using some measured RSSI values as data of the GM. Different authors apply some filtering techniques including GM to RSSI values to predict handover [63]. Grey predictor is also used to predict the RSSI values which are the input of another filter (fuzzy decision system) that produces the handover factor [66].

Different works have been interested in RSSI filtering. A Kalman filter for RSSI was used to traduce the RSSI current value into a geographical area value for MC positioning. The Extended Kalman filter was used to train an Artificial Neural Network [67], which is used to train the measured signal strength from the *Global System for Mobile* communications (*GSM*) for mobile positioning. In this technique, the Extended Kalman filter depends mainly on the GSM feature that measures the signal strength from many nearby BS. In the other hand, the measured RSSI values could be converted to distances depending on the previous position estimation [68], these distances are used as inputs for the Kalman Filter to give the next position estimation; also the Extended Kalman Filter could be applied on the distance estimated from converting RSSI values [69].

Some authors evaluated the different RSSI filtering techniques including Discrete Kalman; these techniques provide information of available AP for handover in an instant of time [65]. While other authors used an Extended Kalman Filter for the location and velocity estimation of a tracked node. An improved version was used to correct the state estimation of Kalman filter, because it works well only if the tracked node moves at a constant speed and does not change its direction [70].

The buffer management and control mechanisms are effective solutions for the video streaming loss caused by service disruptions, some works proposed buffer management schemes [57] [71]-[74] to provide solutions just for the case of video streaming disruption during handover. However, other cases of disconnections such as holes were not studied. Also, buffer management schemes are used to improve connection capacity for real time streaming [75] or to enhance the QoS [76].

One of the proposed schemes consists of an agent located between the wired and the wireless part of the network to replace the *BS Buffer* (*BSB*) [71]. The agent has a buffer to control the transmission speed of the server, when the occupancy of the agent buffer increase, the agent would send more *Acknowledge* (*ACK*) packets to the server to

decrease its sending rate. In case of handover, the MC stops receiving packets and the occupancy of the agent buffer increases that duplicate the ACK packets number up to 3, causing inhibition of sending packets by the server. When MC reconnects, it will consume the buffered packets from the agent, this latter will send the normal ACK packets increasing the sending rate of the server. In this scheme, three points have to be clarified: 1) how the client buffer is affected, 2) how the sending speed of the agent is controlled by the MC and 3) what happen during the handover in the client side.

Other reports used a buffer management technique to solve multimedia services disruption of less than one second [72], the authors used server and client proxies with buffers, the proxy server forwards its buffered packets followed by ping messages to the proxy client. In case of receiving pong messages with correct coding from the proxy client, the proxy server ensures a good connection. If any signal deterioration happens, the client could not respond with pong message or the coding will not be correct, after sending many ping messages without response, this means that no connection is available. In this case the proxy server asks the server to pause the streaming without terminating the session and in the same time the client is warned to change its CA.

The main idea of the frame rate control mechanism proposed in [73] depends on the buffered frames in MC, as the number of buffered frames decreases, the playing bit rate decreases gradually. If any disconnection happens, no frames will reach the MCB causing a decrease in the amount of buffered video, thus the playing bit rate will also decrease until service stops if no new connection is found.

Another proposed mechanism used two buffers located at the *Previous Access Router* (*PAR*) and the *New Access Router* (*NAR*) [74], the PAR forwards the real time packets to the NAR during the handover process, and after MC connects with the NAR it receives these packets. One disadvantage of this mechanism is the buffer size limitation, it lacks specific size for each buffer, thus in sometimes the buffer could be unavailable in both routers, and therefore real time packets will not be buffered. Also using a buffer in the NAR is not useful because most of access routers have not enough memory for buffering real time packets. In addition, this mechanism is just suitable for disconnection of handover of about 200 ms maximum, hence for other disconnections types that could long more there will be lost in the packets.

Furthermore, some other works presented comprehensive QoS performance study of buffer management schemes and handover mechanisms that are used to solve

service disruption during the handover [77]. The authors used MPEG-4 video sources to evaluate the various buffer management mechanisms, where the video is encoded using a layered coding scheme. They showed that the handover using multicasting mechanism and the push out buffer management mechanism exhibit the best results. In the push-out mechanism, when high priority packets arrive and the buffer is full, any low priority packets will be discarded and will be replaced by the arrived packets [78], whereas in case that there are not low priority packets, the arrived packets will be discarded.

Moreover, other researchers focused their work particularly on the avoidance of interruptions of RTMA when MC makes handover at run-time by predicting handover exploiting first order GM [57]. This enables the mobile proxies to be moved to WiFi area where MC will reconnect, and then it will proactively reorganize user sessions in the new network. In addition they proposed a proactive management of proxy-sided buffers by increasing the size of the pre-fetched streaming contents in the buffer only before handovers.

In addition, many works focus on the disconnection caused by the handover and disrupts video streaming. Some reports assumed a MC with two WNIC as a base for their solutions [79]-[81]. A MC was used with two WNIC to make two connections to the IPTV server in the same time by accessing two different AP simultaneously [79]. One connection is used to transfer video streams and the other one to look for another AP, when the current connection starts to be congested and the measured *Moving Average of Negative Jitter* (*MANJ*) exceed a specific threshold (determined by the service provider), at that moment a new connection is established to the server with identical video stream, then it generates the MANJ value to evaluate which is the most congested connection to drop it down, while in other report authors compared the packet delay of the two streams [80]. However, other authors proposed The *Smooth Adaptive Soft- Handover Algorithm* (*SASHA*) which is an application layer handover algorithm [81]. It is based on exploiting the old and new connections over the overlapped area of the two networks. Thus, the quality of the multimedia delivery process increases. The authors assumed that MC has two WNIC and can open two links with the server in the same time. If MC finds a new connection, it will evaluate the quality of multimedia streaming. While the quality of the new connection is increasing, it will increase the load of the new connection and decrease the old connection load until routing all multimedia traffic to over the new AP.

A dynamic handoff mechanism was proposed for mobility management designed to minimize the handoff latency in IEEE 802.11 [38], which reduces the data loss and the signaling overhead in RTMA. In this mechanism, threshold points are considered to provide better solution for fast and ping-pong MC in a campus wide network; because threshold based prediction method with dynamic channel-scanning mechanism is more suitable for RTMA like VoIP over WLAN. It is demonstrated that the handoff latency is reduced from 310 to 33 ms and the throughput in the overlaid area is increased by 51.6% [38].

Furthermore some handover prediction techniques were the subject of interest for many researchers. A predictive handover framework was presented by some authors [82]; it relies on the neighbor network information to estimate the required handover type and the time to finish all handover procedures. This framework is performed by three steps: 1) The initial configuration and measurement step, 2) the neighbor discovery and prediction step and 3) the handover execution step. In the proposed method, the service disruption time needs 55 ms compared to 450 ms for other method.

A fast mobile IP handover protocol with multiple pre-registration was proposed [61]. The authors prepared new IP addresses of multiple locations where MC can move to. When the received signal is low, it will move to the next network with the strongest signal from the prepared locations, and if it was higher than the defined threshold then handover would succeed, so delay time for generating new *Care of Addresses* (*CoAs*) is saved and reduces the handover latency. In other hand, some authors proposed the variable hysteresis handover technique to minimize the handover probability by using hysteresis with a variable margin [83], this can reduce the probability of handover when the signal strength is high (increasing hysteresis), and increasing the probability of handover when signal strength is lower (decreasing hysteresis). Also they proposed an improvement technique for video quality by reducing *Groups of Video* (*GoV*) objects lost due to frame interdependence by breaking off the natural sequence of frames and controlling the initiation frame of the GoV. They showed that the expected number of frames lost depends on position of handover initiation in the GoV and it is possible to estimate the lost frames number.

Other authors developed handover management scheme for VoIP which is sensitive to packet loss [84]. This scheme employs a transport protocol that supports multiple connections for VoIP communication and makes handover decisions based on

the number of retries experienced by a data frame, it minimizes packet loss in addition to redundant traffic due to parallel transfer of identical packets, by predicting the packet loss in advance based on the number of retries and properly selecting a single-path or multi-path by examining the communication quality on the wireless link.

The performance of the handover process in an IEEE 802.11b network was evaluated by other previous work [17] using bandwidth and handover latency. The authors calculated the handover latency depending on the distance between the two AP and the speed of MC, and the VoIP was an example of an application sensitive to delay and jitter supported on the system. The results showed that handover latency (due to the discovery phase in which MC scans the set of RF channels and waits for signal strength conditions received from the AP to be satisfied) and delay can be reduced by choosing suitable positions of the AP and definition of the sweep phase (series of scans on different channels).

Most of the previous proposals deal with special cases of service disruptions, some works focus only on the handover prediction, and in many cases failed to filter the sudden service disruption occurring in holes. Some of them address only the case of handover with limited time interval. Others provide a solution to control the video transmission speed in the server side without referring to the client side. In addition most of the buffer management solutions suffer buffer size control, overflow or underflow. These solutions were tested by already existing simulators in the market such as NS-2 and OPNET; that has a disadvantage that these simulators are not always suitable for the network characteristics that are considered, which need a lot of modifications in the simulator settings in case that is allowed. Therefore, there is a lack of a comprehensive and integrated solution for all the previous problems. Accordingly, this thesis is a timely contribution addressing an effective solution to many challenges in multimedia services disruptions during service disruptions.

This work presents a new effective protocol to mitigate video streaming packets loss during service disruptions. This protocol consists of two parts:

- A new filtering technique represented by the new RSSI Gradient Predictor and Filter to predict the next MC state and to mitigate the adverse effects of coverage holes [85]-[87]. The RSSI Gradient Predictor has a gradient behavior due to the regular MC movement. Accordingly, the average gradient calculated from a sample set of measured RSSI values, is used to predict future RSSI values. We

derived the predictor especially for RSSI, thus it was improved to work as a filter of holes.

- A buffer management and transmission speed control technique; it is developed in order to mitigate video streaming packets loss during service disruptions [87] [88]. It is based on a mathematical specification for the CA of WiFi AP and a definition for MC movement's models. From these definitions we developed a state diagram to generate MC transitions between coverage zones, each transition generates some commands to control the video transmission speed in the BS and the VoD server, and to manage the buffered video in BSB and MCB, offering sufficient amount of video frames in MCB to be consumed during the service disruption duration.

The SDL was used for the verification process, and for implementing our specific Java simulator, we used the SDL diagram to generate the basic classes, and an external graphical library to produce a detailed graphics for the results.

1.7 Organization of the Thesis

The present thesis is organized as follows: Chapter 2 includes an introduction about the CA of WiFi AP, detailed mathematical specifications for the CA are presented. In addition, definitions of disconnections zones and MC movements tracking inside the CA are also discussed.

Chapter 3 presents the new mathematical RSSI Gradient Predictor and Filter, followed by a synthetic test and performance evaluation in comparison with the Grey Model and the Kalman Filter. Moreover, an experimental test and linearity study for the Gradient Predictor and Filter are clarified.

Chapter 4 describes the effective buffer management and transmission speed control technique; it presents complete specifications for the technique in SDL and discusses the verification results.

Chapter 5 provides detailed explanation of the new specific Java simulator, which was generated and developed from the SDL diagram. It combines the RSSI Gradient Predictor and Filter with the buffer management and transmission speed control technique. Moreover, it displays several charts of the results with detailed information about MC, buffers and transmission speed.

Chapter 6 presents conclusions and future work. Chapter 7 is a Spanish resume of the thesis, and then the references are listed. Finally, the Appendix includes information about the contents of the attached CD.

CHAPTER 2

MODELING OF THE WIFI COVERAGE AREA FOR THE PROTOCOL

The AP provides wireless network services to MC as long as it is inside the CA. The signal is measured in many forms as the RSSI% where it is used to classify the CA, thus a simplified model for the CA is defined. The coverage zones such as handover area, holes, and black area where service disruptions occur are mathematically specified and discussed, the MC movements are also defined considering the CA specifications.

2.1 The Coverage Area of a WiFi Access Point

As explained in the previous chapter, the CA fails are responsible for short disconnections in wireless networks causing RTMA services disruptions. Thus the CA should be defined and specified.

The AP is the central device in a WLAN where it acts as RF transmitter and receiver; it could be used to provide a communication between wireless devices and wired network, or to expand the range of wireless network [14] [89]. The wireless AP could typically support up to 255 clients; it is commonly used in offices, commercial centers, homes or schools. The AP used in homes and small offices is a small device with a build in WNIC, radio transmitter and antenna.

The first AP appeared in 1999 after the approval of the IEEE 802.11b standard, and supported many control functions such as security features, access control and RF channel selection by using a simple graphical user interface. The AP could have additional features like internet gateway, switching hub, wireless bridge or repeater and network storage server [89].

Each AP could provide connection for a limited area around it to form the CA. Recently some articles studied the nature of CA, since understanding the CA helps to study several topics such as the signal behavior, handover prediction and network development. Some published works focused mainly on the CA estimation [90], many MCs connected to AP were used to report their positions and to estimate the CA depending on these periodic reports [91].

2.1.1 Simplistic Model for the Coverage Area

In the vertical radiation diagram explained in Figure 1.3 the shape of the CA can be approximated by a circular or an oval figure. The IEEE 802.11 always uses the oval shape to represent the CA, however, a defined shape does not exist actually, since the propagation characteristics are not predictable [14] [91]. But some authors approximate the CA by a circle [38].

We will make some simplifications in order to model the CA for treating the movement of MC inside it. First of all we simplify the area that covers the radiation of an AP to a plane parallel to the ground (distance 0 to the ground without taking into account the different elevations of the ground closed to it). That is, the CA of an AP

could be considered as a plane in an Euclidean space belonging to $\Re^2$. Once we have done this approximation, the second consideration is that the CA is a circle. That is, CA is all the points characterized by the equation $x^2 + y^2 \leq r^2$, where *r* is the radius of the CA centered in point (*0*, *0*). The AP that defines the CA is allocated exactly in the center of the circle. This simplification for the CA is shown in Figure 2.1.

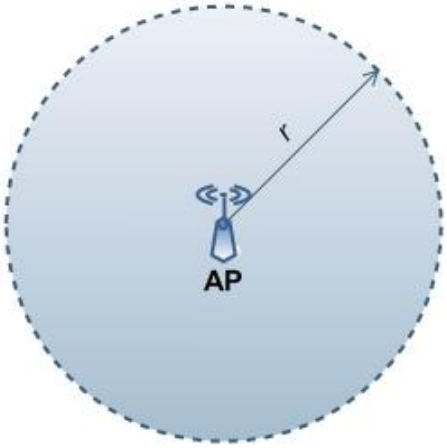

Figure 2.1: Simplified CA

Another simplification is that the points which have the same level of radio antenna radiation inside the CA are all those matching the equation $x^2 + y^2 = r_1^2$. This implies that all the MCs located at a distance r_1 from the AP have the same level of coverage.

The last simplification of the CA is that the level of coverage decreases with longer values of *r*. That is, in the center of the CA (where the AP is allocated), the signal is in its best state and near the boundary of the CA the signal is in the worst state (Figure 2.2).

As a conclusion of the last two simplifications, we can consider that the CA is the union of a set of *concentric circles*. The concentric circles concept could be applied to classify the CA into different coverage zones. The concentric circles have the same center as the CA but different radiuses; hence, all coverage zones are concentric circles with the CA (Figure 2.3). Let $\vec{r} = (r_1, r_2, ..., r_n)$ be the set of different radiuses defined inside the CA, where $r_i \in \Re$. We can define *n* concentric circles (points of CA we name *Sub-set*s (*Ss*)). The Ss_i is defined by the inequality: $r_{i-1}{}^2 < x^2 + y^2 \leq r_i^2$ (taking into account the special value $r_0 = 0$).

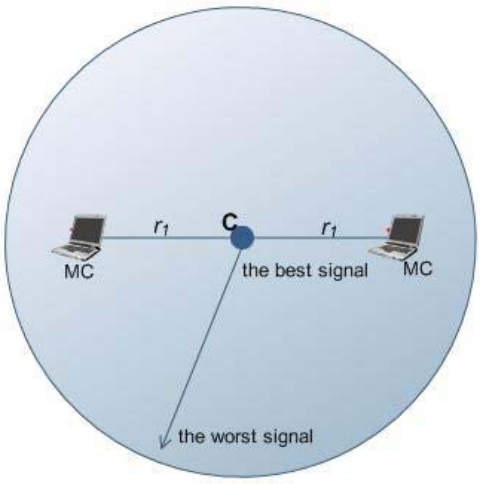

Figure 2.2: The level of coverage

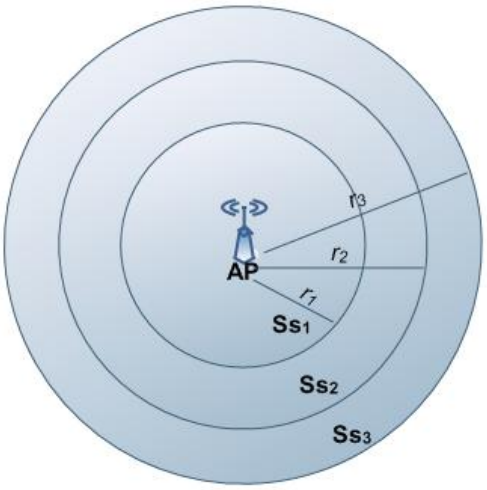

Figure 2.3: The concentric circles and subsets

2.2 The CA Classification Based on Received Signal Strength Indicator

Many parameters related to the wireless connection could be measured while MC moves inside a CA of a WiFi AP, such as data rate, noise, received signal, *Signal to Noise Ratio* (*SNR*) and beacon interval.

In this work, the *Signal Strength* which is measured in the form of RSSI is used; it indicates the received amount of power of radio frequency that is transmitted from AP and measured by the WNIC, the power is measured using two units, by Watts general unit (or mW) or by dBm. The dBm = 10 log10 (power in mW) [89]. The IEEE 802.11 standard defines the RSSI as an integer with allowed values in the range from 0 to 255

(1 byte of size) [14] but vendors do not use 256 values actually; therefore, they defined maximum RSSI (*RSSI_Max*) in the allowed range [9]. For example *Cisco* have chosen *RSSI_Max* = 100, *Symbol* uses an *RSSI_Max* value of 31, while *Atheros* uses *RSSI_Max* = 60 [Web-11]. This integer does not represent the real power value in decibels; however, many signals scanning programs use SNR in db, or % to represent the measured signal. SNR is the difference between the signal strength and the noise level, it measures signal quality in dB [Web-12]. The dBW is a unit relative to power of 1 watt, while the dBm is relative to a power of 1 mW (hence 0 dBm = - 30 dBW). In case of RSSI = - 6 dBm, the signal is equal to 0.25 mW. Sometimes the RSSI% level is used instead of dBm, and could be calculated from the measured RSSI by mapping methods depending on its maximum and minimum values.

There are several tools in the market to scan the WiFi signal and to monitor all changes, they measure also other parameters related to connection. Many existing tools are software tools, while the commercial hardware tools are limited and do not give details like *Raytac Mini Professional WiFi Signal & Hotspot Finder DK-2401* [Web-13]. *MetaGeek's Wi-Spy 2.4i* is a tool that can be connected to the computer via USB port to scan, monitor and analyze any WiFi signal with its supported software that gives a 3D animation [Web-14]. Likewise, many software tools scan and monitor the WiFi signal received by the WNIC of Laptop, some ones list all APs that are in the range and their signal strength (RSSI), and others give many choices to display the signal graph. Moreover, each program can display the signal with different units, some ones with dBm and others with the RSSI%. The *inSSIDer* program [Web-15] has a lot of possible choices to display the received signal in dBm related to time or frequency, and it can show all possible channels with their maximum signal strength. Furthermore, the *Network Stumbler* [Web-12] can display details about all APs in the range with the possibility to export all data to a .txt file, in addition to control three levels of detection speed, and it displays the SNR in dBm. The *WirelessMon Professional* [Web-16] is good software to display the received signal with RSSI% on a specific map of real area.

2.2.1 RSSI% for Coverage Area Classification and modeling

The distribution of RSSI inside the CA could be used to find a relation between MC movement and the CA as it has a regular shape. If MC moves in straight line toward or backward the AP, the signal will increase or decrease respectively. In the other hand,

other movement shapes have different relations with the RSSI, which will be described in details later.

IEEE 802.11 indicates that RSSI can be defined using relative values *RSSI_Max*, this enables the researchers to choose a relative value suitable to their research subject, for example some needs to study the relation between RSSI and time, distance, position, or height, thus each case should has different calculations on RSSI.

This work uses the relative value RSSI%, the *RSSI_Max* refers to a 100% RSSI and the minimum RSSI (*RSSI_Min*) refers to 0% RSSI. In an open area with perfect conditions and no obstacles, RSSI% could be 100% in the center of the CA (position of WiFi AP), and decreases as MC moves far from the AP. When the detected values of RSSI are less than 20%, channel conditions will deteriorate, consequently the data will be lost and the medium will saturates with retransmitted failed data, which causes poor multimedia reproduction quality at MC [46]. As a result, sporadic disruptions could occur.

The RSSI is influenced by the obstruction, diffusion, reflection and multi-path fading causing the fluctuation [51], since the signal is affected by human bodies, walls and the surrounding climatic conditions [21] [92] being difficult to timely detect the unavailability of the signal [51]. The variation, caused by the previous conditions, affects the connection state; hence, discovering positions where disconnections could occur requires more attention.

2.2.2 Coverage Area Zones Simplistic Modeling

The RSSI% range from 0% to 100% can be categorized to different levels associated to different Sub-sets, in order to classify the CA into sub coverage zones. Thus, it facilitates the MC localization inside the CA, and a *Global Position System* (*GPS*) set is not necessary as the exact position of MC is not important.

We assumed three concentric circles with different radiuses r_1, r_2 and r_3 associated to Ss_1, Ss_2 and Ss_3 respectively inside CA, where $r_3 > r_2 > r_1$. If we consider $\Omega(r_i)$ as the coverage level measured by RSSI% at radius r_i, therefore we can define the following coverage zones depending on the coverage level (Figure 2.4):

- *Area1* (A_1) is related to $Ss_1(r_0^2 < x^2 + y^2 \leq r_1^2)$, where $\Omega(r_0) = 100\%$ and $\Omega(r_1) = 60\%$. That is, A_1 is the area of coverage associated to the set of coverage

points in which the levels of coverage are according to the inequality $60 < \Omega(r_i) \leq 100$, where $r_0 < r_i < r_1$.

- *Area2* (A_2) is related to $Ss_2(r_1^2 < x^2 + y^2 \leq r_2^2)$ where $\Omega(r_2) = 40\%$. That is, A_2 is the area of coverage associated to the set of coverage points in which the levels of coverage are according to the inequality $40 < \Omega(r_i) \leq 60$, where $r_1 < r_i < r_2$.
- *Area3* (A_3) is related to $Ss_3(r_2^2 < x^2 + y^2 \leq r_3^2)$ where $\Omega(r_3) = 20\%$. That is, A_3 is the area of coverage associated to the set of coverage points in which the levels of coverage are according to the inequality $20 \leq \Omega(r_i) \leq 40$, where $r_2 < r_i < r_3$.

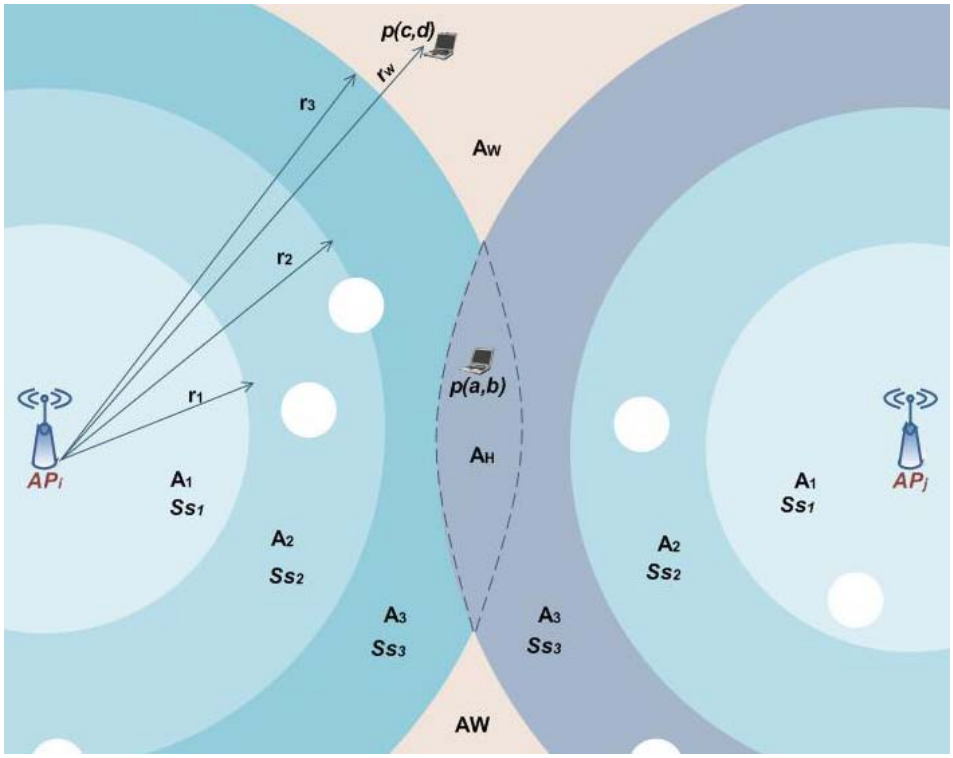

Figure 2.4: Classification of CA

Other researchers chose different limits for classification, some authors classified the $\Omega(r_i)$ values to three levels, the good level ($\Omega(r_i) > 40\%$), the acceptable level ($35\% < \Omega(r_i) < 40\%$) and the poor level ($\Omega(r_i) < 35\%$) [93], while others supposed just two zones with two threshold limits: The good zone and the average zone followed by the overlapped area where the handover occurs [38].

Before transmitting, MC WNIC checks whether the current measured RSSI is less than the *Clear Channel Threshold* (*CCT*) to start transmitting. In case it is greater

or equal to CCT, the wireless channel will not be clear to transmit. When MC is ready to receive, its WNIC must test if the received RSSI (transformed in dBm) is greater than the *Reception Sensitivity Threshold* (*RST*) that is measured in dBm (a value very close to 0 but not 0). If RSSI is equal to RST, WNIC cannot differentiate between noise and signal [Web-11]. If the signal level received from the associated AP drops to a low value, which is called the *Roaming Threshold* (*RT*), then a roaming or handover process should start to other available AP. This zone, where the handover occurs, is called the *Handover Area* (A_H).

Let A_i^j be the coverage zone A_i inside CA_j (where j = 1 or 2) then we can define the handover area A_H as the intersection between A_3^1 and A_3^2 ($A_H = A_3^1 \cap A_3^2$) where $20\% \le \Omega(r_i < r_3) < 35\%$ (Figure 2.4). Accordingly, if MC crosses from A_3 to A_H, a handover process could occur, it will cross to A_H of the other AP and later to A_3. With this consideration, MC cannot cross from A_3 of one AP to A_3 of the other AP directly.

The last zone is the *WiMAX Area* (A_W) which is outside the CA of AP and can be characterized by the subset $Ss_w(r_w^2 > x^2 + y^2)$ that belongs to the CA of the WiMAX BS where $0\% \le \Omega(r_w > r_3) < 20\%$.

2.2.3 Hole Simplistic Modeling

The holes are positions inside the CA where the signal drops suddenly to very low value and cause disconnections; therefore, it is important to define the holes as another zone in the CA. Let us define the vector $\vec{d}(t) = \{d_1(t), d_2(t), ..., d_n(t)\}$ that defines the distances from the center of the CA to holes positions, where each hole is characterized by H_i^j and allocated at distance d_i from the center of the CA_j. The holes, which are allocated in A_W, belong to the CA_j that has the minimum distance from its center to the hole. The hole has some properties:

1. At any hole H_i^j the coverage level $\Omega(d_i) \approx 0\%$. If we suppose the hole (Figure 2.5) has a radius r_i', at distance d_i from the center of the CA (x, y), the center of the hole will be at the point $(x - d_i, y - d_i)$, then all the points that achieve the equation of the circle $(x - d_i)^2 + (y - d_i)^2 \le r_i'^2$ belong to this hole and have the same coverage level $\Omega(d_i) \approx 0\%$.

2. We also define other properties of the hole depending on the presence of the holes; there are two types of holes: Dynamic and static holes.
   2.1 The static hole has constant characteristics (d_i and r_i') and appears always in the same position with the same size.
   2.2 However, the dynamic hole appears at different instances of time and disappears with time, and it has variable characteristics that could have different values (such as its size) depending on time and the positions of its appearance. That means for the dynamic hole we could define the vector $\vec{d} = \{d_1, d_2, ..., d_n\}$ as a function of time $\vec{d}(t) = \{d_1(t), d_2(t), ..., d_n(t)\}$, because these distance values vary with time. Also r_i' could be defined as a function of time $r_i'(t)$ because the size of dynamic hole could be changed, therefore, in general we could say that r_i' and d_i are random variables. #

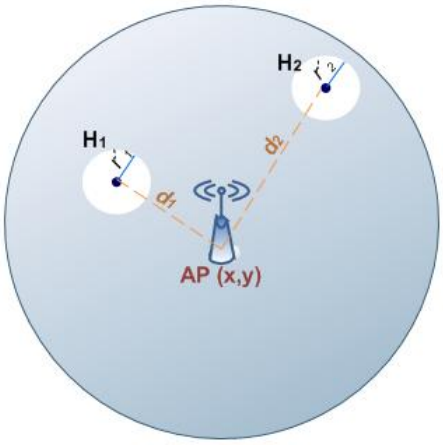

Figure 2.5: Hole simplistic modeling

In this thesis, we are interested in a static hole that has constant d_i and r_i' (do not depend on time) this kind of holes appear always in the same position with the same size. Up to our knowledge, there is not any previous work that has described the hole in this mathematical way and with all these details. Accordingly this study presents new actual description about holes, which are a very special case of real disconnection less studied by previous works. Understanding the holes is the best way to provide a solution for treating them, thus a new mathematical filter was derived specially for these holes, to enhance the signal by treating its fluctuations and output the new $\Omega(r_i)$ without any hole despite of its size. Holes filtering were not considered in most of the published

work, which make the proposed solutions not effectives, therefore, our new RSSI% Gradient Filter is a timely valuable filter, and it is described in the next chapter.

2.3 Examples of Service Disruption Due to Coverage Fails

As long as there are factors affecting the signal and coverage, the MC will suffer disconnections or very low value of $\Omega(r_i)$ leading to poor service quality. Three cases could cause the disconnection: Handover areas, black areas and holes.

In Figure 2.6, these cases of disconnection are shown, the violet zone between the two CA is the handover area, the black zone outside the CA is the black area where there is no WiFi coverage and the white circles are holes. As shown in the figure, MC1 has a good connection with AP_1 and MC2 has a good connection with AP_2, but the rest of them have problems.

In Figure 2.6, MC4 is connected to AP_1 and moves toward AP_2, when its received signal drops to RT, then it will be in A_H, where it will disconnect from AP_1 to move its connection to AP_2, where $\Omega(r_i)$ is greater than RT. In this moment of disconnection, service may be lost and any multimedia streaming will stop. Many published works focused on developing handover mechanisms, in order to improve service quality during disconnection in different network standards as WiFi, WiMAX and *Media Independent Handover* (*MIH*) [24] [30] [48] [58] [94].

The black area includes all the positions outside the WiFi CA, where MC cannot connect to any WiFi network. In the proposed network model for the present work, the black area is under the coverage of WiMAX BS; therefore, MC could not connect as it has not WiMAX WNIC, thus MC will loose any service provided by the WiFi AP (MC5 in Figure 2.6).

The existence of a hole inside the CA means that these sub-sets are non convex ones; accordingly, always there is a set of points inside Ss in which $\Omega(r_i)$ is 0%:

In Figure 2.6, MC3 moves inside a CA of AP_1 passing through a hole, in this position $\Omega(r_i) = 0$, this means that MC3 will suffer disconnection for moments, but these moments could not be predicted, estimated or calculated, because the hole could be dynamic hole, thus it could not have priori knowledge to recognize this hole, which leads to quick interruptions in video streams [21].

There is confusion between holes definition and black area. The hole is found for moments just inside the WiFi CA, whereas black area is outside the WiFi CA due to the limited coverage of AP.

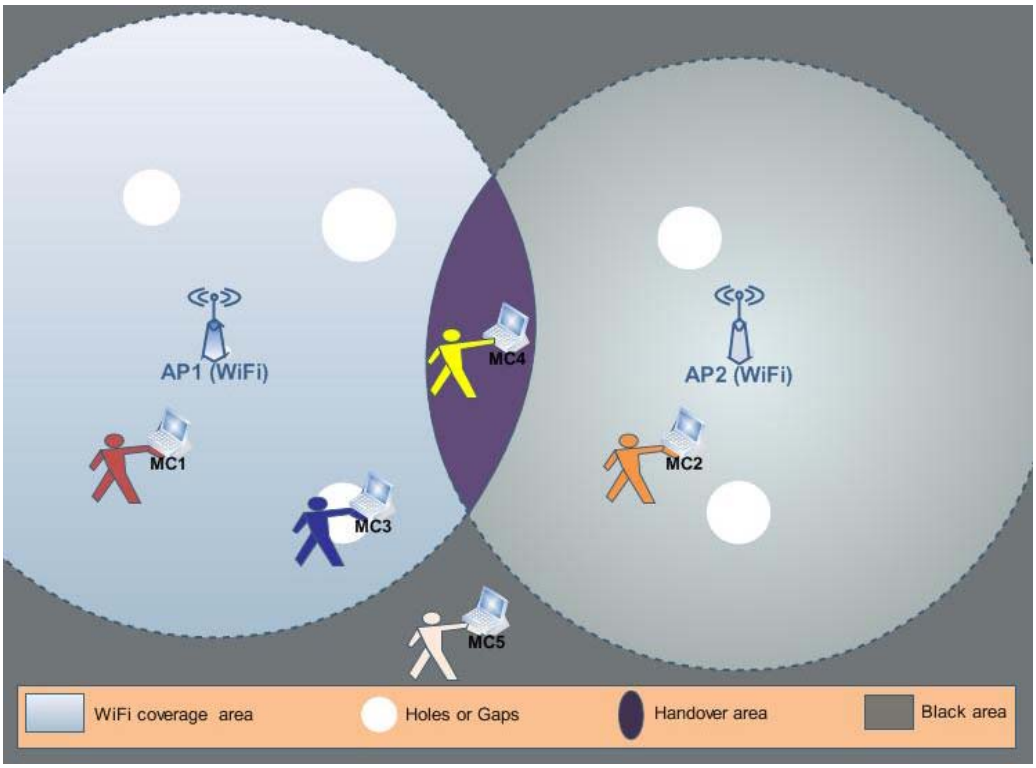

Figure 2.6: Problems of disconnection

2.4 Tracking Modeling for the Mobile Client movements

Studying the relationship between MC movement and the CA is important to discover the situations where disruptions could occur. In the previous section, the CA subsets were described and specified; moreover, their relations with disconnection locations such as holes, handover and out of coverage were also defined. In this section, we will identify the MC movement inside the CA considering the different kinds of movements (Figure 2.7): Straight line (A, B), circular (C), Sine or Cosine (D) and Zigzag (E), where MC could cross one or more coverage zones (or Subset). These kinds of movements could be defined taking into account the previous definitions of coverage zones.

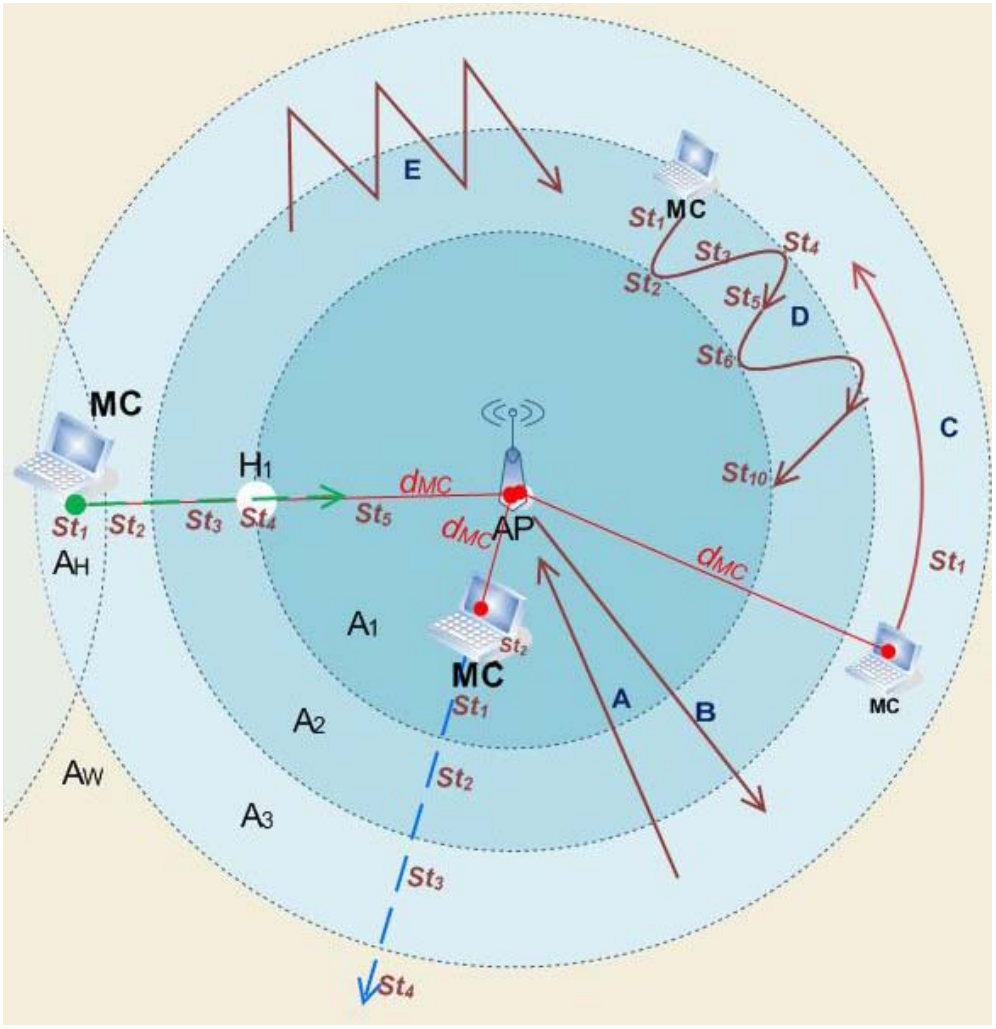

Figure 2.7: Tracking MC movement models

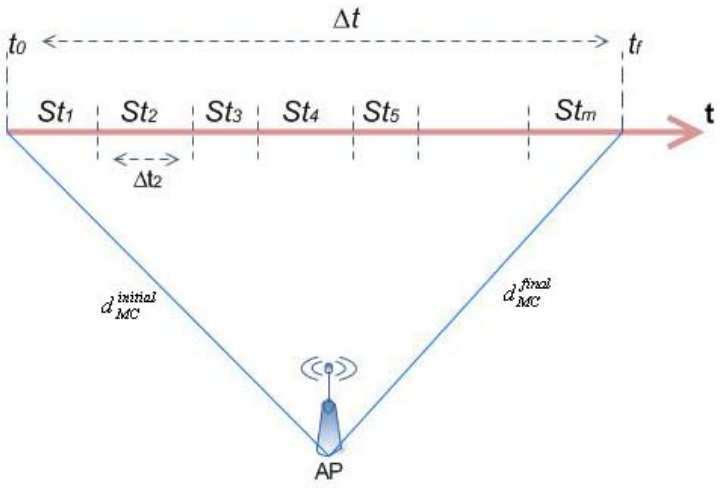

Figure 2.8: The Stage concept

Let us suppose the following assertions (Figure 2.8):

- The MC is moving at a constant speed υ for a duration of time Δt .
- Let d_{MC} be the distance between the MC and the AP, it is located initially at a distance $d_{MC}^{initial}$ of the AP, and finally at a distance d_{MC}^{final} of the AP.
- We define the Stage St_ε (ε = 1, 2……, m) as an interval of time equal Δt_ε of MC movement while d_{MC} is achieving a specific inequality or equation related to r_i .
- The MC can pass through *m* stages during its movement starting at St_1 and terminating at St_m.

Accordingly,

- If $r_{i-1} < d_{MC}^{initial} \le r_i$ then MC is in Ss_i at St_1.
- If $r_w = d_{MC}^{initial}$ then MC is in Ss_w at St_1.
- If $d_{MC}^{initial} = d_1$ then MC is in H_1 at St_1.

For example, in case that MC is moving in straight line from A_1 to A_W (the blue discontinuous line in Figure 2.7), d_{MC} will increase steadily, and the MC will be in several stages:

- St_1, the MC will be in A_1 due to $r_0 < d_{MC}^{initial} \le r_1$.
- St_2, the MC will be in A_2 due to $r_1 < d_{MC} \le r_2$.
- St_3, the MC will be in A_3 due to $r_2 < d_{MC} \le r_3$.
- St_4, the MC will be in A_W due to $d_{MC}^{final} = r_w$.

So we infer that MC started moving with $\Omega(d_{MC}^{initial}) > 60$, which is a very good connection, and finally stopped moving with $\Omega(d_{MC}^{final}) < 20$ which is an out of coverage, thus, $\Omega(d_{MC})$ decreases steadily, being the relation between d_{MC} and $\Omega(d_{MC})$ inversely proportional.

Another example is the case of a MC moving from A_H to A_1 (the green discontinuous line in Figure 2.7) and passing through the hole H_1 (between A_1 and A_2), d_{MC} will decrease steadily, and the MC will be in the following stages:

- St_1, the MC will be in A_H due to $d_{MC} < r_3$ and $\Omega(d_{MC}) < 35$.
- St_2, the MC will be in A_3 due to $r_2 < d_{MC} \le r_3$ and $35 \le \Omega(d_{MC}) \le 40$.
- St_3, the MC will be in A_2 due to $r_1 < d_{MC} \le r_2$.

- *St4*, the MC will be in H_1 due to $d_{MC} = d_1$ and $\Omega(d_{MC}) = 0$. In this stage, a service disruption could happen if MC was moving slowly, this means that it is spending more time in the hole. While in case of moving quickly, it could not detect this hole and the disruption would not occur. Assuming that τ_{hole} is the interval of time required to cross the hole, and the diameter of the hole is $2r_i'$ then $\tau_{hole} = 2r_i'/\nu$; thus the relation between ν and τ_{hole} is inversely proportional, i.e. increasing ν leads to decreasing τ_{hole}. For example, if a signal scanner tool measures the signal every 0.5 s, then MC will move at $\nu > r_i'$ to cross the hole without detecting it, where ν is calculated by the equation $\nu = \frac{d_{MC}^{final} - d_{MC}^{initial}}{t_f - t_0}$ being t_0 and t_f the initial and final time of the movement respectively.
- *St5*, the MC will be in A_1 due to $r_0 < d_{MC} \leq r_1$.

In the final example, d_{MC} fluctuates between two or more values in other types of movements (the shapes D and E in Figure 2.7). The movement type D is characterized by d_{MC} fluctuation between three values:

- *St1*, the MC will be in A_2 due to $r_1 < d_{MC} \leq r_2$.
- *St2*, the MC will be in A_1 due to $d_{MC} = r_1$: At this point $\Omega(d_{MC}) = \Omega(r_1)$.
- *St3*, the MC will be in A_2 due to $r_1 < d_{MC} \leq r_2$.
- *St4*, the MC will be in A_2 due to $d_{MC} = r_2$: At this point $\Omega(d_{MC}) = \Omega(r_2)$.
- *St5*, the MC will be in A_2 due to $r_1 < d_{MC} \leq r_2$.
- *St6*, the MC will be in A_1 due to $d_{MC} = r_1$: At this point $\Omega(d_{MC}) = \Omega(r_1)$.

Let us note that MC will be in different stages: *St1*, *St2*, *St3*, *St4*, *St5* and *St6*, but the zones where it will pass can be repeated defining a *periodic pattern*. In Table 2.1, we show the patterns defined by different kinds of movement (Figure 2.7). We can take advantage of these patterns in order to anticipate the zone where the MC will be in a future stage St_k. For example, we can infer that MC will be in A_1 at St_{10} for the movement shape D in Table 2.1.

While in case of moving in circular form (shape C in Figure 2.7), the periodic pattern (Table 2.1) consists of one stage (A_3), this means that in any stage St_i the MC

will be in A_3. Likewise, following the periodic pattern sequence (Table 2.1) of shape E (Figure 2.7) that consists of A_2 and A_3, we could infer that in St_{10} the MC will be in A_3.

Table 2.1: MC movement's periodic patterns

	St_1	St_2	St_3	St_4	St_5	St_6	St_7	St_8	St_9	St_{10}
Shape D	A_2	A_1	A_2	A_2	A_2	A_1	A_2	A_2	A_2	A_1
Shape C	A_3	A_3	A_3	A_3	A_3	A_3	A_3	A_3	A_3	A_3
Shape E	A_2	A_3	A_2	A_3	A_2	A_3	A_2	A_3	A_2	A_3

Let us consider a different example of movement (shape F in Table 2.2) where MC will be in the sequence: A_1, A_2, A_3, A_W, A_H, A_W, A_3, A_2, A_2 and A_3. Looking at this sequence, we can not find frequent repeated zones, which means that the MC will follow this path only once during the movement. So we can define *non periodic pattern,* when the movement does not contain repeated zones. Another example is shape G (Table 2.2), where MC will be in the sequence: A_3, A_W, A_3, A_2, A_2, A_1, A_2, A_3, A_H and A_3, it defines also a non periodic pattern because we can not find repeated zones. Therefore, inferring future zones where the MC will be is not possible using the periodic pattern. Following the sequence in both cases, we can discover another way to infer future zones. The MC (shape F in Table 2.2) is moving from an excellent connection zone (A_1 at St_1) to good connection zone (A_2 at St_2) and then to weak connection zone (A_3 at St_3), this means that the MC moves gradually from the best to the worst coverage zone; accordingly, we can infer that it will be in out of coverage zone (A_W at St_4) after short time. We refer to this situation as *gradient pattern*.

Table 2.2: MC movement's non periodic patterns

	St_1	St_2	St_3	St_4	St_5	St_6	St_7	St_8	St_9	St_{10}
Shape F	A_1	A_2	A_3	A_W	A_H	A_W	A_3	A_2	A_2	A_3
Shape G	A_3	A_W	A_3	A_2	A_2	A_1	A_2	A_3	A_H	A_3

Some times the MC passes through coverage holes during its movement, thus we will find a stage in which the MC is in H_1, such as St_3 of shape K (Table 2.3). In the sequence of shape K (A_2, A_1, H_1, A_2, A_2, A_1, A_2, A_2, A_2 and A_1) we can not find any periodic pattern, but if we compare the first four stages (A_2, A_1, H_1 and A_2) with the second four stages (A_2, A_1, A_2 and A_2) we will find similarity except the stage where the hole appears. Therefore, we can say in the absence of the hole, this pattern can be considered as periodic pattern; we categorize this type as a *periodic pattern with holes*.

Whereas in other situations (shape L in Table 2.3), we can not find the similarity to discover the periodic pattern. If the hole H_2 (at St_6) appears or disappears, the pattern will not change. This type can be categorized as *non periodic pattern with holes*

Table 2.3: MC movement's in periodic and non periodic patterns with holes

	St_1	St_2	St_3	St_4	St_5	St_6	St_7	St_8	St_9	St_{10}
Shape K	A_2	A_1	H_1	A_2	A_2	A_1	A_2	A_2	A_2	A_1
Shape L	A_1	A_2	A_3	A_W	A_H	H_2	A_3	A_2	A_2	A_3

2.5 The Need of Video Service Disruption Mitigation Protocol

In the previous section we analyzed the effects of holes in the movement of the MC:

- There are movements defining periodic patterns inside the set of visited zones. Only, in case we have no holes, we can predict the future stage St_k in which the MC will be after some time. That is the reason we have defined a ***predictor*** to infer that zone.
- There are some movements that do not define a periodic pattern. For that kind of movements we try to find our gradient definition in order to anticipate information, but it will not work with totally random movements.
- Just in case there are holes in the MC path, we will try to eliminate the effects they provoke in the periodic and non periodic movements. To do this we need a ***filter*** to eliminate the holes' adverse effect. That is interesting because we again could predict the stage St_k using our predictor. In this way we mitigate the adverse effects of holes.
- For movements defining gradient patterns, we can use our predictor when there are no holes in the path. But holes can be filtered and then we can predict the future St_k for gradient pattern's movements using our predictor

In Table 2.4, we sum up our technique to mitigate the adverse effect of holes.

Table 2.4: Holes effects mitigation

		Holes	
		No	Yes
Movement types	Periodic	Predict	Filter Predict
	Non periodic	---	---
	Gradient	Can predict	Can filter

The main idea of our protocol was based on the mentioned definitions of the CA and MC movements. The first part of the protocol: The RSSI Gradient Predictor and

Filter was derived depending on the gradient and the periodic patterns in addition to the gradient behavior of $\Omega(d_{MC})$. To proceed from this behavior, we studied the possible movement models of the MC, and we classified them to regular and irregular movements, because the regular movement is a condition to have a steadily behavior. Therefore, the predictor used the average gradient that was calculated using a sample set of $\Omega(d_{MC})$, then the instant gradient could be calculated from the average gradient for any instant time even if for the future. Taking into account the presence of holes, the predictor was improved to work as a filter for these holes, this was achieved by detecting the hole and correcting it to a value related to the previous correct $\Omega(d_{MC})$ sample.

The second part of the protocol: The buffer management and transmission speed control technique. For this technique, we considered a network with two APs connected to a WiMAX BS. The BS is connected to a wired network where a VoD server streams multimedia packets to MC which is connected to the WiFi AP. The technique is based on the CA classification into different coverage levels. Depending on the subset and stage concepts, we analyzed the MC movement between these subsets to build a state diagram. Several MC transitions could be generated from the state diagram, where each transition is a change in the subset or the coverage level. While $\Omega(d_{MC})$ is related to MC position, then it will be related to the transitions. Some commands were associated to each transition in order to control the transmission speed in the VoD server and BS, and to manage the buffered video in BSB and MCB. This process achieved by 1) increasing the BS transmission speed in two cases: When the MCB is under its upper limit, and in case of any expecting disconnection. 2) Decreasing the BS transmission speed in two cases: When the MCB is over its upper limit, and in case the MC is going back to good coverage level.

For the verification process of the buffer management and transmission speed control technique, we used the SDL to define and describe the technique, then to verify the possibility of exchanging the messages and signals which carry the commands. The SDL diagram was used to generate the main classes of the new specific Java simulator; it was supported by an external library for generating special graphs with information about the MC movement, RSSI, the transmission speed and the buffered video. All the protocol details will be explained in the following chapters.

CHAPTER 3

THE RSSI GRADIENT PREDICTOR AND FILTER

Many filters and models such as Grey model and Kalman filter were used as predictors in the field of wireless connections, especially for handover prediction. In the new RSSI Gradient Predictor and Filter, samples of RSSI% were used to predict next MC coverage level where holes are filtered and the signal is enhanced. The RSSI Gradient Predictor and Filter were tested on RSSI measured values. The signal scanning experiment was done in an open area with no obstacles to avoid their effects. The Gradient Filter showed linear behavior. Likewise, it displayed good results in detecting and filtering holes.

3.1 Grey Model

Referring to the *Black Box* concept, *White System* can be defined when we have all information about it, unless that, it is called *Black System* [65] [Web-17]. A system with partial information known and partial information unknown is called *Grey System* [65] [66]. The Grey System works mainly on system analysis which has produced poor, incomplete or uncertain messages. The advantages of the GM are its ability to estimate an unknown system using only a few data. Furthermore, it can use a first-order differential equation to characterize the unknown system behavior [Web-17]. The most commonly used GM is the GM (1, 1), which is a single variable first-order GM. The modeling procedure is summarized as follows:

1. Given the original data set ($\Omega(d_{MC})$ values): $X^0 = \left[x^0(1), x^0(2), ..., x^0(n)\right]$, where $x^0(i)$ corresponds to the system output at time i.
2. A new sequence $X^1 = \left[x^1(1), x^1(2), ..., x^1(n)\right]$ is generated, where $x^1(k) = \sum_{m=1}^{k} x^0(m)$.
3. From X^1, the first-order differential equation $\frac{dx^1(k)}{dk} + ax^1(k) = u$ is formed
4. From which it is possible to obtain ***a*** and ***u*** with $\begin{bmatrix} a \\ u \end{bmatrix} = (B^T B)^{-1} B^T y_n$

   Where:

$$B = \begin{bmatrix} -1/2\,(x^1(1) + x^1(2)) \\ -1/2\,(x^1(2) + x^1(3)) \\ ..... \\ -1/2\,(x^1(n-1) + x^1(n)) \end{bmatrix}, \; y_n = \left[x^0(2), x^0(3), ..., x^0(n)\right]^T$$

5. The predictive function is $\hat{x}^1(k) = (x^1(1) - u/a)e^{-ak} + u/a$ and the predicted value at time $k+1$ is $\hat{x}^0(k+1) = \hat{x}^1(k+1) - \hat{x}^1(k)$ which can be written as:

$$\boxed{\hat{x}^0(k+1) = (x^0(1) - u/a)(e^{-a} - 1)e^{-ak}}$$

The detailed derivations of GM equations are as follows:

Starting from step 4 we will find the equation of u and a.

$$B^T = \left[-1/2\,(x^1(1) + x^1(2)), -1/2\,(x^1(2) + x^1(3)), ..., -1/2\,(x^1(n-1) + x^1(n))\right]$$

$$B^T.B = \begin{bmatrix} 1/4\sum_{i=1}^{n-1}(x^1(i)+x^1(i+1))^2 & -1/2\sum_{i=1}^{n-1}(x^1(i)+x^1(i+1)) \\ -1/2\sum_{i=1}^{n-1}(x^1(i)+x^1(i+1)) & n-1 \end{bmatrix}$$

$$(B^T.B)^{-1} = \frac{1}{w}\begin{bmatrix} n-1 & 1/2\sum_{i=1}^{n-1}(x^1(i)+x^1(i+1)) \\ 1/2\sum_{i=1}^{n-1}(x^1(i)+x^1(i+1)) & 1/4\sum_{i=1}^{n-1}(x^1(i)+x^1(i+1))^2 \end{bmatrix}$$

Where $w = \left[\frac{n-1}{4}\sum_{i=1}^{n-1}(x^1(i)+x^1(i+1))^2\right] - \left[\frac{1}{4}\left(\sum_{i=1}^{n-1}(x^1(i)+x^1(i+1))\right)^2\right]$

$$B^T.y_n = \begin{bmatrix} -1/2\sum_{i=1}^{n-1}\left(x^0(i+1)(x^1(i)+x^1(i+1))\right) \\ \sum_{i=1}^{n-1}x^0(i+1) \end{bmatrix}$$

$$\begin{bmatrix} a \\ u \end{bmatrix} = \frac{1}{w} \begin{bmatrix} \left[\frac{1-n}{2}\sum_{i=1}^{n-1}\left(x^0(i+1)(x^1(i)+x^1(i+1))\right)\right] + \left[\frac{1}{2}\left(\sum_{i=1}^{n-1}x^0(i+1)\right)\left(\sum_{i=1}^{n-1}(x^1(i)+x^1(i+1))\right)\right] \\ \left[\frac{-1}{4}\left(\sum_{i=1}^{n-1}(x^1(i)+x^1(i+1))\right)\left(\sum_{i=1}^{n-1}x^0(i+1)(x^1(i)+x^1(i+1))\right)\right] + \left[\frac{1}{4}\left(\sum_{i=1}^{n-1}x^0(i+1)\right)\left(\sum_{i=1}^{n-1}(x^1(i)+x^1(i+1))^2\right)\right] \end{bmatrix}$$

$$a = \frac{\left[\frac{1-n}{2}\sum_{i=1}^{n-1}\left(x^0(i+1)(x^1(i)+x^1(i+1))\right)\right] + \left[\frac{1}{2}\left(\sum_{i=1}^{n-1}x^0(i+1)\right)\left(\sum_{i=1}^{n-1}(x^1(i)+x^1(i+1))\right)\right]}{\left[\frac{n-1}{4}\sum_{i=1}^{n-1}(x^1(i)+x^1(i+1))^2\right] - \left[\frac{1}{4}\left(\sum_{i=1}^{n-1}(x^1(i)+x^1(i+1))\right)^2\right]}$$

$$u = \frac{\left[\frac{-1}{4}\left(\sum_{i=1}^{n-1}(x^1(i)+x^1(i+1))\right)\left(\sum_{i=1}^{n-1}x^0(i+1)(x^1(i)+x^1(i+1))\right)\right] + \left[\frac{1}{4}\left(\sum_{i=1}^{n-1}x^0(i+1)\right)\left(\sum_{i=1}^{n-1}(x^1(i)+x^1(i+1))^2\right)\right]}{\left[\frac{n-1}{4}\sum_{i=1}^{n-1}(x^1(i)+x^1(i+1))^2\right] - \left[\frac{1}{4}\left(\sum_{i=1}^{n-1}(x^1(i)+x^1(i+1))\right)^2\right]}$$

From the relation between $x^0(i)$ and $x^1(i)$, four equations are correct:

$$x^1(i+1) = x^0(i+1) + x^1(i)$$

$$\sum_{i=1}^{n-1} x^0(i+1) = x^1(n) - x^0(1)$$

$$\sum_{i=1}^{n-1} \left((x^0(i+1))(x^1(i) + x^1(i+1)) \right) = \sum_{i=1}^{n-1} ((x^1(i+1))^2 - (x^1(i))^2)$$

$$\sum_{i=1}^{n-1} (x^1(i) + x^1(i+1)) = x^1(n) - x^0(1) + 2\sum_{i=1}^{n-1} x^1(i)$$

Then we have the following

$$\frac{u}{a} = \frac{\left[\left(\sum_{i=1}^{n-1} (x^1(i) + x^1(i+1)) \right) \left(\sum_{i=1}^{n-1} ((x^1(i+1))^2 - (x^1(i))^2) \right) \right] - \left[(x^1(n) - x^0(1)) \left(\sum_{i=1}^{n-1} (x^1(i) + x^1(i+1))^2 \right) \right]}{\left[2(n-1) \sum_{i=1}^{n-1} ((x^1(i+1))^2 - (x^1(i))^2) \right] - \left[2(x^1(n) - x^0(1)) \left(\sum_{i=1}^{n-1} (x^1(i) + x^1(i+1)) \right) \right]}$$

$$a = \frac{\left[2(n-1) \sum_{i=1}^{n-1} \left((x^1(i+1))^2 - (x^1(i))^2 \right) \right] - \left[2(x^1(n) - x^0(1)) \left(\sum_{i=1}^{n-1} (x^1(i) + x^1(i+1)) \right) \right]}{\left[(1-n) \sum_{i=1}^{n-1} (x^1(i) + x^1(i+1))^2 \right] + \left[\left(\sum_{i=1}^{n-1} (x^1(i) + x^1(i+1)) \right)^2 \right]}$$

Finally the predicted value at time k+1 is $\hat{x}^0(k+1) = \hat{x}^1(k+1) - \hat{x}^1(k)$. Referring to step 5:

$$\hat{x}^1(k) = (x^1(1) - u/a)e^{-ak} + u/a$$

Then:

$$\hat{x}^0(k+1) = \left((x^1(1) - u/a)e^{-a(k+1)} + u/a \right) - \left((x^1(1) - u/a)e^{-ak} + u/a \right)$$

$$\boxed{\hat{x}^0(k+1) = (x^0(1) - u/a)(e^{-a} - 1)e^{-ak}}$$

3.2 Kalman Filter

The *Kalman filter* is a set of mathematical equations that provides an efficient computation (recursive) means to estimate the state of a process, in a way that minimizes the mean of the squared error. The filter is very powerful in several aspects: It supports estimations of past, present and even future states and it can do so even when the precise nature of the modeled system is unknown [66].

The *Discrete Kalman filtering* module tries to estimate RSSI values by representing the RSSI time evolution as a combination of signal noise (measurement noise) and maximum signal evolving (process noise) [63].

The filter is used to estimate the state $x \in R^n$ of a discrete time controlled process, $\hat{x}_k^- \in R^n$ is a *Priori state* estimate at step k, given knowledge of the process prior to step k and $\hat{x}_k \in R^n$ is a *Posteriori state* estimate at step k given measurement z_k.

The Discrete Kalman filter algorithm consists of two phases:

1. Time update (predictor): Projecting forward the current state and error covariance estimates to obtain a priori estimate for the next time step.
   a. To project the state ahead
      $\hat{x}_k^- = A\hat{x}_{k-1} + Bu_{k-1}$
   b. Project the error covariance ahead
      $P_k^- = AP_{k-1}A^T + Q$
2. Incorporating a new measurement into a priori estimate to obtain an improved a posteriori estimate.
   a. Compute the Kalman gain:
      $K_k = P_k^- H^T (HP_k^- H^T + R)^{-1}$
   b. Update estimate with measurement z_k
      $\hat{x}_k = \hat{x}_k^- + K_k (z_k - H\hat{x}_k^-)$
   c. Update the error covariance:
      $P_k = (1 - K_k H) P_k^-$

As initial step for the first state, initial estimates for $\hat{x}_{k-1}$ and P_{k-1} used as inputs:

1. $A(n \times n)$: A matrix relates the step of $k-1$ to current state k
2. $B(n \times 1)$: A matrix relates u to the state x
3. u: Optional control input
4. P_k^-: A priori estimation error covariance
5. Q: Process noise covariance

6. With a real measurement $z \in R^m$ that is: $z_k = Hx_k + v_k$
7. v_k: A random variable represents a measurement noise that has normal probability distribution $p(v) \approx N(0, R)$
8. R: The measurement noise covariance. While Q and R constant → P_k and K_k are constant.
9. $H(m \times n)$: A matrix relates the state x to the measurement z_k.

The following assumptions are considered as in [66]: $A = I$ (if the state does not change from step to step), where I is the identity matrix, $u = 0$ (there is not control input), $Q = 0$ (assumed to be very small). $R = 0.01$, in [66] authors used Q/R as standard deviation, and Q is the initial state of P_k, and $H = I$ is a noisy measurement of the state directly; accordingly,

$$x_k = x_{k-1} + w_{k-1}$$

$$z_k = x_k + v_k$$

Consequently, the following equations are generated:

1. Time update:

$$\hat{x}_k^- = \hat{x}_{k-1}$$

$$P_k^- = P_{k-1} + Q$$

2. Measurement update:

$$K_k = P_k^-(P_k^- + R)^{-1}$$

$$\hat{x}_k = \hat{x}_k^- + K_k(z_k - \hat{x}_k^-)$$

$$P_k = (1 - K_k)P_k^-$$

By solving the previous equations, two equations are obtained to be used in the RSSI filtering:

$$P_k = \frac{R(P_{k-1} + Q)}{P_{k-1} + Q + R}$$

$$\boxed{\hat{x}_k = \hat{x}_{k-1} + \frac{(P_{k-1} + Q)(z_k - \hat{x}_{k-1})}{P_{k-1} + Q + R}}$$

3.3 The Basics of RSSI Gradient Predictor and Filter

The existing filters used actually have many disadvantages such as the disability to filter holes and enhance the signal; moreover, some predictors are not precise and do not work with special cases such as the constant $\Omega(d_{MC})$. Therefore, it is important to develop a new Predictor and Filter especially for $\Omega(d_{MC})$ predicting and filtering simultaneously.

3.3.1 Basic Definitions

Referring to the calculus definition of the gradient vector field, $\Omega(d_{MC})$ gradient can be defined in the same way being used in estimating the next area where MC could be, $\Omega(d_{MC})$ is related to MC location.

Definition 1: CA Scalar Field is a 2-Dimentional space with a real RSSI value attached to each point in the space.

Definition 2: CA Vector Field is a scalar field with a vector associated to each point in the space; the vector field defines the gradient of these scalar values which are RSSI values. The gradient has the direction to the greatest value of RSSI in the field, which is the center where the AP is positioned. It means, if the gradient has the opposite direction, it will be a negative value as in Figure 3.1.

The gradient can be a function of other variables like the velocity (it is a function of time). This leads to define the gradient of RSSI with respect to time (time is needed to predict the next connection state of MC).

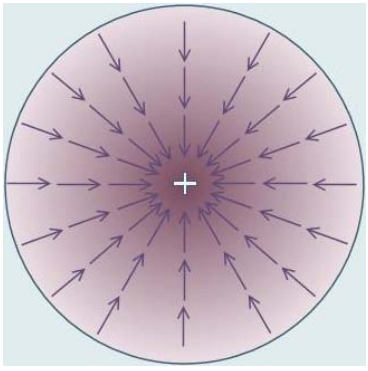

Figure 3.1: CA scalar field

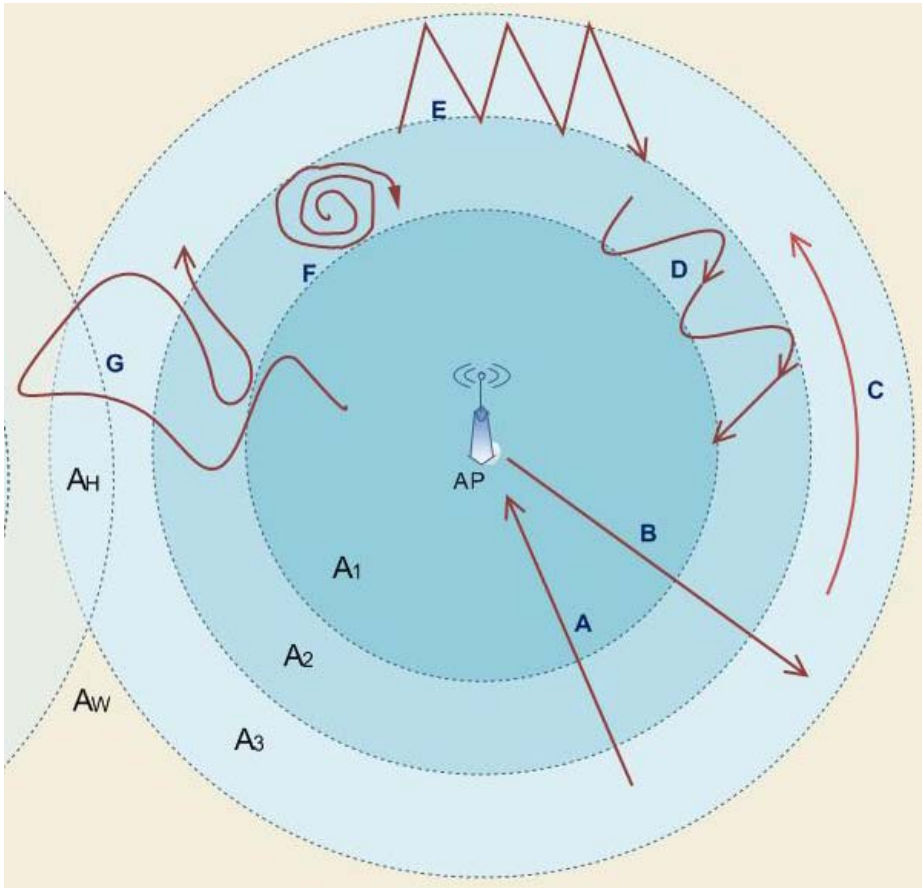

Figure 3.2: CA vector field and RM classes

Definition 3: Regular Movement (*RM*) is defined if the absolute value of RSSI gradient is constant along the time of this movement, and MC speed is constant. Global contribution of a RM can be done following the direction of the *CA Vector Field* (forward to the AP position, shape A) or on the contrary (backward to the AP position, shape B). There are different classes of RM (Figure 3.2): Straight line (A, B), *Sine* (*SIN*) or *Cosine* (*COS*), Zigzag, Spiral (D, E, F)... in each class MC can cross one or more times the limits of a particular zone [88].

Definition 4: Irregular Movement (*IM*) is defined when the absolute value of RSSI gradient is not constant. This means that the speed and direction of MC are not constant. Likewise, its movement has not a known regular shape (G).

3.3.2 The RSSI Gradient Predictor

Predicting the next MC connection state is crucial for any protocol to solve the problem of disrupting multimedia services during disconnections. Predicting the next state allows the MC to take actions in advance especially if the time of disconnection is predicted.

The MC is considered moving at constant speed and RM, measuring *n* values of $\Omega(d_{MC})$ (as a sample set) within an interval of time t, then the vector $\vec{x} = [x_0, x_1, ..., x_n]$ represents these values, where x_0 was measured at time t_0 and x_n was measured at time t. ∇x_k is the instant gradient of $\Omega(d_{MC})$ at any time:

$$\nabla x_k = x_k - x_{k-1}$$

Then, the gradient vector is:

$$\nabla \vec{x} = [\nabla x_1, \nabla x_2, ..., \nabla x_n]$$

And the instant gradient with respect to time at any time:

$$\nabla(x_k)_t = \frac{\nabla x_k}{\Delta t_k}, \text{ where: } \Delta t_k = t_k - t_{k-1}$$

The average gradient, with respect to time, after an interval of time equal t is:

$$\nabla(x_n)_t = \frac{\nabla x_n}{\Delta t}, \text{ where } \nabla x_n = x_n - x_0 \text{ and } \Delta t = t - t_0.$$

If x_n was unknown and all the other variables were known, it could be calculated from the equation:

$$x_n = \nabla(x_n)_t \times \Delta t + x_0$$

To calculate x at any time t_k, the same equation can be used changing the interval of time where this value of x is called the predicted value $\hat{x}_k^-$:

$$\hat{x}_k^- = (\nabla(x_n)_t \times \Delta t) + x_0, \text{ where } \Delta t = t_k - t_0$$

It is correct that the average gradient equals the average of the summation of all instants gradient in the same interval of time in case of RM, where MC moves at constant speed and direction, accordingly:

$$\nabla(x_n)_t = \frac{1}{n}\sum_{k=1}^{n} \nabla(x_k)_t$$

The predicted value of x will be:

$$\hat{x}_k^- = (\nabla(x_n)_t \times \Delta t) + x_0$$

$$\hat{x}_k^- = x_0 + \frac{\Delta t}{n}\sum_{k=1}^{n}\nabla(x_k)_t$$

$$\hat{x}_k^- = x_0 + \frac{(t_k - t_0)}{n}\sum_{k=1}^{n}\left(\frac{x_k - x_{k-1}}{t_k - t_{k-1}}\right)$$

Any $\Omega(d_{MC})$ value can be estimated using this formula, at the exact requested time. Using Table 3.1, the zone where MC will be connected can be easily estimated.

Table 3.1: RSSI values and areas estimation

$\hat{x}_k^-$	**Area**
$100\% \geq \hat{x}_k^- > 60\%$	A_1
$60\% \geq \hat{x}_k^- > 40\%$	A_2
$40\% \geq \hat{x}_k^- \geq 20\%$	A_3
$20\% > \hat{x}_k^-$	A_W

The RSSI Gradient Predictor does not behave well in a non straight line RM. The predictor was tested on a set of synthetic movements and gave good prediction results with movements similar to the ones following shape A due to its linearity (Figure 3.3). It was a trouble with different directions because the predictor can only detect the global contribution of the $\Omega(d_{MC})$ gradient. For example in Figure 3.4 (spiral movement, shape F), when the movement detection started at 2 s and finished at 23 s, the predictor did not detect the instant variation. Still, it worked well; it predicted the final value of $\Omega(d_{MC})$.

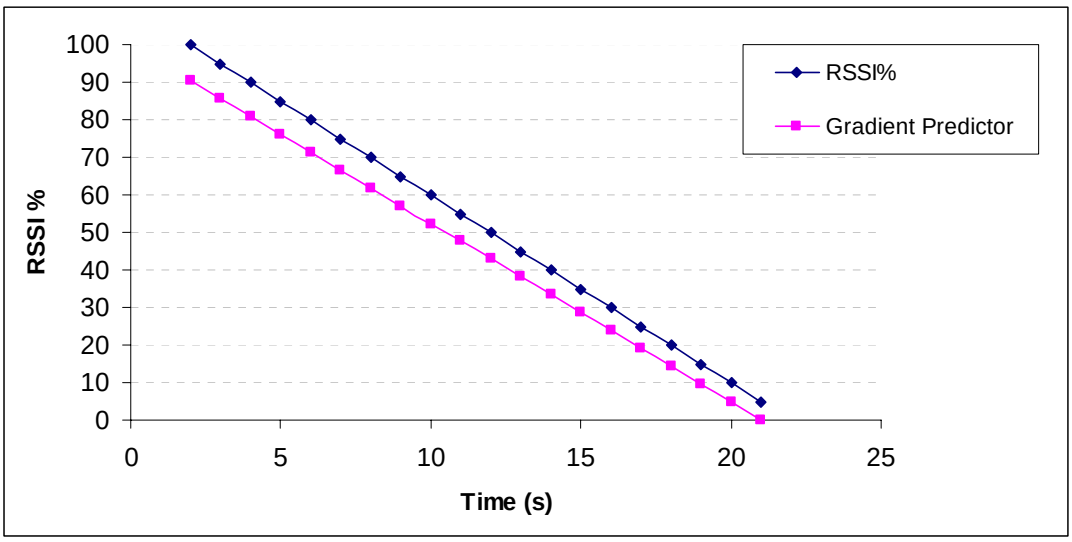

Figure 3.3: Prediction result of synthetic values when MC moves as shape A

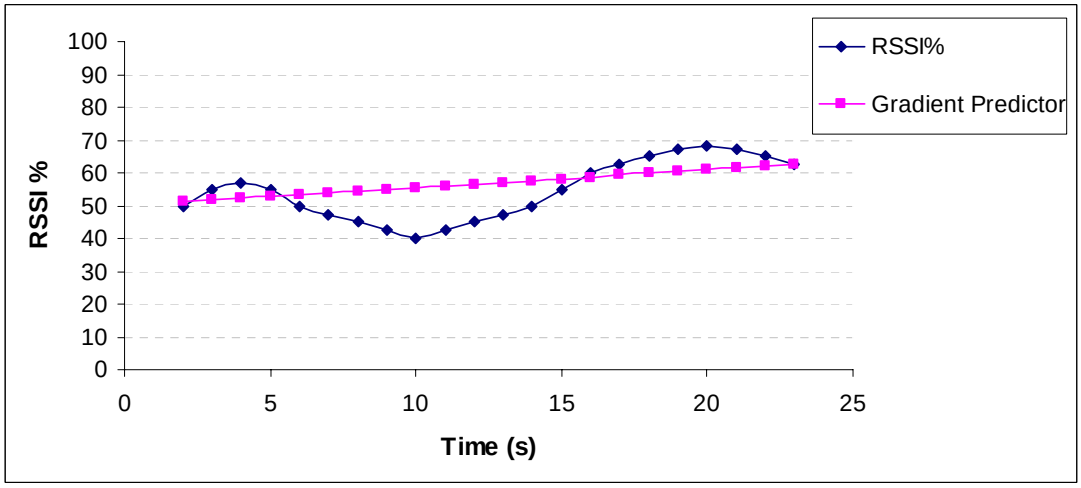

Figure 3.4: Prediction result of synthetic values when MC moves as shape F

3.3.3 The RSSI Gradient Filter

In some cases, when the RSSI gradient is fluctuating, the formula of Gradient predictor is no longer giving correct estimation for all movement shapes. Thus, it is important to take into account the error of estimation between the current predicted value and the previous measured value. This error is calculated using the standard deviation by the equation:

$$\sigma(x_{k-1}, \hat{x}_k^-) = \sqrt{\frac{1}{2}(x_{k-1} - \hat{x}_k^-)^2}$$

By adding or subtracting this standard deviation to the predicted value, the estimated values of $\Omega(d_{MC})$ will be:

$$\hat{x}_k = \hat{x}_k^- \pm \sigma(x_{k-1}, \hat{x}_k^-)$$

In each case of x, adding or subtracting the value of the standard deviation must be decided. This is solved by multiplying the standard deviation by the SIGN function (SIGN of the difference between the two inputs of the standard deviation), because the SIGN function gives 1 in case of positive input and -1 in case of negative.

The formula of the estimated value will be:

$$\hat{x}_k = \hat{x}_k^- + SIGN\,(x_{k-1} - \hat{x}_k^-) \cdot \sigma(x_{k-1}, \hat{x}_k^-)$$

When applying this formula to $\Omega(d_{MC})$ values, which include zero values as holes, the formula does not estimate correct value. One solution to correct the formula consists of two steps:

- To find a condition that detects the zero values. It can be solved by multiplying the previous measured value by the current value; if the result is zero, one of them must be zero.
- Removing the effect of the error part from the formula as the first condition is achieved without changing the original value.
- To achieve that, multiplying by zero is required if the first condition is achieved; otherwise, multiplying by 1. The SIGN function solves this:

$$SIGN\,(x_{k-1} \cdot x_k)^2 = \begin{cases} 0 \\ 1 \end{cases}$$

The final formula of the filtered predicted (estimated) value or the new Gradient Filter is:

$$\boxed{\hat{x}_k = \hat{x}_k^- + SIGN(x_{k-1} - \hat{x}_k^-) \cdot \sigma(x_{k-1}, \hat{x}_k^-) \cdot SIGN(x_{k-1} \cdot x_k)^2}$$

3.3.4 The RSSI Gradient Filter Synthetic Test and Performance Evaluation

The detailed results of testing GM, Kalman filter and RSSI Gradient Filter on some synthetic proposed values of $\Omega(d_{MC})$ are in the attached CD, where MC moved in RM at constant speed and irregular movement, these values were supposed to be measured every 1 second to have $k = t$ (Figure 3.5).

For the Kalman filter we considered $P_{k-1} = 1$ as an initial state which arrives 2.4 after 20 iterations in all cases; moreover, other values were tested and gave the same

results in all cases, while in GM and Gradient Filter there was not any initial consideration affecting the results.

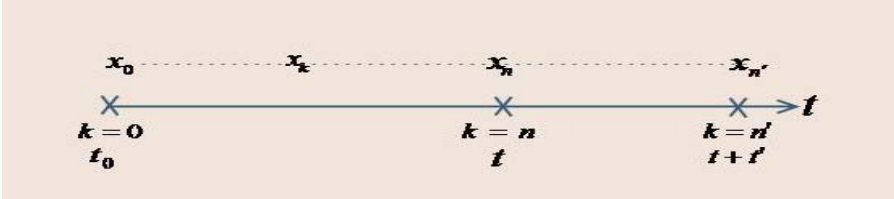

Figure 3.5: Relation between Time t and k

To clarify the results, the performance was evaluated by taking five examples of RM (shapes A-F) and one IM (shape G) shown in Figure 3.6. Results of testing the supposed synthetic values of these shapes are shown in the following figures and discussed considering holes of coverage.

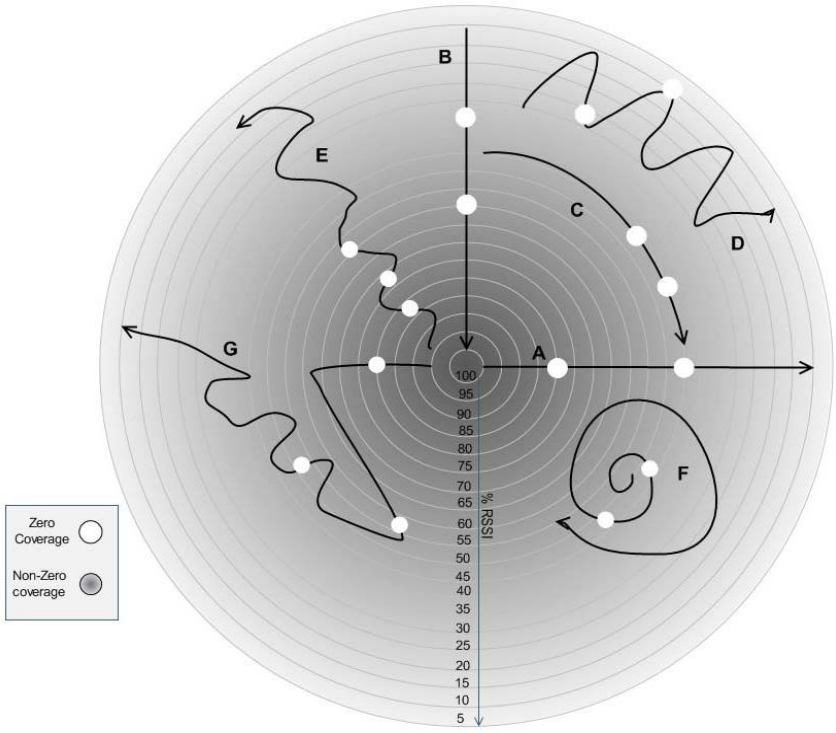

Figure 3.6: Examples of MC movements

Figure 3.7 represents the proposed synthetic values of the straight line movement far from the AP (decreasing values), it is clear how the Gradient Filter is a good predictor, it gave a very closed values to $\Omega(d_{MC})$, at time 5 s and 12 s, it detected the holes in addition it filtered them. Likewise, the Kalman filter detected these holes with high variation in the $\Omega(d_{MC})$, while the GM did not.

Figure 3.8 shows the proposed synthetic values of the straight line movement toward the AP (increasing values). The Gradient Filter performance is very good especially holes detection, whereas the Kalman filter gave bad values with holes detection at 6 and 11 seconds, while GM did not detect these holes. The GM predicted results higher than the $\Omega(d_{MC})$ in the last part of movement.

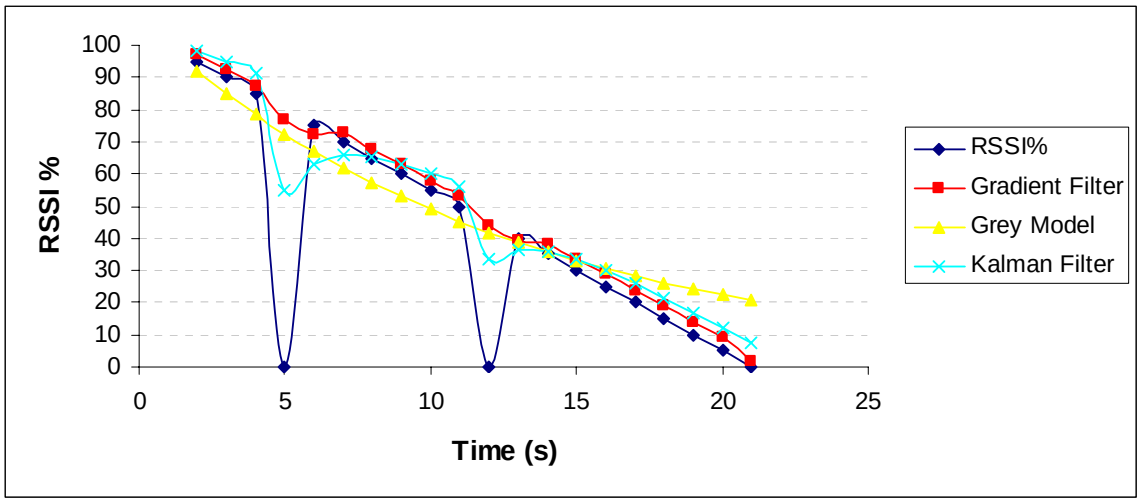

Figure 3.7: Filters results on synthetic RSSI values of shape A

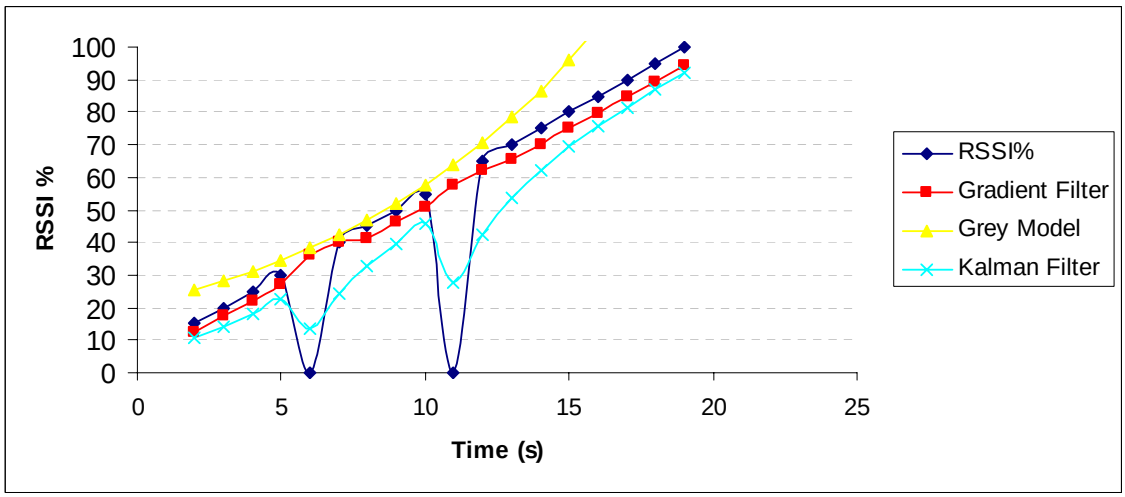

Figure 3.8: Filters results on synthetic RSSI values of shape B

The special case represented in Figure 3.9 shows the movement at constant speed around the AP (circular shape), the GM did not work because $a = 0$ in this case; however, the problem of holes affected the results of Kalman filter with high variation, whereas the Gradient Filter demonstrated the best results.

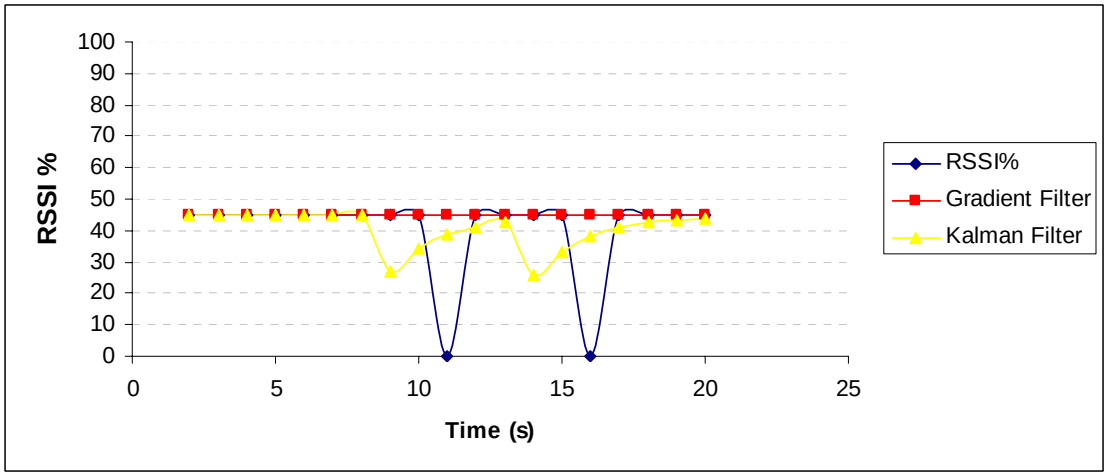

Figure 3.9: Filters results on synthetic RSSI values of shape C

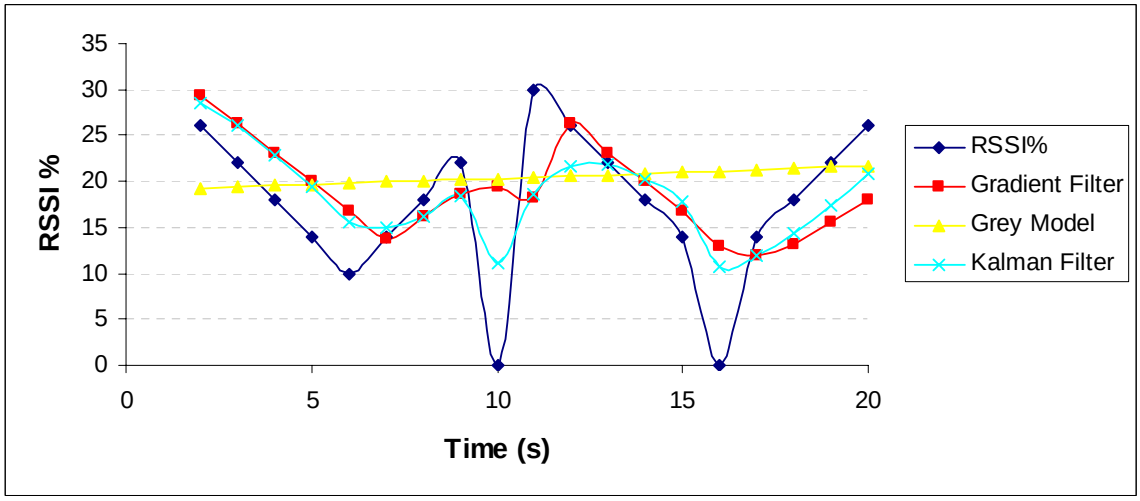

Figure 3.10: Filters results on synthetic RSSI values of shape D

Different case of movement is represented in Figure 3.10, MC moved with zigzag shape around the AP, this movement combined many straight lines movements increasing and decreasing. The presence of holes made the prediction very difficult. The instant variation in $\Omega(d_{MC})$ could not be detected by GM because it is a linear model, it can just predict the final state, whereas the Kalman filter worked good with this class of movement except for holes detection. The Kalman filter behaved differently when it detected the holes found at 10 s and at 16 s, in the first one it gave high variation, while in the second it was good. The Gradient Filter was good and gave the same results, as the Kalman filter in some moments during movement.

In shape E (Figure 3.11), MC moved in zigzag motion going far from the AP, in general these values must be the same as the straight line of shape A but with low decreasing speed. GM had the same performance, it did not detect holes, Kalman filter detected holes with high variation in the $\Omega(d_{MC})$ value and the Gradient Filter performance was very good.

The spiral motion (Figure 3.12) shows increasing and decreasing values in very small range all the time, filters behavior was the same except for the Gradient Filter at 13 s where it detected holes with results higher than the expected values.

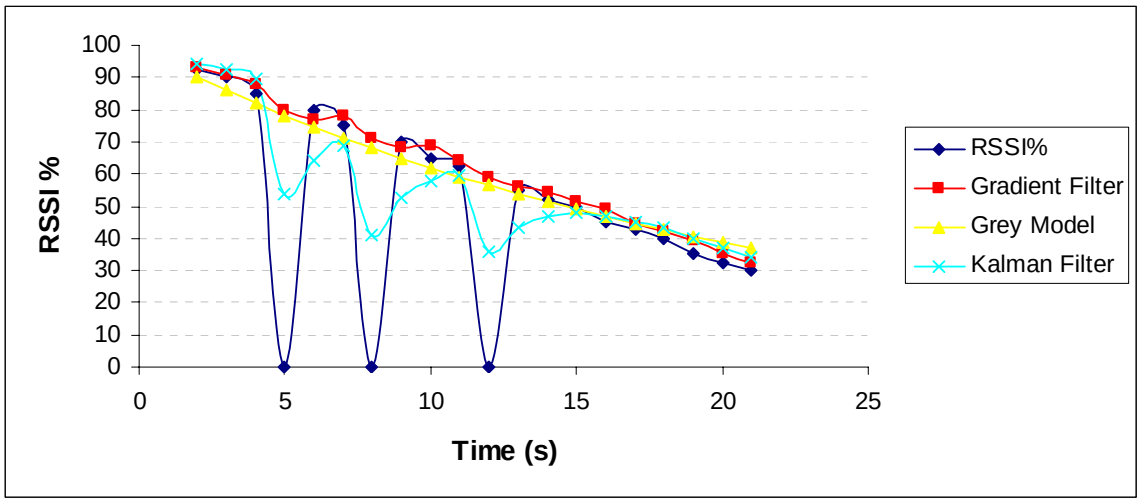

Figure 3.11: Filters results on synthetic RSSI values of shape E

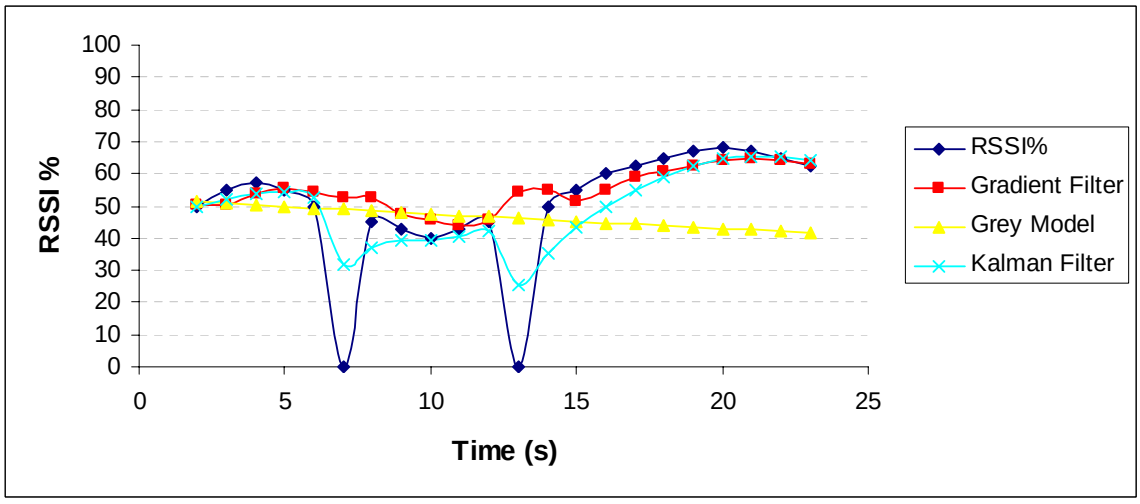

Figure 3.12: Filters results on synthetic RSSI values of shape F

The last case of movement is the IM (Figure 3.13) considered as the complex one, the IM in general consists of many parts, and each part should be a regular motion.

In some moments it seems as straight line, others as SIN or COS…etc. Also in this case, the GM could not detect the instant variation and the holes, while the Kalman filter gave a good values; however, it showed high variation with holes, and the Gradient Filter was not very good in the last hole at second 26. this special case represents the non periodic pattern with holes.

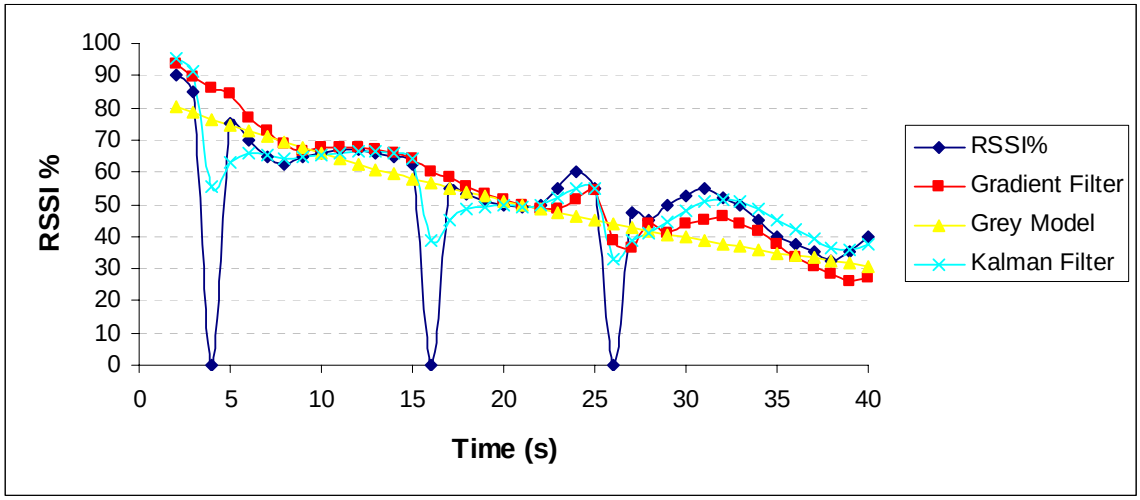

Figure 3.13: Filters results on synthetic RSSI values of shape G

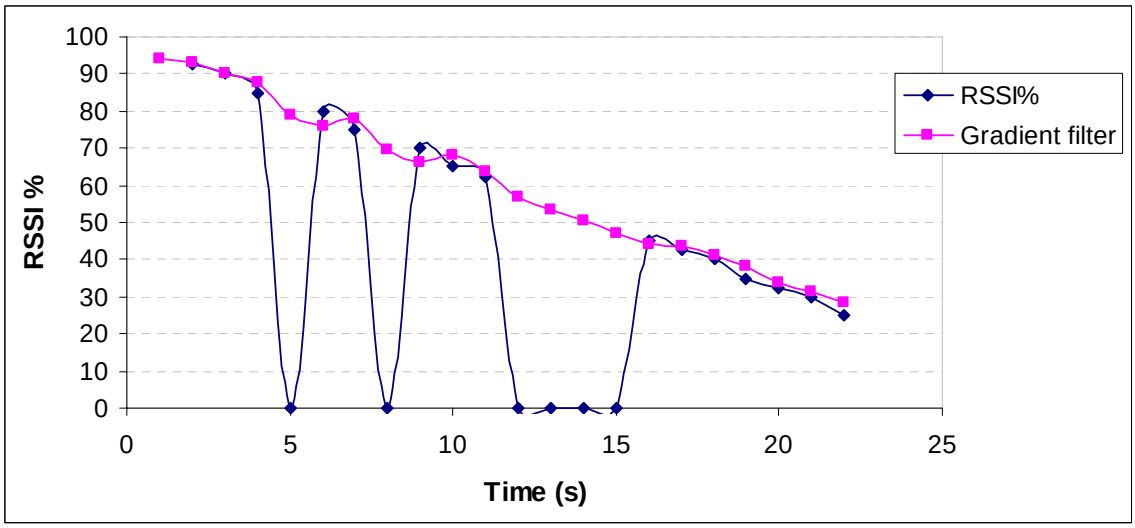

Figure 3.14: Gradient Filter output in the presence of continuous zeros

In Table 3.2, a qualitative evaluation for the three filters performance is shown; numbers 1, 2, 3 and 4 are used as an indicator of each filter. (1) is the best filter, (2) is good, (3) is the worst filter and (4) means the filter does not work. In the same table, from precision of prediction we understand how the filter output is close to the synthetic value of $\Omega(d_{MC})$.

Table 3.2 displays the best results for the RSSI Gradient Filter in all situations of holes detection and support, the Gradient Filter detected the zero value (hole) of $\Omega(d_{MC})$ except a light variation as in Figure 3.14 (this zero does not indicate a constant out of coverage state), in addition of best prediction precision in all cases. The Kalman filter gave good prediction accuracy and detected holes in most of these cases (Figure 3.10, Figure 3.12 and Figure 3.13); however, it could not filter them since it shows a high variation, which could indicate an out of coverage state even if the terminal was in a CA (Figure 3.11 and Figure 3.8). The GM did not detect and support holes in addition to its prediction precision, it is the worst (Figure 3.7 and Figure 3.8). It is important to note that GM did not work in case of constant $\Omega(d_{MC})$ gradient all the time, because $a = 0$; consequently, u/a could not be calculated in the formula (Figure 3.9).

To outline the previously introduced ideas, the Gradient Predictor was developed to predict the next MC state based on the RSSI Gradient in case of regular movement, and then it was improved to the Gradient Filter to solve the problem of holes by filtering them. The predictor and filter were compared to other models producing good results and performance.

Table 3.2: Filters evaluation

Shape	Filter	Holes detection and support	Precision of Prediction
A	Kalman	3	2
	GM	4	3
	Gradient	1	1
B	Kalman	3	2
	GM	4	3
	Gradient	1	1
C	Kalman	3	1
	GM	-	-
	Gradient	1	1
D	Kalman	2	2
	GM	4	3
	Gradient	1	1
E	Kalman	3	2
	GM	4	3
	Gradient	1	1
F	Kalman	3	2
	GM	4	3
	Gradient	1	1
G	Kalman	3	1
	GM	4	3
	Gradient	1	2

3.4 The RSSI Gradient Filter Experimental Test

The main objective of this experiment was the Gradient Filter performance evaluation on $\Omega(d_{MC})$ measured values from a WiFi AP. Likewise, studying the behavior of CA and signal behavior in different surrounding conditions.

3.4.1 Experiment Settings and Equipments Used

The football playground at the *University of Las Palmas de Gran Canaria* (*ULPGC*) was chosen to be the open area to do the experiment, where there were no obstacles or buildings effects on the signal.

The straight line was the shape of MC movement at constant speed 1 mps. Eight directions are considered on the playground (Figure 3.15), in each direction MC scanned the signal 4 times backward (far from) the AP and 4 times forward to the AP. In total, 192 groups of values were measured in 3 days. The directions shown in Figure 3.15 are as follow:

1. *GS-A*: Goal Soccer A.
2. *GS-B*: Goal Soccer B.
3. *F*: Front.
4. *S*: Seats.
5. *F-GS-A*: Diagonal direction between the GS-A and F.
6. *F-GS-B*: Diagonal direction between the GS-B and F.
7. *S-GS-A*: Diagonal direction between the GS-A and S.
8. *S-GS-B*: Diagonal direction between the GS-B and S.
9. *FOR*: Forward the AP.
10. *BAC*: Backward (far from) the AP.

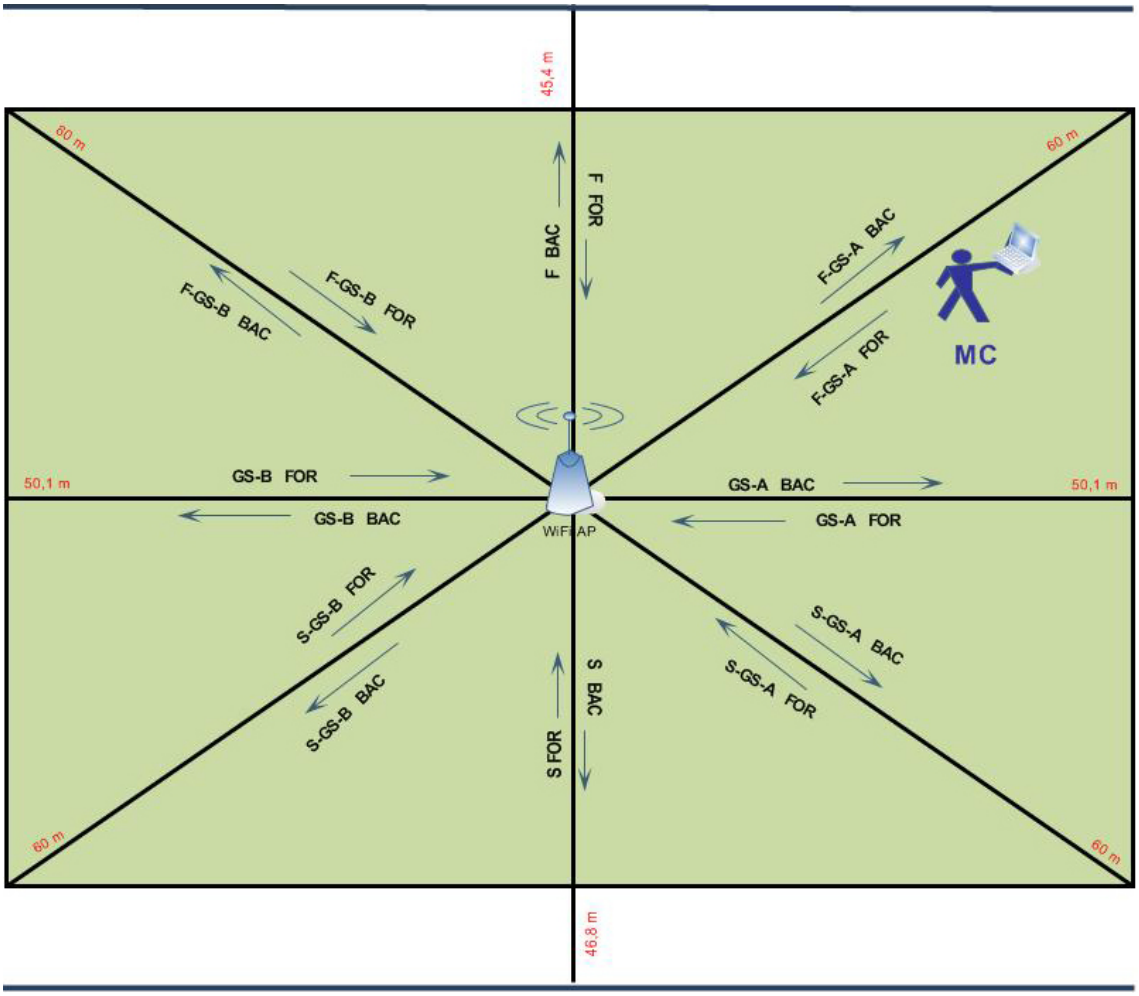

Figure 3.15: Football playground of ULPGC

The measurements were done in different hours each day, the weather conditions were natural with alternating sunny and cloudy days; all these considerations are explained in Tables 5.3, 5.4 and 5.5.

The AP used was *ANSONIC USB wireless adapter* (*model number: AN-W541USB*) which works as an AP or wireless adapter; it can be connected to any laptop in the center of the football playground. The MC was a laptop *Sony VAIO PCG-TR5MP* with WNIC *Intel*(*R*) *PRO/Wireless 2200BG Network Connection* (*model number: WM3B2200BG*). The *Network Stumbler Version 0.4.0* software was installed on laptop to scan the signal.

Table 3.3: Considerations of the first day (16/11/2008) of the experiment

CONSIDERATIONS	
Weather	Clear No winds
Sunset	18:08 h.
AP	Placed on 40 cm of height above the ground In the center of the football camp Vertically oriented position to Seats Other 16 AP were discovered in all channels

Table 3.4: Considerations of the second day (30/11/2008) of the experiment

CONSIDERATIONS	
Weather	Partially Cloudy North wind Completely coludy at 15:00 h. Start raining at 15:19 h. after 16:00 h. Partially Cloudy
Sunset	18:05 h.
AP	Placed on 40 cm of height above the ground In the center of the football camp Vertically oriented position to Seats Other 17 APs were discovered in all channels

Table 3.5: Considerations of the third day (07/12/2008) of the experiment

CONSIDERATIONS	
Weather	Partially Cloudy Some winds
Sunset	18:05 h.
AP	Placed on 45 cm of height above the ground In the center of the football camp Vertically oriented position to Seats Other 17 APs were discovered in all channels

3.4.2 Results and Discussion

In *Network Stumbler* [Web-12], the scanning frequency is controlled only by speed controller range between slow and fast, we could not determine exactly the speed of scanning. In the actual scanning results it scanned the signal 2 times each 1 second, and we are interested in scanning frequency 1scan/s, so we calculated the medium of each two measurements.

As there are 192 groups of values, we preferred to calculate the medium of values in the repeated directions of each day, for example, there are 4 times of scanning in the direction SG-A (FOR) in the first day, we calculated the medium of these four values, as a result 2 groups of values are still in each direction for each day, last values in total are reduced to 48 groups (3 days, 8 directions, 2 groups FOR and BAC).

In all figures and tables, *m1* indicates the medium of the first day, *m2* is the medium of second day and *m3* is the medium of the third day.

Comparison between Measured and Synthetic RSSI%

Figure 3.16 shows 3D graph represents the WiFi CA in the football playground, which is clear that the CA is not circular in actual situation, and there are different colored zones classifying the signal strength in CA. Some important differences and similarities between theoretical assumptions and actual situation are extracted from Figure 3.16:

- Different colors appear in the figure represent different zones of CA depending on the RSSI which is similar to my previous assumption where the CA was classified to different zones.
- It is clearly shown how the signal drops to low values in many positions of CA to form holes, this is the same as assumed before.
- The CA is not circular in the actual situation; it can take any shape depending on the surrounding conditions that affect the signal. Theoretically, the CA was considered to be circular in ideal conditions and this may be impossible.
- One important notice is the continuity of each colored zone, the color in some cases is found in distinct places like the blue color, which is caused also by factors that affect on the signal such as reflection.

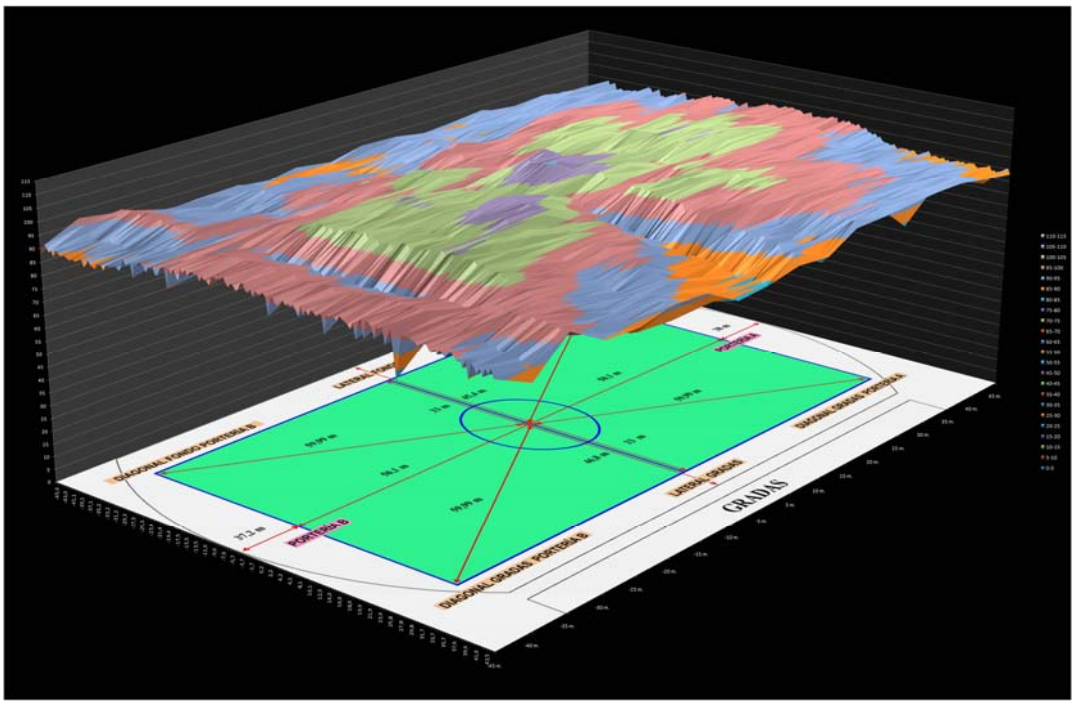

Figure 3.16: RSSI distribution in the CA

Previously, we proposed some synthetic values of $\Omega(d_{MC})$ to evaluate the Gradient Filter compared with other models. After measuring RSSI, a comparison between these synthetic values and the measured ones will be presented.

In Figure 3.17, the pink line represents these synthetic values and the blue line represents measured values *S-GS-A* (*BAC*). Speed in the experiment was 1 mps, whereas it was just assumed to be constant speed in synthetic values, then speed in synthetic case could be very high such as MC moving by a car. It is clear that $\Omega(d_{MC})$ changes quickly in a very small period of time, so MC arrived to the last zone of coverage along the straight line from AP. The general behavior of the signal is the most important in Figure 3.17, they are the same; moreover, in other cases of measurements the signal may have more holes or variations depending on the surrounding conditions.

In previous assumptions, the signal in ideal condition was supposed to be 100% adjacent to the AP. Nevertheless it was different in the actual measurements (80% - 90%). Due to the limited area of the football playground, MC did not arrive to the boundary of CA; consequently, the signal behavior in the boundary zone was not studied.

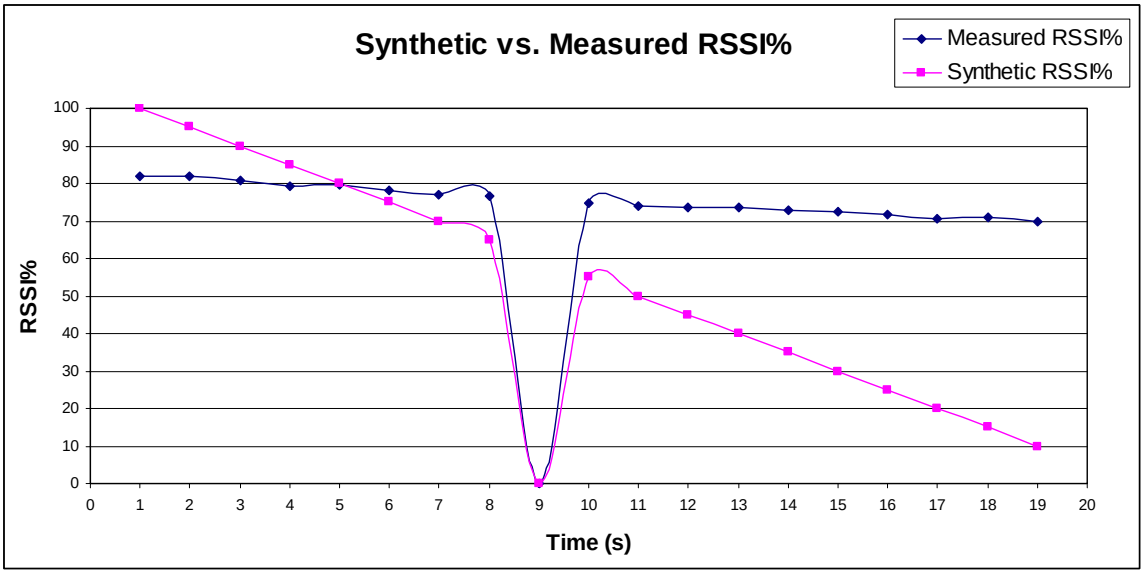

Figure 3.17: Comparison between synthetic & measured RSSI%

Gradient Linearity

Filters and models that were used by other researchers, were linear or exponential, whereas the Gradient Filter is linear; accordingly, studying the linearity of $\Omega(d_{MC})$ gradient is important as indicator for any inaccurate values.

There were variations in the actual values between the three days and in the same day also, because the measured signal was affected by other signals and weather; consequently, it is not precise that relation between signal and distance is linear or exponential. Thus, a range of these values was chosen as sample. Then we put the trend line[1] with R^2 (linear: LIN, and exponential: EXP) in each graph to illustrate how much this line is close to the real values.

[1] ***Trendline****: A graphic representation of trends in data series, such as a line sloping upward to represent increased sales over a period of months. Trendlines are used for the study of problems of prediction, also called regression analysis)*
R-squared value*: R-squared value: A number from 0 to 1 that reveals how closely the estimated values for the trendline correspond to your actual data. A trendline is most reliable when its R-squared value is at or near 1. Also known as the coefficient of determination)[http://office.microsoft.com/en-us/excel/HP100074611033.aspx]*

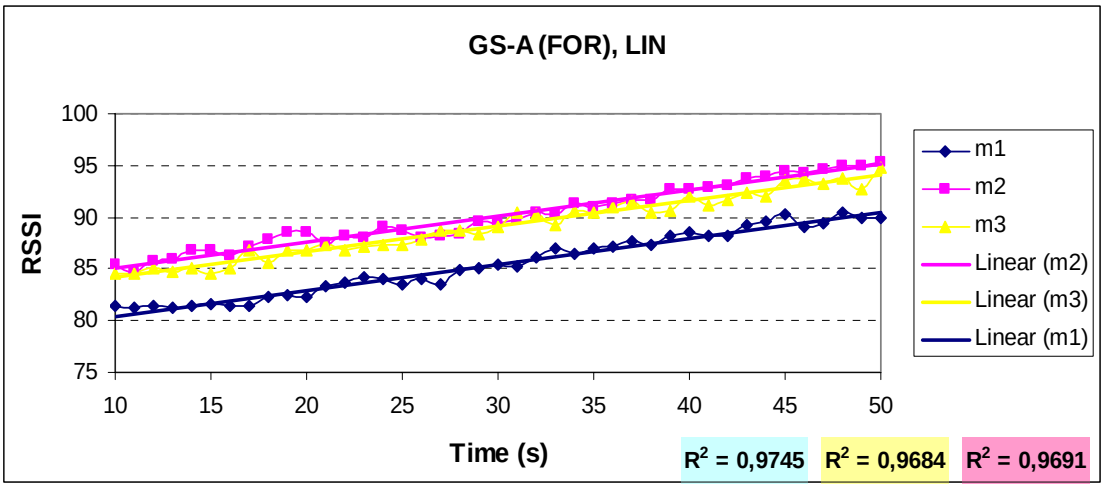

Figure 3.18: Linear trendline of RSSI% in the direction GS-A (FOR)

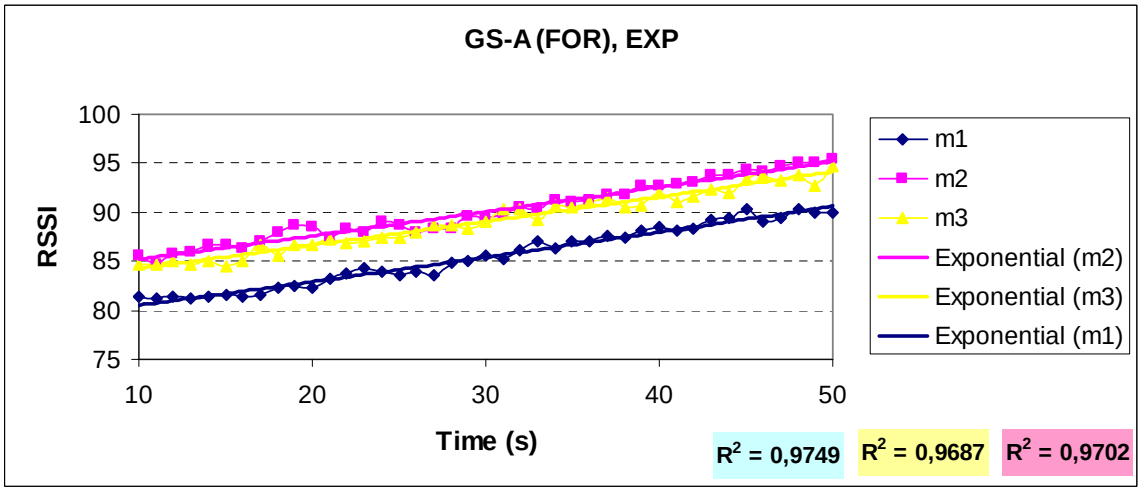

Figure 3.19: Exponential trendline of RSSI% in the direction GS-A (FOR)

Figure 3.18 shows the linear trend line with R^2 for the direction GS-A(FOR) and Figure 3.19 shows the exponential trend line with R^2 for the direction GS-A(FOR). As a comparison, the difference between R^2 for the first day (*m1*) is 0.0004 which is very low value, for *m2* the difference is 0.0011 and for *m3* is 0.0003, it is very small value, so the Gradient Filter can be assumed to be linear or exponential.

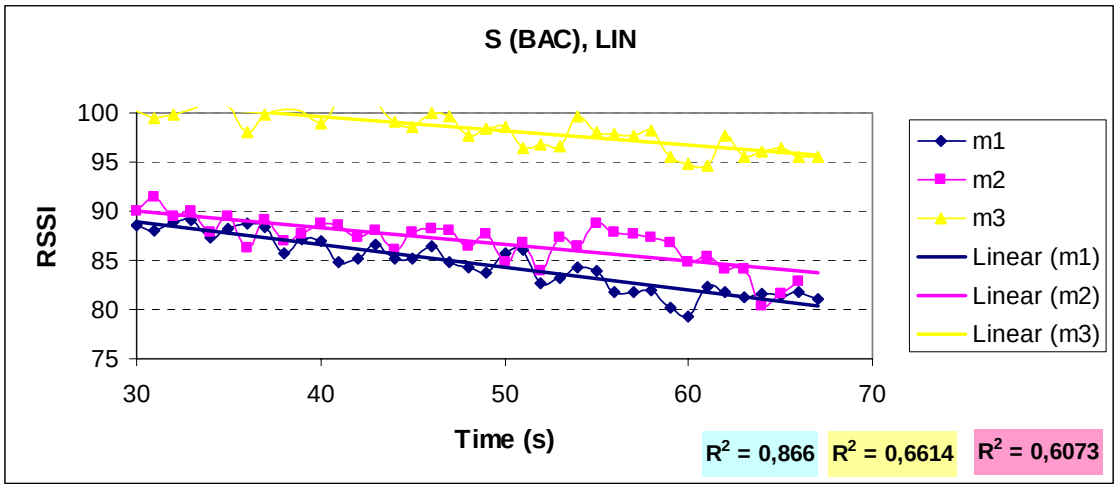

Figure 3.20: Linear trendline of RSSI% in the direction S (BAC)

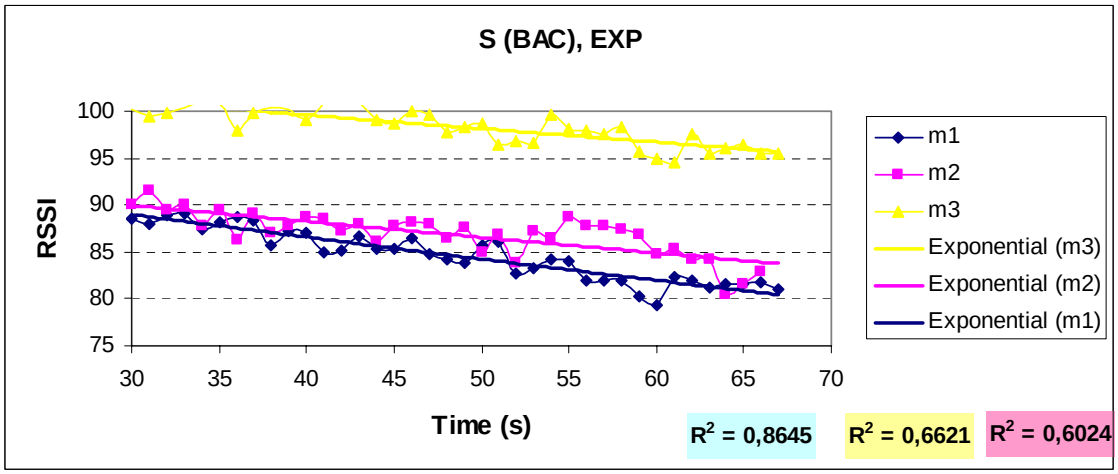

Figure 3.21: Exponential trendline of RSSI% in the direction S (BAC)

The second case is the direction S (BAC) (Figure 3.20 and Figure 3.21). As a comparison, the difference between R^2 for the first day (*m1*) is 0.0015, for *m2* the difference is 0.0049 and for m3 is 0.0007, so the gradient can be assumed to be linear in this case.

All R^2 results are concluded in Table 3.6 and Table 3.7. In this test of linearity we used the original RSSI values exported from the program:

- In the first day: The sky was clear and windless and the signal was linear as exponential, in 7 cases the signal behavior was very close to be linear as in other 7 cases it was very close to be exponential.

- In the second day: The sky was cloudy and there were winds from the north, at 15:20 it was raining but the linearity was clear, because in 10 cases it was very close to be linear and just in 6 cases it was very close to be exponential.
- In the third day: The sky was semi cloudy and there were little winds; however, the exponential relation was clear, because in 4 cases the signal was very close to be linear whereas in 11 cases it was exponential

The evaluation of signal behavior is difficult, because there were not ideal conditions, especially there were 17 AP detected in the same time; therefore, the signal each time demonstrates different behavior. Still, the Gradient Filter could be tested on these actual values.

Table 3.6: Results of the linear and exponential trendlines for all measurements

		GS-A		GS-B		F		S		S-GS-B		S-GS-A		F-GS-B		F-GS-A	
	R^2	LIN	EXP	LIN	EXP	LIN	EXP	LIN	EXP	LIN	EXP	LIN	EXP	LIN	EXP	LIN	EXP
BAC	m1	0,616	0,613	0,950	0,950	0,786	0,788	0,866	0,865	0,795	0,794	0,616	0,614	0,823	0,823	0,758	0,757
	m2	0,780	0,779	0,769	0,767	0,882	0,880	0,607	0,602	0,836	0,833	0,753	0,750	0,803	0,801	0,931	0,931
	m3	0,946	0,947	0,934	0,934	0,706	0,705	0,661	0,662	0,866	0,870	0,942	0,943	0,882	0,885	0,918	0,917
FOR	m1	0,975	0,975	0,975	0,976	0,896	0,895	0,914	0,914	0,956	0,956	0,931	0,933	0,956	0,956	0,970	0,974
	m2	0,969	0,970	0,975	0,976	0,945	0,943	0,917	0,914	0,968	0,970	0,973	0,973	0,973	0,974	0,977	0,979
	m3	0,968	0,969	0,969	0,971	0,945	0,945	0,853	0,852	0,942	0,943	0,954	0,956	0,955	0,955	0,966	0,965

Table 3.7: Comparison between R^2 of the linear and exponential trendlines for all measurements

Number of R^2	First day	Second day	Third day	Total of 48 group
R^2 Linear	7	10	4	21
R^2 Exponential	7	6	11	24
L & E the same	2	0	1	3

3.4.3 Gradient Filter Test

The *Network Stumbler* program exported a data file that contains the signal values as RSSI (an integer in the range 0-255). We used a mapping method to convert these integer values to RSSI% ($\Omega(d_{MC})$) values by taking maximum RSSI value (*RSSI_Max* = 122), and the minimum (*RSSI_Min* =0), which was obtained during all measurements, in order to calculate RSSI% by the formula:

$$\Omega(d_{MC}) = RSSI\% = \frac{RSSI}{(RSSI\_Max - RSSI\_Min)/100}$$

Some figures are presented here to explain the performance of the Gradient Filter.

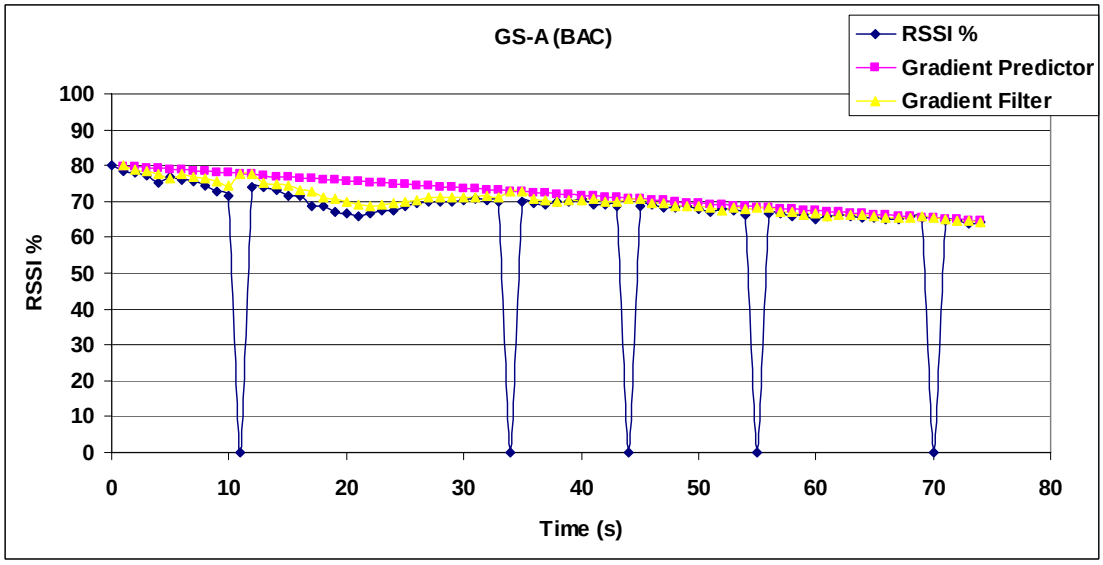

Figure 3.22: Gradient Filter test on RSSI measured values in the direction GS-A (BAC)

In Figure 3.22, holes appeared five times during signal scanning, $\Omega(d_{MC})$ in general did not has a lot of variation, the variation in the first part of the $\Omega(d_{MC})$ appeared in most of all measurements in (BAC) direction and at the end part of (FOR) directions, that assisted the presence of some effects on that zone of CA.

In Figure 3.23, there were a lot of holes and more variations in $\Omega(d_{MC})$ in the first part. The Gradient Filter demonstrated good results in detecting these holes and filtering them; moreover, the results were very close to the actual values. The Gradient

Predictor works as linear predictor, it predicted precisely the last value, while it could not detect instant variations of the signal; therefore, it did not detect holes.

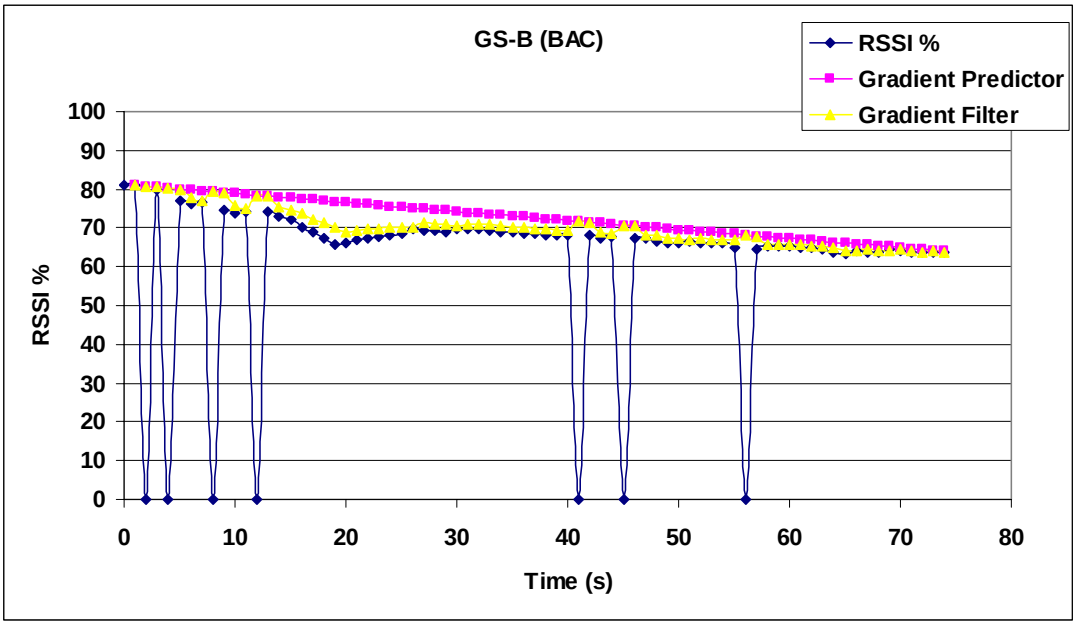

Figure 3.23: Gradient Filter test on RSSI measured values in the direction GS-B (BAC)

In Figure 3.24, the gradient is smooth except the last part that has a small variation, as explained before, these variations appeared lastly in the (FOR) direction. In this case the predictor was very good in predicting until 45 s, because the signal was very smooth and very close to be linear.

Figure 3.25 demonstrates high variation in $\Omega(d_{MC})$ at 88 s; in addition the hole was between the decreasing part and the increasing part. The predictor did not detect this variation and produced higher value, which affected directly the filter leading to unexpected rise in the filtered $\Omega(d_{MC})$ value.

In this study, the Gradient Filter demonstrated better results than other models and filters in detecting and filtering holes. Also the predictor produced good results in predicting the last $\Omega(d_{MC})$ value as the linear behavior was illustrated.

The RSSI Gradient Predictor and Filter was the first part of our protocol, it is responsible for filtering the holes and enhance the signal, in addition to predict the next MC state. Whereas the second part of our protocol is the buffer management and speed control technique, to keep the MCB and BSB filled usually, which offer video frames

during short disconnections that could not be filtered, this part will be specified and described in the next chapter using the *SDL*.

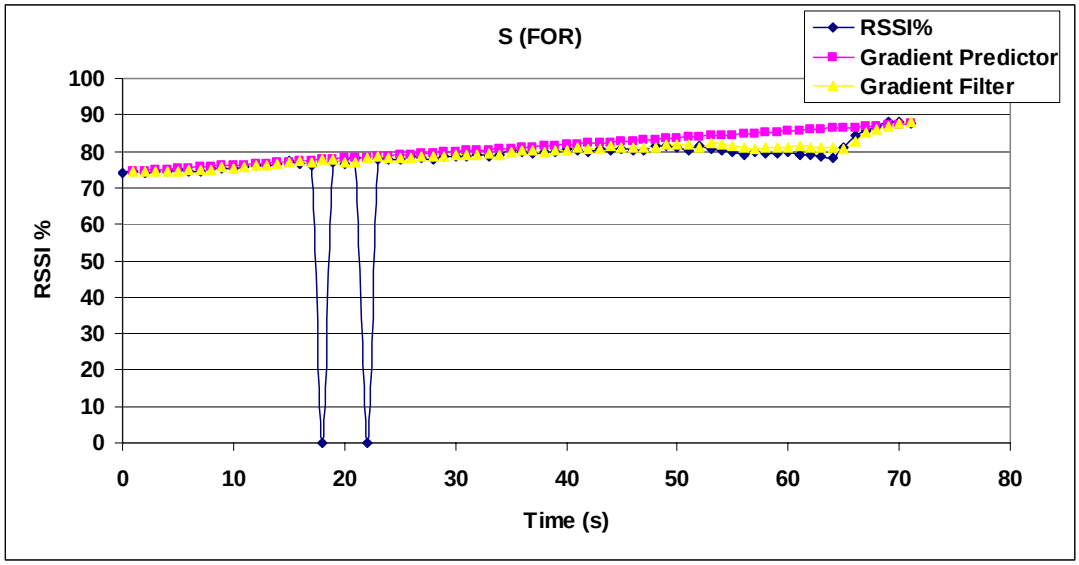

Figure 3.24: Gradient Filter test on RSSI measured values in the direction S (FOR)

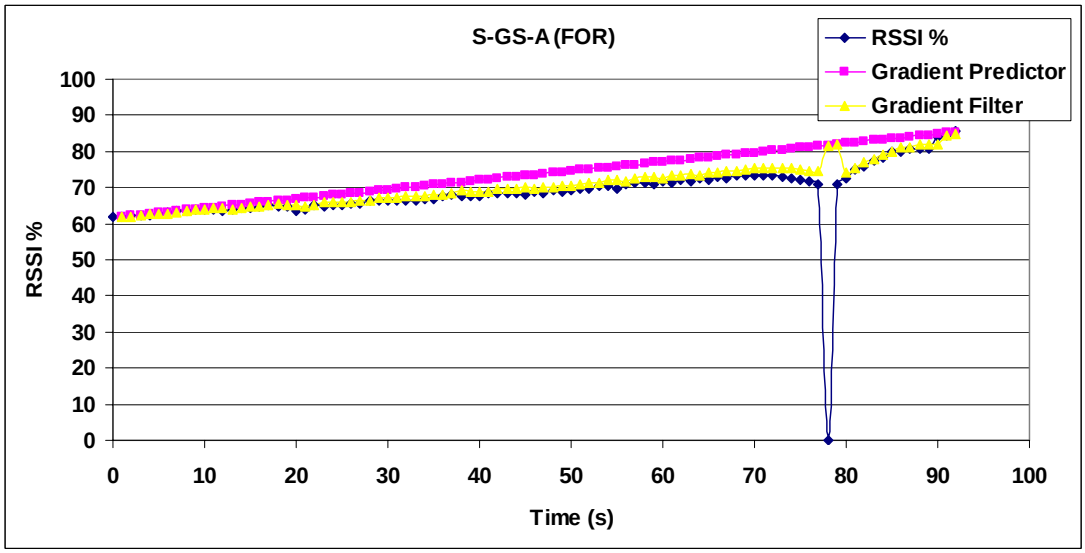

Figure 3.25: Gradient Filter test on RSSI measured values in the direction S-GS-A (FOR)

CHAPTER 4

THE SDL SPECIFICATION FOR THE BUFFER MANAGEMENT TECHNIQUE

Our protocol provides solution to mitigate the video streaming loss by offering sufficient amount of buffered video in MCB before disconnection. This was achieved by managing the MCB and BSB controlling the video transmission speed. The Cinderella *SDL* was used to verify the possibility of controlling these buffers by exchanging messages between MC, AP and BS. Likewise, a simple monitor was designed to show the buffered video changes.

4.1 Network Structure and Mobility Conditions

The network which is considered for the the protocol combines infrastructure of two WiFi cells, where the APs are connected to a WiMAX BS and each AP has two WNICs: One for the WiFi cell and the other to communicate with the BS. The BS is connected to a wired backbone (wired Internet) where a VoD server streams multimedia packets to MC which is connected to the WiFi AP. The server and the client use TCP and UDP for signaling and multimedia data communication respectively, other multimedia protocols like RTSP for video communications can be used.

The MC is supposed to be outdoor and no important obstacles are present in the surrounding area, ignoring the presence of complex buildings, cars or other elements that provoke strong interferences in wireless channels. Under these assumptions, the wireless channel behavior is not strongly chaotic, because interferences and path loss conditions are moderated. Figure 4.1 represents the above assumptions where the CAs of two WiFi APs are overlapped to form the handover area.

It is important for our technique to know how MC is moving in the CA considering the random walk mobility model based [92]. Most of researchers choose a special case of mobility to be studied, because it is a challenge to consider all mobility situations; consequently, we should take into account two important mobility factors:

- *Constant terminal speed*: MC is supposed to move at constant speed, the speed which is used to calculate the time or the distance in a limited area with regular motions, this facilitates predicting disconnection time and estimating the video size required for this period.
- *Movement kinds*: MC is assumed to move in regular motion in the CA of a WiFi AP (as supposed in chapter 2), some regular motions are considered such as: Straight lines (A & B), SIN or COS (D), ZigZag (E), Spiral (F) or circular (C) as shown in Figure 4.2. These kinds of movements give us an idea about the distribution of RSSI and its relation with MC movement; thus, obtaining a mathematical relation could predict the anticipated values of RSSI.

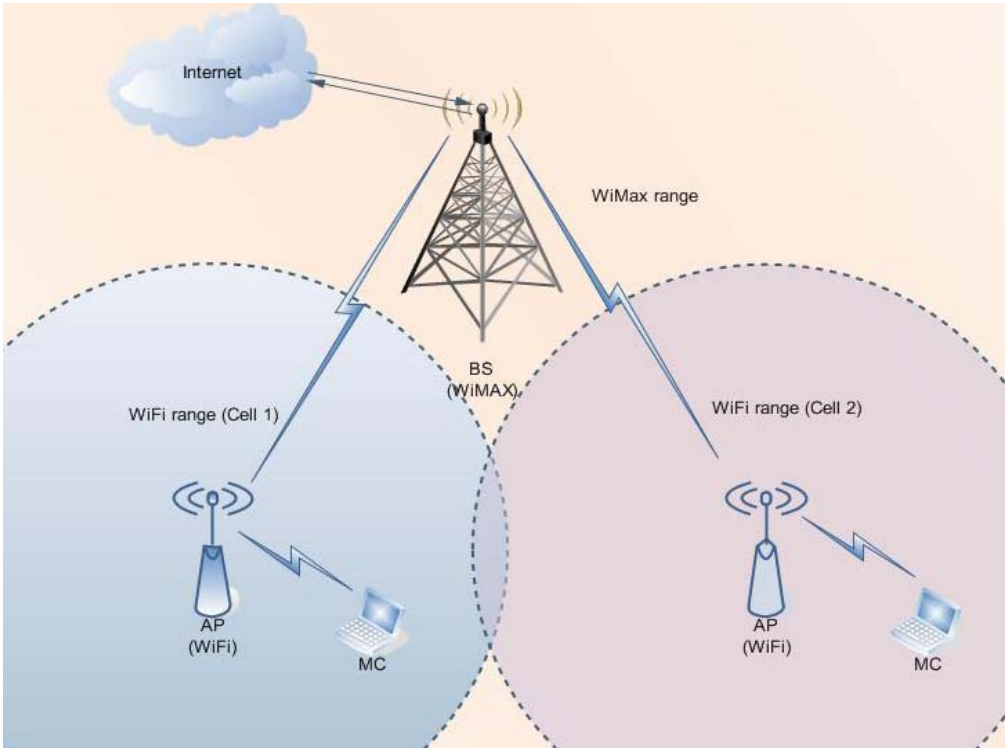

Figure 4.1: The proposed network architecture

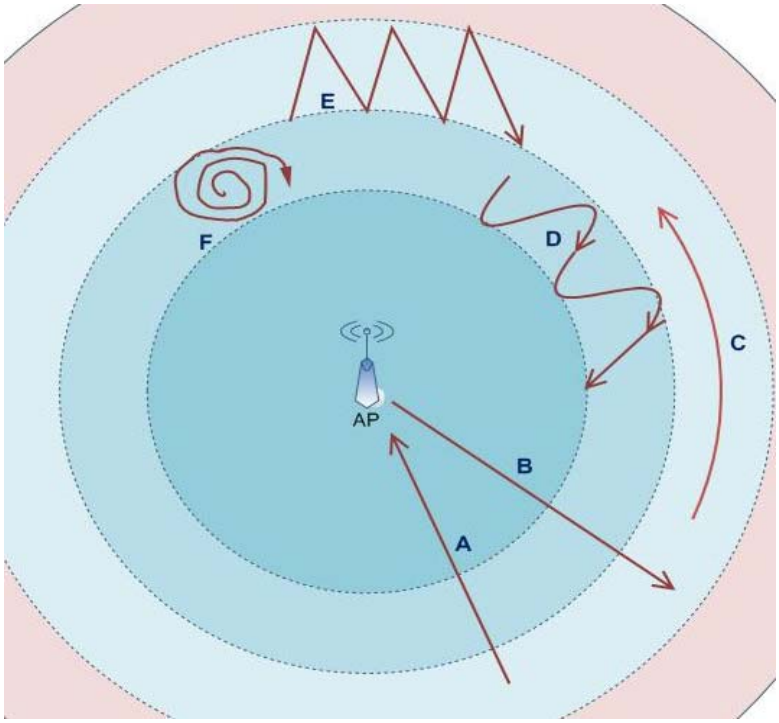

Figure 4.2: Regular motion shapes

4.2 State Diagram for Mobile Client Movements

While a particular MC is moving inside the CA of WiFi AP, or crossing from its CA to another one, it could disconnect due to different situations:

- MC is in A_H, connection could be lost when MC transfers its connection from the associated AP to another one with better signal strength.
- MC is in A_W (the black area) and the WiFi connection is lost. In this case, it can reconnect to the previous or to a new one.
- MC is passing through a hole, sudden disconnection occurs due to obstacles.

In all cases, receiving video frames is interrupted for a moment; furthermore, video frames could be lost in the way before reaching the MC, and this problem is solved in this work by the buffer management and transmission speed control technique. In this chapter we present a specification for the transmission speed control and buffer management part. More details about simulating the complete protocol including the prediction and filtering technique will be presented in chapter 5.

4.2.1 Description of the State Diagram

Let us suppose a MC moving at constant speed v inside the CA of a WiFi AP. Accordingly, an assumed MC's state $S(t)$ [1] could be defined considering the previous definitions of the CA as:

$$S(t) = A_x, \text{ where } x = 1, 2, 3, \text{H or W.}$$

The instantiation of A_x is done by the following inequalities:

$$\text{If } 100 \geq \Omega(d_{MC}) > 60 \rightarrow x = 1, \text{ then } S(t) = A_1.$$

$$\text{If } 60 \geq \Omega(d_{MC}) > 40 \rightarrow x = 2, \text{ then } S(t) = A_2.$$

$$\text{If } 40 \geq \Omega(d_{MC}) \geq 20 \rightarrow x = 3, \text{ then } S(t) = A_3.$$

In case that MC detects two signals $\Omega_1(d_{MC})$ and $\Omega_2(d_{MC})$ from AP_1 and AP_2 respectively then:

$$\text{If } (20 \leq \Omega_1(d_{MC}) < RT) \text{ and } (\Omega_2(d_{MC}) \geq 20) \rightarrow x = H, \text{ then } S(t) = A_H.$$

[1] Let us note that we are only interested in the movement of one MC. That is, our formulation is valid for the movement of any MC, but only one. That is the reason we not annotate the name of the MC in the formula $S(t)$.

If $(\Omega_1(d_{MC}) < 20)$ and $(\Omega_2(d_{MC}) < 20) \rightarrow x = W$, then $S(t) = A_W$.

In the state diagram (Figure 4.3), each state represents a coverage zone considering that the MC could only cross to consecutive zones, or it could continue in the same zone. When MC changes the zone, a transition will be generated being used by all entities (BS, AP and MC) to control all buffers and transmission speed. The number of transitions that are generated in 1 s depends on MC speed, in case of moving with very high speed, more transitions could be generated, but some of them could be detected as unexpected transitions. Thus, to avoid any transition problems, MC speed must be specified. The measurements of the experiment (chapter 3) demonstrated that the $\Omega(d_{MC})$ changed 0.5% with human walking speed of 1 mps. Therefore, the gradient $\Delta\Omega(d_{MC})$ should not exceed 5% that is the maximum possible change $\Omega(d_{MC})_{\max}$ to have a transition, accordingly, the speed must be less than or equal to 10 mps (36 kph). Since $RT = 35\%$ and $\Omega(r_2) = 40\%$, then the distance which can be crossed between the two limits to have a transition is very short.

$$\nabla\Omega(d_{MC})_{\max} = \Omega(r_i) - RT = 5\%$$

$$\nabla\Omega(d_{MC}) = 0.5\% \rightarrow v = 1mps$$

$$\nabla\Omega(d_{MC})_{\max} = 5\% \rightarrow 10mps$$

Let $TR(t)$ be a transition generated when MC changes its state from $S(t-1)$ to $S(t)$, then $TR(t)$ can be defined:

$$TR(t) = Cross\,(S(t-1), S(t)) \ldots\ldots\ldots\ldots\ldots\ldots \text{If } S(t-1) \neq S(t)$$

$$TR(t) = Still\_in(S(t)) \ldots\ldots\ldots\ldots\ldots\ldots\ldots \text{If } S(t-1) = S(t)$$

Where $t \geq 1$ because the first transition is generated at $t = 1$ as the MC has two generated states.

Consequently, it is easy to discover the trajectory of MC following its transitions and the duration of each state, and memorizing MC trajectories in a profile could be used to infer future possible movements and disconnections, e.g. an employee probably defines every day the same trajectory from home to work and it could be disconnected in case of passing through a tunnel.

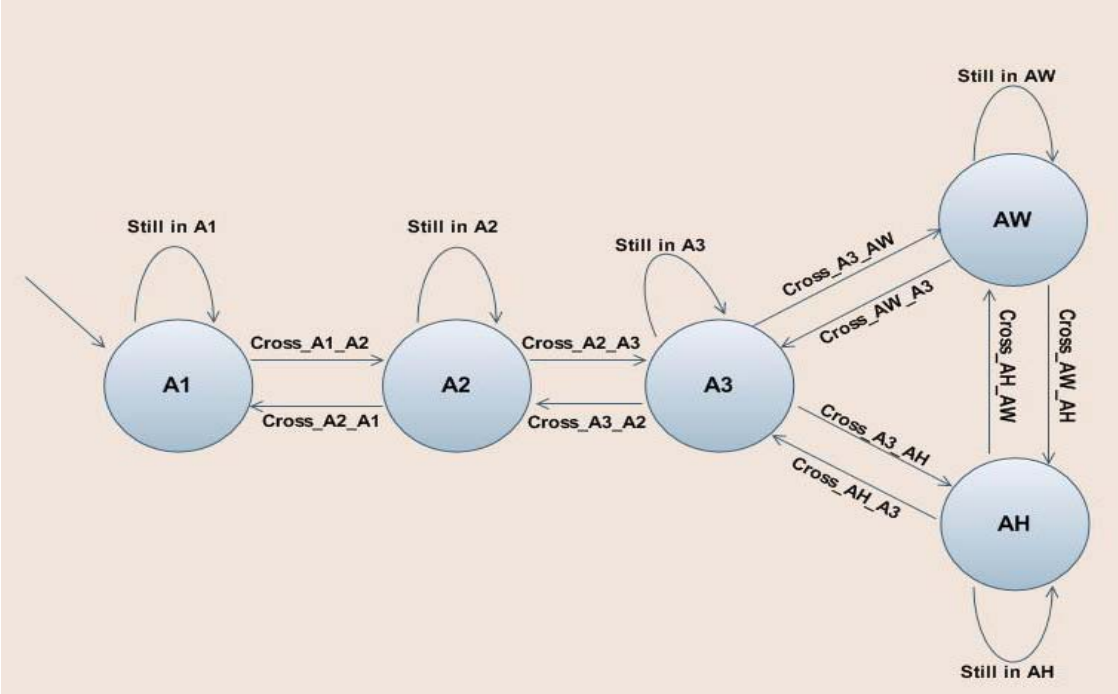

Figure 4.3: State diagram for MC transitions

4.2.2 SDL for The State Diagram

The state diagram was verified using the *Cinderella SDL* application [Web-18], the system in *SDL* consists of a set of different *instances*: *Processes* or *blocks* (the *block* could contain *processes*), where the *process* was chosen to represent an entity, part of entity or a function, all *processes* communicate by exchanging *signals*, each *signal* could carry parameters as inputs, outputs or messages.

- **MC State:**

The state diagram is represented in a process called *state_diagram*, it has an input signal *RSSI*, which takes the values of the *RSSI_1* ($\Omega_1(d_{MC})$) and *RSSI_2* ($\Omega_2(d_{MC})$) from the MC WNIC, *RSSI_1* and *RSSI_2* are the RSSI of *AP_1* and *AP_2* respectively, then it outputs a signal *MC_state* to carry the MC state to the *transition* process. The *transition* process takes the current and the old MC state to generate the signal *MC_transition* that is an input for the *transitions_actions* process (Figure 4.4).

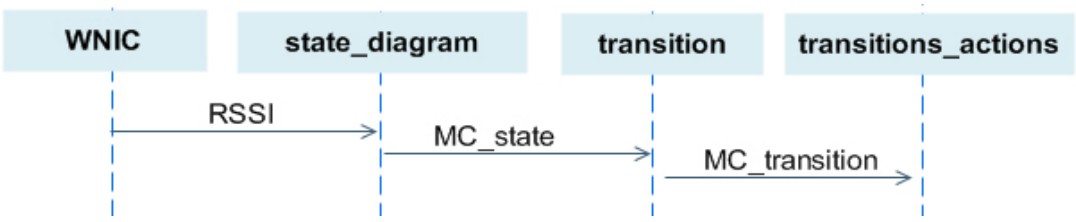

Figure 4.4: Signal exchange to generate MC state and transition

- **Signals Generated by the *state_diagram* Process**

The *state_diagram* process produces four signals: *MC_state*, *handover_process*, *handover* and *state_information*. The main signal is *MC_state*(*state*): *State* (*CharString* data type) could be A_1, A_2, A_3, A_H or A_W. A_H and A_W are special cases that will generate more signals depending on the situation of MC:

- *state* = "A_H", as long as MC is still under the connection of the original AP, only the *MC_state*(*state*) signal will be generated. Unless RSSI of another AP is measured (higher than the RT), it will generate another signal called *handover_process*. When it sends the *handover*(*to_handover_AP*) signal to the new AP (where *to_handover_AP* is the *Service Set Identifier* (*SSID*) of *CharString* data type), the handover will start immediately (Figure 4.5). If the handover succeed, MC could be in the CA of the other AP (after the handover).
- *state* = "A_W", it will generate the signal *message*(*state_information*), *state_information* (*CharString* data type) has one of the following values:

  a. "Very week signal from *AP_1*".

  b. "Very week signal from *AP_2*", in this case it will try to connect to *AP_2*.

  c. "No connection".

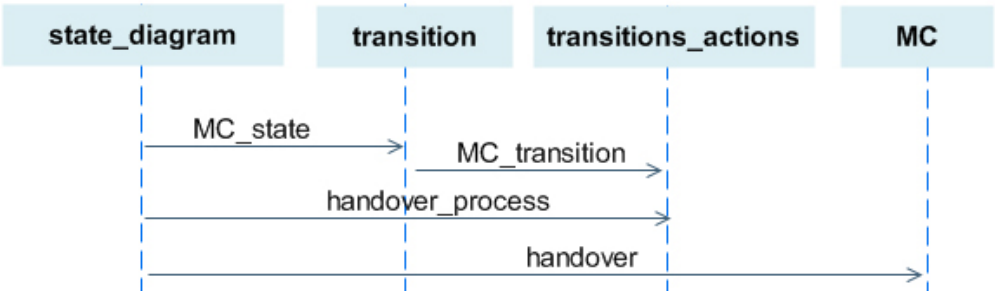

Figure 4.5: Signals generated by *state_diagram* in case of handover

- **MC Transition**

The MC moves in regular motion at constant speed, and the WNIC driver measures some parameters of coverage such as RSSI each 1 s, as soon as it calculates $\Omega(d_{MC})$, the state diagram will discover in which state is the MC. Hence, the transition of MC is generated immediately producing messages to execute some actions, except the *Still_in* transitions (MC is still in the same zone) in which each entity continues doing the same last actions.

A_W and A_H are sensitive states; MC will suffer weak signal in both of them, then it could handover to better CA of another AP in A_H , or it could disconnect totally in A_W, but disconnection does not occur always in the two zones because it could return to the better coverage zone of the same CA. Thus, it is necessary to distinguish between disconnection and connection situations in the same zone.

Other special case: MC moves from A_H to A_W (*Cross_*A_H-A_W) or the contrary, where it could connect to the original AP or another one. Other cases, such as moving from A_H to A_3 (*Cross_*A_H-A_3) or from A_W to A_3 (*Cross_*A_W-A_3) will be described.

- **Signals Generated by the *transition* Process**

MC_transition(*trans*) is the only signal generated by *transition* process (Figure 4.4), it includes the *trans* message (*CharString* data type), it could be of *Cross* type as follows: *Cross_*A_1-A_2, *Cross_*A_2-A_1, *Cross_*A_2-A_3, *Cross_*A_3-A_2, *Cross_*A_3-A_H, *Cross_*A_H-A_3, *Cross_*A_3-A_W and *Cross_*A_W-A_3, or it could be of *Still* type as follows: *Still_in_*A_1, *Still_in_*A_2, *Still_in_*A_3, *Still_in_*A_H and *Still_in_*A_W. After receiving this signal by the *transitions_actions* process, it will generate the corresponding signals to execute some actions; moreover, the *buffer_management* process puts limits associated to each transition in each buffer.

4.3 The Buffer Management Technique

Real time video is a complex task to support, because MC or BS can not request its peer to increase or decrease the video frame transmission speed. Future frames, which have not been produced at any time, could not be consumed before, whereas controlling the VoD transmission speed is possible, because the video is already produced and stored in the server and ready to be transmitted when it is requested.

The BS (Figure 4.1) communicates with a VoD server via internet, and there is a buffer located in the BS, whereas the MC is communicating with the BS through the AP, and also the MC has a buffer. A VoD server can increase or decrease its speed of video transmission until reaching the maximum bandwidth allowed. In the same way, MC could request the BS to increase or decrease transmission speed in order to store the biggest amount of video frames in its buffer. In this way, it could support a wireless disconnection by taking frames from MCB.

The proposed solution takes into account the diagram state of Figure 4.3, where MCB and BSB are managed depending on the MC transition. The BSB and MCB are divided into several parts defining a series of limits associated to transitions, as described in Table 4.1, which could help controlling the video consumed in each state.

Our proposed technique is performed in four steps:

- Discovering the state of MC every Δt (1 s for example).
- Generating MC transition immediately after that time using a state diagram.
- Informing the MC transition to different entities allocated in the AP, BS and MC, the first entity is *AP Proxy* (*APP*), it is a simple proxy that forwards signaling information from MC to BS and data from BS to MC. The second one is the *BSB Manager* (*BSBM*) and the last is the *MCB Manager* (*MCBM*). Where BSBM is responsible for managing the BSB and the MCBM is responsible for managing the MCB.
- Each entity executes some actions depending on the generated transition.

The buffer is working depending on the principle of *First In First Out* (*FIFO*). Hence, the first frame stored in the BSB will be transmitted firstly to the MC, which controls the order of buffered frames. The main idea of the proposed solution is buffering an additional amount of video frames, in MCB before disconnection, to be consumed when MC disconnects. At the moment of disconnection, video frames transmitted from VoD server are buffered in the BSB. Later, these frames will be consumed when MC returns to connect to the original AP or to a new one. By this way, no frames will be lost during disconnection period.

Table 4.1: Buffer limits

Transition	Buffer limits
Still_in_A1	$LimA_1$
Cross_A1-A2	$LimA_2$
Cross_A2-A3	$LimA_3$
Cross_A3-AW	$LimA_w$
Cross_A3-AH	$LimA_H$

4.3.1 Analysis of The Amount of Buffered Video

The video which is localized in a VoD server is packetized into N packets, each packet PK that has size s is streamed from the VoD server to BS with transmission speed V_x (packets per second), and from the BS to MC with transmission speed V_y (packets per second), while the playing bit rate at MC is assumed to be V_p (packets per second). The disconnection caused by handover is supposed to start at time t_h then video packets in MCB will be consumed from packet PK_h during the disconnection of the handover. As the disconnection duration is τ_h, then at $t_h + \tau_h$ is consumed the last packet of disconnection PK_τ from MCB. Accordingly, if the last packet which arrived correctly and buffered in MCB before disconnection at t_{h-1} is identified by PK_L, then video packets in BSB will be consumed after MC reconnection, BSB will send the first packet after reconnection that is identified by PK_{L+1}. MC sends the PK_{L+1} packet id to BS with the des-association message of the handover process (Figure 4.6).

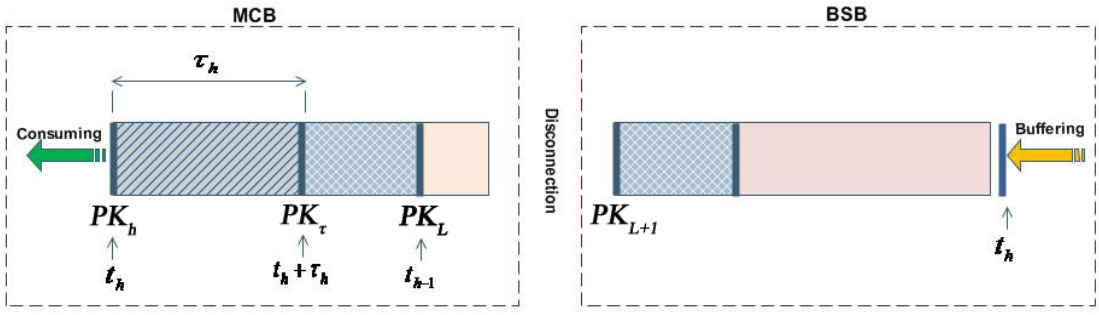

Figure 4.6: Packets and buffers state when handover disconnection start

At this moment, the following two exceptional cases could occur:

- If MC consumed all buffered video during handover disconnection period τ_h, PK_L and PK_τ will be the same packet.
- If the buffered packets were consumed before reconnection, video play could stop until reconnection but no packets would be lost.

Let $C_{MC}(\tau)$ be the number of video packets consumed from MCB during an interval of time τ :

$$C_{MC}(\tau) = \tau \times V_p$$

Then the amount of video packets consumed from MCB during handover disconnection τ_h:

$$C_{MC}(\tau_h) = \tau_h \times V_p$$

Likewise, let $B_{MC}(\tau)$ be the amount of video packets buffered in MCB during an interval of time τ :

$$B_{MC}(\tau) = \tau \times V_y$$

In the other hand, $B_{BS}(\tau)$ is supposed to be the amount of video packets buffered in BSB during an interval of time τ :

$$B_{BS}(\tau) = \tau \times V_x$$

To calculate the amount of video packets buffered in BSB during handover disconnection τ_h:

$$B_{BS}(\tau_h) = \tau_h \times V_x$$

Moreover, let $C_{BS}(\tau)$ be the amount of consumed packets from BSB during an interval of time τ :

$$C_{BS}(\tau) = \tau \times V_y$$

4.3.2 SDL for Buffer Management

The BSB and MCB are managed depending on the MC transition; accordingly, for each *Cross* transition the *transitions_actions* will send signals to the *MCBM* process and *BSBM* processes in order to manage the buffered video, these signals carry a message to

describe the action being executed, the sent signals to *BSBM* must pass through the *APP*. the *buffer_management* process is responsible of calculating the amount of buffered video and it is shared for both *MCBM* and *BSBM* (Figure 4.7).

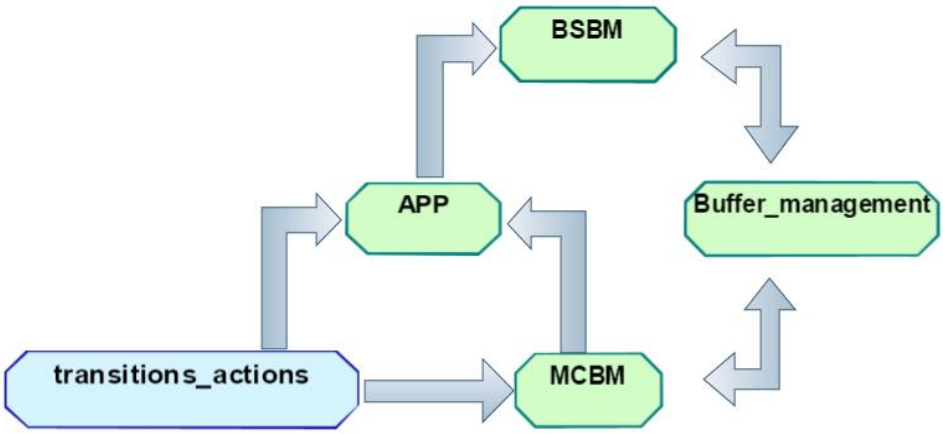

Figure 4.7: Communication between entities to manage buffers

There are four types of the exchanged signals:

1. Messages to *Control the Buffered Video* (*CBV*):
   - *StBAF*: Start Buffering Additional Frames.
   - *SpBAF*: Stop Buffering Additional Frames.
   - *CVF*: Consume Video Frames from the buffer.
2. Messages to *Control the Transmission Speed* (*CTS*):
   - *ISVF*: Increase Speed of Video Frames transmission.
   - *DSVF*: Decrease Speed of Video Frames transmission.
3. There are additional messages from MC to inform the BS about *Handover State* (*HS*):
   - *Send_hd*: Handover is done successfully.
   - *Send_hc*: Handover cancelled for any reason and MC is still connected with the associated AP.
   - *Send_rc*: MC returns to coverage after disconnection.
4. The last message, which is left for future use with predictor, is the *PDT*: *Predict Disconnection Time*.

- **Signals Generated by *transitions_actions***

The *transitions_actions* process generates three types of signals (Figure 4.8):

- The first signal *request_to_BS*(*server*, *message*, *only_BS*) for BS to control the *BSBM* or to control the speed of VoD server, it passes through the *APP*:
  a. *Server*: Is a *CharString* data type, and it could be "BSBM" or "VoD".
  b. *Message*: Is a *CharString* data type, when *server* is "VoD", the message must be one of CTS, and if *server* is "BSBM", the message could be one of the CTS or CBV.
  c. *Only_MC*: Is a *Boolean* data type, it indicates if this transition action is for the *BSBM* only (true) or there are more actions for the *MCBM* (false).
- The second signal *request_to_MC*(*entity, message, only_MC*) for MC to control the *MCBM* or to inform the BS about the state of the handover process:
  a. *Entity*: Is a *CharString* data type, and it must be "MCBM".
  b. *Message*: Is a *CharString* data type, and it could be one of the CBV or the HS messages.
  c. *Only_MC*: Is a *Boolean* data type, it indicates if the actions of this transition are for the *MCBM* only (true) or there are more actions for the *BSBM* (false).
- The last signal is the *error_message* signal, which indicates an impossible transition case.

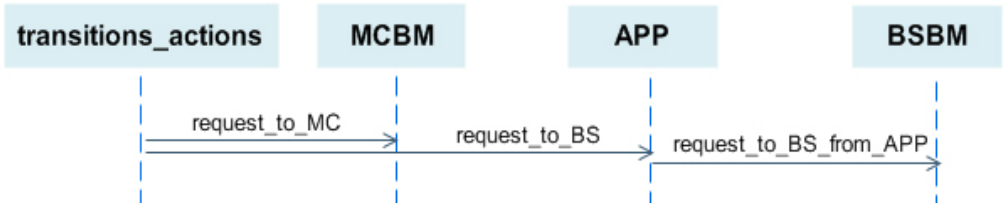

Figure 4.8: Signals generated by the *transitions_actions* process

- **Signal Exchange to Control Video Transmission Speed**

When the *APP* receives a request from *transitions_actions* to change the transmission speed, the *APP* will forward the request to the *BSBM*, if the transition action requires change in BS transmission speed, the *BSBM* will change the transmission speed

(increase or decrease) and manage the BSB by sending a *request_to_manage_BSBM* signal to the *buffer_management* process to execute the action, and then it will respond to *APP* with *ok* message. While in case that the transition action requires change in the transmission speed of the VoD server, the *BSBM* will send *video_speed* signal to the *VoD* process to increase or decrease the speed of transmission, in this moment, the *VoD* will send a *speed_ok* message to *BSBM* indicating that speed has been changed (Figure 4.9).

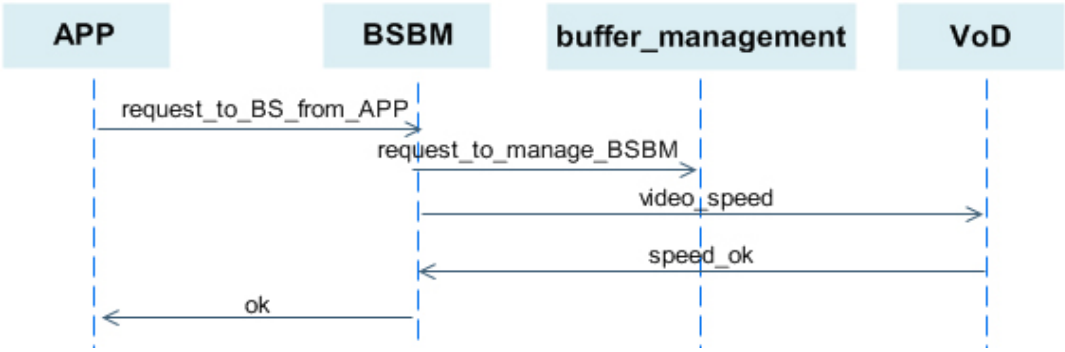

Figure 4.9: Signals exchange to control video transmission speed

- **Transitions and Their Associated Actions**

In the *transitions_actions* process, after receiving the transition signal, some signals will be generated to carry command to the destination entity to execute an action. Table 4.2 describes transitions with their associated signals. All transitions in this table are *Cross* transitions; any other transition of *Still_in* type has no actions, because the entity (BS or MC) will continue executing its last *Cross* transition actions.

Table 4.2: MC Transitions and their associated actions

Transition	Signal	Description
Cross_A1-A2	*request_to_BS('VoD', 'ISVF', true)* *request_to_BS('BSBM', 'StBAF', true)*	
Cross_A2-A1	*request_to_BS('VoD', 'DSVF', true)* *request_to_BS('BSBM', 'SpBAF', true)*	
Cross_A2-A3	*request_to_BS('BSBM', 'ISVF', false)* *request_to_MC('MCBM', 'StBAF', false)*	
Cross_A3-A2	*request_to_BS('BSBM', 'DSVF', false)* *request_to_MC('MCBM', 'SpBAF', false)*	

Transition	Signal	Description
Cross_A_3-A_H	*request_to_BS('BSBM', 'ISVF', false)* *request_to_MC('MCBM', 'StBAF', false)* *request_to_MC('MCBM', 'CVF', false)* *request_to_BS('BSBM', 'StBAF', false)* *request_to_MC('MCBM', 'send_hd', true)* *request_to_BS('BSBM', 'CVF', true)*	Before handover process When handover start After handover, MC state change to A_3 of the new AP, BS transmit it buffered video to MC
Cross_A_H-A_3	*request_to_MC('MCBM', 'send_hc', true)*	Handover cancelled and MC return to coverage of original AP
Cross_A_3-A_W	*request_to_MC('MCBM', 'CVF', false)* *request_to_BS('BSBM', 'StBAF', false)* *request_to_MC('MCBM', 'PDT', false)*	
Cross_A_W-A_3	*request_to_MC('MCBM', 'send_rc', false)* *request_to_BS('BSBM', 'CVF', false)* *request_to_BS('BSBM', 'ISVF', false)* *request_to_MC ('MCBM', 'StBAF', false)*	
Cross_A_H-A_W	*request_to_MC('MCBM', 'CVF', false)* *request_to_BS('BSBM', 'StBAF', false)* *request_to_MC('MCBM', 'PDT', false)* *request_to_MC('MCBM',send_hc', false)*	
Cross_A_W-A_H	*request_to_MC ('MCBM','CVF', true)*	

4.3.3 Signaling Sequence for Handover

When the signal *handover*(*to_handover_AP*) is generated by the process *state_diagram* the handover process will start. There are four processes: *MC*, *BS*, *AP_1* and *AP_2* cooperate to execute the handover process. As MC receives the *handover*(*to_handover_AP*) signal, it will ask its associated AP to disconnect, followed by a requests to the new AP to connect, by exchanging many signals as follows (Figure 4.10):

- First, the *MC* sends the *des_association*(*mac*) signal with its MAC address to the associated *AP* (the original) to disconnect.
- Then it sends an *association_request*(*frame_request*) signal to the new *AP* with request frame including its MAC address and data rate information.

- When the new *AP* receives the association request from the *MC*, it will send an acknowledgment signal *association_ack*(*ack*), which carries *ack* (*Boolean* data type). If *ack* is true then *AP* will accept the request, in case of false, it could not connect (e.g. because its clients number is full) and *MC* must cancel the handover or repeat its request.
- If the new *AP* accepts the request by sending true *ack*, it will send an *association_response*(*frame_response*) signal with a response frame including its SSID and data rate information.
- When *MC* receives *AP* information in its association response, it will send *re_association* signal to the *AP* to start receiving video frames from *BS*.
- After the re-association request, the *AP* sends an information message in *inform_BS* signal to the *BS* (with its SSID and MC MAC) to ask the *BS* to continue video frames transmission for *MC*. In this moment, the BS consumes the video, which was buffered during the disconnection of the handover, and continues the normal transmission.

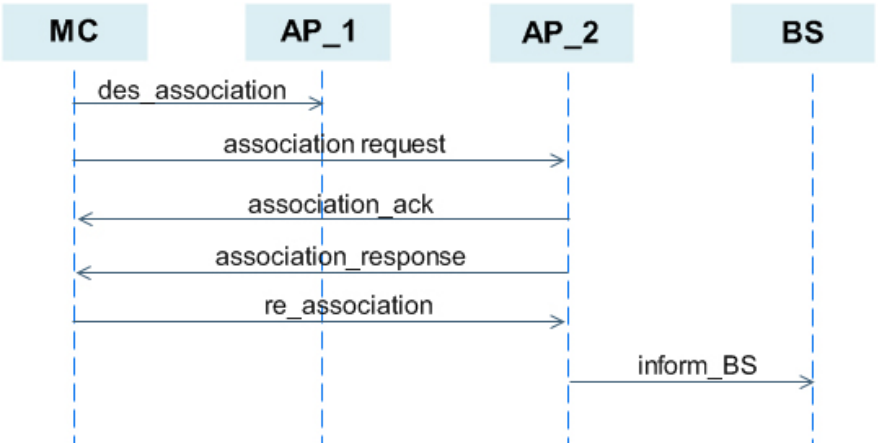

Figure 4.10: Signaling sequence for handover

Figure 4.11 shows the supposed impact of the transitions actions on the previous variables V_x, V_y, $B_{BS}(\tau)$ and $B_{MC}(\tau)$ with the $\Omega_1(d_{MC})$ of a MC connected to AP_1 and then did handover to AP_2, $\Omega_1(d_{MC})$ and $\Omega_2(d_{MC})$ are the measured RSSI% of the two APs respectively. The first transition is *Cross_A1-A2* which produces an increment in V_x and increment in $B_{BS}(\tau)$ also, because the two signals *request_to_BS*('*VoD*', '*ISVF*', *true*) and *request_to_BS*('*BSBM*', '*StBAF*', *true*) are generated, while in the second

transition *Cross_A2-A3* a rise in the value of V_y and $B_{MC}(\tau)$ is illustrated, because the two signals *request_to_BS*(*'BSBM', 'ISVF', false*) and *request_to_MC*(*'MCBM', 'StBAF', false*) are generated, and this rise goes on with the transition *Cross_A3-AH*. Moreover, the $B_{BS}(\tau)$ is increased while the $B_{MC}(\tau)$ is decreased during the handover because the MC consumes its buffered video without buffering additional video, by contrast, the opposite occurs with the BS.

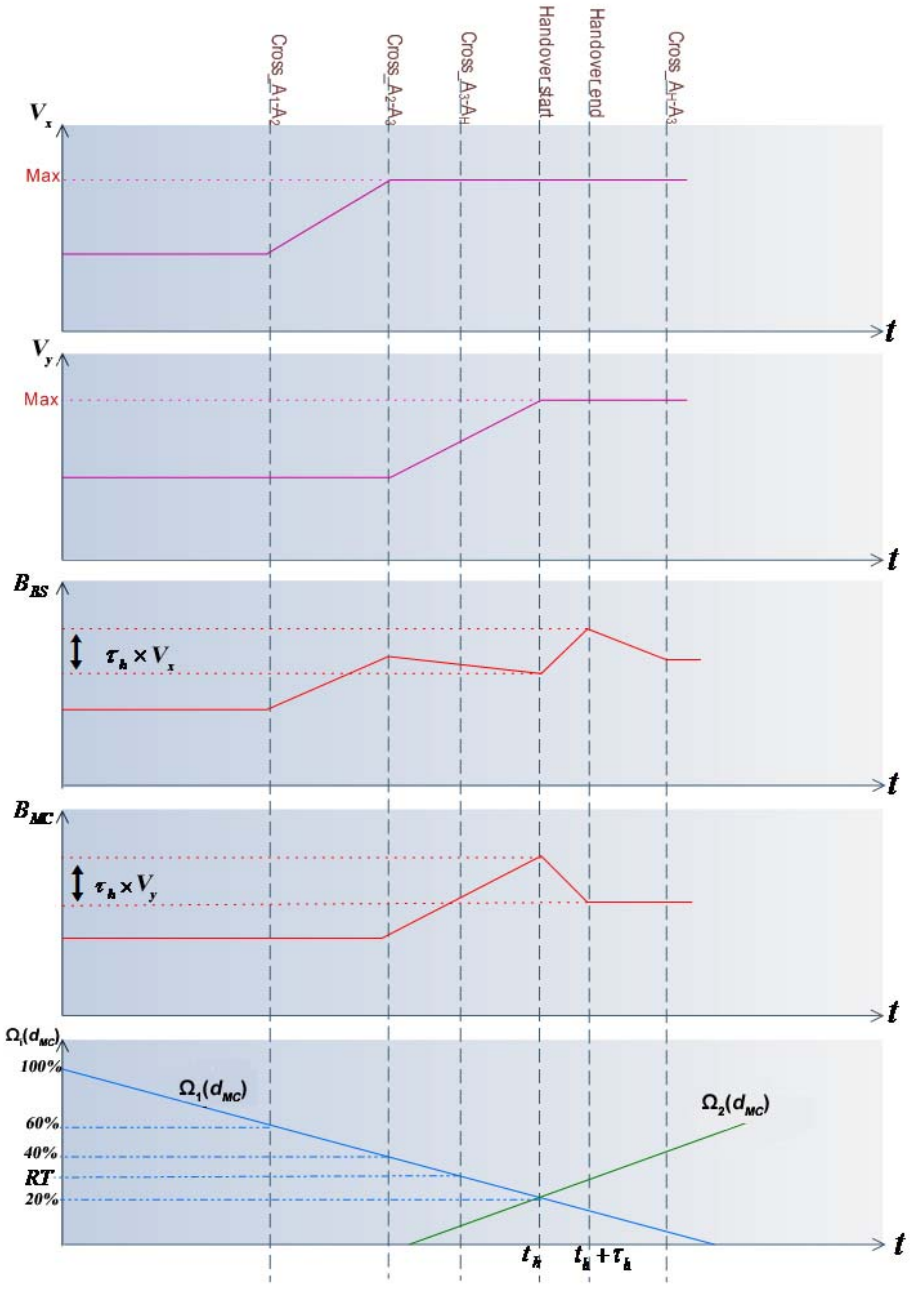

Figure 4.11: Impact of transitions actions on transmission speed and buffered video

4.4 Verification Results

The results are shown by monitoring MCB and BSB to aware about their video frames content, in order to study the effect of different movement shapes and speeds with the change of RSSI; accordingly, a simple monitoring *SDL* diagram was designed to display MCB and BSB buffered video, then it is tested on many cases of movements (Figure 4.12). The most important in movements is the transition of MC among different coverage zones. After the analysis and simulation, a *Message Sequence Chart* (*MSC*) is extracted (Figure 4.13) then all the yields results are used to illustrate the charts which show the buffered video only.

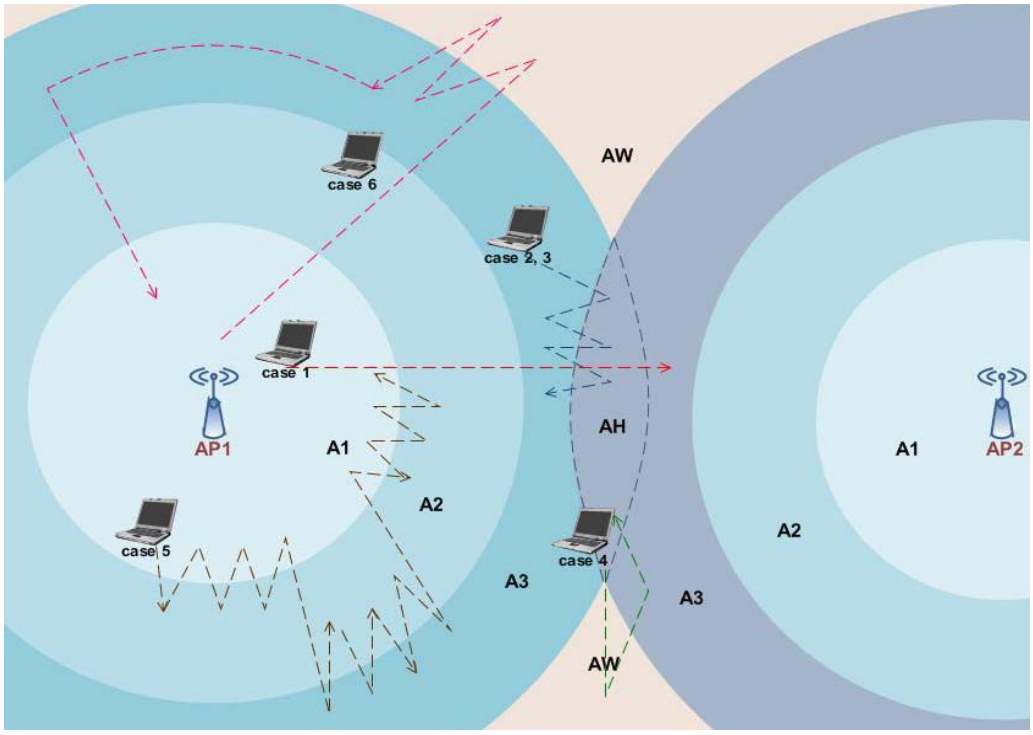

Figure 4.12: MC movements cases

In the *Buffer_Monitor* diagram (Figure 4.14), the *message_sequence* process receives two information signals from the *buffer_management* process each 1 s with the following considerations:

- *MCB_size* = *BSB_size* =10240 KB, MC is supposed to be a mobile device or a laptop.
- The initial *MCB_buffered_video* = the initial *BSB_buffered_video* = 5120 KB, because the previous state of buffer is unknown.

- The *VoD_original_video_size* = 382771 KB, the video, which is chosen as example, has 382771 MB in one hour of type AVI with video codec DivX and has bit rate 128 KBps, the video is high quality with full screen mode.
- V_x initial value: V_x^0 = 80 KBps (in reality, it is the downlink speed in BS when video is transmitted from VoD).
- V_y initial value: V_y^0 = 20 KBps (in reality, it is the downlink speed in MC when video is transmitted from BS).
- V_P = 128 KBps.

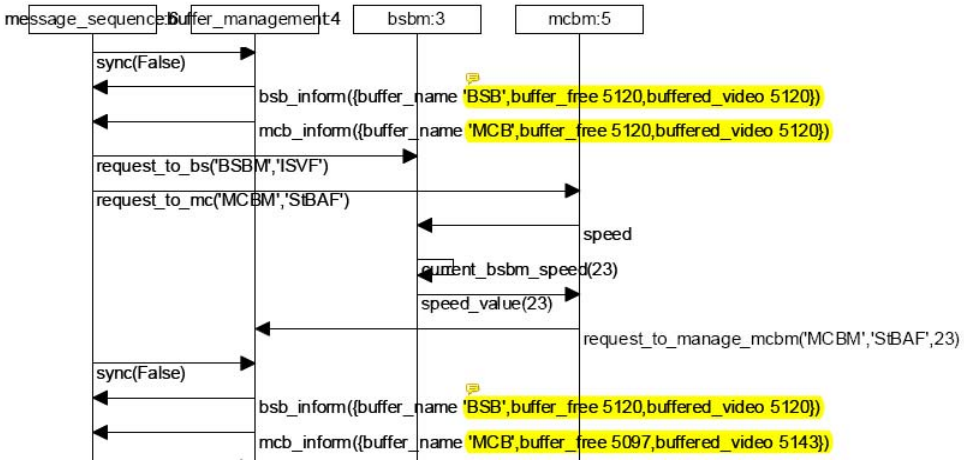

Figure 4.13: Part of the buffer monitoring MSC

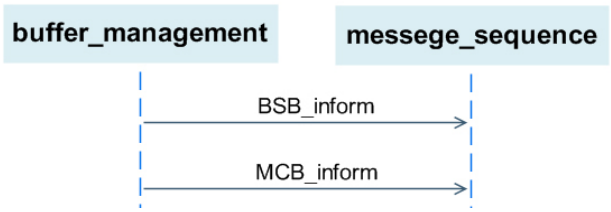

Figure 4.14: Buffer monitoring

The MC movement cases of Figure 4.12 with their results are described below:

- Case 1 (MC moving in straight line): MC was moving in regular motion at constant speed 10 mps (Figure 4.12), initially from an excellent coverage with $\Omega_1(d_{MC})$ = 80% in zone A_1, then moved towards AP_2 passing through A_2, A_3 and A_H with a success handover process to A_3 of AP_2. In this case, it is shown how buffered video was affected by the handover process (Figure 4.15), the curve

during the period of the handover process (11-12 s) is distinct from the rest of movement. During the disconnection of the handover process, the MC buffered video was consumed and BS buffered video frames. After the handover, the MC would receive the video, which was buffered in BSB during disconnection, through AP_2. The handover here is supposed to happen in 1 s, in reality it has its time, but the same shape of buffering will occur, MC is interested not to loose any video frames during disconnection and this was achieved by buffering these frames.

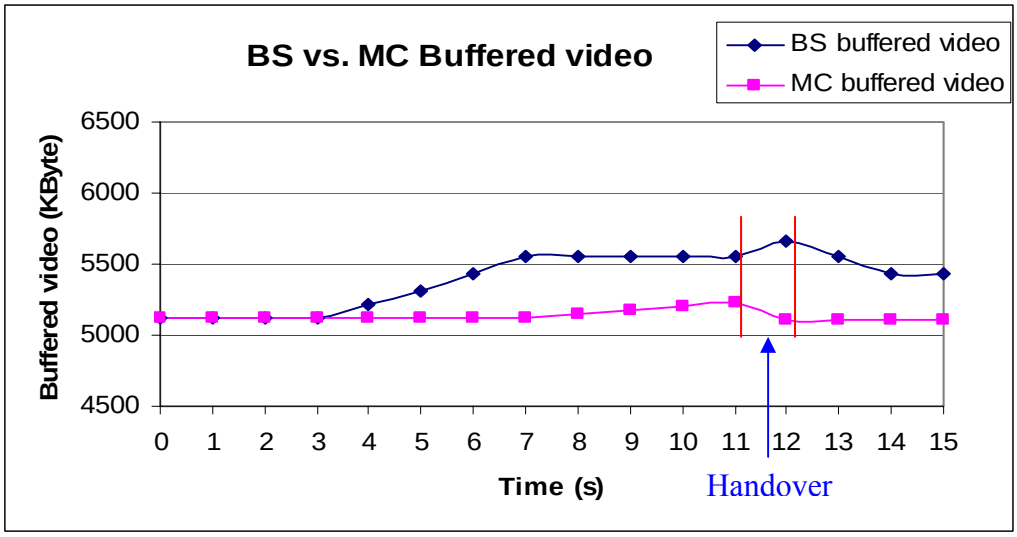

Figure 4.15: MC vs. BS buffered video of case 1

- Case 2 (MC moving in zigzag): MC was moving in zigzag motion between A_3 and A_H without handover, at constant speed (6 mps), starting from A_3 with $\Omega_1(d_{MC})$ = 39% (Figure 4.12). In Figure 4.16, the pink line shows the change in the MC buffered video, it appears like a stairs because MC was buffering additional video frames for the handover, as it returned to A_3, it did not use buffered video. What will happen if MC goes on this movement for a long time? The buffer would be full and no space would remain. The solution is to discard the oldest buffered video frame and store the newest one, this keeps the buffer always refreshed with new video frames.

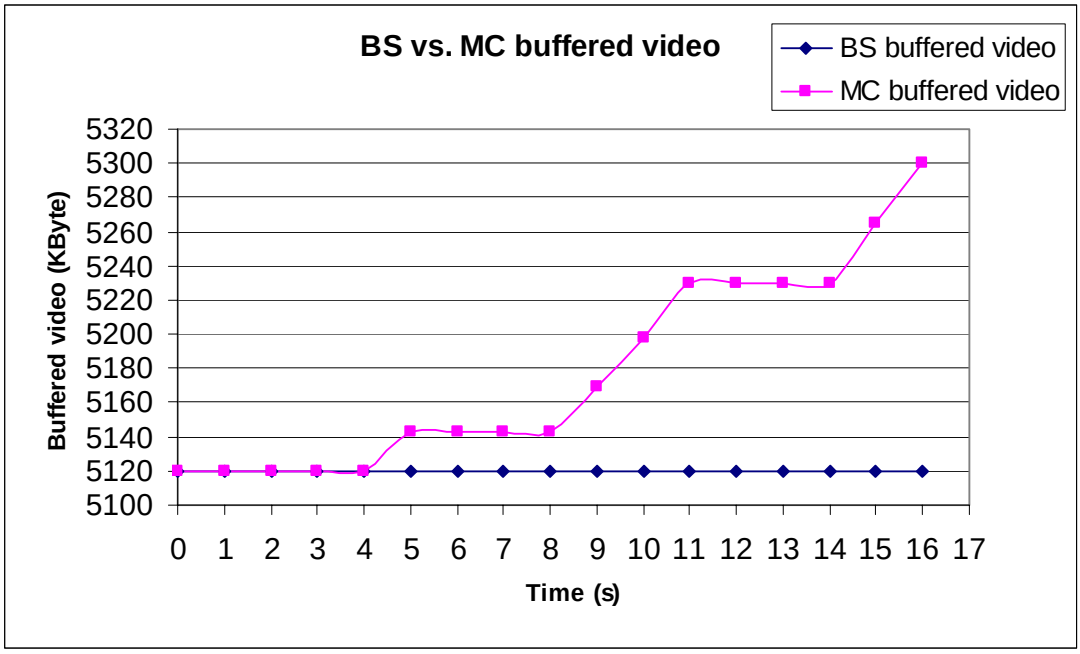

Figure 4.16: MC vs. BS buffered video of case 2

- Case 3 (MC moving quickly in zigzag): The same MC (case 2) was moving in zigzag motion between A_3 and A_H without handover at constant speed (10 mps), starting from A_3 with $\Omega_1(d_{MC})$ = 39%. In this case, as the speed increased, the change in the coverage zone occurred rapidly. For example, the MC generated the *Cross* transition between A_3 and A_H nine times as it was faster, whereas in the previous case were just five times. Figure 4.17 shows the same behavior in MCB values. Each time, the MC crossed from A_3 to A_H, it buffered more frames in case it did handover, as it returned, buffered frames were not consumed. In both cases, the value of BSB was constant, because BS was just requested to increase its transmission speed to provide the MC with more frames.

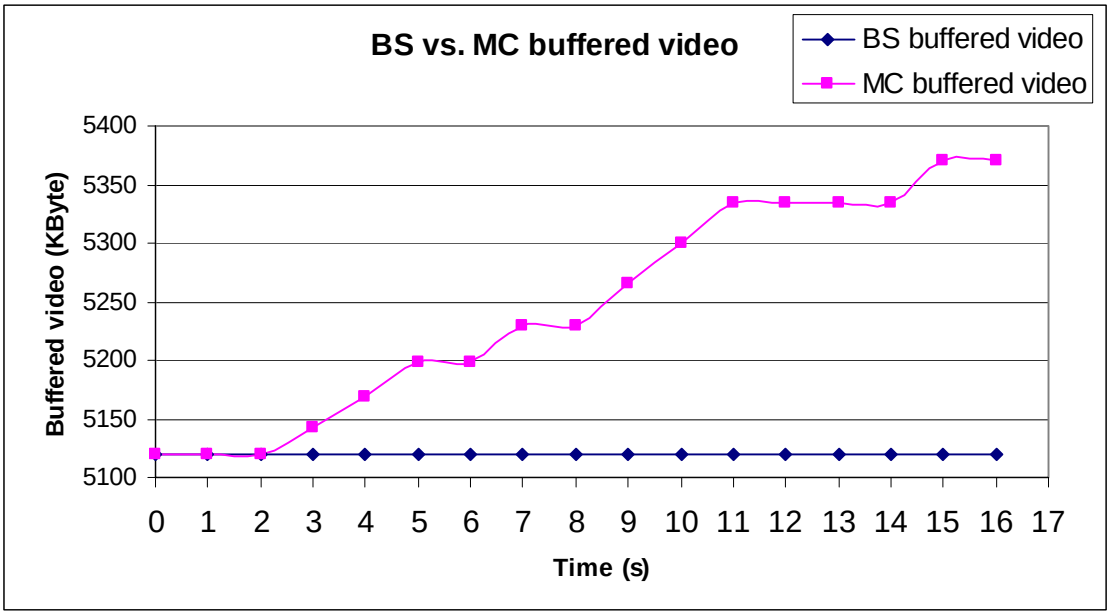

Figure 4.17: MC vs. BS buffered video of case 3

- Case 4 (MC is out of coverage): In this special case, a very short movement with many changes in coverage zones is shown, MC was moving in regular motion at constant speed 4 mps with $\Omega_1(d_{MC})$ = 20% and $\Omega_2(d_{MC})$ = 20% in zone A_H, next it moved to A_W without handover process, the connection of AP_1 was lost and it found new connection with AP_2, followed by A_3 and A_H of AP_2 (Figure 4.12). MC would consume video frames from its buffer during its movement in A_W while BS was buffering the video during disconnection. When MC returned to A_3 of AP_2, it received video frames, which were buffered in BSB during the disconnection, through AP_2. In Figure 4.18, it is obvious that MC buffered video was decreasing and BS buffered video was increasing in A_W case. By contrast, the opposite happened in A_3 and A_H where MC did not handover, because in these states MC was preparing its buffer for any new handover or disconnection.

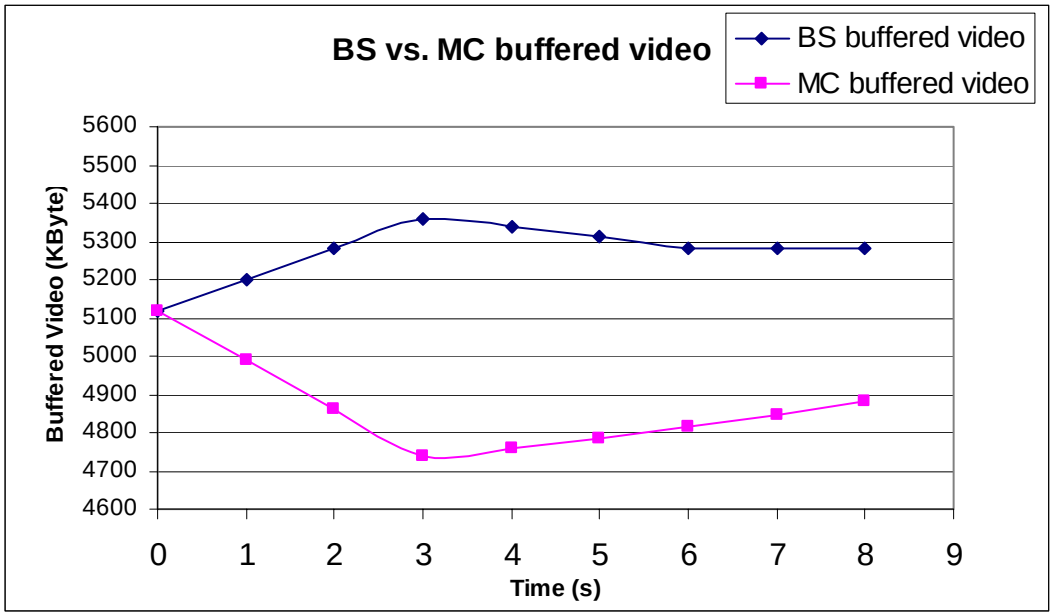

Figure 4.18: MC vs. BS buffered video of case 4

- Case 5 (MC moving in different zigzag motions for a long time): MC was moving in different zigzag motions (Figure 4.12), initially in A_1, A_2 and it moved to A_3 following zigzag motion between A_2 and A_3, after that it returned to zigzag motion between A_1 and A_2, it was moving at constant speed (10 mps), starting with $\Omega_1(d_{MC})$ = 70% with total moving time 60 s. Previously, where the zigzag happened between A_3 and A_H, there was not any change in the BSB. Nevertheless, the zigzag in this case is occurred in A_1 and A_2, so the BS buffered video frames; however, MC buffered video frames when crossing from A_2 to A_3 to prepare the buffer for handover, as shown in Figure 4.19 for buffered video. In case of continuation in zigzag motion, the buffer could be filled, one solution (as proposed for case 2) is discarding old frames; or emptying the buffer as MC enters state A_1, where any buffered frames are not necessary.

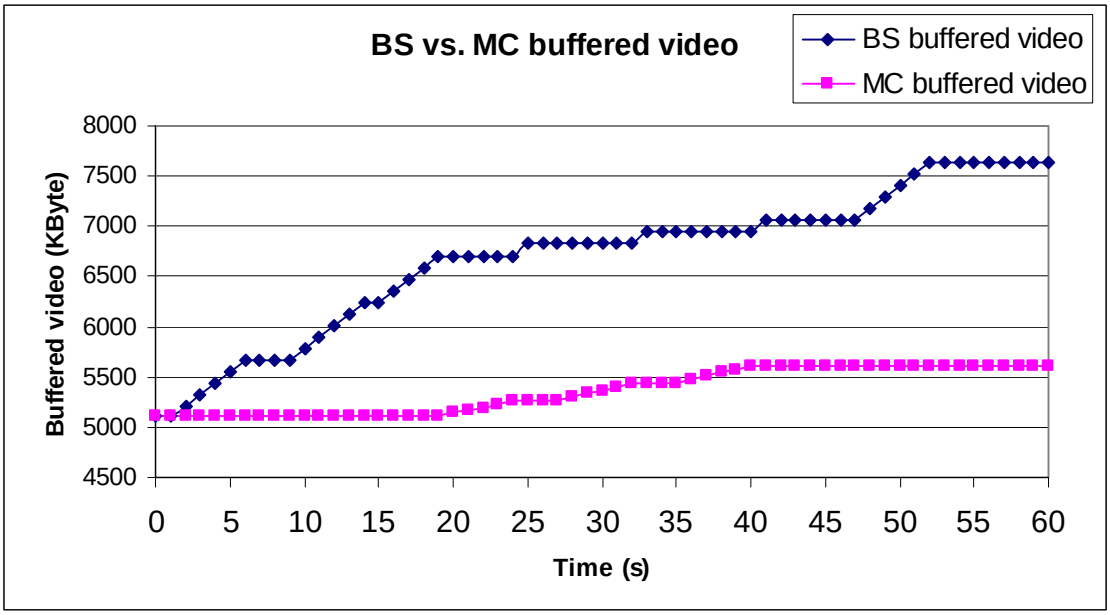

Figure 4.19: MC vs. BS buffered video of case 5

- Case 6 (MC moving in different directions): MC was moving at constant speed (6 mps) in the CA_1 (Figure 4.12), starting from Ω_1 (d_{MC}) = 90%, moving towards A_2, A_3 then A_W, after that it returned to A_3 proceeded to A_W, next it came back another time to A_3 to move with circular motion and constant Ω (d_{MC}) around the AP. Finally it returned to A_2 then to A_1, to complete 75 s of movement. The curve of buffered video did not indicate what was the partial moving shape in the same coverage zone where no *Cross* transitions were generated. As MC is moving with circular motion in A_3, the same transition, which is *Stil_in_A3,* was generated always; the important is the zone where MC is located. In Figure 4.20, MC consumed video frames from its buffer during the disconnection of A_W while BS was buffering video. When MC returned to A_3, it received video frames from the BSB, at the same time it buffered video frames for any possible disconnection (that occurred in zigzag motion between A_3 and A_W). At the end, MC returned to A_2 and A_1. Thus, no changes happened in the two buffers as the probability of disconnection was very low.

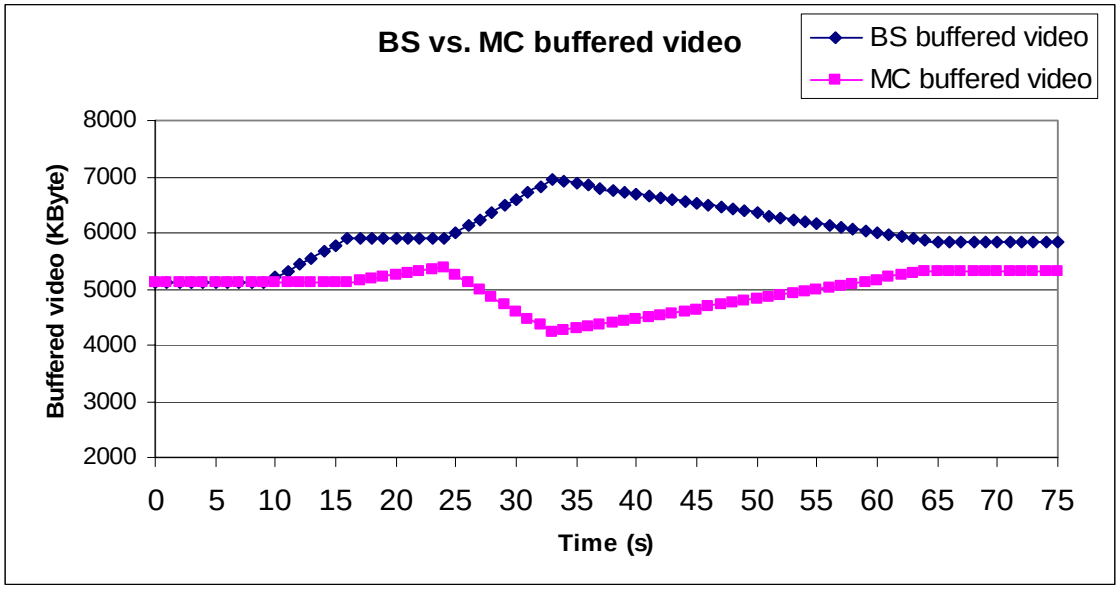

Figure 4.20: MC vs. BS buffered video of case 6

In this work, we did not study all the physical properties related to wireless communication and handover, such as delay and jitter, the most interesting is video frames. The results proved that managing the buffered video and controlling the transmission speed are possible, this could be achieved by exchanging messages between MC and BS which was demonstrated by the *SDL*. In the next chapter this technique will be combined with the Gradient Predictor and Filter to form a comprehensive protocol being simulated by our developed Java simulator.

CHAPTER 5

SIMULATION OF THE PROTOCOL

The proposed protocol was simulated implementing a specific Java simulator; this later combines the Gradient Predictor and Filter with an improved version of the technique specified by SDL for buffer management and transmission speed control. Interestingly, we derived this simulator from the SDL specification we previously implemented.

5.1 Derivation of the Java Simulator Classes from the SDL Diagram

The *SDL* specification was important to implement the technique in diagrams, which was easier to verify the protocol specification among entities, then using these diagrams to extract the Java code giving the possibility to develop the graphical user interface. Using the *SDL* specification diagram, the Java simulator classes and functions were derived directly to execute the same actions but with some necessary modifications to correct some unexpected results, and to improve the technique by adding the new RSSI Gradient Predictor and Filter giving better results after holes filtering. Furthermore, the simulator was provided with new classes to generate special chart forms to monitor the buffers, including all information necessary to understand the MC movement with related changes in all parameters (buffered video, transmission speed, filtered $\Omega(d_{MC})$), these charts could not be generated by any existing simulator, it was designed specially for this technique.

Figure 5.1 shows a simple diagram describing the principal *Java* classes derived from the main *Block* in the *SDL* diagram. The blue blocks in both sides are responsible for the state diagram and the generation of the states, transitions and actions related to transitions, while the green blocks are responsible for managing the MCB and BSB, and controlling the transmission speed in the VoD server and BS.

5.2 Impact of Holes on the State Diagram

While the signal is affected by surrounding conditions, holes will appear suddenly for a limited interval of time. Accordingly if MC is moving in any coverage zone it could pass through holes; therefore, new unexpected transitions will be generated such as *Cross_A1-AW* because the case of holes is the same as the case of out of coverage in A_W; the difference is the amount of time. All transitions caused by holes are shown in Figure 5.2. The dashed pink lines represent these transitions. It is important to refer to four transitions that were already found in the figure: *Cross_A3-AW*, *Cross_AW-A3*, *Cross_AH-AW* and *Cross_AW-AH*, they can be generated by the normal disconnection caused by handover or out of coverage, or could be caused by holes. Therefore, hole's size can distinguish between the true state of A_W and the one caused by holes. Other transitions such as *Cross_A1-AW*, *Cross_AW-A1*, *Cross_A2-AW* and *Cross_AW-A2* are just derived if holes are present in A_1 and A_2. After the filtering process, these four transitions are removed and the state diagram becomes as it was.

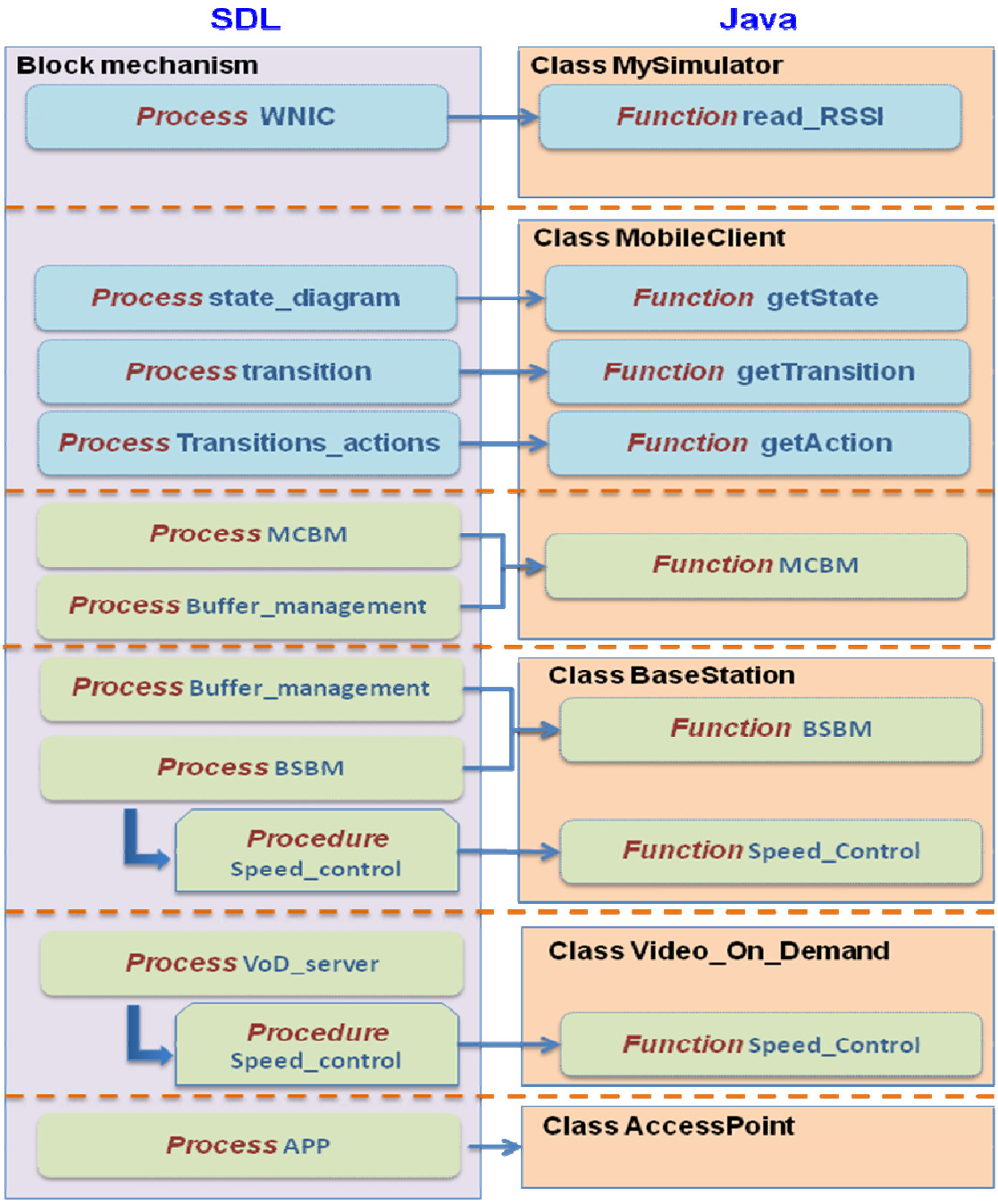

Figure 5.1: Derivation of the simulator from the SDL diagram

We used the second time unit (s) to measure hole's size, but to distinguish the hole from the A_W state; the hole's size must be less than the size of filter samples. For example, if the filter works on samples of 20 s, hole's size will be less than or equal to 18 (Hole's size < = sample size - 2) because starting and ending values of samples can not be included in holes as zeros except in case it was a true disconnection (A_W).

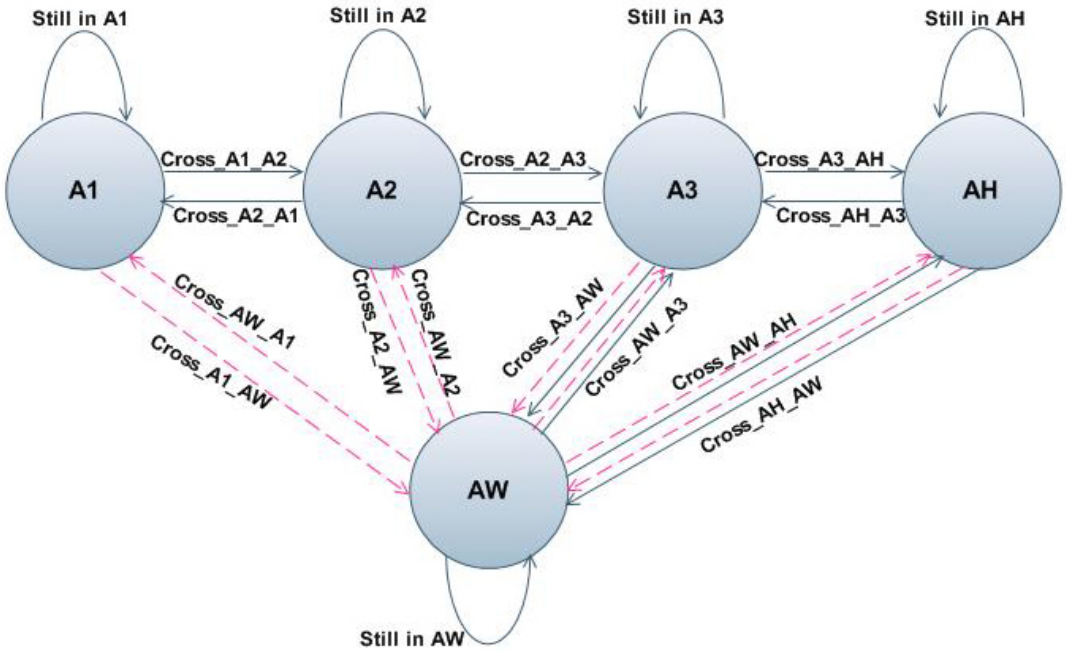

Figure 5.2: The state diagram considered in presence of holes

5.3 Buffer Management and Transmission Speed Control

Managing the buffering process in each entity and the transmission speed control separately is not efficient or logical because both of them are respectively related. That means, any change in the transmission speed must be controlled by buffer's capacity, and buffering process depends on the transmission speed. In the previous technique in chapter 4, buffer's and speed's values were calculated separately which produced unexpected behavior in some moments during the verification process. Hence, some modifications in the technique are necessary:

- VoD Server.
- BS.
- AP.
- MC.
- Transitions Actions to Control Transmission Speed.

VoD Server

The size of VoD buffer is supposed to be ∞ because we are not interested in it, and the total consumption of buffer is: a) the total size of transferred video during the simulation

process in case that the simulation time is less than total video time, and b) the total size of transferred video if the total video time is less than simulation time.

Let V_x be the VoD server transmission speed; it is increased or decreased according to the BS request. V_x has two limits: Maximum (V_x^{max}) and minimum (V_x^{min}) and starts with initial value (V_x^0) which will be defined later. The following values were considered:

- V_x^{max} = 1280 KBps is the transmission speed of the wired network which could be Gigabit Ethernet.
- V_x^{min} = 256 KBps is considered to be as the maximum possible speed of the WLAN.
- $V_x = V_x^0$.

When the VoD server is requested to increase its transmission speed, the speed will increase gradually, so we chose to increase and decrease it by 10% each step, but after testing many cases with different values 10%, 5% and 20%, we found that increasing each step by 5% and decreasing it by 10% giving best results. There is one process located in the VoD server to control V_x:

- *Process* (*VoD-1*): *VoD SPEED CONTROL* shows how *Vx* is increased or decreased by the BS request, which is conditioned by being between V_x^{max} and V_x^{min}.

Process (VoD-1): VoD SPEED CONTROL

```
Switch ( command ) {
 Case ISVF : { // Increase speed of video frames transmission
   If ( Vx < max_Vx - max_Vx / 20 )  { Vx = Vx + max_Vx / 20 }
   Else                              { Vx = max_Vx           }
 }
 Case DSVF : { // Decrease speed of video frames transmission
  If ( Vx > = min_Vx + max_Vx / 10 ) { Vx = Vx - max_Vx / 10 }
  Else                              { Vx = min_Vx           }
 }
 Otherwise: // Stop transmission       Vx = 0
}
```

BS

The BSB's size is controlled by limits: The maximum (*BSB_max*), minimum (*BSB_min*), upper limit (BSB_LIMIT_s) and lower limit (BSB_LIMIT_i). Always the BSB_LIMIT_s must be less than *BSB_max*, and the BSB_LIMIT_i must be greater than *BSB_min*. The upper limit is important for preventing from loss the video frames, that are still in the way after the disconnection. In case that these frames arrive to the buffer whereas it is full, then they will not find enough space and will be discarded. Let *cur_BSB_size* be the current BSB´s size which is calculated each 1 s and set initially to 0. The buffer has a delay of buffering equal N_1, which is the time required to fill the buffer to be greater than the BSB_LIMIT_i to start transmission. All the variables values were chosen after many retries and tests until we reached the suitable values that achieved the best results. The following values were considered for BSB:

- *BSB_max* = 10 MB is considered to be the same as the mobile device memory.
- *BSB_min* = 0 MB, the minimum possible value is zero because the lower limit of the buffer keeps the buffer from reaching to zero, except in few cases of long disconnections.
- *cur_BSB_size* = 0, initially is set to zero.
- BSB_LIMIT_i = 10% *BSB_max*, the lower limit was chosen to be higher than the minimum value with an amount suitable to keep the buffer in a good state, and this amount of buffered video is also sufficient for the buffer to start streaming to MC initially without problems.
- BSB_LIMIT_s = 90% *BSB_max*, the same thing with the upper limit, the two limits have the same percentage of buffered video from the maximum and the minimum values. These values were tested and verified.

Let V_y be the transmission speed of the BS, it is increased or decreased according to MC request and position; it is controlled also by the BSB limits. V_y has two limits and initial value: The maximum (V_y^{max}), the minimum (V_y^{min}), and K_y is the initial transmission speed value that is calculated from the signal initial value. Always V_y must be under the transmission speed threshold (*TH*) of the current zone where MC is located [95]:

- V_y^{max} = 256 KBps is the same transmission speed of the WLAN.
- V_y^{min} = 64 KBps (the minimum speed suitable to keep the buffer in a good state).

- $V_y = K_y = V_y^{max}$ / 100 * RSSI[0], it is calculated by this formula because the transmission speed decreases as the $\Omega(d_{MC})$ increases.

Two processes are located in BS, the first one for managing the BSB and the second process to control V_y:

- *Process* (*BS-1*): *BSBM* calculates the size of BSB considering BSB limits and correct speed values to keep the BSB in the required range. The BSB´s size is calculated by $cur\_BSB\_size += V_x - V_y$.
- *Process* (*BS-2*): *BS SPEED CONTROL* shows how V_y is increased or decreased by the request of MC, always V_y is controlled by BSB limits in order to keep the BSB always on the upper limit.

Process (BS-1): BSBM

```
If ( cur_BSB_size < BSB_LIMITi )
 // Increase speed of video frames transmission from VoD
                                          { VoD ( ISVF )
 // Stop video transmission from BS          Vy = 0       }

 // Set the same speed for video frames transmission
If ( cur_BSB_size > BSB_LIMITs & Vy > 0 )   Vx = Vy

 // Stop video frames transmission
If ( cur_BSB_size > BSB_LIMITs & Vy = 0 )  VoD ( STOP )

// Calculate buffered video in BSB
cur_BSB_size = cur_BSB_size + Vx - Vy
```

```
Process (BS-2): BS SPEED CONTROL
Switch (command) {
 Case: ISVF {        //Increase speed of video frames transmission
      If ( Vy  > TH )                                  Vy = TH
      Else { If(BSB_LIMITs > cur_BSB_size > BSB_LIMITi)
                                                       Vy = TH
            Else if (cur_BSB_size < BSB_LIMITi){VoD ( ISVF )
                                                       Vy = Vy + TH / 5}
            Else                                      {Vy = TH
                                                       VoD ( STOP ) }
     }
 }
 Case: DSVF {        //Decrease speed of video frames transmission
      If ( Vy  > =  min_Vy  +  max_Vy / 10 )
      { If ( BSB_LIMITs > cur_BSB_size > BSB_LIMITi )
                                              Vy = Vy - max_Vy / 10
        Else if ( cur_BSB_size <  BSB_LIMITi )
                                              VoD( ISVF )
        Else                                 { VoD ( STOP )
                                              Vy = Vy - max_Vy / 10 }
      }
     Else                                     Vy = min_Vy
 }
 Otherwise: Vy = 0 //Stop transmission
}
```

AP

We supposed the AP with transmission speed $V_z = V_y$, and the delay of buffering and retransmission $N_2 = 0$, which means it has buffer size equal 0, V_z has the same values as V_y and starts with initial value V_z^0:

- $V_z^{max} = V_y^{max} = 256$ KBps is the same maximum transmission speed of the BS.
- $V_z^{min} = V_y^{min} = 64$ KBps is the same minimum transmission speed of the BS.
- $V_z^0 = V_y = K_y = V_y^{max} / 100 * \text{RSSI}[0]$, this formula is used because the transmission speed decreases as the $\Omega(d_{MC})$ increases.

- $V_x^0 = V_z^0 * 2$; initially the transmission speed in the wired network (from VoD to BS) is two folds the transmission speed in the wireless network, it was chosen after a lot of tests, and this value achieved best results.

MC

The MCB's size is controlled by limits: The maximum (*MCB_max*), minimum (*MCB_min*), upper limit (MCB_LIMIT_s) and lower limit (MCB_LIMIT_i). Always the MCB_LIMIT_s must be less than *MCB_max*, and the MCB_LIMIT_i must be greater than *MCB_min*, The upper limit is important for preventing from loss the video frames that are still in the way after the disconnection. In case that these frames arrive to the buffer whereas it is full, they will not find empty space and will be discarded. Let *cur_MCB_size* be the current MCB´s size which is calculated each 1 s and set initially to 0. The buffer has delay of buffering equal N_3 which is the time required to fill the buffer to be greater than the MCB_LIMIT_i to start playing video.

All the variables values were chosen after many retries and tests until we reached the suitable values that achieved the best results. The following values were considered for MCB:

- *MCB_max* = 10 MB is the possible memory size available in mobile devices.
- *MCB_min* = 0 MB is zero because there is a lower limit that keeps the buffer from being empty.
- *cur_MCB_size* = 0 is the initial value of the buffer.
- MCB_LIMIT_i = 10% *MCB_max*, the lower limit was chosen to be higher than the minimum value with an amount suitable to keep the buffer in a good state, and this amount of buffered video is also sufficient for the buffer to start playing video without problems.
- MCB_LIMIT_s = 90% *MCB_max*, the same thing with the upper limit, the two limits have the same percentage of buffered video from the maximum and the minimum values. These values were tested and verified.

Let V_P be the playing video bit rate in MC; it is increased or decreased according to MCB state. V_P has three values K_P, ½K_P, and Zero. V_P takes the value of K_P when MCB is in its upper limit, and K_P = 128 KBps which is the playing bit rate for a good quality

video, but in cases of disconnections it could drop to ½K_P. One process is located in MC to control MCB and V_P:

- *Process* (*MC-1*): *MCBM* calculates the size of MCB taking into account MCB limits and BS requests to change V_y, to keep the MCB in the required range. The MCB´s size is calculated by *cur_MCB_size* + = $V_z - V_P$.

Process (MC-1): MCBM

```
If( cur_MCB_size >= MCB_max ){                    Vp = Kp
    If( Vz > min_Vz && state ≠ AW )               Vz = min_Vz
}
Else If((MCB_max > cur_MCB_size >= MCB_LIMITs) && state ≠ AW)
                                                  Vp = Vz = Kp
Else If (cur_MCB_size < MCB_LIMITi){
                                                  Vp = 0
   If(Vz < TH && state ≠ AW) //increase transmission speed
                                                  BS (ISVF)
}
Else If (MCB_LIMITs > cur_MCB_size >= MCB_LIMITi){
   Switch (state){
      Case AW :                                   Vp = Kp / 2
      Otherwise:  {   If(Vz < TH )                BS (ISVF)
                                                  Vp = Kp
                  }
               }
}
Else If (cur_MCB_size <= 0 && Vz <= 0){
                                                  cur_MCB_size = 0
                                                  Vp = 0
                                                  Vz = 0
}
Else                                              Vp = Kp
//calculate buffered video
cur_MCB_size = cur_MCB_size + Vz - Vp
```

Transitions Actions for Controlling Transmission Speed

Some MC transitions produce commands to control transmission speed of VoD and BS, which lead to changes in the BSB and MCB.

Table 5.1: Transitions with Speed control commands

Transition	Speed control
Cross_A1-A2	`VoD ( ISVF )` // increase VoD transmission speed
Cross_A2-A1	`VoD ( DSVF )` // decrease VoD transmission speed

Cross_A2-A3	// if MCB did not reach its upper limit, then ask the BS to increase its transmission speed
	`If ( cur_MCB_size < MCB_LIMITs && Vz < TH )`
	`BS ( ISVF )`

Cross_A3-A2	// if MCB is over its upper limit then ask the BS to decrease its transmission speed `If ( cur_MCB_size > MCB_LIMITs ) BS ( DSVF )`

Cross_A3-AH	// during the handover process the transmission speed of the BS and AP is zero because of disconnection
	`If ( handover process start ) Vz = Vy =0`
	// if the handover process did not start and the MCB is less than its upper limit, then ask the BS to increase its transmission speed
	`Else`
	`If ( cur_MCB_size < MCB_LIMITs && Vz < TH )`
	`BS ( ISVF )`

Cross_AH-A3	-
Cross_A3-AW	// transmission speed is zero because of disconnection state `Vz = Vy = 0`

Cross_AW-A3	// if MCB is less than its upper limit, then ask the BS to increase its transmission speed
	`If ( cur_MCB_size < MCB_LIMITs && Vz < TH )`
	`BS ( ISVF )`

Cross_AH-AW	// transmission speed is zero because of disconnection state `Vz = Vy = 0`

Cross_AW-AH	// during the handover process the transmission speed of the BS and AP is zero because of disconnection
	`If ( handover_process start ) Vz = Vy = 0`
	// if the handover process did not start and the MCB is less than its upper limit, then ask the BS to increase its transmission speed
	`Else`
	`If ( cur_MCB_size < MCB_LIMITs && Vz < TH )`
	`BS ( ISVF )`

Cross_A1-AW	`Vz = Vy = 0` // transmission speed is zero because of hole
Cross_AW-A1	-
Cross_A2-AW	`Vz = Vy = 0` // transmission speed is zero because of hole
Cross_AW-A2	-

All transitions with their commands are explained in Table 5.1. There are four important commands to control the speed:

- *VoD* (*ISVF*): The BS asks the VoD server to increase the speed of video frames transmission. This command leads to increase in the BS buffered video. It is requested just in case of *Cross_A1-A2*.
- *VoD* (*DSVF*): The BS asks the VoD server to decrease the speed of video frames transmission. It is requested just in case of *Cross_A2-A1*.
- *BS* (*ISVF*): The MC asks the BS to increase the speed of video frames transmission. This command leads to increase the MC's buffered video. To execute this command, the MCB must be under its upper limit. It is requested in cases of *Cross_A2-A3* and *Cross_AW-A3,* and in cases of *Cross_A3-AH* and *Cross_AW-AH* if the handover process has not been started yet.
- *BS* (*DSFV*): The MC asks the BS to decrease the speed of video frames transmission. To execute this command, the MCB must be higher than its upper limit. It is requested in case of *Cross_A3-A2*.

In the next cases of disconnection, the normal result is stopping the BS transmission, then $V_z = V_y = 0$ that leads to decreasing in the MC's buffered video:

- Disconnections happen during the handover (*Cross_A3-AH* and *Cross_AW-AH*).
- The out of coverage state A_W (*Cross_A3-AW* and *Cross_AH-AW*).
- The holes (*Cross_A1-AW* and *Cross_A2-AW*).

5.4 Simulation Process

The simulator was implemented using *Java programming language* [Web-19] and for drawing graphs of charts we have used the external library *chartDirector* [Web-20].

The simulator consists of eight classes; some of them were generated from the *SDL* as shown before:

1. Class **`MySimulator`**: Is the main class which includes the *main* function, where all objects creation and initialization, and simulation process are found.
2. Class **`MobileClient`**: Contains all functions of MC such as **`setBufferInitialValues`**, **`getState`**, **`getTransition`**, **`getAction`**, **`MCBM`**, and **`handover`**.
3. Class **`AccessPoint`**: The AP is only responsible of forwarding messages and

data between MC and BS, it contains functions such as: **`connect_To_BS`**, **`request_To_BS_From_MC`**.

4. Class **`BaseStation`**: Includes all functions related to BS operations.
5. Class **`Video_On_Demand`**: Includes all functions related to VoD operations.
6. Class **`SimulationResults`**: Organizes the results.
7. Class **`SplineLine`**: Is responsible of displaying the charts with all results.

The simulation process consists of many steps:

1. Create objects of all entities and set their initial values.
2. Get $\Omega(d_{MC})$ values of the associated AP from the data files (*RSSI_1.txt* for the first AP and *RSSI_2.txt* for the second AP) using the ***`read_RSSI`*** function, and set the simulation time to be equal to the total time of scanned RSSI.
3. Apply the Gradient filter on these values to remove holes (using *Process SIM-1*: *Gradient Filter*), in the same process the filter will call the Gradient Predictor to predict next MC state (*Process SIM-2*: *Gradient Predictor*).
4. Initialize connections between entities (BS with VoD, AP with BS, MC with AP).
5. Create arrays to store $\Omega(d_{MC})$, transmission speed and buffer's values during the simulation time.
6. Run the next steps while the total time of simulation does not finish:
   - Store the current measured $\Omega(d_{MC})$ of the associated AP.
   - Get MC state: ***`getState`*** function.
   - Get MC transition: ***`getTransition`*** function.
   - Get actions associated to MC transition: ***`getAction`*** function.
   - Call BSBM: ***`BSBM`*** function.
   - Store current BSB´s size.
   - Call MCBM: ***`MCBM`*** function.
   - Store current MCB´s size.

- Store current V_x, V_y (V_z), V_P. Note that if BS has received the complete video, then $V_x = 0$; If MC has received the complete video, then $V_y = V_z = 0$ and simulation will be terminated.

7. Show charts of results taking stored data.

Process (SIM-1): Gradient Filter

```
Variables: x,y,z,w,m,Filtered_value
x = Gradient Predictor (t,RSSI)
m = ( RSSI[t-1] + x ) / 2
y = square root (0.5 * ( RSSI[t-1] - m)^2 + (x - m)^2)
z = signum ( RSSI[t-1] – x )
w = signum ((RSSI[t] * RSSI[t-1])^2)
Filtered_value = (y * z * w) + x
```

Process (SIM-2): Gradient Predictor

```
// The predictor starts working when there are 20 sample values
minimum, So t must be greater than 20
Variables i=0, j=0, predicted, gradient_sum=0, x =0, y=0
Array RSSI_No_Holes[20]
For ( i = t-20, i < t-1, i++){
      If (RSSI[i] ≠ 0){      RSSI_No_Holes [j] = RSSI[i]
                             j++
                      }
}
For( i = 1, i < j, i++)
                   x = x + (RSSI_No_Holes[i] - RSSI_No_Holes[i-1])
gradient_sum = x / 20
predicted = ( gradient_sum *(21))+ RSSI_No_Holes[0]
```

5.5 Simulation Results

Several models of MC movement were simulated, some of them with long time holes, with constant $\Omega(d_{MC})$, with handover and others with long disconnection period.

In the simulation results graphs, there are two charts; the first one illustrates BSB and MCB, and transmission speed (V_x, V_y, V_P) along the time of simulation. The second chart shows $\Omega(d_{MC})$ filtered values, with colored background to differentiate

coverage zones: The light green color (A_1), the light orange color (A_2), the light blue color (A_3) and the light pink color (A_W), whereas A_H is not shown as colored zone because it is an overlapped zone over A_3. The horizontal dashed red line shows the handover threshold while the vertical dashed red lines show when MC is in A_H. In the second chart, the dot black line explains the current connected AP filtered $\Omega(d_{MC})$ values, while the red balls show all *Cross* transitions happened with the time noted on a label beside each ball.

- Case 1: MC movement includes different transitions in sensitive zones (Figure 5.3), starting in CA of AP_1, Crossing from A_1 to A_2 at t = 79 s, from A_2 to A_3 at t = 129 s, and go out of coverage in A_W at t = 210 s, connecting another time to AP_1 at t = 280 s, crossing to A_H at t = 348 s and to handover to AP_2 at t =363 s. After handover MC continuo connected to AP_2, crossing from A_3 to A_2 at t = 369 s, from A_2 to A_1 at t = 389 s, going back to A_2 at t = 439 s, then to A_3 at t = 459 s, to go out of coverage in A_W at t = 480 s, elsewhere a special transition from A_W to A_H happened at t = 510 s to connect another time to AP_1 at t = 522 s, disconnecting in A_W at t = 557 s to connect then to AP_2 at 607 s, crossing to A_2 at t = 628 s and finally to A_3 at t = 667 s. Figure 5.3 shows that the BSB starts buffering until arrives the *BSB_LIMITs* and BSB level is maintained always on this level by controlling the transmission speed, at this level VoD transmission speed V_x is decreased to be equal to BS transmission speed V_y and the buffer is kept on this level. In the other side, it is impossible to keep the MCB in one level, because video will be consumed in the time of disconnection while there is not buffering which leads to gradual decline (t =210 s to 280 s) until MC connects another time producing gradual rise (t = 280 s to 348 s) with slower speed than decline because buffering happen in the same time with consuming. Video playing speed (black line of first chart) is always in its max value except in some times of disconnection periods drop to the medium such as the period between t = 210 s and 280 s, t = 480 s and 510 s, t = 557 s and 607 s.
- Figure 5.4 is the same as case 1 except seven sites where there are continuous zeros (long holes). The first hole appears between t = 22 s and 44 s, the second between 44 s and 60 s, the third between 88 s and 110 s which is the longest one (15 s), the fourth between 132 s and 154 s, the fifth between 286 s and 308, the sixth between 330 s and 348 s, and the last one between 374 s and 396 s. All

these long holes were filtered successfully by the Gradient filter and did not affect buffers or the playing video.

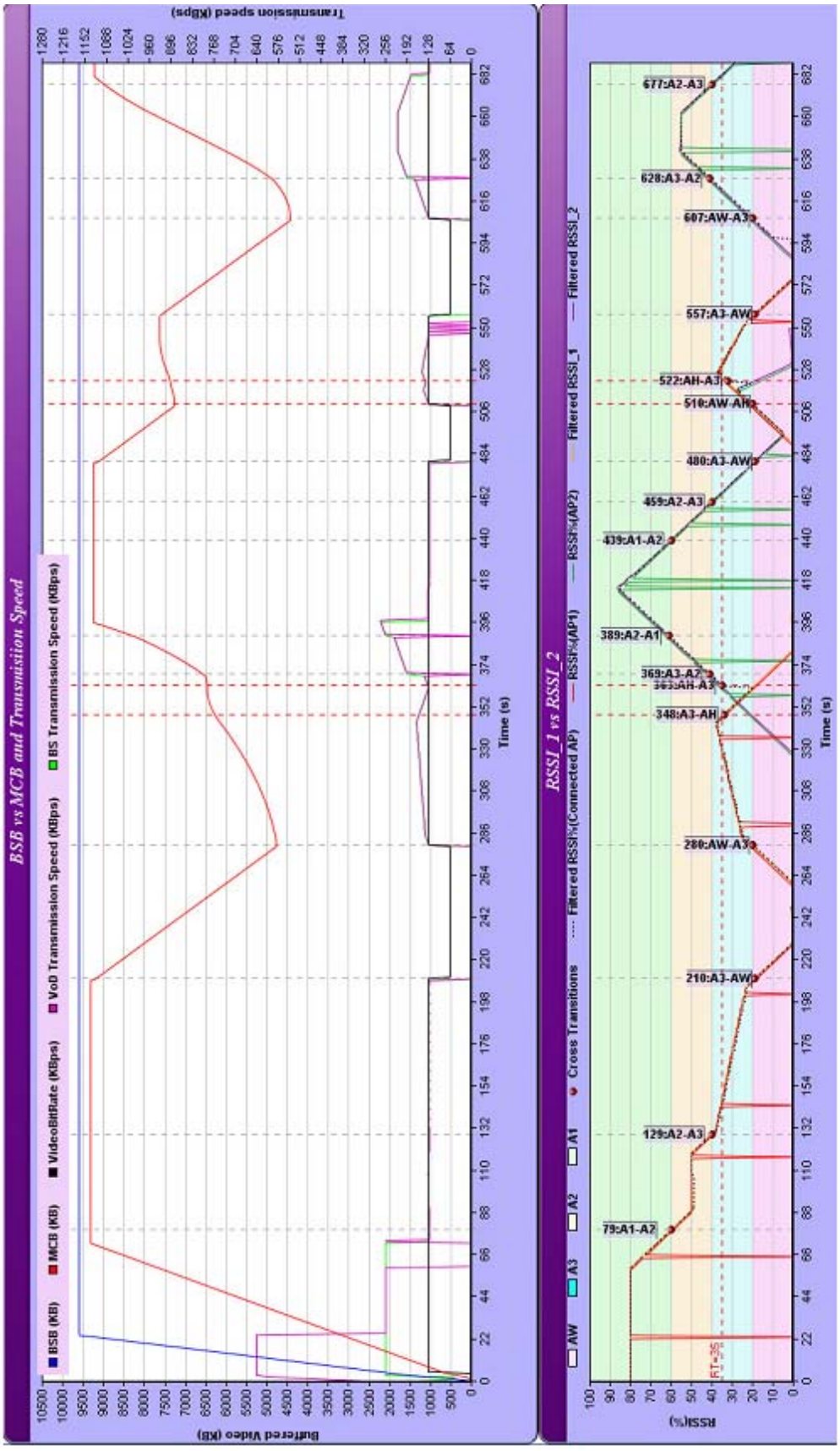

Figure 5.3: Case1, many Cross transitions and handover process in the presence of holes

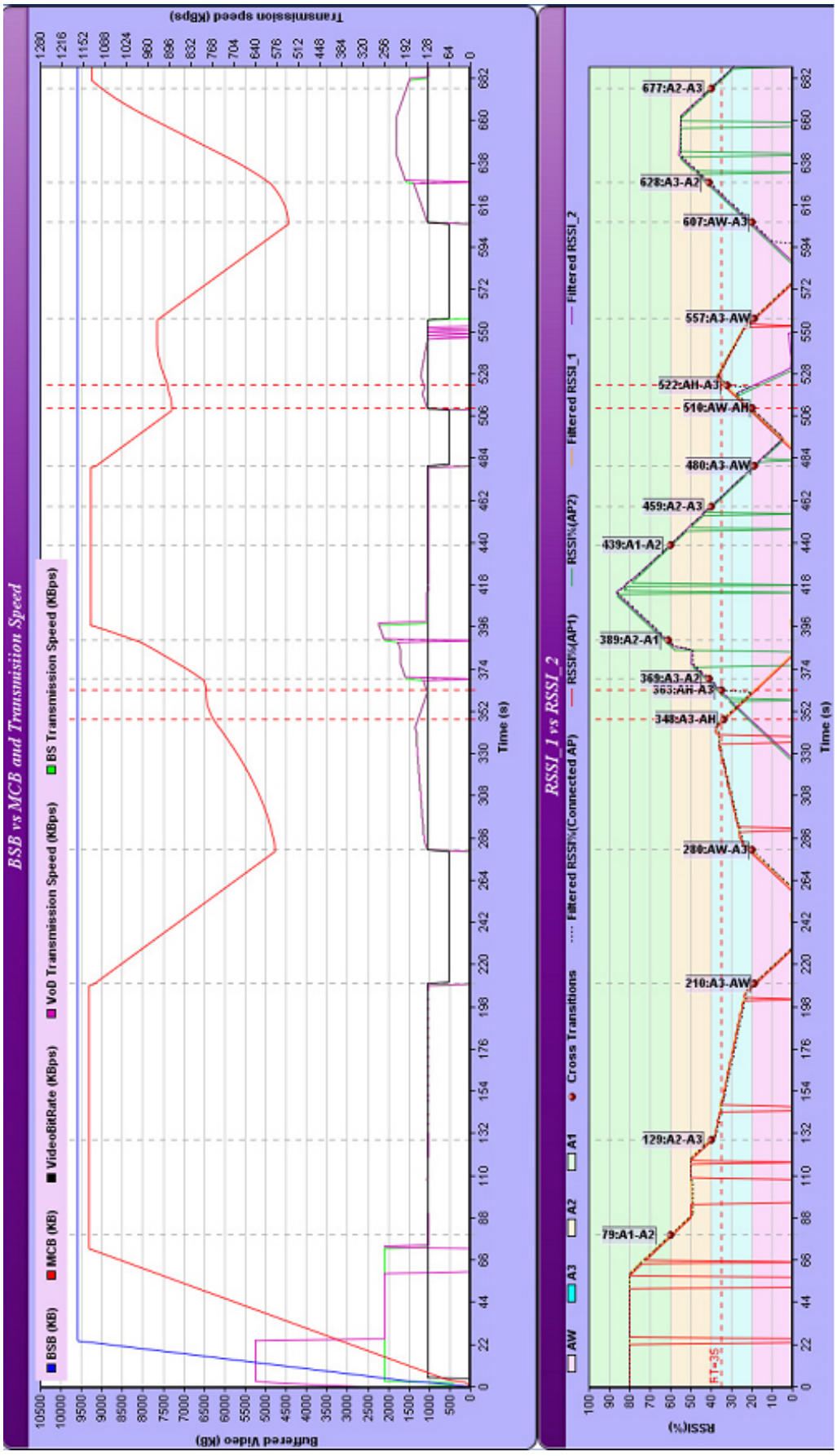

Figure 5.4: Case 1 with long time holes

- Case 2: In Figure 5.5, MC started at A_1 of AP_1, passing to A_2 at t =19 s, to A_3 at t = 40 s, then going back to A_2 at t = 88 s, then to A_3 at t = 129 s for a long time, next disconnecting in A_W at t = 210 s, going back to A_3 of AP_1 at t = 254 s for a very short time, then to A_W at t = 258 s, another time to A_3 at t = 280 s, entering in A_H (t = 351 s to 363 s) to handover to the CA of AP_2 , then to A_2 at t = 372 s, A_1 at t = 391 s, and another time to A_2 at t = 460 s, A_3 at t = 480 s, and disconnecting in A_W at t = 501 s then reconnected to AP_2 at t = 588 s.

  The BSB started buffering before because the BSB needs some time to arrive to the level where it could transmit to MC, the two buffers were maintained at high level till the MC entered A_W (t = 210 s) where it disconnected, then MCB decreased till it connected another time to AP_1 at t = 254 s, after connection in A_3, MCB increased slowly until crossing to A_H to handover to AP_2, where it increased rapidly to arrive another time to MCB_LIMIT_s as BSB. At t = 500 s, MC disconnects in A_W and the MCB went back to decrease till reconnection to increase another time at t = 588 s.

  The playing video speed $V_P = K_P$ all the time except in disconnection periods, it dropped to the medium as clear from Figure 5.5. In this movement also there were many holes that were filtered well by the Gradient Filter and did not affect on the buffer or the transmission speed.

- However in Figure 5.6 is shown the same case 3 but with long holes filtered by the Gradient filter, the first and the longest happened between t = 20 s and 45 s, the second one between t = 100 s and 120 s, and another long one between t = 420 s and 450 s.

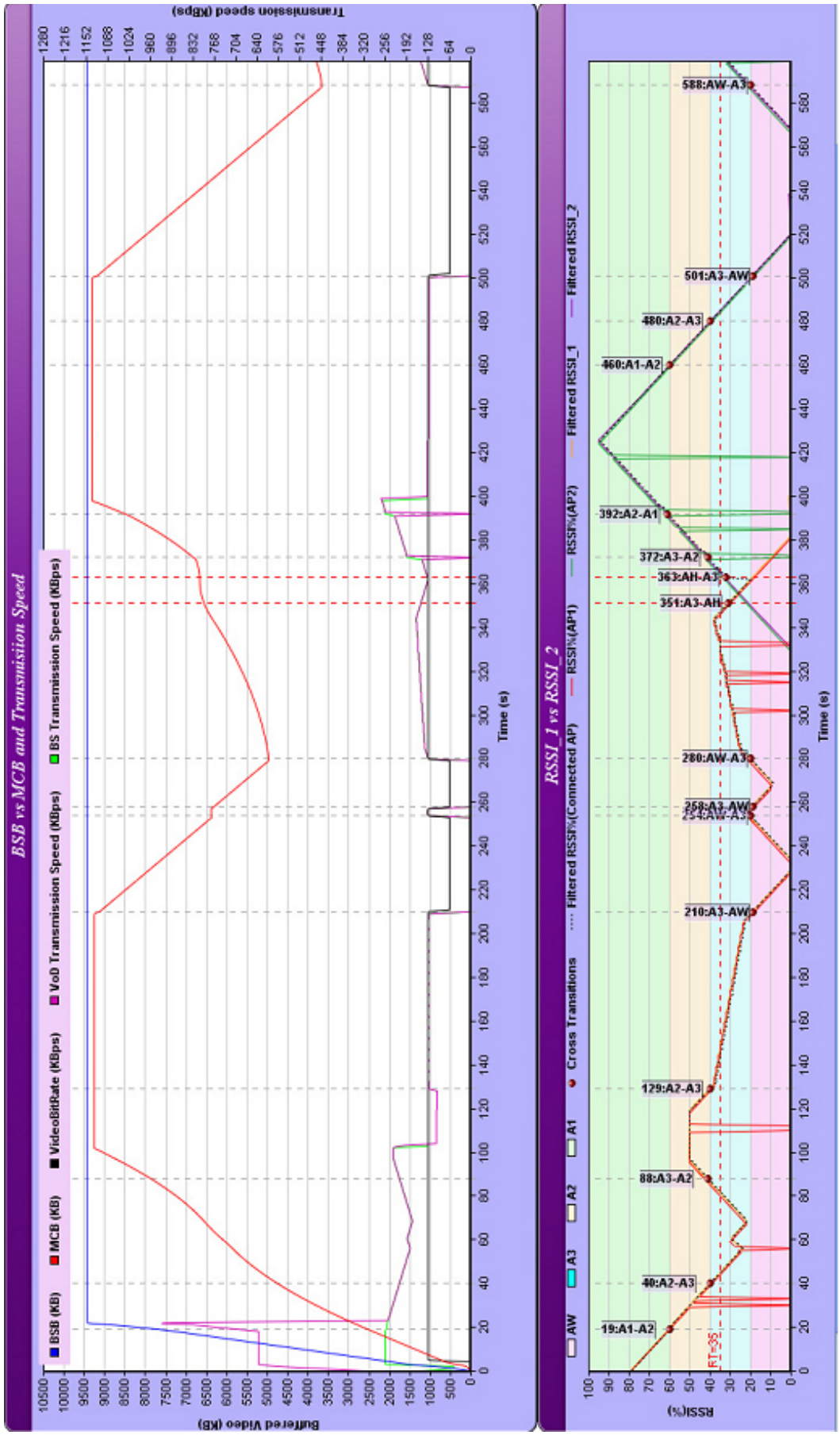

Figure 5.5: Case 2, many holes, handover and out of coverage

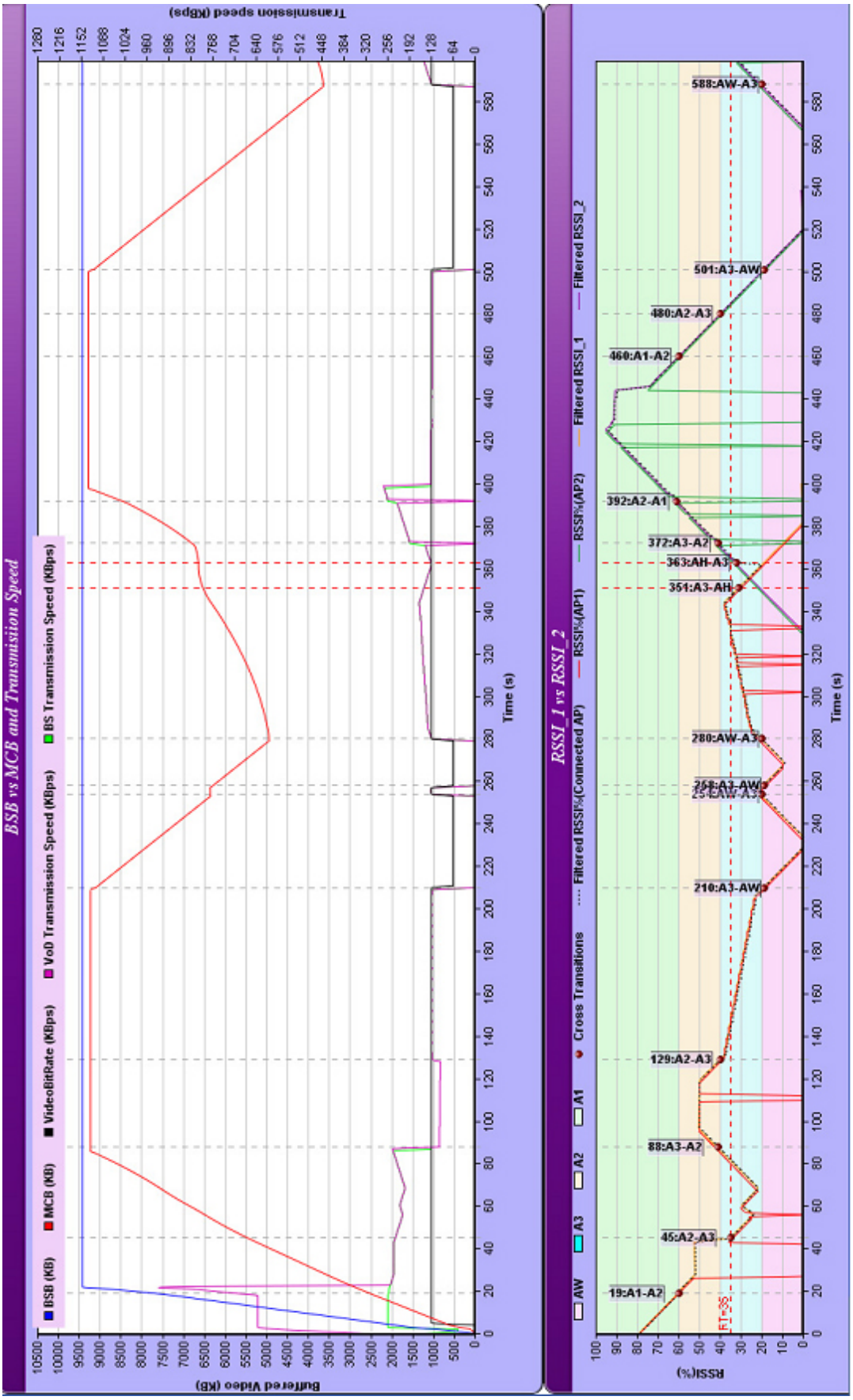

Figure 5.6: Case 2 with long time holes

- Case 3: In Figure 5.7, MC started at A_2 of AP_1, passing to A_1 at t = 22 s, going back to A_2 at t = 44 s, then to A_3 at t = 64 s, next to A_W at t = 85 s, going back to A_3 at t = 91 s, A_2 at t = 112 s then to A_3 at t = 126 s and A_W another time at t = 147 s, going back to A_3 at t = 199 s and A_2 at t = 234 s, finally it continued with zigzag motion between A_2 and A_3. This motion includes some holes. The first transition *Cross_A_2-A_1* happened at t = 22 s which generated *DSVF* command to decrease V_x, then the transition *Cross_A_1-A_2* happened at t = 44 s which generated *ISVF* command to increase V_x till filling the BSB to the BSB_LIMIT_s, when it arrived this limit, V_x would decrease to be equal to the BS transmission speed V_y which happened at t ≈ 50 s. V_y also decreased as the $\Omega(d_{MC})$ decreased, so during the disconnection of A_W (t = 147 s to 199 s) $V_x = V_y = 0$, while V_p had a good value to display the video. After reconnection V_y increased and MCB increased also to arrive to MCB_LIMIT_s. As shown inFigure 5.7, MCB remained in this limit because there was not any disconnection during the zigzag motion. It is illustrated the relation between V_y and $\Omega(d_{MC})$, as the $\Omega(d_{MC})$ decreased, V_y decreased.

- In Figure 5.8, MC has the same movements as case 4, but in this case there were some long holes which were filtered by the Gradient filter, and they did not affect on buffers, thus the same curve of buffer's values yielded this case. The first long hole appeared between t = 20 s and 40 s, the other one between t = 100 s and 120 s. It is clear from Figure 5.7 that the filter works very well.

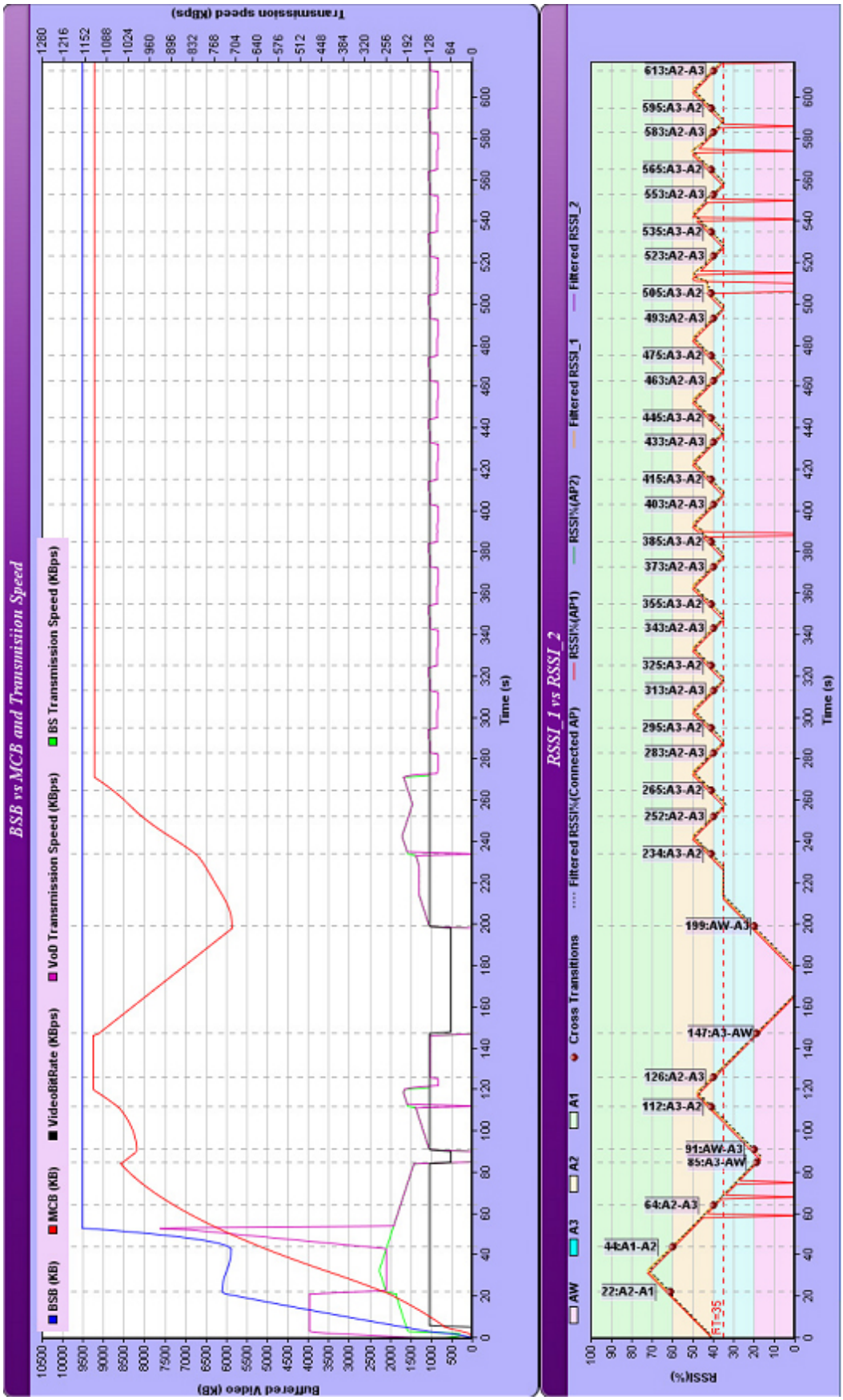

Figure 5.7: Case 3, MC movement in zigzag motion

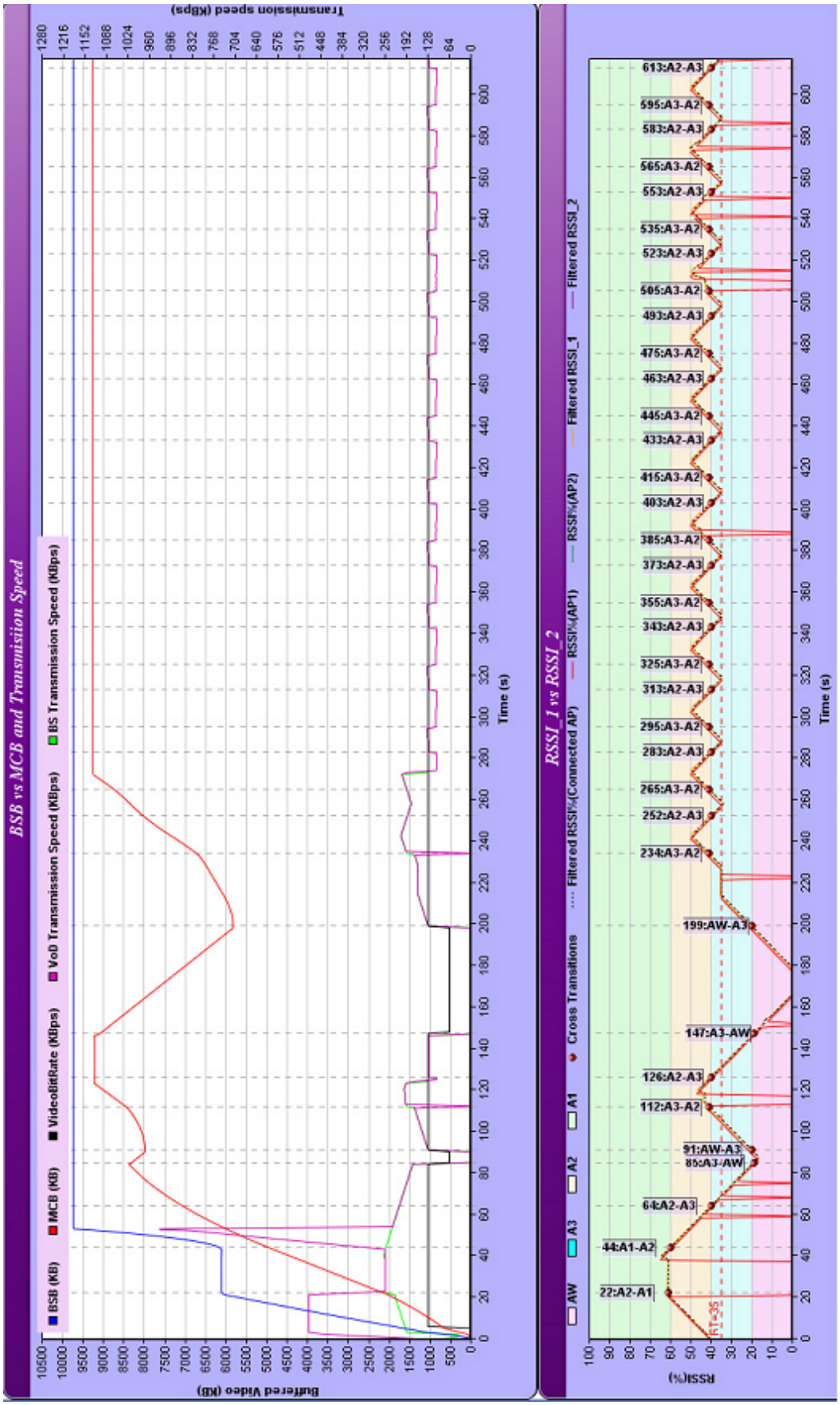

Figure 5.8: Case 3 with long time hole

- Case 4: It is a special case of movement (Figure 5.9) where MC has constant $\Omega(d_{MC})$ all the time, this case demonstrates how the technique works to keep the level of BSB and MCB in the BSB_LIMIT_s and MCB_LIMIT_s respectively, and the playing video speed V_P remains all the time in its maximum value.
- Case 5: It is shown in Figure 5.10, MC started from A_3, crossing to A_2 at t = 16 s then A_1 at t = 37 s, going back to A_2 at t = 74 s, A_3 at t = 120 s to stay there with constant $\Omega(d_{MC})$ for a long time, then crossing to A_W at t = 263 s and going back to A_3 at t = 279 s, A_2 at t = 320 s, and finally to A_1 at t = 360 s to stay there with constant $\Omega(d_{MC})$ for a long time, there was not any handover process because there was not any other AP detected. In this case there were some long holes as the one appeared between t = 44 s and 66 s, another one between t = 374 s and 396 s.
- Case 6: MC started at A_3 of AP_1 as shown in Figure 5.11, then crosses to A_W at t = 26 s where it found another connection with AP_2 at t = 77 s to stay in A_3 for along time, next it moved to A_2 at t = 193 s and A_1 at t = 212 s to continuo in constant $\Omega(d_{MC})$ all the time. When MC entered in disconnection state, MCB was not full because MC just started its connection before a very short time, therefore the playing video $V_P = 0$ during this disconnection as long as the MCB in its MCB_LIMIT_i. Also VoD transmission speed and BS transmission speed $V_x = V_y = 0$, because BSB in its BSB_LIMIT_s. At t = 77 s MC connected to AP_2 and MCB started buffering to exceed MCB_LIMIT_i then $V_P = K_p$. In this movement, some long holes were found, one at t = 140 s and another long hole between t = 320 s and 340 s.

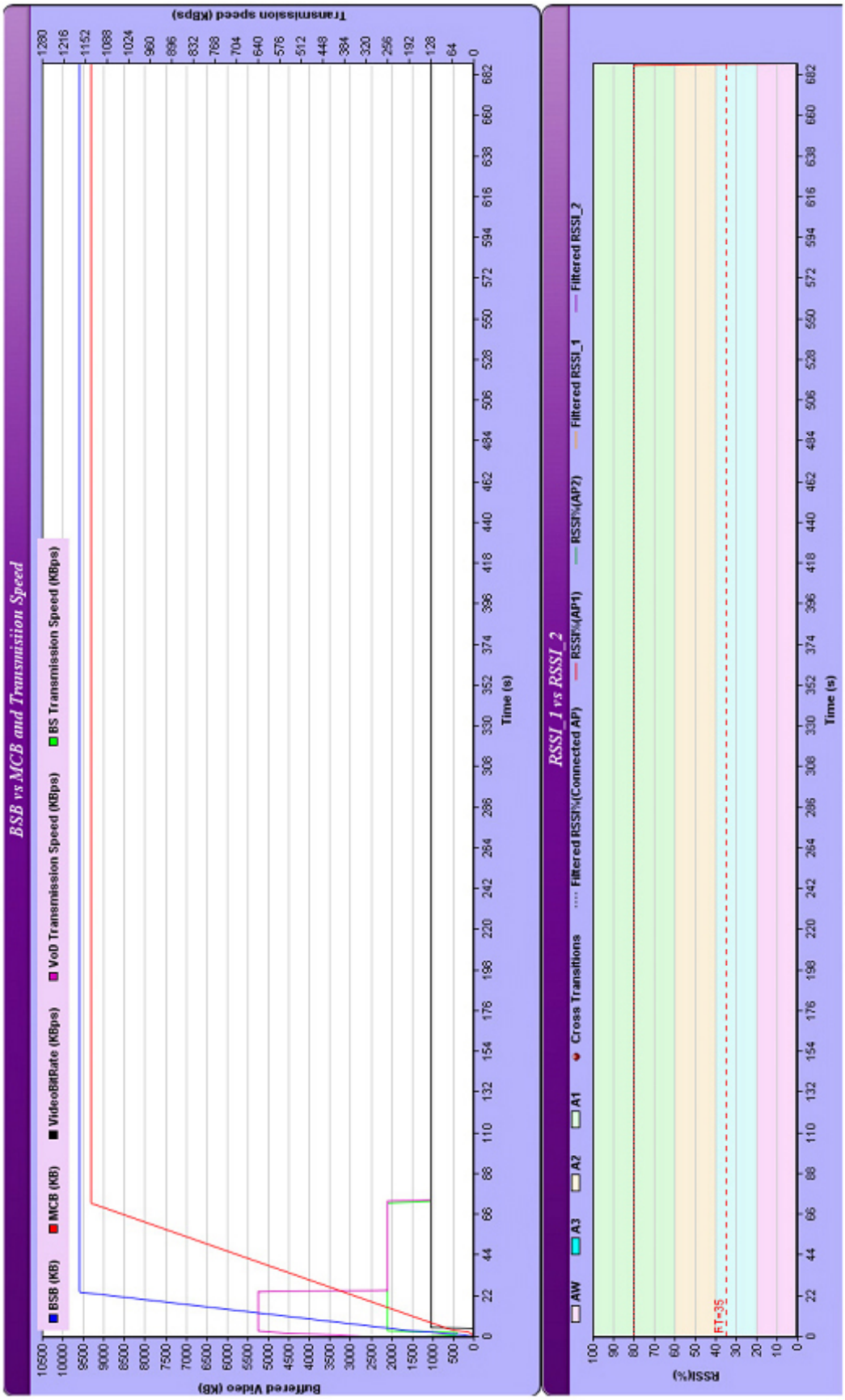

Figure 5.9: Case 4 is special case of constant RSSI% in A_1

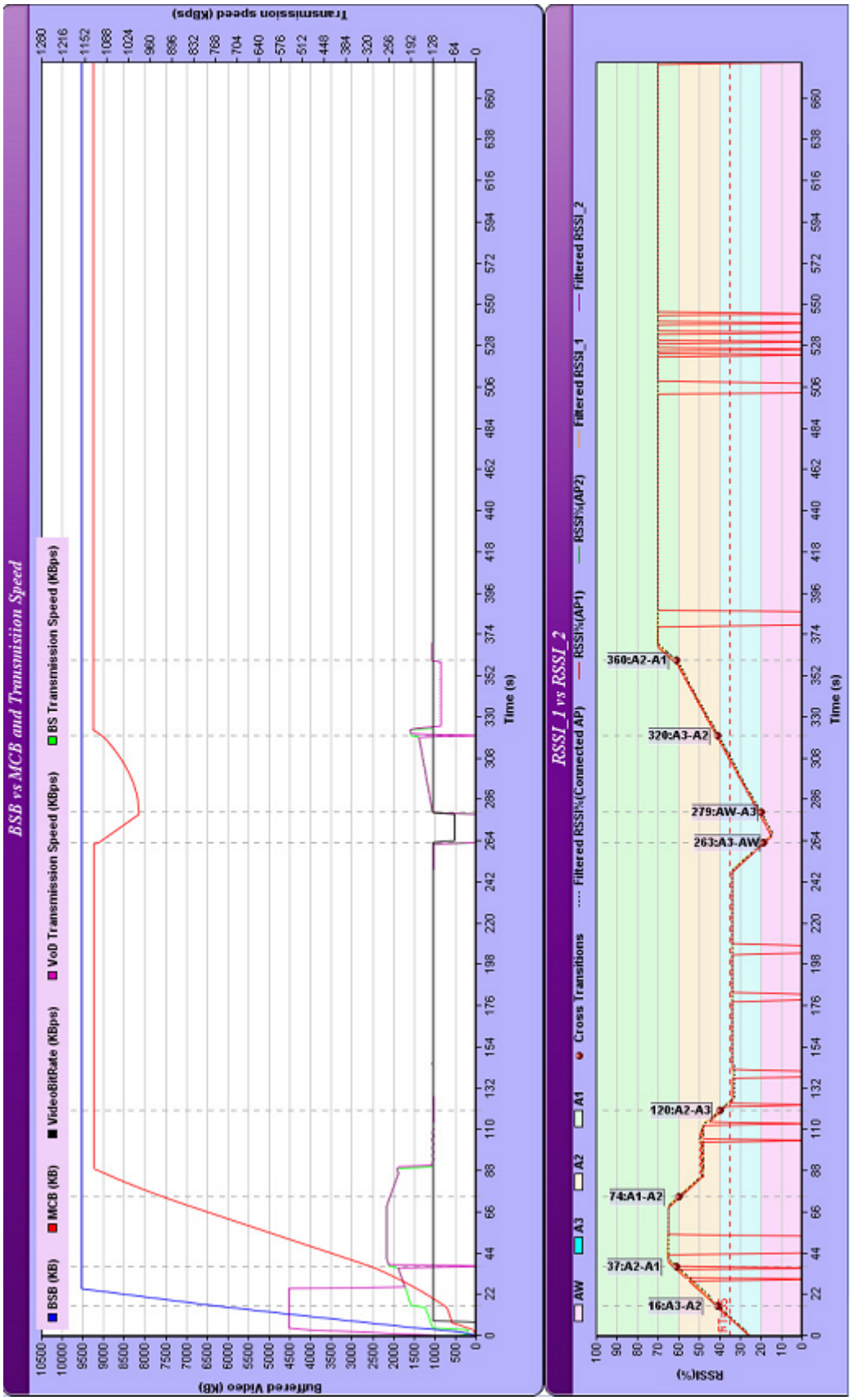

Figure 5.10: Case 5, MC starts in A3, constant RSSI% in some times and long time hole

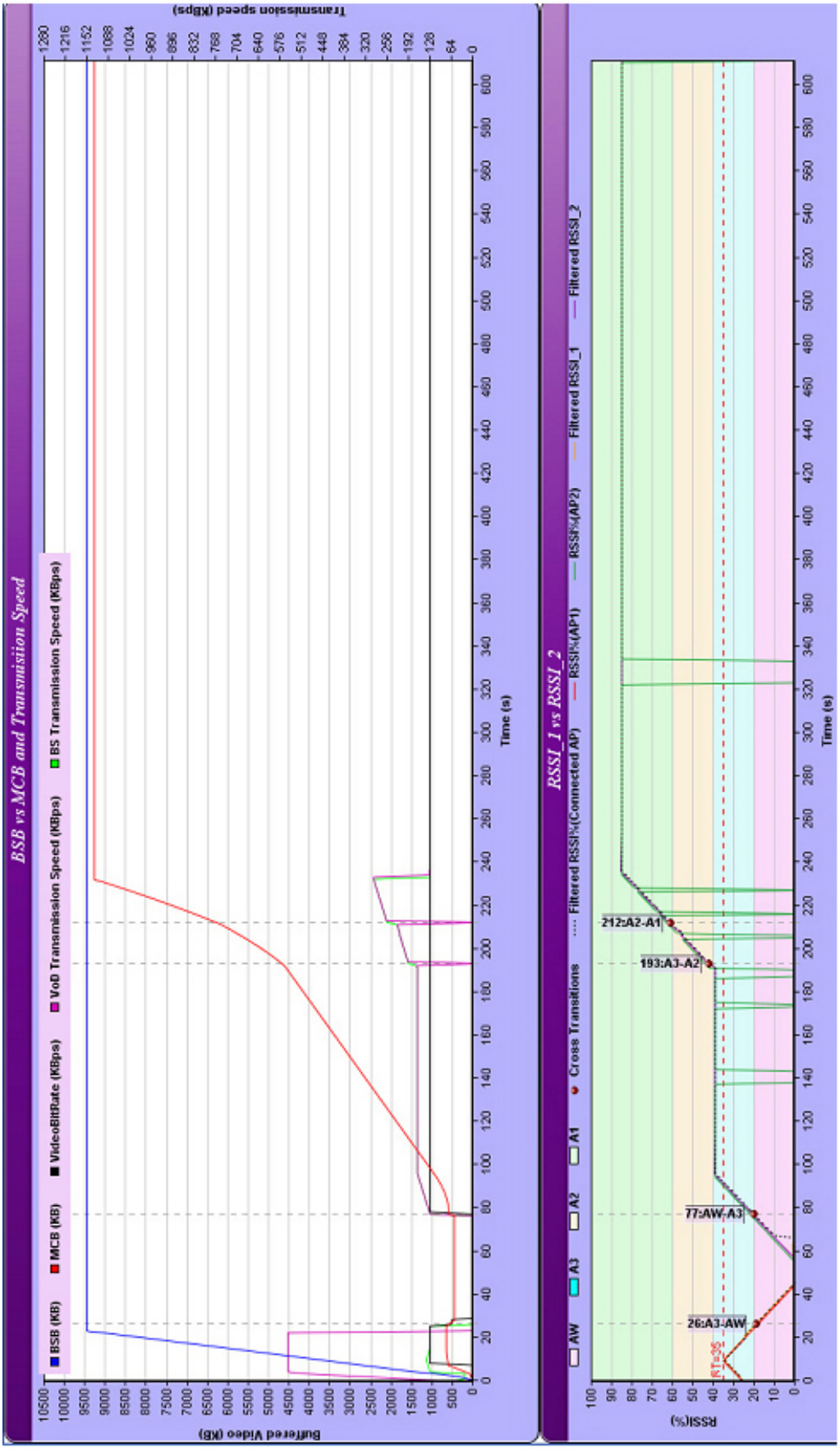

Figure 5.11: Case 6, early disconnection

- Case 7: In Figure 5.12 is shown a test for a long disconnection period, MC started moving in the first part as the previous case, whereas in the second part from t = 212 s, $\Omega(d_{MC})$ decreased till disconnection state which lasted a long time until MCB arrived to the MCB_LIMIT_i between t = 384 s and 400 s causing the V_P = 0, that means the MCB needed about 135 s ≈ 2.5 m to arrive its MCB_LIMIT_i. An important relation between this duration of time needed to disconnect and the difference between the MCB_LIMIT_s and MCB_LIMIT_i, as the difference increased the duration of time increased also.
- Case 8: It is shown in Figure 5.13, in this case also a long disconnection period is illustrated after a long constant $\Omega(d_{MC})$ in A_1, MC started disconnection at t = 354 s and MCB arrived to its MCB_LIMIT_i at t = 490 s, so it took the same duration as the previous case.

As a conclusion, the proposed and simulated protocol provided solutions for three problems:

- Transmission speed control is sufficient to manage the buffering process which avoids streaming packets loss during short disconnections. As demonstrated above, the buffer was kept near its upper limit, and just during the disconnections it was under this level, while the playing video had adequate quality always (Figures 5.3, 5.4, 5.5, 5.6, and 5.10). it could support disconnection periods up to 135 s.
- The Gradient predictor could predict the next state of MC allowing the speed control commands to be executed before disconnections. As shown in all the previous figures, the values of the filtered and predicted $\Omega(d_{MC})$ were very close to the real values, which indicate that the predictor performance is very good and precise, in accordance with the synthetic test comparing to other predictors.
- The Gradient filter provided a very powerful solution for holes problem. It is an effective filter, which was proved in all the discussed cases of holes: Short holes (1 s) and long holes (18 s).

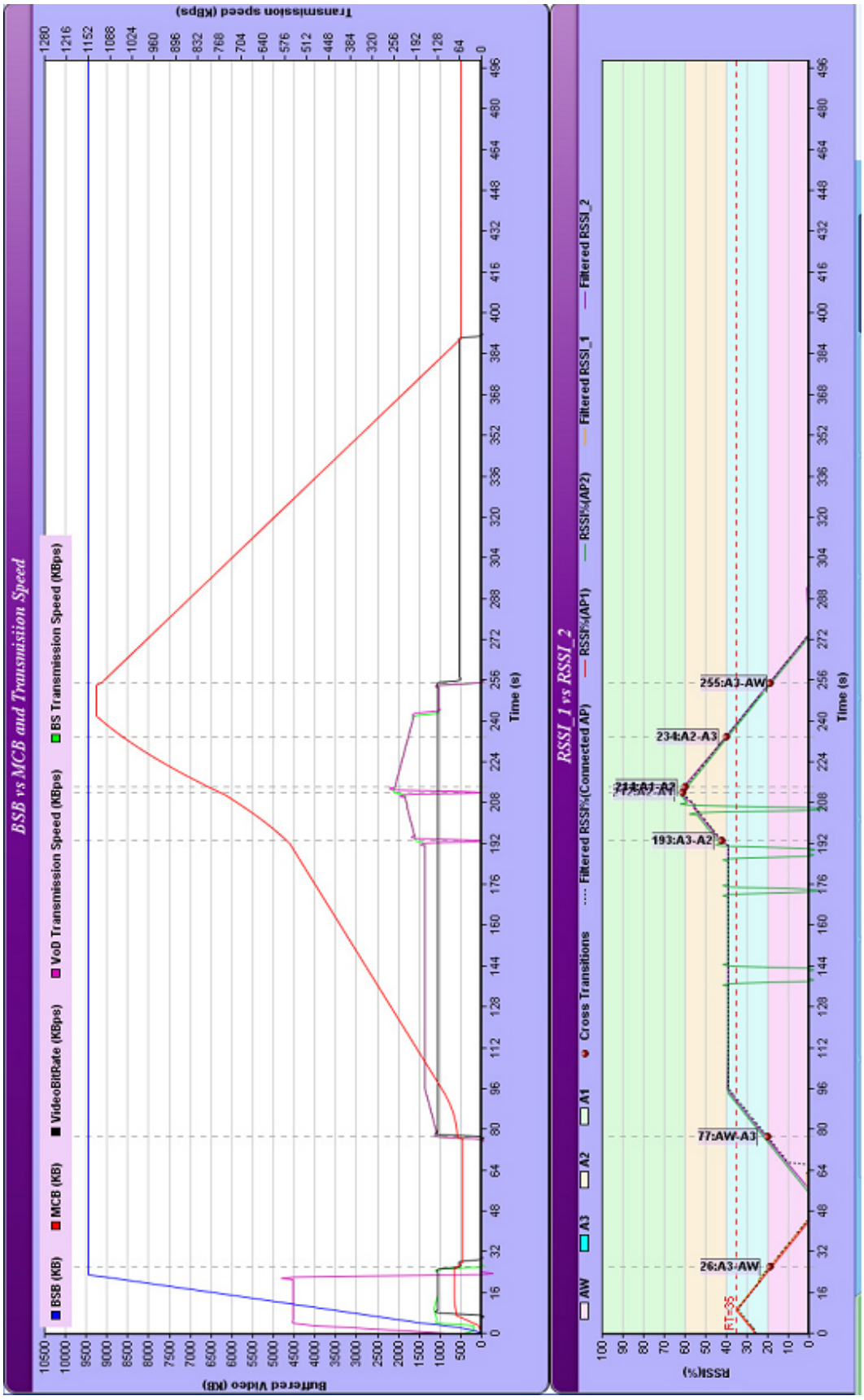

Figure 5.12: Case 7, disconnection for a long time

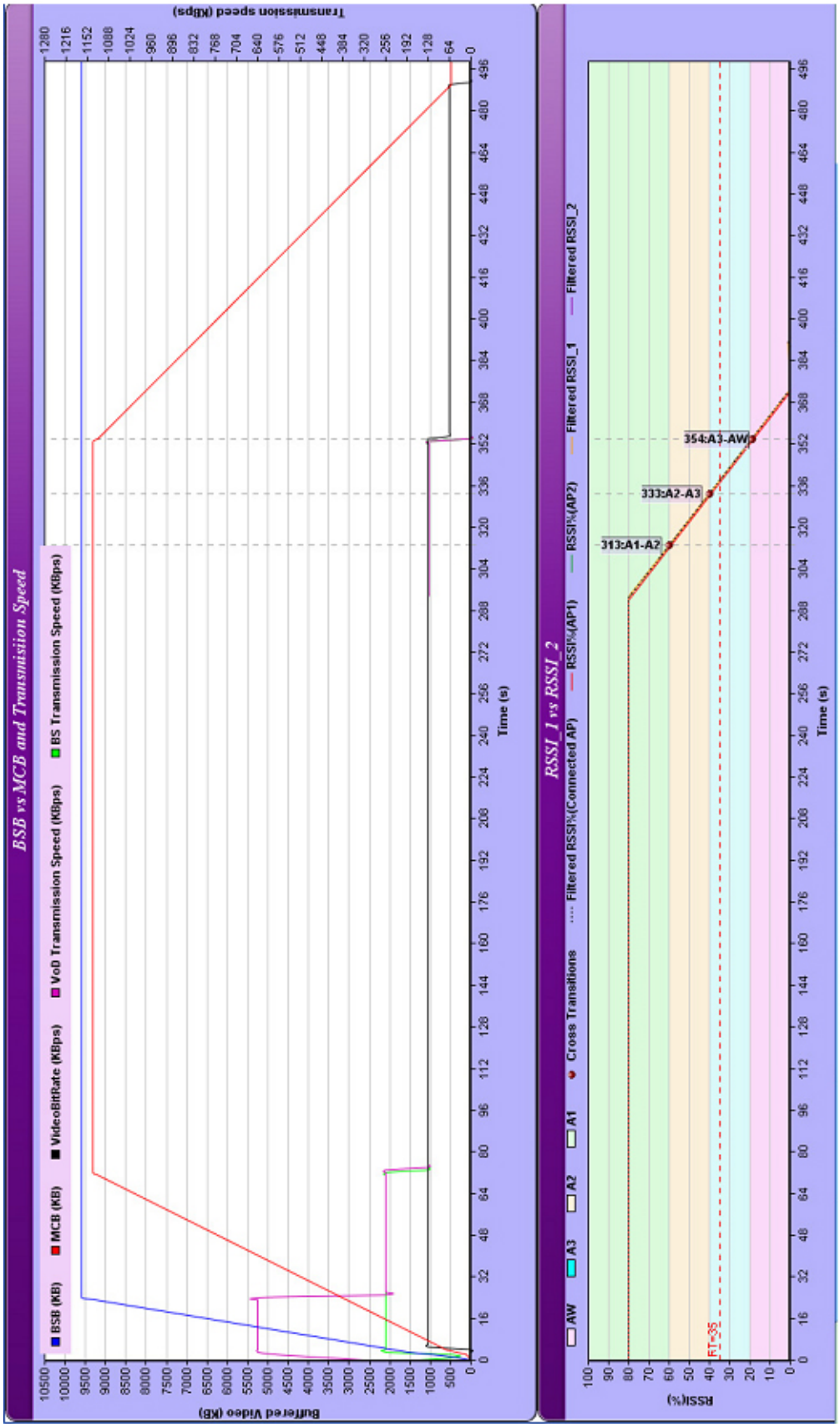

Figure 5.13: Case 8, constant RSSI% and long disconnection period

CHAPTER 6

CONCLUSIONS AND FUTURE WORK

After three years working in my PhD Thesis we summed up our principal future work.

6.1 Conclusions

Nowadays, multimedia services are experiencing rapid development due to the growing popularity of RTMAs. Most of these applications use the streaming technology to offer services via Internet such as VoIP and VoD. Thus, WiFi and WiMAX wireless networks support RTMAs and provide the user with variety of multimedia services.

The MC can request video streaming services while it is inside CA of WiFi AP. During its movement it could experiment disconnections due to signal fluctuations, which are caused by coverage holes, handover, or when the MC is out of CA. Consequently, there were many works addressed this problem, some of them were interested only in the disruption caused by handover, others focused in the prediction.

The holes are positions inside CA where the signal drops suddenly and sporadically. This makes the holes provoke sporadic and impossible to predict disconnections of the MC. If the MC spends a considerable amount of time inside hole then it will suffer a long and unexpected disconnection. In case it spends a short interval of time some video frames could be lost. Up to our knowledge, minor amount of works focused in the coverage holes due to the associated disconnections are very difficult to control.

In these situations the MC will suffer video services disruptions during the mentioned disconnections, causing a big degradation of QoS and QoE.

Many papers have presented buffer management techniques to reduce the degradation of QoS controlling the size of the buffer to be consumed by the MC before it will be disconnected. But there is a lack of an effective protocol to mitigate the disruption caused by the mentioned disconnections caused by holes.

Therefore, we developed an effective protocol based on a new mathematical specification for the CA, and MC movement's identification considering the holes. The protocol consists of two techniques:

- The RSSI Gradient Predictor and Filter were developed as a filtering technique to mitigate the adverse effects of coverage holes. The filter was derived from the average gradient of RSSI sample set when the MC moves in regular motions at constant speed. It used the average gradient to calculate the RSSI in future instant time.
- The buffer management and transmission speed control technique to mitigate the video streaming packets loss. A state diagram for MC movements was used to

generate transitions in case that the MC crossed different coverage zones. Every transition generated commands to control the transmission speed of the VoD server and the BS, leading to effective BSB and MCB management. This technique keeps both of them in the upper limit as long as possible to provide the MC with the required video frames during the disruption duration.

The synthetic and the experimental tests of the RSSI Gradient Predictor and Filter demonstrated that it has the best results comparing with the Kalman filter and the Grey model. It filtered all the existing holes of different sizes in all cases and predicted the next MC coverage level accurately.

The protocol verification and simulation results proved its efficiency, the protocol was suitable for all types of disruptions caused by holes, handover, or out of coverage, it offered sufficient amount of video frames to be consumed during the mentioned disconnections, even for long time disruptions of about 135 s. resulting in continuous adequate video playing bit rate and offering enough time to the user to move from a CA to another without interruptions.

6.2 Future Work

We provided the predictor and filter that were based on regular motions considerations, the periodic patterns of MC movement were addressed whereas the non periodic patterns could not be treated. Therefore we consider it is important to develop our work in the future through improving three important lines:

- Studying more complex non-periodic patterns of MC movement models in order to find new mathematical specifications for these patterns.
- Developing the filter using the new specification to be suitable for any movement models including patterns of unexpected coverage levels.
- Developing the protocol using the improved filter will provide it with high capabilities to treat complex disruptions cases.

CAPITULO 7

RESUMEN AMPLIO

7.1 Aplicaciones Multimedia a Tiempo Real

Las Aplicaciones Multimedia a Tiempo Real (*RTMA* del inglés *Real Time Multimedia Applications*) son aplicaciones que necesitan enviar y recibir media streams a través de los canales de comunicación, los paquetes de datos recibidos deben ser decodificadas antes de emitir el audio y el vídeo en el receptor final [1]. Hoy en día, las RTMAs están experimentando un rápido desarrollo debido a la creciente popularidad de las aplicaciones de vídeo [2]. Por lo tanto, una *Red Inalámbrica de Área Local* (*WLAN* del inglés *Wireless Local Area Networks*) como IEEE 802.11 soporta RTMA, principalmente como *Voz sobre Protocolo de Internet* (*VoIP* del inglés *Voice over Internet Protocol*) y servicios de vídeo [3]. Por otra parte, una *Red Inalámbrica de Área Metropolitana* (*WMAN* del inglés *Wireless Metropolitan Area Network*) como IEEE 802.16 ofrece mejor capacidad de ofrecer servicios inalámbricos, como la transmisión de multimedia, y vigilancia a tiempo real [4].

La mayoría de los tipos de RTMA utilizan la tecnología de streaming para ofrecer los servicios de audio y vídeo vía Internet. *Streaming* es el método de distribución de audio y vídeo que se distribuyen a través de redes de telecomunicaciones, y transmitidos a través de una red de *Protocolo de Internet* (*IP* del inglés *Internet Protocol*), desde un host de origen hasta un host de destino. Muchos protocolos de red han sido diseñado específicamente para el streaming media [4], así algunas de ellas proporcionan soporte a los servicios básicos de red en la capa de red, otros funcionan en la capa de transporte como el *Protocolo de Datagramas de Usuario* (*UDP* del inglés *User Datagram Protocol*) y el *Protocolo de Control de Transmisión* (*TCP* del inglés *Transmission Control Protocol*) [5], pero algunos protocolos definen los mensajes y procedimientos en la capa de aplicación para controlar la entrega de datos multimedia como el *Protocolo de Streaming de Datos a Tiempo Real* (*RTSP* del inglés *Real-Time Streaming Protocol*), y el *Protocolo de Inicio de Sesiones* (*SIP* del inglés *Session Initiation Protocol*) [4].

El *VoIP* es un protocolo importante que utiliza la tecnología IP para transmitir paquetes de datos de voz. En este proceso, la voz es convertida a una señal digital, que es comprimido y luego dividido en una serie de paquetes que se transportan a través de la red IP, luego estos paquetes se reúnen y descifraran en el host receptor [6]. *Skype*, *MSN*, *Google Talk* y *VoipBuster* son ejemplos de las aplicaciones VoIP.

El *Streaming de Multimedia a Tiempo Real* es un RTMA que incluye dos mecanismos comunes de distribución sobre la red IP que son streaming en directo y streaming bajo demanda. En el *streaming en directo*, hay una conexión directa entre el codificador y el servidor donde el codificador esta capturando, digitalizando y comprimiendo la señal analógica recibida de vídeo y audio, y pasando el archivo comprimido resultante al servidor. Mientras que el *streaming bajo demanda* no tiene una conexión directa entre el codificador y el receptor ya que el vídeo comprimido debe ser almacenado y luego el usuario puede utilizarlo para la distribución. Por otra parte, la comunicación entre el servidor y el cliente para el contenido bajo demanda es lo mismo como el contenido en directo, la principal diferencia es que en el contenido bajo demanda, el usuario puede retroceder o adelantar el vídeo, sin embargo esta opción no es disponible en el streaming en directo. Así, el vídeo a tiempo real constituye un ejemplo de transmisión en directo [4], y el *Vídeo bajo Demanda* (*VoD* del inglés *Vídeo on Demand*) constituye un ejemplo de streaming bajo demanda. Este último es un sistema multimedia interactivo, donde el cliente puede elegir una película de una base de datos de vídeo almacenados en un servidor de vídeo. Además, el sistema puede proporcionar al usuario unas funciones, incluyendo: pausa, avance rápido, retroceso rápido, lento avance y retroceso lento, ir al anterior / futuros frames.

La mayoría de RTMA necesitan *Calidad de Servicio* (*QoS* del inglés *Quality of Service*) alta y una demanda alta de red debido a los requisitos especiales de la percepción de vídeo y audio, que son muy sensibles al retraso y al jitter, y requieren un gran ancho de banda [5]. Esto significa que los RTMA requieren un rendimiento especial de la red que se mide por parámetros tales como: la pérdida de paquetes, jitter, ancho de banda, puntualidad, confiabilidad y el coste [7]. Por ejemplo, la videoconferencia requiere un retraso de end-to-end que no se demore más de 200 ms, y como resultado la posibilidad de retransmitir los paquetes perdidos es limitada [3]. Sin embargo, las características del canal inalámbrico, tales como el sombreado, desvanecimiento de multi-ruta, y las interferencias siguen limitando el ancho de banda disponible para las aplicaciones desplegadas. Todos los usuarios de RTMA buscan la continua recepción del streaming real de vídeo y audio. Además, muchos requisitos son importantes como imágenes de alta calidad, debido a que los sistemas de imágenes pueden introducir cierta cantidad de distorsión o artefactos en la señal, por lo que la evaluación de la calidad es muy importante [8]. Asimismo el usuario desea recibir audio

de alta calidad (la cantidad de claridad del audio), que es muy difícil porque se ve afectada por muchos factores, como el retraso prolongado de la trayectoria de la voz [Web-1]. Algunos códigos de audio han sido desarrollados para mejorar la calidad de audio como la *Alta Eficiencia Codificación de Audio Avanzado* (*HE-AAC* del inglés *High-Efficiency Advanced Audio Coding*). *La Puntuación Media de Opinión* (*MOS* del inglés *Mean Opinion Score*) proporciona una indicación numérica de la calidad percibida de los medios recibidos después de la compresión y transmisión, MOS se expresa como un número único en el rango de 1 a 5, donde 1 es la menor calidad percibida (inaceptable), y 5 es la calidad percibida más alta (excelente) [4].

7.1.2 Estándares de las redes inalámbricas

Hoy en día muchas redes inalámbricas están disponibles para soportar RTMA WiFi y IEEE 802.11; algunos ejemplos de estas tecnologías son WiFi y *Interoperabilidad Mundial para Acceso por Microondas* (*WiMAX* del inglés *Worldwide Interoperability for Microwave Access*).

7.1.2.1 WiFi y IEEE 802.11

WiFi es la tecnología inalámbrica que se basa en el estándar IEEE 802.11 y está certificada por la WiFi Alliance, es una asociación global especializada en la certificación para mejorar la experiencia de usuario para dispositivos móviles inalámbricos [Web-2].

WiFi puede proporcionar datos a alta velocidad para zona limitada hasta 200 m, IEEE 802.11a puede proporcionar hasta 54 Mbps a 5 GHz en banda sin licencia [9], y IEEE 802.11b permite hasta 11 Mbps a 2,4 GHz en banda sin licencia [10], y IEEE 802.11g ofrece hasta 54 Mbps en banda de 2,4 GHz sin licencia [11]. IEEE 802.11 Grupo-n de Trabajo publico la nueva especificación IEEE 802.11n que se basa en la tecnología de interfaz aérea *Múltiples Entradas Múltiples Salidas* (*MIMO* del inglés *Multiple Input Multiple Output*), que incluye la mejora de rendimiento, seguridad, y el roaming, y soporta la operación ya sea en la banda de 2,4 GHz o las bandas de 5 GHz, que permite un flujo de datos de hasta 600 Mbps que operan en 20 MHz o 40 MHz de ancho de banda [12].

El IEEE 802.11 es el actual estándar líder de WLAN que soporta RTMA como VoIP y la videoconferencia [3] para las estaciones móviles y portátiles [13] [14], que se

logra por las dos altas velocidades IEEE 802.11g y IEEE 802.11n y la capa 802.11e QoS basada en *Control de Acceso Medio* (*MAC* del inglés *Medium Access Control*) [13]. IEEE 802.11 especifica dos capas físicas [15]: *Espectro Ensanchado por Secuencia Directa* (*DSSS* del inglés *Direct Sequence Spread Spectrum*) y la *Espectro Ensanchado por Salto de Frecuencia* (*FHSS* del inglés *Frequency Hopping Spread Spectrum*).

En el mercado, hay una gran cantidad de dispositivos WiFi que soportan la RTMA, tales como los teléfonos VoIP, TV, reproductores de MP3, consolas de videojuegos, y otros reproductores multimedia. Por ejemplo, en casa, los dispositivos inalámbricos pueden utilizarse para proporcionar conectividad inalámbrica de voz a través de los teléfonos VoIP WiFi, además, una WLAN podría ser utilizada para distribuir los contenidos de un servidor multimedia a cualquier dispositivo en el hogar [Web-3].

El estándar IEEE 802.11 es caracterizado por su sencillez y robustez frente a los fallos debidos al enfoque distribuido de su protocolo MAC [16].

IEEE 802.11 LAN puede funcionar en el modo de red Ad-Hoc, donde MC puede comunicarse directamente con otro *Cliente Móvil* (*MC* del inglés *Mobile Client*) sin la necesidad de un *Punto de Acceso* (*AP* del inglés *Access Point*) para conectarlos, en este caso forman el *Conjunto Independiente de Servicios Básicos* (*IBSS* del inglés *Independent Basic Service Set*) [14] [17].

El protocolo básico IEEE 802.11 MAC es la *Función de Coordinación Distribuida* (*DCF* del inglés *Distributed Coordination Function*) [15] [16] que emplea *Acceso Múltiple por Detección de Portadora con Evasión de Colisiones* (*CSMA*/*CA* del inglés *Carrier Sense Multiple Access with Collision Avoidance*) como método de acceso [13], pero IEEE 802.11e introduce el protocolo *Función de Coordinación Hibrida* (*HCF* del inglés *Hybrid Coordination Function*) para soportar QoS. El HCF define dos mecanismos de acceso al medio: acceso de canal contención-basado y acceso de canal controlado [16].

En el modo de infraestructura de IEEE 802.11 (Figura 7.1) todos los MCs están asociados a AP. La estructura de interconexión forma el *Conjunto de Servicio Básico* (*BSS* del inglés *Basic Service Set*). La conexión de más de AP puede extender un BSS a un *Conjunto de Servicio Extendido* (*ESS* del inglés *Extended Service Set*) [17].

Cualquier MC puede seguir en comunicación con los otros MCs que se encuentran dentro de la *Área de Cobertura* (*CA* del inglés *Coverage Area*) de su BSS, que es conocida como *Área de Servicio Básico* (*BSA* del inglés *Basic Service Area*) [14][18]. En otro lugar, hay muchas posibles ubicaciones físicas de BSS, que pueden solapar parcialmente, separarse físicamente, colocarse físicamente, o pueden estar presentes físicamente en el mismo espacio [14].

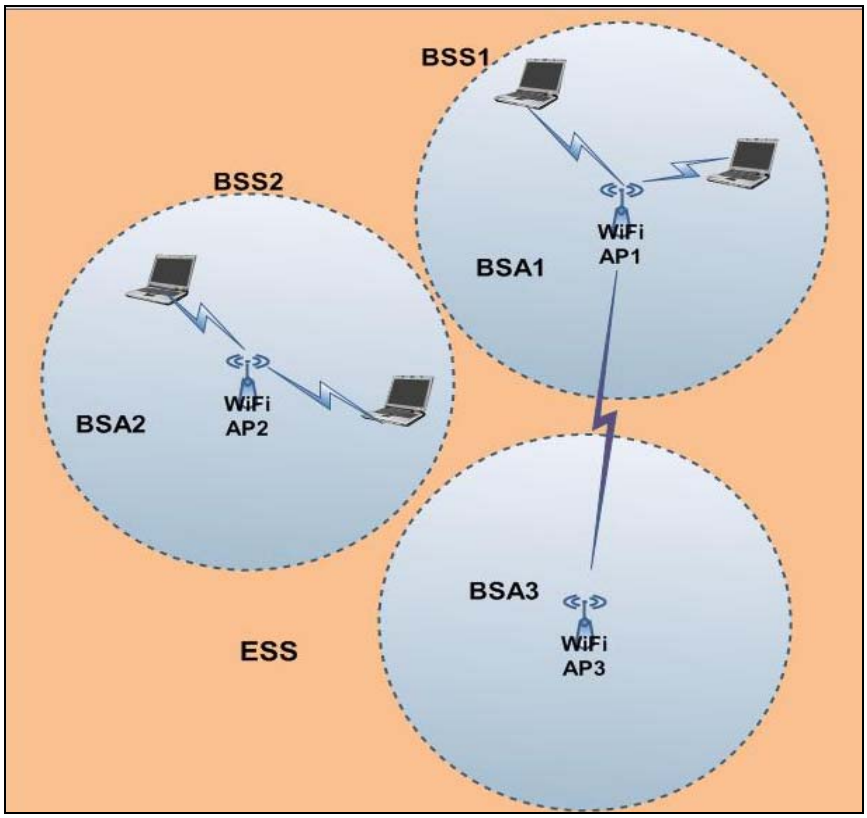

Figura 7.1: Topologías de redes WiFi

Soporte del QoS enWiFi*: *IEEE 802.11e

Con el control de QoS, el AP WiFi puede priorizar el tráfico y optimizar la manera de compartir recursos de red entre las diferentes aplicaciones. Así, todas las aplicaciones dentro las redes WiFi requieren un control QoS, e en su ausencia, todas las aplicaciones que se ejecutan en diferentes dispositivos tienen la misma prioridad para transmitir frames de datos [Web-3]. Por lo tanto, no es posible dar prioridad a los paquetes de datos de dichas aplicaciones con el DCF enfoque predeterminado, de modo que las correcciones del IEEE 802.11e se introducen para proporcionar características necesarias para priorizar los paquetes de RTMA [19][20]. La única característica del IEEE 802.11e que esta incluida por el WiFi Alliance en el programa de certificación del

Multimedia Inalámbrico (*WMM* del inglés *Wireless Multi-Media*), es *El Canal de Acceso Distribuida Mejorada* (*EDCA* del inglés *Enhanced Distributed Channel Access*) que es soportado por muchos dispositivos [21].

El WMM define cuatro clases de prioridad: voz, vídeo, fondo y mejor esfuerzo, para cada uno de ellos se especifica el valor máximo del temporizador aleatorio. Como el temporizador aleatorio es menor que la posibilidad de un dispositivo para acceder a la interfaz de aire es mayor. WMM también define el tiempo máximo permitido para un fotograma de cierta clase de bloquear la interfaz de aire. El vídeo tiene un valor de temporizador ligeramente superior a la voz, y los frames de datos de VoIP pueden siempre ser enviados antes de paquetes de datos en la cola del mejor esfuerza. Estas aplicaciones, utilizan el campo *Servicios Diferenciados* (*DiffServ* del inglés *Differentiated Services*) de la cabecera de un paquete IP para informar la capa del protocolo sobre la cola de prioridad, mientras que el AP o el módem de *Línea de Suscriptor Digital* (*DSL* del inglés *Digital Subscriber Line*) es responsable del QoS en las conexiones de red [21].

7.1.2.2 WiMAX y IEEE 802.16

WiMAX es una reciente tecnología de acceso inalámbrico basada en IP [Web-4], y permite los operadores a proporcionar clientes con múltiples servicios de multimedia a tiempo real [22]-[25] como VoD, VoIP, chatear en tiempo real, *El Internet Móvil* (*MI* del inglés *Mobile Internet*) [Web-4].

El sistema WiMAX publicación 1 se basa en el IEEE 802.16e-2005 y IEEE 802.16e-2009, mientras que publicación 2 es basado en IEEE 802.16m que es previsto ser completado próximamente. Estas versiones de los estándares IEEE 802.16 son las claves del programa certificado del Foro de WiMAX [Web-5] [Web-6].

El IEEE 802.16d (o IEEE 802.16-2004), para un WiMAX fijo, no suportan la movilidad, mientras que el IEEE 802.16e-2005 para el WiMAX Móvil lo suporta. Este último funciona en las frecuencias entre 2 y 11 GHz, y ofrece escalabilidad tanto en la tecnología de acceso de radio y canales de red de 1,25 a 20 MHz [Web-7]. Por otra parte, WiMAX publicación 2 suporta varios canales de 20 MHz [Web-8].

El WiMAX Móvil publicación 1 es capaz de soportar un sector de *Enlace Descendente* (*DL* del inglés *DownLink*) de picos con una velocidad de datos de hasta 46

Mbps, suponiendo una relación de DL/UL de 3:1, y el pico *Enlace Ascendente* (*UL* del inglés *UpLink*) sector de velocidad de datos de hasta 14 Mbps, suponiendo un DL/UL ratio de 1:1, en un canal de 10 MHz. Además, el WiMAX móvil puede cubrir una célula de 2-5 Km. [Web-8]. El IEEE 802.16e es una tecnología basada en la *Multiplexación por División de Frecuencias Ortogonales* (*OFDM* del inglés *Orthogonal Frequency Division Multiplexing*), que es una tecnología que permite al WiMAX lograr un rendimiento y una capacidad óptimos, y mejora la cobertura interior [Web-8] [26].

El WiMAX soporta varias características claves [Web-9], tales como: la tolerancia a múltiples rutas y auto-interferencia, *Duplex2 de División de Tiempo* (*TDD2* del inglés *Time Division Duplex2*), *Petición de Repetición Automática Híbrida* (*H-ARQ* del inglés *Hybrid-Automatic Repeat Request*), la programación de frecuencia selectiva, gestión de la conservación de energía, handoff exigente de la red optimizada, *Multidifusión y Difusión de Servicios* (*MBS* del inglés *Multicast and Broadcast Service*), asignación flexible de recursos de radio, dispositivo de móvil de bajo consumo de energía. En la tecnología WiMAX móvil (Figura 7.2), la *Estación Base* (*BS* del inglés *Base Station*) está conectado a una red IP con cable, y conecta muchos *Estaciones Suscritores* (*SS* del inglés *Subscriber Stations*) que puede ser fijo o móvil [27], y deben ser apoyadas con una WiMAX *Tarjeta de Interfaz de Red Inalámbrica* (*WNIC* del inglés *Wireless Network Interface Card*). WiMAX tiene el potencial de reemplazar varias infraestructuras de telecomunicaciones como las redes de cables de teléfono y las redes celulares.

Además, proporcionar RTMA con los requisitos avanzados de QoS constituye un gran desafío. WiMAX soporta avanzada QoS y baja latencia para mejorar RTMA [Web-4], y también soporta diferentes duraciones de frame [28], y porque su frame enfoque basado en MAC se controla centralmente, lo que ofrece una QoS de multimedia garantizada [20].

El IEEE 802.16 específica la capa física y la capa MAC, y define un protocolo MAC de conexión orientada, con cada conexión entre la SS y BS se identifica mediante un identificador de 16 bits de *Identificador de Conexión* (*CID* del inglés *Connection Identifier*). WiMAX utiliza dos formas de asignar ancho de banda: *Subvención por Conexión* (*GPC* del inglés *Grant per Connection*), donde el ancho de banda es asignado

a cada conexión, y *Subvención por SS* (*GPSS* del inglés *Grant per SS*) donde SS re-distribuye las ranuras de transmisión asignado por el BS a todas sus conexiones [28].

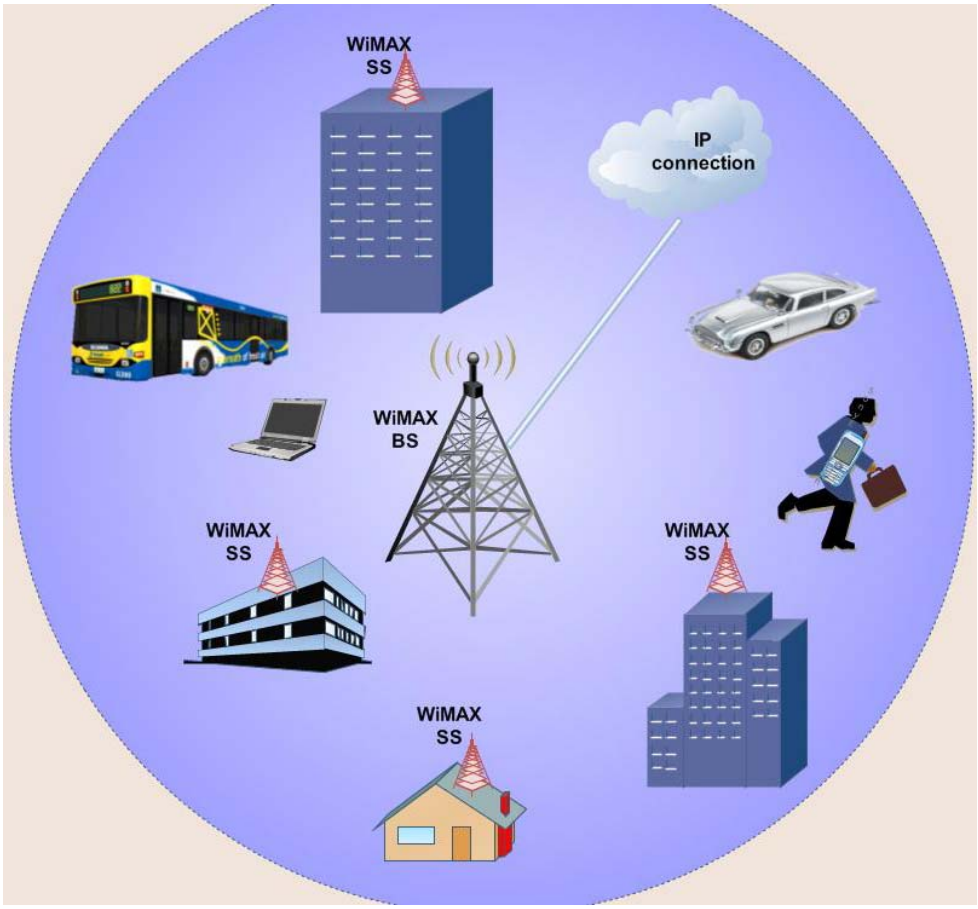

Figura 7.2 : Arquitectura de red WiMAX móvil

EL IEEE 802.16e define cinco clases de programación de servicios [28]-[31]:

- *Unsolicited Gran Service* (*UGS*) para suportar los flujos de servicio a tiempo real que generan un tamaño fijo de paquetes como el VoIP.
- *Real Time Polling Service* (*rtPS*) para suportar flujos de servicio a tiempo real que producen un tamaño variable de paquetes. El usuario debe identificar el tamaño de cada paquete antes de recibir el permiso para mandarlo, como el vídeo MPEG [31].
- *rtPS Extendida* (*ertPS*).
- *Non-real time polling service* (*nrtPS*) para suportar los flujos que no son a tiempo real, que requieren tamaños variables de datos de subvenciones.

- *Mejor Esfuerza* (*BE* del inglés *Best efforts*) para suportar el mejor esfuerzo de trafico como el email.

Las tres primeras clases requieren data y retraso, y sus aplicaciones son afectadas por el proceso de handover [32]. Además, IEEE 802.16 usa cinco QoS parámetros para reservar recursos para el flujo de trafico del usuario: flujo mínimo de datos, flujo máximo de datos, retraso máximo, el jitter y el nivel de la prioridad [31].

7.1.3 Problemas de cobertura enredes inalámbricas para RTMA

Recientemente, diferentes RTMA han sido propuestos para ser implementados en redes inalámbricas:

- El *juego de móvil* es un RTMA que se juega sobre un teléfono móvil, teléfono inteligente, *Asistente Digital Personal* (*PDA* del inglés *Personal Digital Assistant*), ordenador portátil o cualquier tipo de dispositivo de mano o inalámbricos. Actualmente, los juegos móviles en un entorno inalámbrico están recibiendo mucha atención e importancia, pero no todos los teléfonos móviles se utilizan como una plataforma de juego. Además, la mayoría de los productos actuales tienen uno o dos juegos en su versión comercial [33].
- Uno de los RTMA recientes es el *Televisión sobre el protocolo IP* (*IPTV* del inglés *Internet Protocol TV*), es un nuevo protocolo que ofrece al usuario una forma interactiva de TV a través de redes informáticas existentes en lugar de los sistemas de televisión tradicional. IPTV proporciona un buen nivel de QoS y *Calidad de Experiencia* (*QoE* del inglés *Quality of Experience*), seguridad, interactividad y fiabilidad [4].
- La *Televisión Móvil* es otro RTMA, que puede ser transmitido por una red inalámbrica móvil o de forma independiente por el sistema de radiodifusión dedicado como el *Radiodifusión de Vídeo Digital – de Mano* (*DVB-H* del inglés *Digital Vídeo Broadcasting – Handheld*), como consecuencia los dispositivos móviles requieren un hardware dedicado al receptor. La televisión móvil no se espera que tenga éxito, hasta que supere la competencia con el streaming de audio y vídeo bajo demanda porque estas aplicaciones son mejores para el uso móvil donde el contenido se puede consumir cuando el usuario quiere, mientras

que la televisión móvil es transmitida en directo, lo que significa que necesita la cobertura de red para permitir la transmisión continua [21].

- Las técnicas de compresión de vídeo como *Grupo de Expertos en Imágenes Móviles* (del inglés *Moving Picture Experts Group*) *MPEG*-2/4 y H.264/AVC (del inglés *Advanced Vídeo Coding*) son una parte critica del RTMA sobre WLAN [4][13][21][34].

En las redes inalámbricas, hay una variedad de diferentes características y requisitos de servicio para soportar RTMA como alto nivel de calidad, velocidad, tasa de bits, tasa de error máximo tolerable de paquetes, y límites de retardo [35]. En RTMA, los paquetes deben llegar al cliente antes de su tiempo de juego y con un tiempo suficiente para ser decodificados y para mostrar el contenido del paquete [5], así los paquetes del streaming de RTMA deberían tener mayor prioridad que otros paquetes para reducir las vibraciones [21].

7.1.3.1 QoS para RTMA Considerando el Movimiento del Cliente

Hoy en día, hay un número creciente de RTMA que son suscritos por los usuarios de móviles, lo que urge proporcionar QoS garantizada en las redes inalámbricas [15], debido a la falta de mecanismos integrados que soportan RTMA y a las limitaciones de recursos, considerándose como un desafío para garantizar QoS para el rendimiento y el retardo sensibles del RTMA [15] [36]. Esto significa que, las redes inalámbricas existentes proporcionan un QoS limitado para RTMA [37] y esto depende de la capacidad de cada red [5]. En algunos casos, es muy difícil garantizar QoS para RTMA especialmente para terminales inalámbricos en movimiento [38], donde la necesidad de la detección de una ubicación y el proceso de handover hacen que sea difícil determinar la razón de la pérdida de paquetes y el intervalo de pérdida [39]. Además, cuando el MC se mueve sobre los agujeros de cobertura, la baja cobertura causa una interrupción en el streaming de audio [21]. Hay muchos modelos para soportar QoS, como los modelos *Servicios Integrados* (*IntServ* del inglés *Integrated Services*) y DiffServ, mientras que *Conmutación Multi-Protocolo mediante Etiquetas* (*MPLS* del inglés *MultiProtocol Label Switching*) es un protocolo de garantía de QoS [4] [34].

RTMA depende principalmente de la métrica de QoS que es proporcionada por la red inalámbrica, y la sensibilidad de cada uno de estos indicadores varía ampliamente

de una aplicación a otra. Los siguientes parámetros pueden ser considerados como los indicadores básicos de QoS [34] [40] [41]:

- *Throughput*: el número efectivo de unidades de datos transportados por unidad de tiempo (por ejemplo bps) [40]. El throughput máximo de medio de transmisión es igual a la capacidad del canal [4], VoIP, streaming de vídeo y juegos interactivos son aplicaciones multimedia muy sensibles a las reducciones del throughput [Web-3]. Hoy en día algunas MC son compatibles con múltiples interfaces inalámbricas de diferentes tecnologías que permiten al MC aumentar el ancho de banda necesario para la RTMA cuando es posible conectarse a más de una red, esto puede ser en las áreas superpuestas de estas tecnologías diferentes [36].
- *Retraso*: el intervalo de tiempo entre la entrega de información desde el origen hasta el destino [4] [40].
- *Jitter*: se refiere generalmente como "variación de retraso" [40], es la fluctuación del retraso de un paquete a la siguiente en el flujo de la misma conexión [4]. RTMA tiene requisitos estrictos en el retraso y el jitter, que es necesario para las comunicaciones interactivas como VoIP y videoconferencia. El retraso de transmisión de un trayecto debe ser inferior a 150ms. Está demostrado que el streaming de audio o de vídeo es menos sensible al retraso o jitter que el tráfico en tiempo real [41].
- *Pérdida de paquetes*: el porcentaje de unidades de datos que no llegan a su destino en un intervalo de tiempo específico [40]. La pérdida de paquetes puede ser debido al ancho de banda baja de la conexión inalámbrica, la atenuación de la señal o la obstrucción, o handover [39]. RTMA no es muy sensible a la tasa de pérdida de paquetes. Por ejemplo, una tasa de pérdida del 1% es aceptable para el vídeo en tiempo real con una tasa de 16-384 Kbps [41]. Para IPTV, videoconferencia y telefonía de vídeo, la pérdida de paquetes a causa del retraso excesivo es el principal factor que afecta a la calidad requerida [5]. Existen varias técnicas para recuperar la pérdida de paquetes, como la retransmisión de paquetes en la capa de transporte, la corrección de errores en la capa física, o el uso de los códigos en la capa de aplicación [4].

7.1.3.2 Definición del área de cobertura

El CA no tiene una forma esférica perfecta, porque en realidad hay algunos lugares sin potencia de la señal dentro de CA, que se relacionan con el patrón de radiación de la antena o a la presencia de agujeros. Por otra parte, las fluctuaciones de la señal y el proceso de handover podrían causar desconexiones.

El CA es el patrón de radiación de la antena que tiene diferentes formas dependiendo del diseño de la antena y la frecuencia, también representa el campo en relación a la fuerza (potencia) gráfica, o simplemente la distribución del *Indicador de la Potencia de la Señal Recibida* (*RSSI* del inglés *Received Signal Strength Indicator*) en el espacio [42]. El RSSI es un indicador de la intensidad de la señal, y es afectado por las condiciones naturales como el clima y la presencia de obstáculos, y las fluctuaciones en la señal podrían producir desconexiones y la pérdida de transmisión dentro del CA.

La Figura 7.3 muestra la CA (diagrama de radiación) de una antena al aire libre que está situada en el centro. En la trama vertical, se muestra que la radiación no tiene una esférica forma consistente en varios lóbulos: el anterior se llama el lóbulo principal y es el más grande, el menor se llama el lóbulo posterior, y el resto de los lóbulos se llaman lóbulos laterales [43]. Esta forma de radiación precisa la presencia de muchas posiciones que no tienen cobertura, o con una señal débil, también los puntos blancos representan la presencia de agujeros donde ninguna señal podría ser detectada.

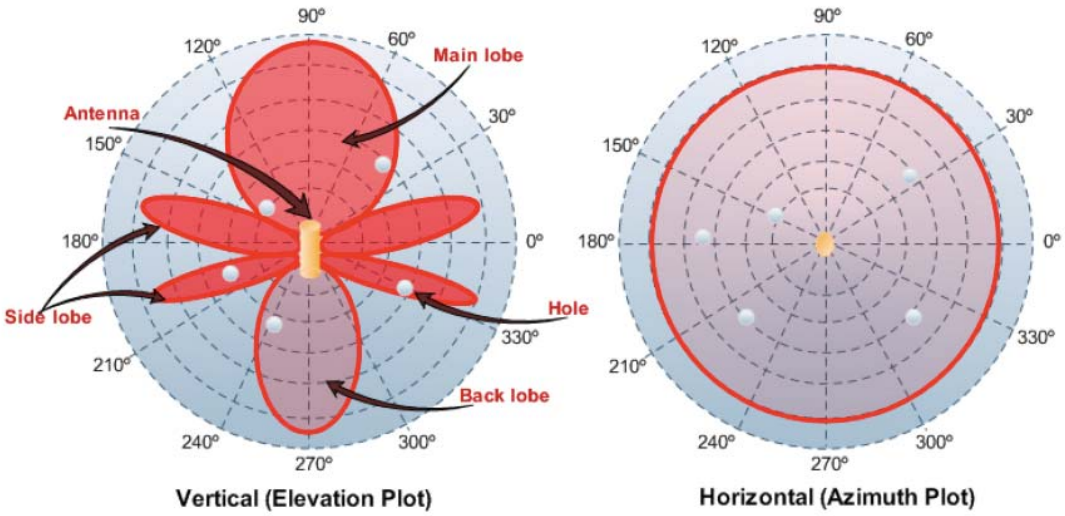

Figura 7.3 : CA Real (Antena de radiación)

7.1.3.3 Agujeros

En todas las redes inalámbricas, donde MC recibe señales de AP o BS, las señales se ven afectadas por las condiciones circundantes, tales como el clima o los obstáculos, tales como túneles causando variación de la señal y la caída en algunos momentos. Las posiciones de la caída de la señal (RSSI = 0) se llaman agujeros. Las desconexiones causadas por los agujeros no se pueden prever, salvo para algunos casos raros en que la desconexión se produce con frecuencia en la misma posición, lo que permite al MC memorizar las posiciones.

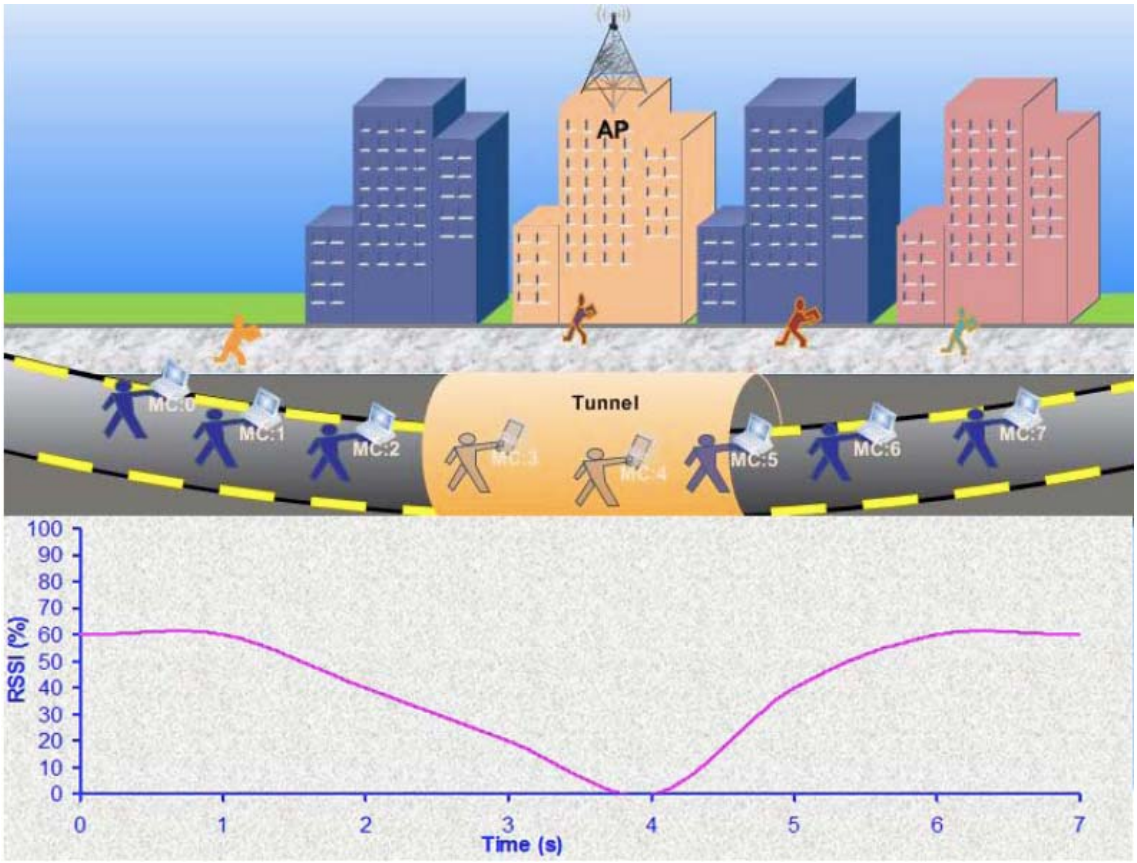

Figura 7.4 : Los agujeros en el caso de el MC pasando por un túnel

Por ejemplo, cuando MC conectado está pasando por un túnel, se desconecte perdiendo frames de vídeo. En la Figura 7.4 el MC con el ordenador portátil está caminando en una calle y tiene conexión con el AP montado sobre el edificio, y tiene una buena señal hasta t = 2 s la señal disminuye gradualmente a medida que entra en el túnel, la conexión se pierde totalmente en el instante t = 4 s como se explica en el diagrama, la caída de la señal en t = 4 s se denomina agujero. Más tarde, la señal es mayor cuando el MC sale del túnel, como se ilustra con la curva ascendente en el

diagrama. En este caso de los agujeros, si MC pasa con frecuencia por la misma ruta, el agujero se podía prever, mientras que en otras situaciones de un obstáculo móvil, como un tren, es muy difícil predecir el posición de agujero, ya que se presenta de forma esporádica.

7.1.3.4 Handover y Roaming

En nuestros días, MCs se proporcionan con varios WNICs (sistemas de Multi-homed que tienen varias interfaces de red [44]) para permita el acceso a diferentes tecnologías inalámbricas [45] ampliando la zona donde pueden ser conectados. Sin embargo, no hay ningún dispositivo comercial con WiFi y WiMAX. Consecuentemente, cuando MC empieza a perder conexión al AP asociado y deja de recibir datos [38] [46], buscará otro AP o BS para asociarse. Este proceso se llama roaming o handover.

Hay varias definiciones del *Roaming* y el *Handover*. El Roaming se define como la capacidad de un operador de red de ofrecer a sus clientes los mismos servicios disponibles en su red doméstica cuando están utilizando otro sistema dentro o fuera del país [Web-10]. Desde la perspectiva de la compañía local hay dos tipos de roaming: roaming de entrada: donde los clientes de otra red inalámbrica entran en la red de origen y usan sus servicios, y el roaming de salida: los clientes de red de casa están de visita en otra red y utilizan sus servicios.

Desde la perspectiva de la región, los tipos de roaming son los siguientes:

- *Roaming Regional*: la capacidad de moverse de una región a otra región dentro de la cobertura nacional del operador de telefonía móvil.
- *Roaming Nacional*: la capacidad de moverse de un operador móvil a otro en el mismo país.
- *Roaming Internacional*: la capacidad de mover a la red de un proveedor de servicio exterior fuera del país.

Diferentes trabajos han definido el handover como el proceso que ocurre cuando el MC se mueve de su conexión entre diferentes BSs o APs utilizando las mismas o diferentes tecnologías [17] [30] [44] [47]-[49]. Cuando este proceso soporta la continuidad del servicio durante el mantenimiento de la conexión del canal de red, baja latencia (latencia de handover es el tiempo entre cuando el MC pierde la conexión con su actual AP hasta que reciba el primer paquete IP después de conectarse con el nuevo enlace [50]), en este caso el handover se llama *Seameles Handover* [45] [47] [48] [51]- [53]. El

IEEE 802.16 define el proceso de handover en que el MC emigra del aire-interfaz proporcionado por un BS al aire-interfase proporcionada por otro BS [54].

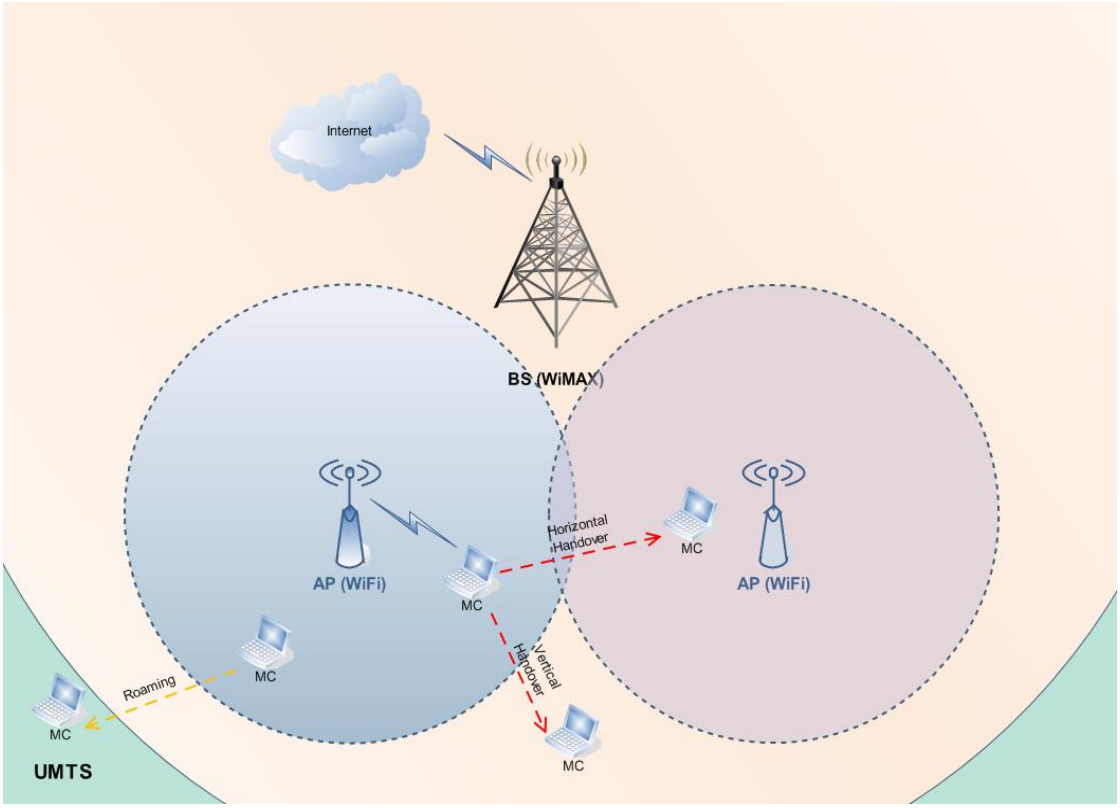

Figura 7.5 : Tipos de Handover y roaming

Hay diferentes tipos del handover (que se muestra en la Figura 7.5) y se clasifican dependiendo sobre muchos factores, desde el punto de vista de tecnología del BS [45] [51] [55], se identifican diferentes clases:

- *Handover Horizontal* (HH) que se produce cuando el MC se mueve entre las redes que utilizan la misma tecnología y el mismo tipo de interfaz de red móvil. Además, las dos redes pueden ser operadas por el mismo operador de red donde la dirección IP del dispositivo móvil puede permanecer sin cambios y el handover se produce en la capa de enlace inalámbrico [31].
- *Handover Vertical* (*VH*), cuando estas redes diferentes utilizan diferentes tecnologías y diferentes interfaces inalámbricas, y el cambio de la dirección IP es necesario [31]. Y en esta clase, hay define dos tipos [55]:

a. *Handover vertical hacia arriba*: es un handover de una superposición de móviles con un tamaño de celda más grande y menor ancho de banda por unidad de área).
b. *Handover vertical hacia abajo*: es un handover a una superposición de móviles con un tamaño de celda más pequeña y mayor ancho de banda por unidad de área).

Algunos trabajos llaman la HH como un handover de intra-tecnología y la VH como handover de Inter-tecnología [56]. Sin embargo el handover de intra-sistema es definido como el handover entre los sectores de un mismo sistema pero el handover de inter-sistema es el handover entre diferentes sistemas [53]. También, diferentes tipos de handover pueden ser distinguidos dependiendo de sus estrategias [57]:

- *Handover Reactivo* (*RH* del inglés *Reactive Handover*) que retrasa el handover al máximo posible por ejemplo, el handover empieza solo cuando el MC pierde completamente su señal de corriente AP [56].
- *Handover Proactivo* (*PH* del inglés *Proactive Handover*) que activa el handover antes de la pérdida completa de la señal de la célula original. Dependiendo del procedimiento de transferencia (se refiere a la secuencia de acciones entre MC y AP [17]), hay dos estrategias disponibles en este tipo:
  a. *Proactiva exigente* (*HP* del inglés *Hard Proactive*) donde el MC se desconecta del AP asociado antes de conectarse al AP visible [24] [47] que permite una conectividad simple con un AP [45]. La misma definición se dio al backward handover [49].
  b. *Proactiva no exigente* (*SP* del inglés *Soft Proactive*): en este caso, el MC hace una conexión correcta con el nuevo AP antes de desconectar del AP actual [47], siendo conectada a mas de un AP al mismo tiempo [24] [45]. Esta definición fue designada a handover adelantado [49].

Es importante reconocer el Ping-Pong handover, que es un proceso de handover innecesario que ocurre cuando el MC handover a BS vecino y vuelve a la BS original después de un corto tiempo [58]. El handover ocurre debido a dos razones:

- El MC puede salir del CA de AP actual y necesita asociarse a un AP nuevo.

- El MC detecta múltiples AP dentro del rango y necesita cambiar entre ellos para mejorar algún aspecto de la comunicación, como reducir las perdidas de paquetes, mejorar el rendimiento o reducir el costo [31].

El proceso del handover requiere dos cosas importantes:

- El mantenimiento de la conexión puesto que el AP asociado esta cambiado debido al cambio de red.
- El mantenimiento de los requeridos QoS de las aplicaciones que están activas en el dispositivo del MC puesto que el AP esta cambiado.

El Soporte del handover en WiFi

El IEEE 802.11 original no especifica los mecanismos del handover [57], pero las dos enmiendas IEEE 802.11f y IEEE 802.11r proporcionan la capacidad del handover entre los APs que están interconectados en la capa de enlace, y este último ocurre entres distintas fases [15] [50] [56]:

1. *Discovery*: la estación detecta la potencia de la señal del AP actual si es baja y comienza a escanear en busca de otras señales disponibles para establecer una nueva conexión [50].
2. *Autenticación*: la estación y el AP seleccionado por la fase de escaneo intercambian los mensajes de autenticación de la estación.
3. *Asociación*: la estación solicita al AP un identificador de asociación que se utilizará para la entrega de datos [56].

El IEEE 802.11r especifica el handover rápido que suporta el QoS [59]; es conocido como transición de BSS rápido que tiene como objetivo reducir el tiempo de desconexión cuando la estación se mueve de su conexión de un BSS a otro. La transición de BSS rápido incluye protocolos que sólo se pueden aplicar en la transición de estación entre el AP dentro de los dominios de la misma movilidad en el mismo ESS [59]; entonces dos de ellos están definidos:

1. *Transición Rápida de BSS*: cuando la solicitud del recurso no es requerida antes de la transición de la estación a un nuevo AP.
2. *Solicitud de Recursos de la Transición Rápida del BSS*: cuando la solicitud de recursos se requiere antes de la transición de la estación.

Estos protocolos necesitan intercambio de información entre el AP y la estación durante la fase de asociación. El intercambio de mensajes se realiza por dos métodos [59]:

1. *Por el Aire*: la estación se comunica directamente con el nuevo AP.
2. *Por los Sistemas Distribuidos*: la estación comunica con el nuevo AP a través del AP actual asociado.

El Soporte del Handover en WiMAX Móvil

El IEEE 802.16 establece el procedimiento del handover para soportar la movilidad entre las BSs [27]. Este último define dos variantes del handover [54].

- *Cortar-antes-hacer handover*: el servicio con el BS objetivo se inicia después de desconectar el servicio con la anterior BS servida.
- *Hacer-antes-cortar handover*: el servicio con la BS objetivo se inicia antes de desconectar el servicio con el anterior BS servida.

IEEE 802.16e proporciona dos modos de handover [Web-4] [27]:

- *Handover exigente*
- *Handover no exigente*, abajo de este modo hay dos procedimientos de handover [27] [30] [24] [54]:
  a. *El Handover de Macro Diversidad* (*MDHO* del inglés *Macro Diversity Handover*).
  b. *Cambio Rápido de BS* (*FBSS* del inglés *Fast BS Switching*).

7.1.4 Interrupción del Servicio de Vídeo Streaming en Redes Inalámbricas

Los problemas discutidos de la cobertura afectan directamente a los servicios de streaming de vídeo, ya que la ubicación de las señales débiles se produce una interrupción de la prestación de servicios vídeo. A continuación, analizamos los problemas que esta interrupción provoca separándolos en tres diferentes situaciones:

- *Problemas con el handover*: el handover tiene un efecto malo sobre los parámetros del QoS del vídeo streaming como el jitter y el retraso durante la sesión del RTMA, causado por varias operaciones ejecutadas durante el handover. El retraso del handover es el intervalo de tiempo desde cuando el MC deja de recibir datos hasta cuando se mueve a una nueva conexión con AP [60]. Para reducir la latencia larga durante el handover, [61] se ha propuesto la técnica del handover rápido para satisfacer la movilidad sin costura para el

servicio de video streaming. El principal problema de los rendimientos durante el período de retraso, la conexión se pierde y no hay más paquetes de vídeo que se almacenan en el MC, con lo que el vídeo aparece carecer de algunos frames y el usuario puede ver el vídeo de baja calidad o una parte podría perderse del mismo. Por lo tanto, para superar este problema, una técnica eficaz es necesaria para proporcionar al usuario frames de vídeo suficientes antes de la desconexión con el fin de mantener el vídeo mostrado con una calidad aceptable.

- *Problemas con los agujeros*: el mismo problema causado por el handover puede ser causada por los agujeros, pero el problema de los agujeros es su predicción imposible cuando ésta causada por objetos móviles. Por lo tanto, las soluciones propuestas del handover no pueden ser eficaces en el caso de los agujeros. Por esta razón, los modelos de filtración y técnicas son mejores puesto que la señal detectada puede ser filtrada para evitar la desconexión repentina y para suavizar la curva de la señal.
- *Problemas de servicio de vídeo streaming en WiFi y WiMAX*: el servicio de vídeo streaming requiere alta tasa de consumo de energía, causando problemas con los dispositivos móviles que dependen de baterías de energía limitada, ya que es poco práctico cargar la batería del dispositivo durante el movimiento. En el servicio de vídeo streaming, la energía se utiliza principalmente para la computación, la transmisión y la mostración. Sin embargo, en la transmisión, la energía se consume para transmitir y recibir la *Radiofrecuencia* (*RF*) de señal audio y vídeo, y también en el cómputo para codificar y descodificar estas señales.

- Por otra parte, el problema de *Mobile IP*, que es un mecanismo de gestión de movilidad de la capa de red, lo que permite a los usuarios de dispositivos móviles mantener su conexión con la red inalámbrica doméstica cuando se mueven a una nueva red. Esto es posible gracias a un túnel de los paquetes transferidos a través de un agente domestico en la misma red [Web-10] [51] [62]. Sin embargo, la desventaja de este esquema es que los agentes domésticos y extranjeros podrían convertirse en cuellos de botella, ya que estos últimos necesitan manejar los paquetes de un túnel para un gran número de hosts móviles [51]. Este esquema utiliza tres procedimientos: El descubrimiento del agente, el registro, la enrutamiento y túneles [7].

7.1.5 Objetivo de la Tesis

El principal objetivo de la tesis fue el desarrollo de un protocolo para mitigar la disrupción de los servicios de vídeo streaming en redes WiFi. Para lograr este objetivo:

- Hemos definido la ***especificación matemática del CA*** y su relación con lugares de desconexión y las diferentes formas del movimiento del MC
- El desarrollado nuevo ***filtro y predictor del RSSI gradiente*** para mejorar la señal mitigando los adversos efectos de los agujeros, y predecir los estados de desconexión del MC.
- Hemos desarrollado una técnica eficaz de ***la gestión del buffer y el control de velocidad de transmisión*** para mantener el *MC Buffer* (*MCB*) en su límite superior durante el mayor tiempo, para consumirlos durante el tiempo de disrupción. Hemos controlado la velocidad de transmisión dependo del estado del MC
- Hemos ***verificado el protocolo*** usando el *Lenguaje de La Especificación y Descripción* (*SDL* del inglés *Specification and Description Language*). Hemos verificado la posibilidad de ejecutar esta técnica por el intercambio de señales y mensajes entre MC, AP y BS.
- Hemos implementado un ***simulador Java*** generado del diagrama del SDL para simular el protocolo e ilustrar su eficiencia y rendimiento.

7.1.6 Trabajos relacionados y motivaciones

La predicción es un paso esencial en el desarrollo de muchas técnicas para resolver el problema de la pérdida de streaming del vídeo durante cortas desconexiones. Varios filtros fueron utilizados como indicadores en la área de las conexiones inalámbricas, donde el valor del RSSI para estos filtros en forma directa o indirecta (por ejemplo, calculándolo utilizando otros parámetros como la distancia). *El Modelo de Grey* (*GM* del inglés *Grey Model*), el filtro de Kalman, transforma de Fourier, Particle [63] y el filtro de Bayesian [64] son filtros utilizados por muchos investigadores.

Como un modelo de predicción, el GM juega un papel importante para hacer una predicción precisa en diversos campos [65]; así podemos predecir el siguiente RSSI usando algunos valores medidos del RSSI como datos para del GM. Diferentes autores aplican algunas técnicas de filtrado incluido el GM a los valores de RSSI para predecir el handover [63]. El predictor de Grey se utiliza también para predecir los valores de

RSSI que son la entrada de otro filtro (sistema de decisión fuzzy) que producen el factor del handover [66].

Diferentes trabajos se han interesado al tema del filtrado de RSSI. El filtro de Kalman para RSSI fue utilizado con el fin de traducir el valor de RSSI actual a un valor de área geográfica para la posición del MC. El filtro de Kalman extendido fue utilizado para capacitar una Red Neuronal Artificial [67], que se utiliza para formar la potencia de la señal medida del *Sistema Global para las Comunicaciones Móviles* (*GSM* del inglés *Global System for Mobile communications*) para el posicionamiento de móviles. En esta técnica, el Filtro Kalman Extendido depende principalmente en las características del GSM que puede medir la potencia de la señal de muchos BS cerca. Por otra parte, los valores medidos del RSSI pueden ser convertido a distancias dependiendo en la estimación anterior de la posición [68], estas distancias son utilizadas como entradas para el filtro de Kalman para dar la estimación de la posición siguiente, también el filtro de Kalman Extendido puede ser aplicado en la distancia estimada desde la conversión de valores RSSI [69].

Algunos autores evaluaron diferentes técnicas para filtrar los valores de RSSI incluido el Kalman discreto, estas técnicas proporcionan información sobre los AP disponible para el handover en un instante [65]. Sin embargo, otros autores utilizaron el filtro de Kalman Extendido para la estimación de la ubicación y la velocidad de un nodo de seguimiento. Se utilizó una versión mejorada para corregir la estimación del estado del filtro de Kalman, porque funciona bien sólo si el nodo de seguimiento se mueve con una velocidad constante y no cambia su dirección [70].

La gestión del buffer y los mecanismos de control son soluciones eficaces para la pérdida de transmisión del vídeo causada por las cortas desconexiones, algunos de los trabajos han propuesto sistemas de gestión del buffer [57] [71]-[74] para proporcionar soluciones solo para el caso de la interrupción de la transmisión del vídeo durante el handover. Sin embargo, otros casos de desconexiones tales como los agujeros no se estudiaron. Además, los sistemas de gestión del buffer se utilizan para mejorar la capacidad de conexión para el streaming a tiempo real [75] o para mejorar la calidad del servicio [76].

Uno de los esquemas propuestos contiene un agente localizado entre el cable y la parte inalámbrica para sustituir el *BS Buffer* (BSB) [71]. El agente tiene un buffer para controlar la velocidad de transmisión del servidor, cuando aumenta la ocupación del

agente buffer, el agente enviaría más paquetes *Acknowledge* (ACK) al servidor para disminuir su velocidad de envío. En caso de handover, el MC deja de recibir los paquetes y la ocupación del agente de buffer aumenta y duplica el número de paquetes ACK de hasta 3, provocando la inhibición del envío de paquetes por el servidor. Cuando el MC vuelve a conectarse, consumirá los paquetes protegidos del agente, este último enviará los paquetes ACK normales aumentando la velocidad de envío del servidor. En este esquema, tres puntos tienen que ser aclarados: 1) cómo el buffer del cliente se ve afectado, 2) cómo la velocidad de transmisión del agente es controlado por el MC y 3) que pasa durante el handover en el lado del cliente.

Otros informes utilizaron una técnica de gestión del buffer para resolver la interrupción de servicios multimedia de menos de un segundo [72], los autores utilizaron el servidor y los proxies de cliente con tampones, el servidor proxy reenvía sus paquetes almacenados seguido de mensajes de ping al cliente proxy. En caso de recibir mensajes pong con codificación correcta desde el cliente de proxy, el servidor proxy asegura una buena conexión. Si ocurre algún deterioro de la señal, el cliente no puede responder con el mensaje pong o la codificación no será correcta, después de enviar muchos mensajes ping sin respuesta, esto significa que ninguna conexión esta disponible. En este caso, el servidor proxy le pide al servidor para interrumpir la transmisión sin necesidad de terminar la sesión y en el mismo tiempo se le advierte al cliente a cambiar su CA.

La idea principal del mecanismo de frame de control de la tasa propuesta en [73] depende de los frames protegidos en MC, como el número de frames de buffer disminuye, la velocidad de bits de juego disminuye gradualmente. Si ocurre cualquier desconexión, los frames no llegan al MCB causando una disminución en la cantidad del buffer de vídeo, por lo tanto la tasa de bits de juego también se reducirá hasta que se detenga el servicio si no se encuentra una nueva conexión.

Otro mecanismo propuesto utiliza dos buffers situado en el *Router de Acceso Anterior* (*PAR* del inglés *Previous Access Router*) y el *Router de Acceso Nuevo* (*NAR* del inglés *New Access Router*) [74], el PAR envía los paquetes a tiempo real a la NAR durante el proceso de handover, y después de MC se conecta con la NAR y recibe estos paquetes. Una desventaja de este mecanismo es la limitación del tamaño de cada buffer, que carece de un tamaño específico para cada buffer, así en ocasiones el buffer podría no estar disponible en ambos routers, y por lo tanto los paquetes a tiempo real no se

almacenaran. También, usando un buffer en la NAR no es útil porque la mayoría de los routers de acceso no tienen suficiente memoria para el almacenamiento temporal de paquetes a tiempo real. Además, este mecanismo es adecuado para la desconexión debido al handover de cerca de 200 ms como máximo, por lo tanto, para otros tipos de desconexiones que podrían ser más largos, se perderán en los paquetes

Además, algunos otros trabajos presentaron un estudio exhaustivo del rendimiento QoS de los sistemas de gestión de almacenamiento y los mecanismos de handover que se utilizan para resolver la interrupción del servicio durante el handover [77]. Los autores utilizaron las fuentes de vídeo MPEG-4 para evaluar la gestión de diversos mecanismos de buffer, donde el vídeo está codificado con un esquema de capas de codificación. También, demostraron que el handover usando el mecanismo de multidifusión y el mecanismo de gestión del push-out buffer dio los mejores resultados. En el mecanismo push-out, cuando los paquetes de alta prioridad llegan y el buffer está lleno, los paquetes de baja prioridad serán descartados y serán reemplazados por los paquetes que llegan [78], mientras que en el caso de que no hay paquetes de baja prioridad, los paquetes que llegan serán descartados.

Por otra parte, otros investigadores centraron su trabajo particularmente sobre evitar la interrupción del RTMA cuando el MC hace handover en tiempo de ejecución mediante la predicción del handover explotando el GM de primer orden [57]. Esto permite a los móviles proxy trasladarse a la zona WiFi donde el MC se reconecta, y luego reorganizar las sesiones de usuario en la nueva red. Además propusieron una gestión proactiva de los buffers proxy-sided a través del aumento del tamaño de los contenidos streaming pre-buscados en el buffer sólo antes del handover.

Además, muchos trabajos se centraron sobre la desconexión causada por el handover e interrumpe el streaming de vídeo. Algunos informes suponen un MC con dos WNIC como base para sus soluciones [79]-[81]. Un MC se utilizó con dos WNIC para hacer dos conexiones con el servidor de IPTV en el mismo tiempo mediante el acceso a dos diferentes AP al mismo tiempo [79]. Una conexión se utiliza para la transferencia del vídeo stream y el otro para buscar otro AP, cuando la conexión actual comienza a estar congestionada y la *Media Móvil de Fluctuación Negativa* (*MANJ* del inglés *Moving Average of Negative Jitter*) medido supera un umbral específico (determinado por el proveedor de servicios), en ese momento una nueva conexión se establece con el servidor con una idéntica de vídeo streaming, que a continuación

genera el valor MANJ para evaluar cuál es la conexión más congestionada para anularla, mientras que en otros comparan el retardo de las dos corrientes [80]. Además otros autores proponen El *Algoritmo de Adaptación Suave del Handover-Suave* (*SASHA* del inglés *Smooth Adaptive Soft-Handover Algorithm*), que es un algoritmo del handover de la capa de aplicación [81]. Se basa en la explotación de las conexiones viejas y nuevas en el área de superposición de las dos redes. Por lo tanto, la calidad del proceso de entrega de multimedia aumenta. Los autores asumieron que el MC tiene dos WNIC y puede abrir dos conexiones con el servidor al mismo tiempo. Si el MC encuentra una nueva conexión, evaluará la calidad del multimedia streaming. Si la calidad de la nueva conexión está aumentando, aumentará la carga de la nueva conexión y disminuye la carga de la conexión anterior hasta el enrutamiento de todos los tráficos de multimedia pasa al nuevo AP.

Un mecanismo de transferencia dinámica fue propuesto para la gestión de la movilidad y fue diseñado para minimizar la latencia del handoff en el IEEE 802.11 [38], lo que reduce la pérdida de datos y la sobrecarga de señalización en el RTMA. En este mecanismo, los puntos de umbral son considerados que ofrecen una mejor solución para una rápida y ping-pong MC en una red amplia de campus, porque el método de predicción establecida en el umbral con un mecanismo dinámico de escanear el canal de es más adecuado para el RTMA como VoIP en WLAN. Se demuestra que la latencia de transferencia se reduce de 310 a 33 ms y el rendimiento en el área superpuesta se incrementa en un 51,6% [38].

Además, algunas técnicas de predicción del handover han sido objeto de interés para muchos investigadores. Un frame de predicción del handover fue presentado por algunos autores [82], este último se basa en la información de la red vecina para estimar el tipo de handover requerido y el tiempo para terminar todos los procedimientos del handover. Este frame se realiza en tres pasos: 1) la configuración inicial y la etapa de medición, 2) El descubrimiento de vecinos y el paso de predicción y 3) El paso de la ejecución del handover. En el método propuesto, el tiempo de interrupción del servicio necesita 55 ms frente a 450 ms para otro método.

Un protocolo del handover rápido del IP móvil con múltiples pre-registros ha sido propuesto por algunos trabajos [61]. Los autores prepararon nuevas direcciones IP de los múltiples lugares a donde el MC puede mover. Cuando la señal recibida es baja, se moverá a la red junto con la señal más fuerte de los lugares preparados, y si es

superior al umbral definido, entonces el handover tendría éxito, así que el tiempo de retraso para la generación de nuevas *Direcciones de Atención* (*CoAs* del inglés *Care of Adresses*) es guardado y reduce la latencia del handover. En cambio, algunos autores han propuesto la técnica del handover histéresis variable para minimizar la probabilidad del handover mediante el uso de histéresis con un margen variable [83], esto puede reducir la probabilidad del handover cuando la intensidad de la señal es alta (histéresis en aumento), y el aumento de la probabilidad del handover cuando la señal es más baja (disminución de histéresis). También se propone una técnica mejorada de la calidad de vídeo mediante la reducción de perdida de los objetos de *Grupos de Vídeo* (*GoV* del inglés *Groups of Vídeo*) debido a la interdependencia de frames por la ruptura de la secuencia natural de los frames y controlar el frame de iniciación de los GoV. Los autores mostraron que el número esperado de frames perdidos depende de la posición de inicio del handover en los GoV y es posible estimar el número de frame perdidos.

Otros autores desarrollaron un plan de gestión del handover de VoIP que es sensible a la pérdida de paquetes [84]. Este plan usa un protocolo de transporte que soporta múltiples conexiones para la comunicación VoIP y toma decisiones de handover en función del número de reintentos experimentados por una trama de datos, también minimiza la pérdida de paquetes, además del tráfico redundante debido a la transferencia paralela de paquetes idénticos, al predecir la pérdida del paquete anticipadamente en función del número de reintentos y adecuadamente selecciona un ruta-única o rutas-múltiple a través del examen de la calidad de la comunicación en el enlace inalámbrico.

El rendimiento del proceso del handover de una red IEEE 802.11b ha sido evaluado por otros trabajos anteriores [17] usando el ancho de banda y la latencia del handover. Los autores calcularon la latencia del handover en función de la distancia entre dos AP y la velocidad del MC, y la VoIP es un ejemplo de una aplicación sensible al retardo y al jitter que esta suportado por el sistema. Los resultados mostraron que la latencia del handover (debida a la fase de descubrimiento en el que MC escanea el conjunto de canales de RF y espera a que las condiciones de intensidad de la señal recibida desdel AP sean cumplidas) y el retraso se puede reducir mediante la elección de las posiciones de AP adecuadas y la definición de la fase de barrido (que son series de escaneo en diferentes canales).

La mayoría de las previas propuestas tratan con casos especiales, algunos trabajos se centraron sólo en la predicción del handover y en muchos casos fallaron en filtrar las interrupciones repentinas que ocurren en los agujeros, algunos de las cuales tratan sólo el caso del handover con un intervalo de tiempo limitado. Otros ofrecen una solución para controlar la velocidad de transmisión de vídeo en el lado del servidor sin hacer referencia al parte del cliente. Además, la mayoría de las soluciones de gestión del buffer sufren el problema de control del tamaño del buffer, exceso o falta. Estas soluciones fueron probadas por los simuladores ya existentes en el mercado como NS-2 y OPNET, que tiene una desventaja que estos simuladores no siempre se adaptan a las características de red que se consideran, que necesitan una gran cantidad de modificaciones en la configuración del simulador en el caso que se permite. Por lo tanto, hace falta una solución completa para todos los problemas anteriores. En consecuencia, esta tesis es una contribución nueva tratando una solución a muchos desafíos en las interrupciones de servicios multimedia durante las desconexiones cortas.

Este trabajo presenta un protocolo nuevo efectivo para mitigar la pérdida de paquetes de video streaming durante las interrupciones del servicio. El protocolo consta de dos partes:

- La nueve técnica de filtración representada por el nuevo Filtro y Predictor del RSSI Gradiente (*RSSI* en inglés *Gradient Predictor and Filter*) para predecir el próximo estado del MC además de mitigar el efecto adverso de los agujeros [85]-[87]. El predictor del RSSI Gradiente tiene un comportamiento gradiente debido al movimiento regular del MC. En consecuencia, el gradiente promedio se calcula de una muestra anterior del conjunto de los valores medidos del RSSI, se utiliza para predecir futuros valores de RSSI, por lo que fue modificado para funcionar como un filtro de agujeros.
- Una técnica de gestión del buffer y del control de transmisión de vídeo; fue desarrollada para mitigar la pérdida de paquetes del vídeo streaming durante la disrupción del servicio [87] [88]. Se basa en una especificación matemática para el CA de WiFi AP y una definición de modelos de movimientos del MC. Desde estas definiciones se desarrolló un diagrama de estado a generar transiciones de MC entre las zonas de cobertura, cada transición genera algunos comandos para controlar la velocidad de transmisión de vídeo en el BS y el servidor VoD, y gestionar el buffer de vídeo en BSB y MCB, que ofrece cantidad suficiente de

vídeo frames en MCB para ser consumidos durante la duración de la interrupción del servicio.

El SDL se utilizó para el proceso de verificación, y para implementar nuestro específico simulador de Java, se utilizó el diagrama de SDL para generar las clases básicas, y una biblioteca gráfica externa para producir una gráfica detallada de los resultados

7.2 Modelación de la zona de cobertura WiFi para el protocolo

El AP proporciona servicios de red inalámbrica para MC siempre cuando esté dentro del CA. En el CA, la señal se mide de muchas formas como el % RSSI donde se utiliza para clasificar el CA. Entonces un modelo simple para el CA se defina. Las zonas de cobertura como la zona del handover, agujeros, y el área negra, donde las interrupciones en el servicio ocurren, son matemáticamente especificadas y discutidas, los movimientos del MC también se definen teniendo en cuenta estas especificaciones del CA.

7.2.1 El Área de cobertura de un AP WiFi

El AP es el dispositivo central de una WLAN, donde actúa como transmisor y receptor de RF, sino que podría utilizarse para proporcionar una comunicación entre dispositivos inalámbricos y red por cable, o para ampliar el rango de las redes inalámbricas [14] [89]. El AP inalámbrico normalmente podría soportar hasta 255 clientes, es común utilizado en oficinas, centros comerciales, hogares o escuelas. El AP que esta utilizado en hogares y pequeñas oficinas es un pequeño dispositivo con WNIC integrado, transmisor de radio y antena.

El primer AP apareció en 1999 después de la aprobación del estándar IEEE 802.11b, y soportó muchas de las funciones de control, como características de seguridad, control de acceso y selección de canales de RF utilizando una simple interfaz gráfica de usuario. El AP podría tener características adicionales como puerta de enlace de Internet, conmutador, puente o un repetidor inalámbrico y el servidor de almacenamiento de red [89]. Cada AP puede proporcionar la conexión de un área limitada alrededor de ella para formar el CA. Recientemente, algunos artículos estudiaron la naturaleza del CA ya que el entendimiento del CA ayuda a estudiar varios temas como el comportamiento de la señal, la predicción del handover y el desarrollo de la red. Algunos trabajos publicados se centraron principalmente en la estimación del CA

[90], muchos MCs conectados al AP se utilizan para informar sus posiciones y para estimar el CA depende de estos informes periódicos [91].

7.2.1.1 El Modelo simple del área de cobertura

Recordemos la diagrama vertical de radiación explican en la Figura 7.3. La forma del CA se puede aproximar por una figura circular o un óvalo. El IEEE 802.11 utiliza siempre la forma oval para representar el CA, sin embargo, una forma definida no existe en realidad, ya que las características de propagación no son predecibles [14] [91]. Pero algunos autores aproximan el CA por un círculo [38].

Vamos a hacer algunas simplificaciones para el modelo de CA para el tratamiento del movimiento del MC dentro del CA.

En primer lugar simplificamos el área que cubra la radiación de un AP a un plano paralelo al suelo (distancia 0 a la tierra sin tener en cuenta las diferentes alturas del terreno cerrado a él). Es decir, el CA de un AP podría ser considerado como un plano en un espacio Euclidiano que pertenece a $\Re^2$. Una vez que hemos hecho esta aproximación, la segunda consideración es que el CA es un círculo. Es decir, CA es todos los puntos se caracterizan por la ecuación $x^2 + y^2 \leq r^2$, donde *r* es el radio del CA centrada en el punto (*0, 0*). Exactamente en el centro del círculo se localiza el AP que define el CA. En la Figura 7.6 se muestra esta simplificación del CA.

Otra simplificación es que dentro del CA de los puntos que tienen el mismo nivel de radiación de la antena de radio son todos los puntos que coinciden con la ecuación $x^2 + y^2 = r_1^2$. Esto implica que todos los MCs situado a una distancia r_1 del AP tiene el mismo nivel de cobertura.

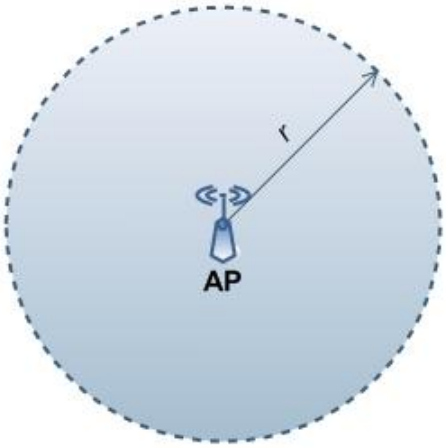

Figura 7.6: El CA simplificada

La simplificación final del CA que hacemos es la siguiente consideración: El nivel de cobertura disminuye con valores mas largas de *r*. Es decir, en el centro del CA (donde se localiza el AP), la señal se encuentra en su mejor estado y cerca de la frontera del CA la señal está en el peor estado (Figura 7.7).

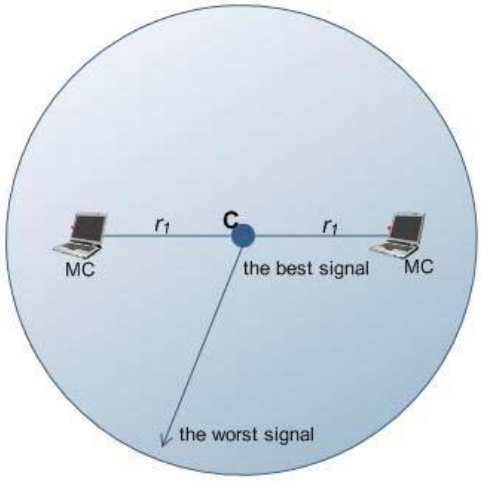

Figura 7.7: El nivel de cobertura

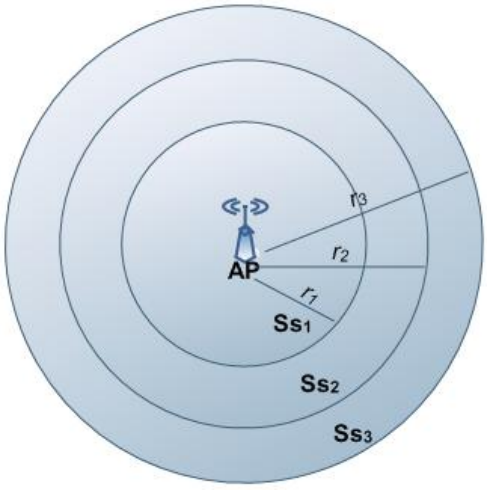

Figura 7.8: Los círculos concéntricos y subconjuntos

Como conclusión de los últimos dos simplificaciones podemos considerar que el CA es la unión de un conjunto de *círculos concéntricos*. El concepto de los círculos concéntricos se podría aplicar para clasificar el CA en diferentes zonas de cobertura. Los círculos concéntricos tienen el mismo centro como el CA, pero diferentes radios, por lo que todas las zonas de cobertura son círculos concéntricos con el CA (Figura 7.8). Sea $\vec{r} = (r_1, r_2, ..., r_n)$ el conjunto de diferentes radios definidos dentro del CA,

donde $r_i \in \Re$. Podemos definir *n* círculos concéntricos (puntos del CA llamamos subconjunto (*Ss*)). El Ss_i es definida por la desigualdad: $r_{i-1}^2 < x^2 + y^2 \leq r_i^2$ (teniendo en cuenta el valor especial $r_0 = 0$).

7.2.2 Clasificación del CA basado en el RSSI

Muchos de los parámetros relacionados con la conexión inalámbrica pueden ser medidos, mientras que se mueve dentro de un MC CA de un AP WiFi, como la velocidad de datos, el ruido, la señal recibida, *Relación Señal a Ruido* (*SNR* del inglés *Signal to Noise Ratio*) y el intervalo de baliza.

En este trabajo, la intensidad de la señal que se mide en la forma de RSSI se utiliza, sino que indica la cantidad recibida de la potencia de la frecuencia de radio que se transmite de AP y medida por el WNIC por la unidad dbm. A veces, el nivel RSSI% se utiliza en lugar de dBm, y podría calcularse a partir del RSSI medido por los métodos de asignación en función de sus valores máximos y mínimo

7.2.2.1 RSSI% para La modelización y clasificación del área de cobertura

La distribución del RSSI dentro del CA puede ser utilizado para encontrar una relación entre el movimiento de MC y el CA, ya que tiene una forma regular. Si el MC se mueve en línea recta hacia o hacia atrás al AP, la señal aumentará o disminuirá respectivamente. Por otro lado, otras formas de movimiento tienen relaciones diferentes con el RSSI, que será descrito en detalle en la sección siguiente.

IEEE 802.11 indica que RSSI se puede definir mediante los valores relativos a la máxima RSSI (*RSSI_Max*), lo que permite a los investigadores a escoger un valor relativo adecuado para su tema de investigación, por ejemplo algunos necesitan estudiar la relación entre RSSI y el tiempo, distancia, posición, o la altura, por lo que cada caso tiene diferentes cálculos de RSSI.

En este trabajo se utiliza el valor relativo RSSI%, el *RSSI_Max* se refiere a un RSSI 100% y el mínimo RSSI (*RSSI_Min*) se refiere a RSSI 0%. En una área abierta con perfectas condiciones y sin obstáculos, RSSI% puede ser de 100% en el centro del CA (posición de WiFi AP), y disminuye que el MC se mueve lejos del AP. En el momento de detectar un RSSI menos del 20%, las condiciones del canal se deteriore, se perderán los datos y el medio se satura con la retransmisión de datos fallados, que causan la mala calidad de reproducción multimedia en el MC [46]. Como resultado, las

interrupciones esporádicas podrían ocurrir.

El RSSI está influenciada por la obstrucción, la difusión, la reflexión y la perdida de múltiples-ruta que causa la fluctuación [51], puesto que la señal se ve afectada por los cuerpos humanos, las paredes y las condiciones climáticas [21] [92] que son difíciles de detectar oportunamente la falta de disponibilidad de la señal [51]. La variación, causada por las condiciones anteriores, afecta el estado de conexión, por lo que descubrir las posiciones donde puede producirse desconexiones requiere más atención.

7.2.2.2 Modelización simple de zonas del CA

El rango de RSSI% de 0% a 100% se puede clasificarlo a diferentes niveles asociados a diferentes subconjuntos, para clasificar el CA en sub-zonas de cobertura. Por lo tanto, facilita la localización de MC dentro del CA, y un *Sistema de Posicionamiento Global* (*GPS* del inglés *Global Positioning System*) no es necesario ya que la posición exacta del MC no es importante.

Asumimos tres círculos concéntricos con diferentes radios r_1, r_2 y r_3 asociados a Ss_1, Ss_2 y Ss_3 respectivamente dentro del CA, donde $r_3 > r_2 > r_1$. Vamos a considerar $\Omega(r_i)$ el nivel de cobertura medido por RSSI% en el radio r_i, por lo tanto podemos definir las zonas de cobertura siguientes en función del nivel de cobertura (Figura 7.9):

- *Area1* (A_1) se relaciona con $Ss_1(r_0^2 < x^2 + y^2 \le r_1^2)$, donde $\Omega(r_0) = 100\%$ y $\Omega(r_1) = 60\%$. Es decir, A_1 es la zona de cobertura asociada al conjunto de los puntos de cobertura en que los niveles de cobertura son de acuerdo a la desigualdad $60 < \Omega(r_i) \le 100$, donde $r_0 < r_i < r_1$.
- *Area2* (A_2) está relacionada con $Ss_2(r_1^2 < x^2 + y^2 \le r_2^2)$ dónde $\Omega(r_2) = 40\%$. Es decir, A_2 es la zona de cobertura asociada al conjunto de los puntos de cobertura en que los niveles de cobertura son de acuerdo a la desigualdad $40 < \Omega(r_i) \le 60$, donde $r_1 < r_i < r_2$.
- *Area3* (A_3) está relacionada con $Ss_3(r_2^2 < x^2 + y^2 \le r_3^2)$ donde $\Omega(r_3) = 20\%$. Es decir, A_3 es la zona de cobertura asociada al conjunto de los puntos de cobertura en que los niveles de cobertura son de acuerdo a la desigualdad $20 \le \Omega(r_i) \le 40$, donde $r_2 < r_i < r_3$.

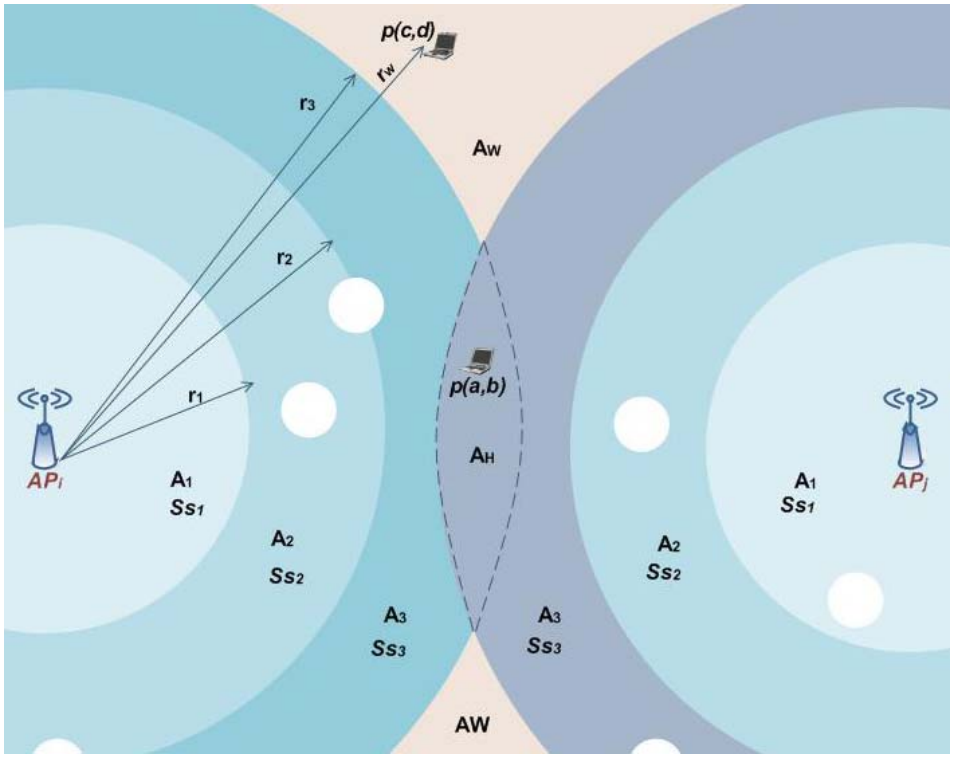

Figura 7.9: Clasificación del CA

Otros investigadores han elegido distintos límites para la clasificación, algunos autores clasifican los valores $\Omega(r_i)$ a tres niveles, el nivel bueno ($\Omega(r_i) > 40\%$), el nivel aceptable ($35\% < \Omega(r_i) < 40\%$) y el nivel débil ($\Omega(r_i) < 35\%$) [93], mientras que en otros supuestos sólo dos zonas con dos umbrales límites: la buena zona y la zona media seguido por el área de superposición donde el handover ocurre [38].

Antes de transmitir, el MC WNIC controla si la medida actual del RSSI es menor que el *Umbral de Canal Desocupado* (*CCT* del inglés *Clear Channel Threshold*) para comenzar a transmitir. En caso de que sea mayor o igual al CCT, el canal inalámbrico no está claro para transmitir. Cuando el MC está listo para recibir, su WNIC debe probar si el RSSI recibido (transformado en dBm) es mayor que el *Umbral de Sensibilidad de Recepción* (*RST* del inglés *Reception Sensitivity Threshold*), que se mide en dBm (un valor muy cercano a 0, pero no es 0). Si el RSSI es igual a RST, WNIC no puede diferenciar entre el ruido y la señal de [Web-11]. Si el nivel de señal recibida del AP cae asociadas a un valor bajo, que se llama el *Umbral de Roaming* (*RT* del inglés *Roaming Threshold*), entonces el roaming o el handover debe comenzar a otro

disponible AP. Esta zona, donde la entrega se produce, se llama la *zona del handover* (A_H).

Sea A_i^j la zona de cobertura A_i dentro de CA_j (donde j = 1 o 2) a continuación, se define la zona del handover A_H como la intersección entre A_3^1 y A_3^2 ($A_H = A_3^1 \cap A_3^2$) donde $20\% \le \Omega(r_i < r_3) < 35\%$ (Figura 7.9). Por consiguiente, si el MC cruza de A_3 *a* A_H, un proceso de handover podría ocurrir, que cruzará a A_H del otro AP y más tarde a A_3. Con esta consideración, el MC no puede cruzar de A3 de un AP a la A3 del otro AP directamente.

La última zona es la *zona del WiMAX* (A_W), que está fuera del CA del AP y se caracteriza por el subconjunto $Ss_w(r_w^2 > x^2 + y^2)$ que pertenece al CA de la BS WiMAX dónde $0\% \le \Omega(r_w > r_3) < 20\%$.

7.2.2.3 Modelización simple de los agujeros

Los agujeros son posiciones dentro del CA, donde la señal cae de repente a un valor muy bajo y causa desconexiones, por lo tanto, es importante definir los agujeros como otra zona del CA. Vamos a definir el vector $\vec{d}(t) = \{d_1(t), d_2(t), ..., d_n(t)\}$ que define las distancias entre el centro del CA a los posiciones de agujeros, donde cada agujero se caracteriza por H_i^j y se localiza a una distancia d_i del centro de la CA_j. Los agujeros, que están localizados en A_W, pertenecen a CA_j que tiene la distancia mínima desde el centro al agujero.

El agujero tiene muchas propiedades:

1. En cualquier agujero H_i^j el nivel de cobertura $\Omega(d_i) \approx 0\%$. Si suponemos que el agujero (Figura 7.10) tiene un radio r_i', a una distancia d_i del centro del CA (x, y), el centro del agujero estará en el punto $(x - d_i, y - d_i)$, entonces todos los puntos que obtienen la ecuación del círculo $(x - d_i)^2 + (y - d_i)^2 < r_i'^2$ pertenecen a este agujero y tienen el mismo nivel de cobertura.
2. También se definen otras propiedades del agujero en función de la presencia de los agujeros, hay dos tipos de agujeros: los agujeros dinámicas y estáticas.
   a. El agujero estático es el agujero que tiene características constantes (d_i y r_i') y aparece siempre en la misma posición con el mismo tamaño.
   b. El agujero dinámica aparece en diferentes instancias de tiempo y desaparece

en otras, y tiene características variables que podrían tener valores diferentes (tales como su tamaño) dependiendo del tiempo y las posiciones de su aparición. Eso significa, por el agujero dinámica que podría definir el vector $\vec{d} = \{d_1, d_2, ..., d_n\}$ en función del tiempo $\vec{d}(t) = \{d_1(t), d_2(t), ..., d_n(t)\}$ debido a que estos valores de distancias varían con el tiempo. También se podría definir r_i' como una función de tiempo $r_i'(t)$ porque el tamaño del agujero dinámico se puede cambiar, por lo tanto, en general podríamos decir que r_i' y d_i son variables aleatorios.

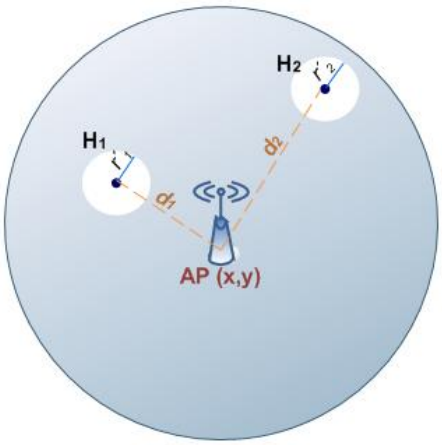

Figura 7.10: El modelo simple del agujero

En esta tesis, estamos interesados en un agujero estático que tiene constante d_i y r_i' (no depende del tiempo) este agujero aparece siempre en la misma posición con el mismo tamaño. Hasta donde sabemos, no hay ningún trabajo previo que ha descrito el agujero de esta manera matemática y con todos estos detalles. En consecuencia, este estudio presenta nueva descripción real sobre los agujeros, que son un caso muy especial de la desconexión real de que los autores no se preocupan de sus investigaciones. El entendimiento de los agujeros es la mejor manera de proporcionar una solución para el tratamiento de ellos, lo que hicimos fue derivar un nuevo filtro matemático especialmente para estos agujeros, para mejorar la señal por tratamiento de sus fluctuaciones y la salida de nuevo $\Omega(r_i)$ sin ningún tipo de agujeros de cualquier tamaño. La filtración de agujeros no se consideran en la mayoría de los trabajos publicados, que hacen propuestas soluciones no eficaces, por lo tanto, nuestro nuevo Filtro del RSSI Gradiente es un filtro de tiempo valioso que se describe en el sección siguiente.

7.2.3 Seguimiento de modelización para los movimientos del cliente móvil

Es importante estudiar la relación entre el movimiento de MC y el CA para determinar cuándo pueden ocurrir las interrupciones. En el apartado anterior se describieron y especificaron los subconjuntos de CA, además de sus relaciones con los tipos de desconexión tales como agujeros, handover y fuera de la cobertura. En esta sección, vamos a identificar el movimiento del MC dentro del CA teniendo en cuenta los diferentes tipos de movimientos del MC, como los que se muestran en la Figura 7.11: línea recta (A, B), circular (C), seno o coseno (D) y Zigzag (E), donde MC podría cruzar una o más zonas de cobertura (o subconjunto). Estos tipos de movimientos podrían definirse teniendo en cuenta las anteriores clasificaciones de las zonas de cobertura.

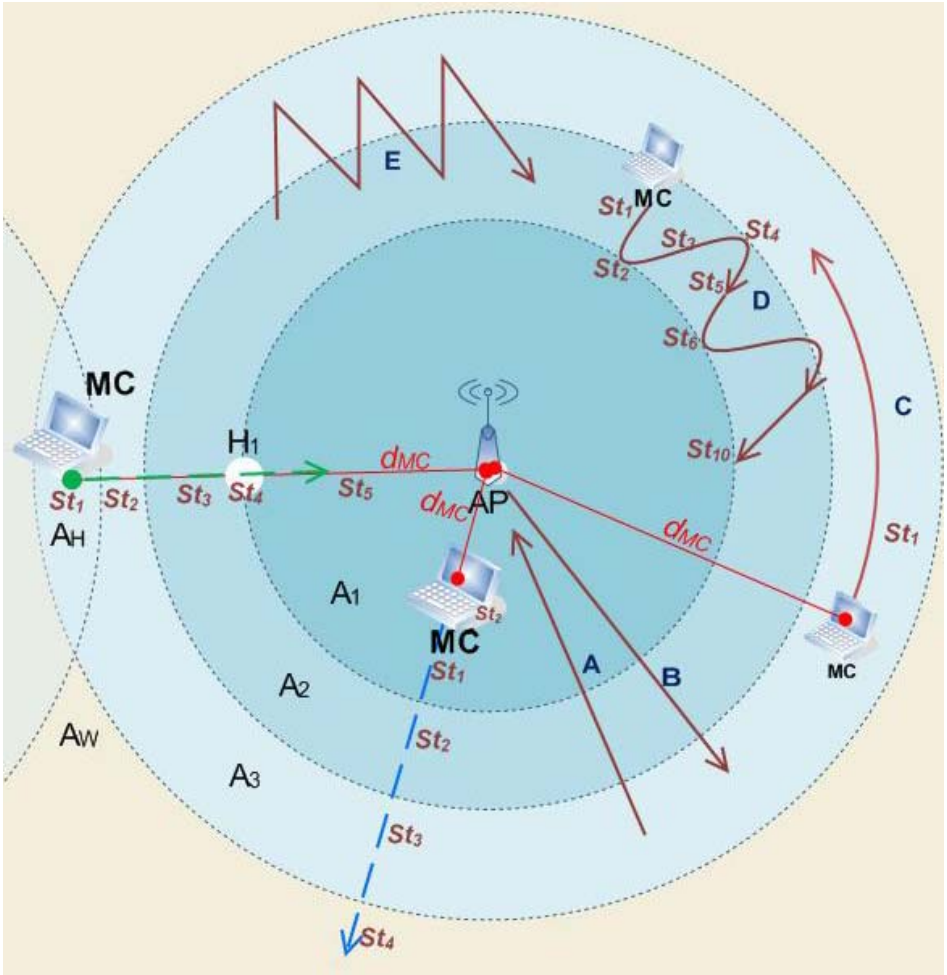

Figura 7.11: Seguimiento de los modelos del movimiento del MC

Supongamos las siguientes afirmaciones (Figura 7.12):

- El MC se mueve con velocidad constante υ por un período de tiempo Δt .

- Sea d_{MC} la distancia entre el MC y el AP, se localiza inicialmente a una distancia $d_{MC}^{initial}$ del AP, y finalmente a una distancia d_{MC}^{final} del AP.
- se define la etapa St_ε (ε = 1, 2 ... ..., m) como un intervalo igual Δt_ε de tiempo del movimiento del MC cuando d_{MC} realiza una desigualdad específica o ecuación relacionados con r_i.
- MC puede pasar a través de las etapas *m* durante su movimiento a partir de St_1 y que termina en St_m.

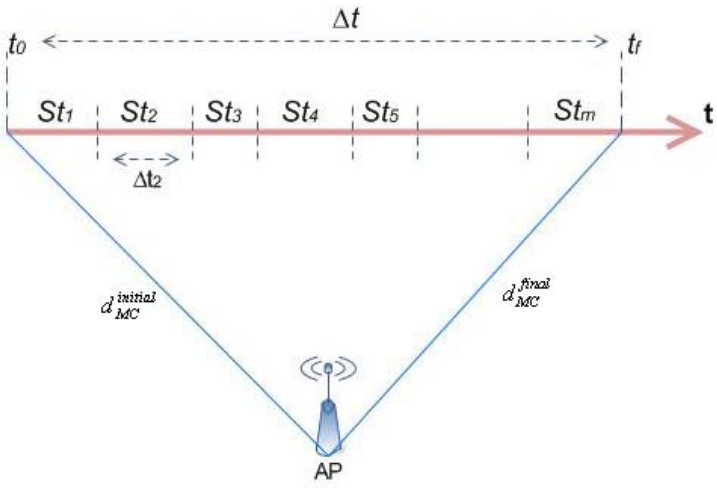

Figura 7.12: El concepto de stage

En consecuencia,

- Si $r_{i-1} < d_{MC}^{initial} \le r_i$ entonces MC está en Ss_i en St_1.
- Si $r_w = d_{MC}^{initial}$ entonces MC está en Ss_w en St_1.
- Si $d_{MC}^{initial} = d_1$ entonces MC está en H_1 en St_1.

Por ejemplo, en caso que el MC se mueve en línea recta desde A_1 a A_W (la línea azul en la Figura 7.11), a continuación, d_{MC} aumentará constantemente pasando por varias etapas:

- St_1, el MC esta en A_1 debido a $r_0 < d_{MC}^{initial} \le r_1$.
- St_2, el MC esta en A_2 debido a $r_1 < d_{MC} \le r_2$.
- St_3, el MC esta en A_3 debido a $r_2 < d_{MC} \le r_3$.
- St_4, el MC esta en A_W debido a $d_{MC}^{final} = r_w$.

Así se infiere que MC empezó a moverse con $\Omega(d_{MC}^{initial}) > 60$, que es una conexión muy buena, y finalmente dejó de moverse con $\Omega(d_{MC}^{final}) < 20$ que es fuera de la cobertura, por lo tanto, $\Omega(d_{MC})$ disminuye de manera constante, es decir, la relación entre el d_{MC} y $\Omega(d_{MC})$ son inversamente proporcionales.

Otro ejemplo es el caso de un MC se mueve de A_H a A_1 (la línea verde discontinua en la Figura 7.11) y pasa por el agujero H_1 (entre A_1 y A_2) d_{MC} disminuirá constantemente pasando por las siguientes etapas:

- St_1, MC esta en A_H debido a $d_{MC} < r_3$ y $\Omega(d_{MC}) < 35$.
- St_2, MC esta en A_3 debido a $r_2 < d_{MC} \le r_3$ y $35 \le \Omega(d_{MC}) \le 40$.
- St_3, MC esta en A_2 debido a $r_1 < d_{MC} \le r_2$.
- St_4, MC esta en H_1 debido a $d_{MC} = d_1$ y $\Omega(d_{MC}) = 0$. En esta etapa, la interrupción del servicio podría ocurrir si el MC se movía lentamente, lo que significa pasar más tiempo en el agujero. Mientras que en caso de movimiento rápido, no pudo detectar este agujero y la interrupción no se produciría. Supongamos que τ_{hole} es el intervalo de tiempo necesario para cruzar el agujero, y el diámetro del agujero es $2r_i'$ entonces $\tau_{hole} = 2r_i'/v$; por lo que la relación entre v y τ_{hole} es inversamente proporcional, es decir, el aumento en v llevar a disminución en τ_{hole}. Por ejemplo, si una herramienta escáner de la señal mide la señal cada 0.5 s, el MC debe moverse con $v > r_i'$ para cruzar el agujero sin detectarlo. v puede ser calculada por la ecuación $v = \frac{d_{MC}^{final} - d_{MC}^{initial}}{t_f - t_0}$ donde t_0 y t_f son el tiempo inicial y final del movimiento, respectivamente.
- St_5, MC esta en A_1 debido a $r_0 < d_{MC} \le r_1$.

En el ultimo ejemplo, d_{MC} fluctúa entre dos o más valores en otros tipos de movimiento (la formas D y E en la Figura 7.11). El movimiento de tipo D se caracteriza por d_{MC} fluctúa entre los tres valores:

- St_1, MC esta en A_2 debido a $r_1 < d_{MC} \le r_2$.
- St_2, MC esta en A_1 debido a $d_{MC} = r_1$: en este momento $\Omega(d_{MC}) = \Omega(r_1)$.
- St_3, MC esta en A_2 debido a $r_1 < d_{MC} \le r_2$.

- St_4, MC esta en A_2 debido a $d_{MC} = r_2$: en este momento $\Omega(d_{MC}) = \Omega(r_2)$.
- St_5, MC esta en A_2 debido a $r_1 < d_{MC} \leq r_2$.
- St_6, MC esta en A_1 debido a $d_{MC} = r_1$: en este momento $\Omega(d_{MC}) = \Omega(r_1)$.

Tengamos en cuenta que MC estará en diferentes etapas: St_1, St_2, St_3, St_4, St_5 y St_6, pero las zonas por donde pasará se puede repetir la definición de un *patrón periódico*. En la Tabla 7.1, se muestran los patrones definidos por diferentes tipos de movimiento (Figura 7.11). Podemos tomar ventaja de estos patrones con el fin de anticipar la zona donde el MC estará en la etapa futura St_k. Por ejemplo, podemos inferir que MC estará en A_1 en ST_{10} para el movimiento de la forma D en la Tabla 7.1.

Mientras que en el caso de moverse en forma circular (forma C en la Figura 7.11), el patrón periódico (Tabla 7.1) se compone de una etapa (A_3), esto significa que en cualquier etapa St_i el MC estará en A_3. Del mismo modo, siguiendo la secuencia patrón periódico (Tabla 7.1) de la forma E (Figura 7.11) que consiste en A_2 y A_3, podríamos inferir que en St_{10} el MC estará en A_3.

Tabla 7.1: Patrones periódicos del movimiento de MC

	St_1	St_2	St_3	St_4	St_5	St_6	St_7	St_8	St_9	St_{10}
Forma D	A_2	A_1	A_2	A_2	A_2	A_1	A_2	A_2	A_2	A_1
Forma C	A_3	A_3	A_3	A_3	A_3	A_3	A_3	A_3	A_3	A_3
Forma E	A_2	A_3	A_2	A_3	A_2	A_3	A_2	A_3	A_2	A_3

Vamos a considerar un ejemplo diferente de movimiento (forma F en la Tabla 7.2) donde MC seguirá la secuencia: A_1, A_2, A_3, A_W, A_H, A_W, A_3, A_2, A_2 y A_3. Mirando esta secuencia, no hemos encontrado frecuentes zonas repetidas, lo que significa que el MC sigue este camino sólo una vez durante el movimiento. Así podemos definir *patrón no periódico* cuando el movimiento no contiene zonas repetidas. Otro ejemplo es la forma G (Tabla 7.2), donde MC seguirá la secuencia: A_3, A_W, A_3, A_2, A_2, A_1, A_2, A_3, A_H y A_3. También este caso es un patrón no periódico porque no hemos encontrado repetidas zonas. Por lo tanto, inferir zonas de futuro donde el MC estará no es posible utilizando el patrón no periódico. Siguiendo la secuencia en ambos casos, podemos descubrir otra manera de inferir futuras zonas. El MC (forma F en la Tabla 7.2) está pasando de una zona con excelente conexión (A_1 en St_1) a una zona de conexión buena (A_2 en St_2) y luego a la zona de conexión débil (A_3 at St_3): esto significa

que el MC se mueve gradualmente de una zona de excelente cobertura a otra de cobertura débil, por lo tanto, podemos inferir que estará fuera de la zona de cobertura (A_W at St_4) después de poco tiempo.

Tabla 7.2: Patrones no periódicos del movimiento de MC

	St_1	St_2	St_3	St_4	St_5	St_6	St_7	St_8	St_9	St_{10}
Forma F	A_1	A_2	A_3	A_W	A_H	A_W	A_3	A_2	A_2	A_3
Forma G	A_3	A_W	A_3	A_2	A_2	A_1	A_2	A_3	A_H	A_3

Algunas veces el MC pasa a través de agujeros de cobertura durante su movimiento: encontraremos etapas en el que el MC está en H_1, como St_3 de la forma K (Tabla 7.3). En la secuencia de la forma K (A_2, A_1, H_1, A_2, A_2, A_1, A_2, A_2, A_2 y A_1) no hemos encontrado ningún patrón periódico, pero si comparamos las primeras cuatro etapas (A_2, A_1, H_1 y A_2) con las segundas cuatro etapas (A_2, A_1, A_2 y A_2) se encuentran similitud con excepción de la etapa en la que aparece el agujero. Por lo tanto, podemos decir, en ausencia del agujero, que este patrón puede ser considerado como patrón periódico, y se clasifica como un *patrón periódico con agujeros*. Mientras que en otras situaciones (forma L en Tabla 7.3), no podemos encontrar la similitud para descubrir el patrón periódico. Si el agujero H_2 (en St_6) aparece o desaparece, el patrón no va a cambiar. Este tipo se pueden categorizar como *patrón no periódico con agujeros*.

Tabla 7.3: el movimiento del MC con patrón periódico y no periódico con agujeros

	St_1	St_2	St_3	St_4	St_5	St_6	St_7	St_8	St_9	St_{10}
Forma K	A_2	A_1	H_1	A_2	A_2	A_1	A_2	A_2	A_2	A_1
Forma L	A_1	A_2	A_3	A_W	A_H	H_2	A_3	A_2	A_2	A_3

7.2.4 La Necesidad de un Protocolo para Mitigar la Disrupción de Servicios de Video

En la sección anterior se analizaron los efectos de los agujeros en el movimiento de MC:

- Hay movimientos que definen patrones periódicos en el conjunto de las zonas visitadas. Sólo en el caso en que no hay agujeros, podemos predecir el futuro (etapa St_k) en la que el MC estará después de algún tiempo. Esa es la razón por la que se ha definido un ***predictor*** para inferir esa zona.

- Hay algunos movimientos que no definen un patrón periódico. Para este tipo de movimientos, tratamos encontrar nuestra definición gradiente para anticipar la información, pero no funciona con movimientos totalmente aleatorios.
- Sólo en caso de que haya agujeros en el camino de MC, vamos a tratar de eliminar los efectos que provocan en los movimientos periódicos y no periódicos. Para hacer esto necesitamos un ***filtro*** para eliminar el efecto adverso de los agujeros. Eso es interesante porque podría volver a predecir el St_k. usando nuestro predictor.
- Para los movimientos que definen patrones gradientes, podemos utilizar nuestro predictor cuando no hay agujeros en el camino. Pero los agujeros se pueden filtrar y entonces podemos predecir el futuro St_k de los movimientos de patrón gradiente utilizando nuestro predictor.

En la Tabla 7.4, resumimos nuestra técnica para mitigar el efecto adverso de los agujeros.

Tabla 7.4: Mitigación del efecto de agujeros

		Agujeros	
		No	Si
Tipos de movimiento	Periódico	Predict	Filter Predict
	Non periódico	---	---
	Gradient	puede predict	puede filtrar

La idea principal de nuestro protocolo se basa en las definiciones mencionadas de los movimientos de CA y MC. La primera parte del protocolo, el predictor y el filtro del RSSI gradiente, se deriva en función de las los patrones periódicos y gradientes, además del comportamiento gradiente de $\Omega(d_{MC})$. Para proceder de este comportamiento, se estudió los posibles modelos del movimiento de MC, que se clasificados a movimientos regulares e irregulares, debido a que el movimiento regular es una condición para tener un comportamiento constante. Por lo tanto, el predictor utiliza el gradiente promedio que se calculó utilizando un conjunto de muestras de $\Omega(d_{MC})$, El gradiente instantáneo puede calcularse a partir del gradiente promedio para cualquier instante de tiempo. Teniendo en cuenta la presencia de agujeros, el predictor se ha mejorado para funcionar como un filtro para estos agujeros, esto se logró mediante la detección del agujero y la corrección del valor relacionado con la muestra anterior correcta.

La segunda parte del protocolo incluye una técnica para la gestión del buffer y el control de transmisión de velocidad. Para esta técnica, hemos considerado una red con dos APs conectados a una WiMAX BS. La BS está conectada a una red cableada donde hay un servidor de streaming de video bajo de demanda que sirve paquetes multimedia al MC que está conectado con el AP WiFi. La técnica se basa en la clasificación de CA en los niveles de cobertura diferentes. En función de los conceptos subconjunto y etapa, se analizó el movimiento de MC entre estos subconjuntos para construir un diagrama de estado. Varias transiciones de MC podrían ser generados a partir del diagrama de estado, donde cada transición es un cambio en el subconjunto o el nivel de cobertura. Si $\Omega(d_{MC})$ se relaciona con la posición de MC, entonces estarán relacionados con las transiciones. Algunos comandos fueron asociados a cada transición para controlar la velocidad de transmisión en el servidor VoD y BS, y para manejar el vídeo almacenado en BSB y MCB. Este proceso se logra mediante: 1) el aumento de la velocidad de transmisión de BS en dos casos: cuando el MCB está debajo de su límite superior, y en caso de desconexión esperada. 2) La disminución de la velocidad de transmisión de BS en dos casos: cuando el MCB está por encima del límite superior, y en caso de que el MC se va de nuevo a nivel de cobertura bueno.

Se utilizó SDL para el proceso de verificación de la técnica de la gestión de buffer y de transmisión de control de velocidad y para verificar la posibilidad de intercambiar los mensajes y señales que llevan los comandos. El diagrama de SDL se utilizó para generar las clases principales del nuevo simulador específico de Java, que fue soportado por una biblioteca externa para la generación de gráficos especial con información sobre el movimiento MC, RSSI, la velocidad de transmisión del vídeo y el buffer.

7.3 El predictor y el filtro del RSSI gradiente

Los filtros existentes que se utilizan en realidad tienen muchas desventajas, tales como la incapacidad para filtrar agujeros y mejorar la señal, por otra parte, algunos predictores no son precisos y funcionan con casos especiales como la constante $\Omega(d_{MC})$. Por lo tanto, es importante desarrollar un nuevo predictor y el filtro especial para la predicción y filtración de forma simultánea.

7.3.1 La Derivación del Filtro y el Predictor del RSSI Gradient

Predecir el próximo estado de conexión del MC es crucial para resolver el problema de la interrupción de los servicios multimedia durante las desconexiones. La predicción del siguiente estado permite generar la transición correspondiente antes que el MC cambia su estado de conexión, que le permite tomar acciones con antelación, especialmente si el tiempo de la interrupción se podía estimado.

Si el MC se mueve con velocidad constante y movimiento regular y medimos n valores de $\Omega(d_{MC})$ (como un conjunto de muestra) dentro del intervalo de tiempo *t*, entonces el vector $x = [x_0, x_1, ..., x_n]$ representa estos valores, cuando: x_0 se mide en tiempo t_0, y x_n se mide en tiempo t. El Gradiente instantáneo de RSSI ∇x_k en cualquier momento es:

$$\nabla x_k = x_k - x_{k-1}$$

Entonces tenemos el vector gradiente:

$$\nabla x = [\nabla x_1, \nabla x_2, ..., \nabla x_n]$$

Y el Gradiente instantáneo con respecto al tiempo en cualquier momento:

$$\nabla(x_k)_t = \frac{\nabla x_k}{\Delta t_k}, \text{ en el que: } \Delta t_k = t_k - t_{k-1}$$

El gradiente media con respecto al tiempo después de un intervalo de tiempo igual t es

$$\nabla(x_n)_t = \frac{\nabla x_n}{\Delta t}, \text{ en el que } \nabla x_n = x_n - x_0 \text{ y } \Delta t = t - t_0.$$

Si x_n no se conocía, se puede calcular de la siguiente ecuación, si todas las demás variables se conocen:

$$x_n = \nabla(x_n)_t \times \Delta t + x_0$$

Para calcular x en cualquier momento t_k, la misma ecuación puede ser utilizada con el cambio del intervalo de tiempo, llamaremos este valor de x el valor predicho $\hat{x}_k^-$:

$$\hat{x}_k^- = (\nabla(x_n)_t \times \Delta t) + x_0, \text{ en el que } \Delta t = t_k - t_0$$

Es cierto que el gradiente promedio es igual al promedio de la suma de instantes gradiente en el mismo intervalo de tiempo in caso de movimiento regular, cuando el MC mueve en velocidad y dirección constantes, entonces:

$$\nabla(x_n)_t = \frac{1}{n}\sum_{k=1}^{n}\nabla(x_k)_t$$

El valor predicho de x será:

$$\hat{x}_k^- = (\nabla(x_n)_t \times \Delta t) + x_0$$

$$\hat{x}_k^- = x_0 + \frac{\Delta t}{n}\sum_{k=1}^{n}\nabla(x_k)_t$$

$$\hat{x}_k^- = x_0 + \frac{(t_k - t_0)}{n}\sum_{k=1}^{n}\left(\frac{x_k - x_{k-1}}{t_k - t_{k-1}}\right)$$

Cualquier $\Omega(d_{MC})$ se puede estimar usando esta fórmula, exactamente en el momento que queremos saberlo. Usando Tabla 7.5, la zona donde se conectará el MC puede ser fácilmente estimada.

Tabla 7.5: Valores del RSSI y la estimación de zonas

$\hat{x}_k^-$	**Área**
$100\% \geq \hat{x}_k^- > 60\%$	A1
$60\% \geq \hat{x}_k^- > 40\%$	A2
$40\% \geq \hat{x}_k^- \geq 20\%$	A3
$20\% > \hat{x}_k^-$	A_W

En algunos casos, cuando el gradiente RSSI está fluctuado, la fórmula de predicción no da la correcta estimación de todos los casos de movimiento. Por lo tanto, es importante tener en cuenta el error de estimación entre el valor actual predicido y la medida anterior. Este error se calcula utilizando la desviación estándar como:

$$\sigma(x_{k-1}, \hat{x}_k^-) = \sqrt{\frac{1}{2}(x_{k-1} - \hat{x}_k^-)^2}$$

Al sumar o restar esta desviación estándar para el valor predicho, los valores estimados de $\Omega(d_{MC})$ serán los siguientes:

$$\hat{x}_k = \hat{x}_k^- \pm \sigma(x_{k-1}, \hat{x}_k^-)$$

En cada caso de x, sumar o restar el valor de la desviación estándar deben ser decididas. Esto se puede resolver multiplicando la desviación estándar de la función de SIGNO (SIGNO de la diferencia entre las dos entradas de la desviación estándar), porque la función de signo da 1 si la entrada es positiva y da -1 si es negativo.

Así que la fórmula del valor estimado será:

$$\hat{x}_k = \hat{x}_k^- + SIGN\,(x_{k-1} - \hat{x}_k^-) \cdot \sigma(x_{k-1}, \hat{x}_k^-)$$

Al aplicar esta fórmula a los valores $\Omega(d_{MC})$, que incluyen los valores cero como agujeros, la fórmula no estima el valor correcto. Una solución para la reformulación de la fórmula consiste en dos pasos:

1. Para encontrar una condición que detecta los valores cero. Esto se puede resolver multiplicando el valor anterior medido por el valor actual y si el resultado es cero, uno de ellos debe ser cero.
2. Eliminar el efecto de la parte de la fórmula de error si la primera condición se consigue sin necesidad de cambiar el valor original.

Para ello, la multiplicación por cero es necesario si la primera condición que se logre o multiplicando por 1 en caso de que no logró. Una de las funciones que resuelve esta es la función de signo:

$$SIGN(x_{k-1} \cdot x_k)^2 = \begin{cases} 0 \\ 1 \end{cases}$$

La fórmula final del valor predicida filtrada (estimado) o el nuevo Filtro de Gradiente es:

$$\boxed{\hat{x}_k = \hat{x}_k^- + SIGN(x_{k-1} - \hat{x}_k^-) \cdot \sigma(x_{k-1}, \hat{x}_k^-) \cdot SIGN(x_{k-1} \cdot x_k)^2}$$

El Filtro del RSSI Gradiente demostró los mejores resultados en todas las situaciones de detección de agujeros y los agujeros, además de la mejor precisión en predicción en todos los casos. Y en comparación con El Filtro de Kalman y El Modelo de Grey, El Predictor y el Filtro del RSSI Gradiente dio los mejores resultados, el Filtro de Kalman puede detectar los agujeros pero muestra gran variación en la señal y el Modelo de Grey no puede detectar los agujeros, también el Modelo de Grey no funciona con algunas casos cuando la señal tiene valor constante todo el tiempo.

7.3.2 La Prueba Experimental del Filtro Gradiente del RSSI

El principal objetivo de este experimento es la evaluación del rendimiento del filtro Gradiente en valores medidos del $\Omega(d_{MC})$ de un WiFi AP. Igualmente, el estudio del comportamiento del CA y el comportamiento de la señal en diferentes condiciones del entorno.

El campo de fútbol de la *Universidad de Las Palmas de Gran Canaria* (*ULPGC*) fue elegido para ser el área abierta para hacer el experimento, donde no haya obstáculos o edificios afectan en la señal.

La línea recta era la forma de movimiento con velocidad constante de 1 mps. Ocho direcciones se consideran en el campo, en cada dirección el MC escaneada la señal 4 veces hacia atrás (lejos de) el AP y 4 veces adelante al AP. En total, 192 grupos de valores se midieron en 3 días.

El AP que fue utilizado es *ANSONIC USB wireless adapter* (*model number: AN-W541USB*) que funciona como un AP o adaptador inalámbrico; se puede conectar a cualquier ordenador portátil en el centro del campo de fútbol. El MC era portátil *Sony VAIO PCG-TR5MP* con WNIC *Intel*(*R*) *PRO/Wireless 2200BG Network Connection* (*model number: WM3B2200BG*). El *Network Stumbler Version 0.4.0* software fue instalado en un portátil para escanear el señal. En el *NetStumbler* la velocidad de escanear la señal se controla por un rango entre rápido y lento, entonces no podemos determinar exactamente la frecuencia del escaneo, pero de los resultados el medí la señal 2 veces cada 1 segundo, y estamos interesados en 1 escanear al segundo, así calculo el promedio por cada dos. De esta manera los grupos se reducidos a 48 grupos.

El experimento mostró en una figura de 3D (Figura 7.13) que el CA no es circular en situación real, y hay diferentes zonas de colores clasificando la intensidad de la señal en CA.

Hemos estudiado el comportamiento lineal de la señal utilizando muestras de los valores medidos con la línea de tendencia y el R^2. La evaluación del comportamiento de la señal es difícil, porque no hay condiciones ideales especialmente hay 17 APs detectados en el mismo tiempo, por lo tanto, la señal cada vez muestra un comportamiento diferente. Sin embargo, el filtro de degradado podría ponerse a prueba en estos valores reales. En el primer día del experimento, el filtro mostró en 7 casos comportamiento lineal. En el segundo día 10 casos lineal, y en tercero 4 casos solo mostró el comportamiento lineal.

Para el test del Filtro del RSSI Gradiente, utilizo el método de asignación:

$$\Omega(d_{MC}) = RSSI\% = \frac{RSSI}{(RSSI\_Max - RSSI\_Min)/100}$$

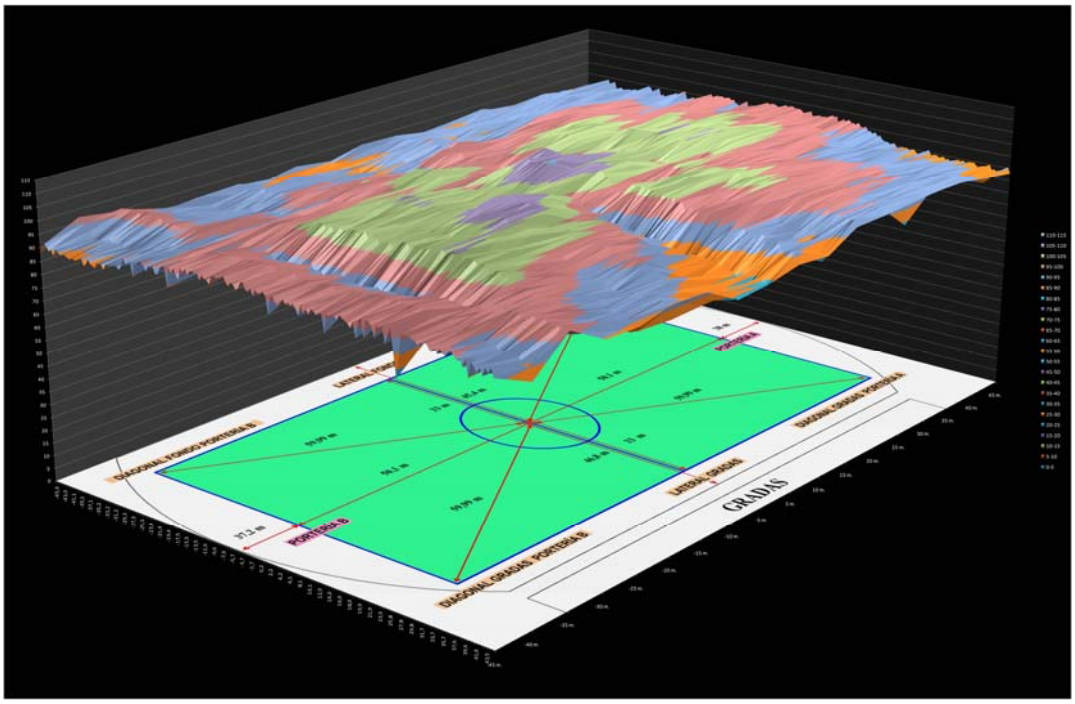

Figura 7.13: Distribución del RSSI en el CA

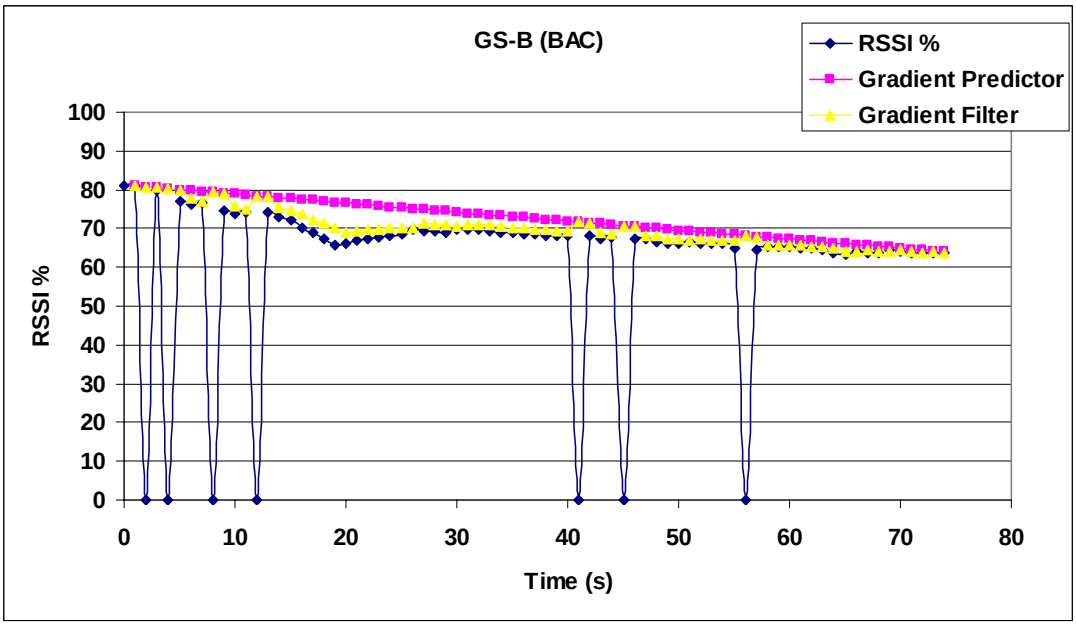

Figura 7.14: Prueba del Filtro Gradiente en valores medidas de RSSI en la dirección GS-B (BAC)

En la Figura 7.13, había un montón de agujeros y más variaciones en la primera parte. El filtro degradado demostrado buenos resultados en la detección de estos agujeros y su filtración, además, los resultados son muy cercanos a los valores reales. El

Predictor del RSSI Gradiente funciona como predictor lineal, que predijo el último valor muy preciso, aunque no pudo detectar variaciones instantánea de la señal, por lo que no detectaron los agujeros.

7.4 La Especificación SDL para la Técnica de la Gestión del Buffer

El protocolo proporciona una solución para la pérdida del vídeo streaming, ofreciendo la suficiente cantidad del vídeo almacenado en MCB antes de la desconexión. Esto se logró mediante la gestión del MCB y BSB controlando la velocidad de transmisión de vídeo. El SDL Cinderella se utilizó para verificar la posibilidad del control de estos buffers por el intercambio de mensajes entre MC, AP y BS. Del mismo modo, un monitor simple fue diseñado para mostrar los cambios de vídeo almacenado en el buffer.

7.4.2 El Diagrama del Estado para los Movimientos del Cliente Móvil

Supongamos que un MC se mueve a velocidad constante v dentro el CA de WiFi AP. Por consiguiente, un supuesto del estado del MC $S(t)$ [1] podría ser definirse teniendo en cuenta la previa definición del CA como:

$$S(t) = A_x, \text{ donde } x=1, 2, 3, \text{ H o W.}$$

La creación de instancias de A_x se realiza por las siguientes desigualdades:

$$\text{Si } 100 \geq \Omega(d_{MC}) > 60 \rightarrow x = 1, \text{ entonces } S(t) = A_1.$$

$$\text{Si } 60 \geq \Omega(d_{MC}) > 40 \rightarrow x = 2, \text{ entonces } S(t) = A_2.$$

$$\text{Si } 40 \geq \Omega(d_{MC}) \geq 20 \rightarrow x = 3, \text{ entonces } S(t) = A_3.$$

En el caso de que el MC detecta dos señales $\Omega_1(d_{MC})$ y $\Omega_2(d_{MC})$ de AP_1 y AP_2, respectivamente, entonces:

$$\text{Si } (20 \leq \Omega_1(d_{MC}) < RT) \text{ y } (\Omega_2(d_{MC}) \geq 20) \rightarrow x = H, \text{ entonces } S(t) = A_H.$$

$$\text{Si } (\Omega_1(d_{MC}) < 20) \text{ y } (\Omega_2(d_{MC}) < 20) \rightarrow x = W, \text{ entonces } S(t) = A_W.$$

En el diagrama de estado (Figura 7.15), cada estado representa una zona de cobertura teniendo en cuenta el MC sólo podían cruzar a las zonas consecutivas, o

[1] Tengamos en cuenta que sólo estamos interesados en el movimiento de un MC. Es decir, nuestra formulación es válida para el movimiento de cualquier MC, pero sólo uno. Esa es la razón por la que no anotar el nombre del MC en la fórmula *S (t)*.

podría continuar en la misma zona. Cuando el MC cambia la zona, una transición se generará siendo utilizado por todas las entidades (BS, AP y MC) para controlar todos los bufferes y velocidad de transmisión. El número de transiciones que se generan en un segundo depende de la velocidad del MC, en caso de que se mueve con una velocidad muy alta, más transiciones pueden ser generadas, que no se puede detectar que causan las transiciones inesperadas. Por lo tanto, para evitar problemas de transición, la velocidad del MC se debe especificar. Las mediciones del experimento anterior demostraron que $\Omega(d_{MC})$ cambio 0,5% con la velocidad humana a pie de 1 mps. Por lo tanto, la gradiente $\nabla\Omega(d_{MC})$ no debe exceder 5% que es el máximo cambio posible ($\Omega(d_{MC})_{\max}$) para tener una transición, en consecuencia, la velocidad debe ser menor o igual a 10 mps (36 kph). Desde $RT = 35\%$ y $\Omega(r_2) = 40\%$ entonces la distancia que se puede cruzar entre los dos límites para tener una transición es muy corto.

$$\nabla\Omega(d_{MC})_{\max} = \Omega(r_i) - RT = 5\%$$

$$\nabla\Omega(d_{MC}) = 0.5\% \rightarrow v = 1mps$$

$$\nabla\Omega(d_{MC})_{\max} = 5\% \rightarrow 10mps$$

Sea $TR(t)$ una transición genera cuando el MC cambia su estado de $S(t-1)$ a $S(t)$ entonces $TR(t)$ se puede definir:

$$TR(t) = Cross\,(S(t-1), S(t)) \quad \text{.....Si } S(t-1) \neq S(t)$$

$$TR(t) = Still\_in(S(t)) \quad \text{.....Si } S(t-1) = S(t)$$

Cuando $t \geq 1$, debido a la primera transición se genera en $t = 1$ como el MC tiene dos estados generados.

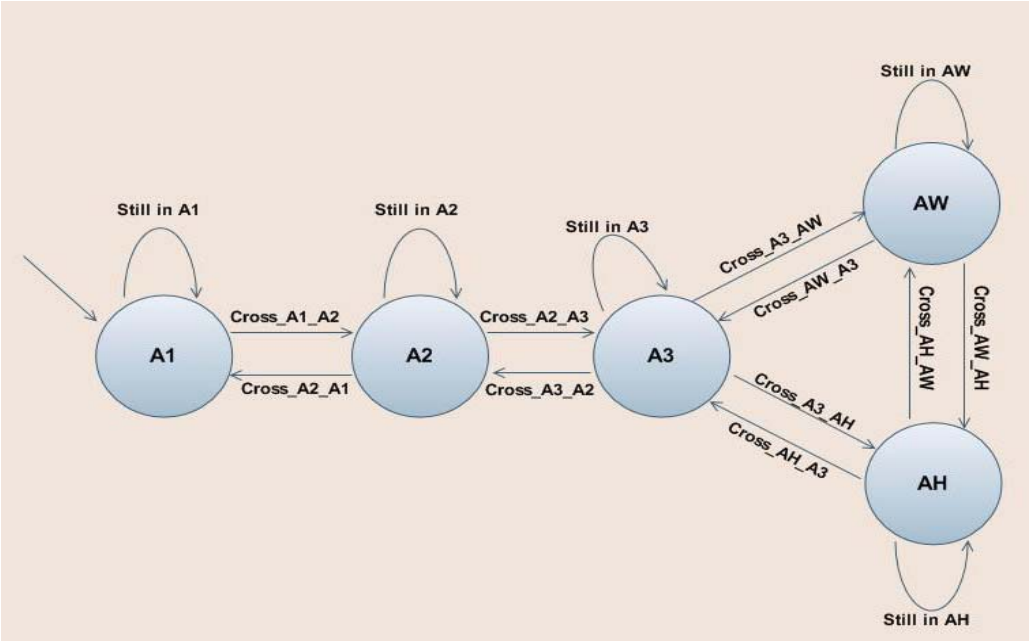

Figura 7.15: Diagrama del estado para los transiciones del MC

7.4.2.1 SDL para el Diagrama de Estado

El diagrama de estado se representa en un proceso llamado *state_diagram*, tiene una entrada de señal *RSSI*, que toma los valores de *RSSI_1* ($\Omega_1(d_{MC})$) y *RSSI_2* ($\Omega_2(d_{MC})$) de la WNIC MC, *RSSI_1* y *RSSI_2* son el RSSI de *AP_1* y *AP_2* respectivamente, entonces sale una señal *MC_state* para llevar el estado de MC al proceso *transition*. El proceso *transition* coge el actual y el antiguo estado del MC para generar la señal *MC_transition* que es un input para el proceso de *transitions_actions* (Figura 7.16).

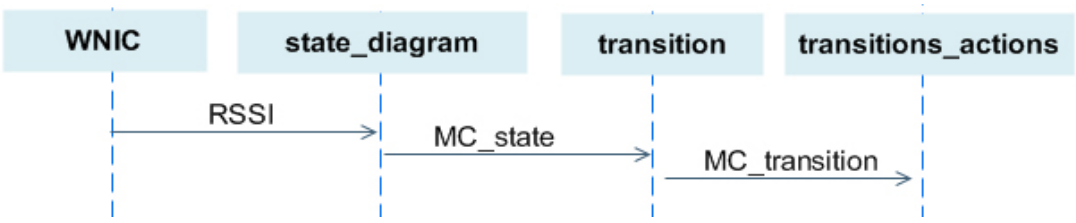

Figura 7.16: El intercambio de señales para generar el estado y la transición de MC

El proceso *state_diagram* produce la señal *MC_state* (estado) podría ser A_1, A_2, A_3, A_H o A_W. *MC_transition*(*trans*) es la única señal generada por el proceso *transition*, que incluye el mensaje *trans*, podría ser de tipo *Cross* como: *Cross_*A_1*-*A_2, *Cross_*A_2*-*A_1, *Cross_*A_2*-*A_3, *Cross_*A_3*-*A_2, *Cross_*A_3*-*A_H, *Cross_*A_H*-*A_3, *Cross_*A_3*-*A_W y *Cross_*A_W*-*A_3, o del tipo *Still* como: *Still_in_*A_1, *Still_in_*A_2, *Still_in_*A_3, *Still_in_*A_H y *Still_in_*A_W.

Después de recibir esta señal por el proceso *transitions_actions*, va a generar las señales correspondientes para ejecutar unas acciones, por otra parte, el proceso de *buffer_management* pone límites asociados a cada transición en cada buffer

7.4.3 La tecnica del gestion del buffer

Nuestra técnica propuesta se realiza en cuatro pasos:

- Descubrir el estado de cada MC cada Δt (1s por ejemplo).
- Generación de MC transición inmediatamente después esta tiempo usando un diagrama de estado.
- Informar la transición MC para diferentes entidades asignados en el AP, BS y MC, la primera entidad es AP Proxy (APP), que es un proxy sencillo que envía la señalización de información del MC a BS y los datos de BS a MC. El segundo es el Gestor de BSB (*BSBM*: del inglés *BSB Manager*) y el último es el *Gestor de MCB* (*MCBM* del inglés MCB Manager). Cuando BSBM es responsable de la gestión de los BSB y MCBM son responsables de la gestión del MCB.
- Cada entidad ejecuta algunas acciones de protocolo en función de la transición generada.

El BSB y MCB se gestionan en función de la transición MC, en consecuencia, para cada transición *Cross* el *transitions_actions* enviará señales a los procesos *MCBM* y *BSBM* con el fin de gestionar el buffer de vídeo, estas señales llevan un mensaje para describir la acción que se ejecuta, señales que se envían a BSBM debe pasar a través del APP. El proceso *buffer_management* es responsable de calcular la cantidad de vídeo protegido y es compartida por ambos MCBM y BSBM (Figura 7.17).

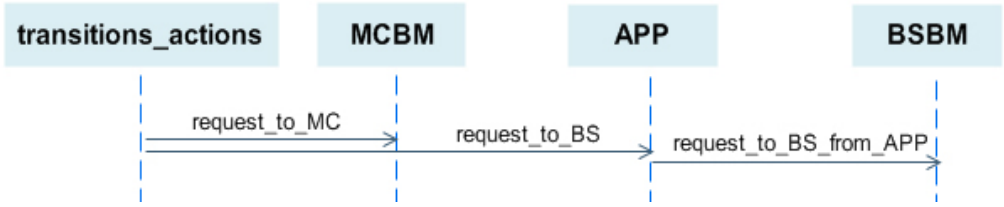

Figura 7.17: Señales generadas por el proceso *transitions_actions*

El proceso *transitions_actions* genera tres tipos de señales (Figura 7.17): la primera señal *request_to_BS* para BS para controlar el BSBM o para controlar la

velocidad del VoD, y pasa a través del APP. La segunda señal *request_to_MC* para MC para controlar el MCBM o comunicar a la BS sobre el estado del proceso de handover. La última señal es la señal *error_message*, que informa un caso de transición imposible

Cuando el *APP* recibe una petición de *transitions_actions* para cambiar la velocidad de transmisión, el APP se remitirá la solicitud al *BSBM* si la acción de transición requiere un cambio en la velocidad de transmisión de BS, el *BSBM* cambiará la velocidad de transmisión (aumento o disminución) y gestiona el BSB por el envío del señal *request_to_manage_BSBM* al proceso *buffer_management* para ejecutar la acción, a continuación dará respuesta al *APP* con el mensaje *ok*. Mientras que en el caso de que la acción de transición requiere un cambio en la velocidad de transmisión del servidor VoD, el *BSBM* enviará señal *vídeo_speed* al proceso *VoD* para aumentar o disminuir la velocidad de transmisión, en este momento, el *VoD* se enviará un mensaje *speed_ok* al *BSBM* para decir que la velocidad se ha cambiado (Figura 7.18).

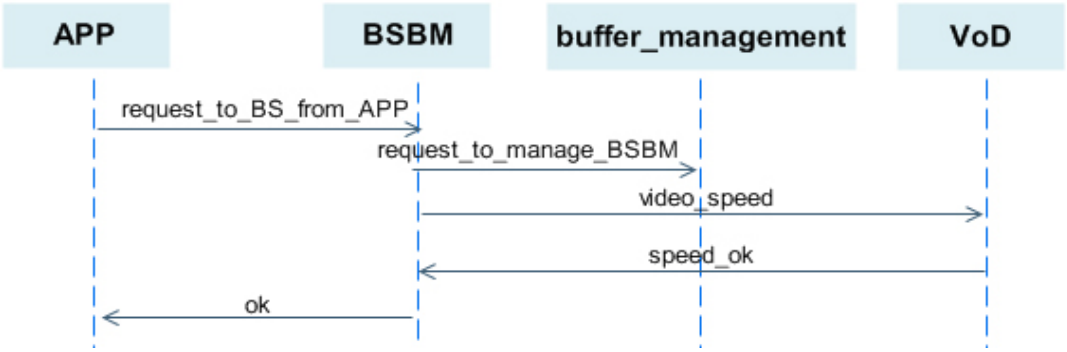

Figura 7.18: El intercambio de señales para controlar la velocidad de transmisión de vídeo

En este trabajo, todas las propiedades físicas relacionadas con la comunicación inalámbrica y el handover, como el retardo y el jitter, no están bajo el foco de este estudio. Los resultados demostraron que la gestión del buffer de vídeo y el control de la velocidad de transmisión es posible, esto es se podría lograr por el intercambio de mensajes entre MC y BS, que fue demostrado por la especificación SDL (los resultados detallados en CD).

7.5 Simulación del protocolo

El protocolo pospuesto se simuló por la implementación de un simulador específico de Java, el simulador combina el Filtro y el Predictor Gradiente con una versión mejorada de la técnica que se ha especificada por SDL para la gestión del buffer y el control de la

velocidad de transmisión. Un punto interesante es que deriva este simulador de la especificación SDL nos implementada anteriormente.

La Figura 7.19 muestra un diagrama simple que describe las principales clases de Java derivados de los principales bloques en el diagrama de SDL. Los bloques de color azul en ambos lados responsable del diagrama de estado y la generación de los estados, transiciones y acciones relacionadas con transiciones, mientras que los bloques verdes son responsables de la gestión de el MCB y BSB, y el control de la velocidad de transmisión en el servidor VoD y BS.

7.5.1 Impacto de los Agujeros en el Diagrama de Estado

Mientras que la señal se ve afectada por las condiciones del entorno, los agujeros que aparecen de repente para un intervalo limitado de tiempo. En consecuencia, si MC se mueve en cualquier zona de cobertura que podría sufrir la presencia de agujeros en el interior del CA, por lo tanto, nuevas transiciones inesperadas se generará como *Cross_*A_1*-*A_W porque el caso de los agujeros es el mismo que el caso de fuera de la cobertura en A_W; la diferencia es la cantidad de tiempo. Todas las transiciones causadas por los agujeros se muestran en la Figura 7.20. Las líneas punteadas de color rosa representan estas transiciones. Es importante hacer referencia a cuatro transiciones que se encuentran ya en la figura: *Cross_*A_3*-*A_W, *Cross_*A_W*-*A_3, *Cross_*A_H*-*A_W y *Cross_*A_W*-*A_H, pueden ser generados por la desconexión normal causado por el handover o fuera de cobertura, o podría ser causado por los agujeros, por lo tanto, el tamaño del agujero se puede distinguir entre el real estado del A_W y la causada por los agujeros. Otras transiciones como *Cross_*A_1*-*A_W, *Cross_*A_W*-*A_1, *Cross_*A_2*-*A_W y *Cross_*A_W*-*A_2 son derivados si los agujeros estarán presentes en A_1 y A_2. Después del proceso de filtración, estas cuatro transiciones se quitan y el diagrama de estado vuelve a ser como era.

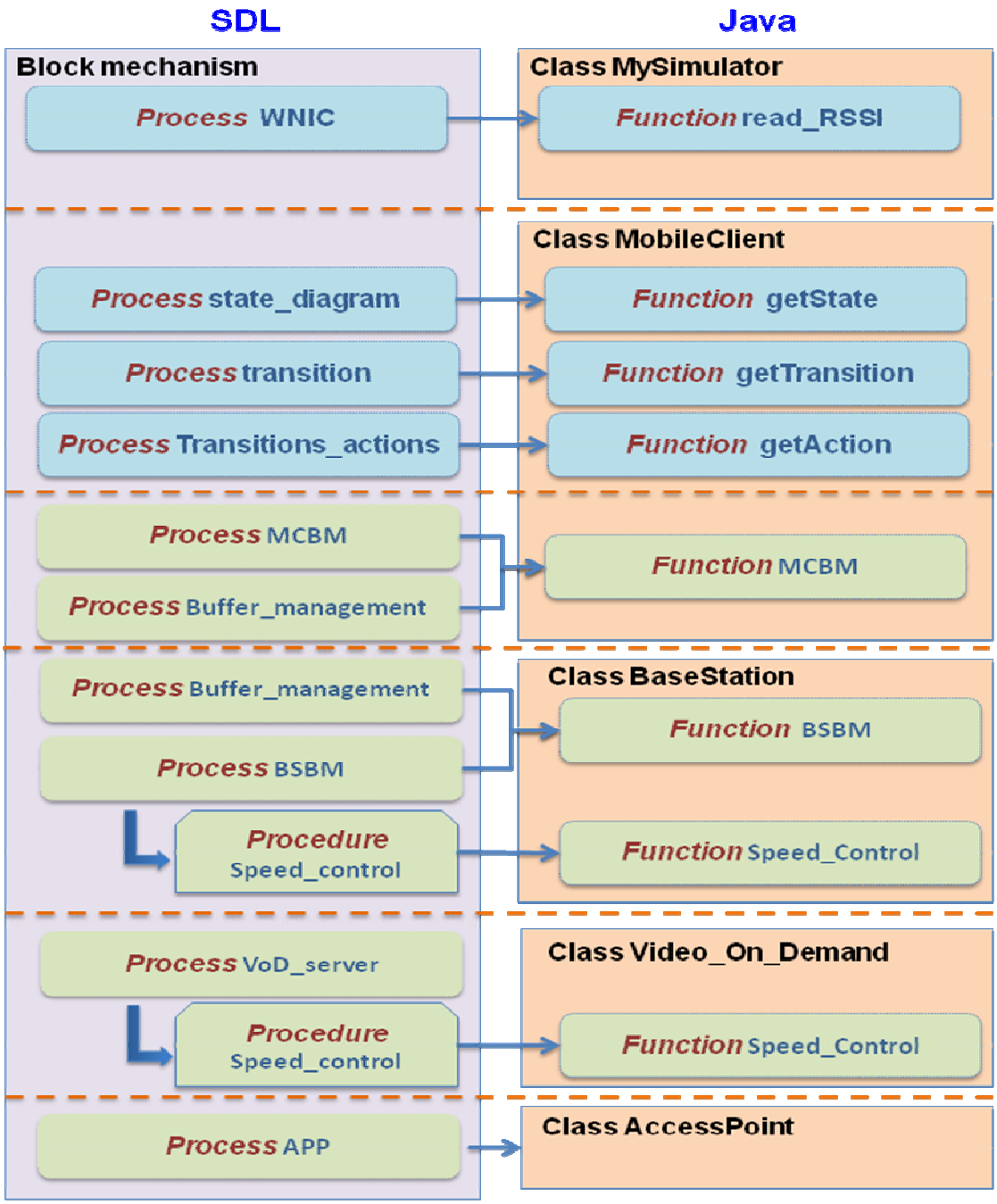

Figura 7.19: Derivación del simulador a partir de la especificación SDL

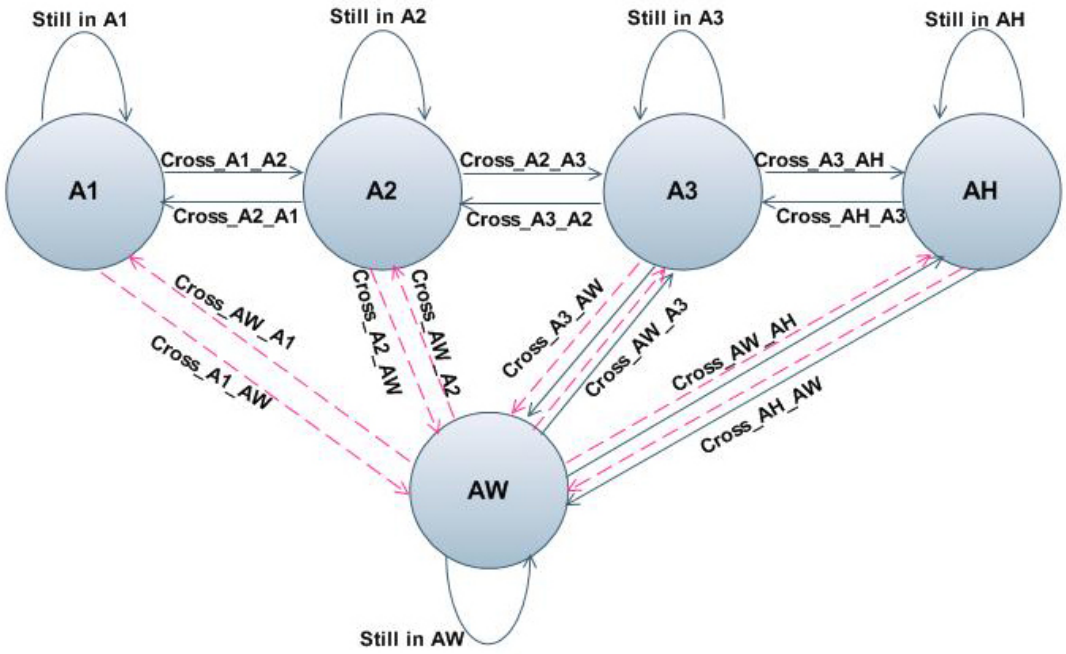

Figura 7.20: El diagrama de estado considerado en presencia de agujeros

7.5.2 Gestión de Buffer y Control de Velocidad de Transmisión

Gestión del buffer y el control de la velocidad de transmisión en cada entidad aparte no es eficiente o lógico, porque ambos están relacionados respectivamente. Eso significa que, cualquier cambio en la velocidad de transmisión debe ser controlada por la capacidad buffer, y el proceso de almacenamiento en el buffer depende de la velocidad de transmisión. Antes, los valores de velocidad han sido calculados por separado, que produce un comportamiento inesperado en algunos momentos durante el proceso de verificación. Por lo tanto algunas modificaciones son necesarias:

1. *Proceso* (*VoD-1*): *CONTROL VELOCIDAD VoD*: muestra cómo V_x se aumenta o disminuye por la solicitud de BS condicionada por estar entre V_x^{max} *y* V_x^{min}.
2. *Proceso (BS-1): BSBM* calcula el tamaño del BSB teniendo en cuenta los límites de BSB los valores correctos de velocidad para mantener el BSB el rango requerido. El tamaño del *BSB* se calcula: *cur_BSB_size* + = V_x - V_y.
3. *Proceso (BS-2): CONTROL VELOCIDAD* BS: muestra cómo V_y se aumenta o disminuye por la solicitud de MC, siempre V_y es controlado por los límites BSB para mantener el BSB siempre en el límite superior.

4. *Proceso* (*MC-1*): *MCBM* calcula el tamaño del MCB, teniendo en cuenta los límites de MCB y las solicitudes del cambio de V_y, para mantener el MCB en el rango requerido. El tamaño de el MCB se calcula: $cur\_MCB\_size += V_z - V_P$

Proceso (VoD-1): CONTROL VELOCIDAD VoD

```
Switch ( command ) {
 Case ISVF : { // Aumentar la velocidad de transmisión de vídeo
   If ( Vx < max_Vx - max_Vx / 20 )  { Vx = Vx + max_Vx / 20 }
   Else                              { Vx = max_Vx           }
 }
 Case DSVF : { // disminuir la velocidad de transmisión de vídeo
  If ( Vx > = min_Vx + max_Vx / 10 ) { Vx = Vx - max_Vx / 10 }
  Else                               { Vx = min_Vx           }
 }
 Otherwise: // parar transmision       Vx = 0
}
```

Proceso (BS-1): BSBM

```
If ( cur_BSB_size < BSB_LIMITi )
 // Aumentar la velocidad de transmisión de vídeo del VoD
                                      { VoD ( ISVF )
 // parar transmision del BS             Vy = 0     }

 // Establecer la misma velocidad de transmisión de vídeo
If ( cur_BSB_size > BSB_LIMITs & Vy > 0 )   Vx = Vy

 // parar transmision
If ( cur_BSB_size > BSB_LIMITs & Vy = 0 )  VoD ( STOP )

// Calcular el vídeo almacenado en BSB
cur_BSB_size = cur_BSB_size + Vx - Vy
```

Proceso (BS-2): CONTROL VELOCIDAD BS

```
Switch (command) {
 Case: ISVF { // Aumentar la velocidad de transmisión de vídeo
      If ( Vy  > TH )                                  Vy = TH
      Else { If(BSB_LIMITs > cur_BSB_size > BSB_LIMITi)
                                                       Vy = TH
             Else if (cur_BSB_size < BSB_LIMITi){VoD ( ISVF )
                                                       Vy = Vy + TH / 5}
             Else                                     {Vy = TH
                                                       VoD ( STOP ) }
     }
 }
 Case: DSVF {  // disminuir la velocidad de transmisión de vídeo
      If ( Vy  > =  min_Vy  +  max_Vy / 10 )
      { If ( BSB_LIMITs > cur_BSB_size > BSB_LIMITi )
                                              Vy = Vy - max_Vy / 10
        Else if ( cur_BSB_size <  BSB_LIMITi )
                                              VoD( ISVF )
        Else                                 { VoD ( STOP )
                                              Vy = Vy - max_Vy / 10 }
      }
     Else                                     Vy = min_Vy
 }
 Otherwise: Vy = 0 //parar transmision
}
```

Proceso (MC-1): MCBM

```
If( cur_MCB_size >= MCB_max ){                    Vp = Kp
    If( Vz > min_Vz && state ≠ AW )               Vz = min_Vz
}
Else If((MCB_max > cur_MCB_size >= MCB_LIMITs) && state ≠ AW)
                                                  Vp = Vz = Kp
Else If (cur_MCB_size < MCB_LIMITi){
                                                  Vp = 0
   If(Vz < TH && state ≠ AW) // Aumentar la velocidad
                                                  BS (ISVF)
}
Else If (MCB_LIMITs > cur_MCB_size >= MCB_LIMITi){
   Switch (state){
      Case AW :                                   Vp = Kp / 2
      Otherwise:  {   If(Vz < TH )                BS (ISVF)
                                                  Vp = Kp
                  }
               }
}
Else If (cur_MCB_size <= 0 && Vz <= 0){
                                                  cur_MCB_size = 0
                                                  Vp = 0
                                                  Vz = 0
}
Else                                              Vp = Kp
//calcular el vídeo almacenado
cur_MCB_size = cur_MCB_size + Vz - Vp
```

Algunas transiciones del MC producen comandos para controlar la velocidad de transmisión de VoD y BS, que conducen cambios en el BSB y MCB. Todas las transiciones con sus comandos se explican en Tabla 7.6.

Tabla 7.6: Transiciones y sus comandos de control de velocidad

Transición	Control de velocidad
Cross_A1-A2	**VoD (ISVF)** // Aumenta la velocidad de transmisión del VoD
Cross_A2-A1	**VoD (DSVF)** // Disminuye la velocidad de transmisión del VoD
Cross_A2-A3	// si el MCB no llegó a su límite superior pede a la BS para aumentar su velocidad de transmisión **If (cur_MCB_size < MCB_LIMITs && Vz < TH)** **BS (ISVF)**
Cross_A3-A2	// si MCB está por encima del límite superior entonces pede la BS para disminuir su velocidad de transmisión **If (cur_MCB_size > MCB_LIMITs) BS (DSVF)**

Cross_A3-AH	// durante el proceso de handover, la velocidad de transmisión de la BS y AP es cero debido a la desconexión
	If (handover process start) Vz = Vy =0
	// si el proceso de handover no se ha iniciado y el MCB es menor que su límite superior, pedir a la BS Aumenta la velocidad de transmisión
	Else
	If (cur_MCB_size < MCB_LIMITs && Vz < TH)
	BS (ISVF)

Cross_AH-A3	-
Cross_A3-AW	// la velocidad de transmisión es cero debido a la desconexión **Vz = Vy = 0**
Cross_AW-A3	// si MCB es inferior a su límite superior, pedir a la BS para aumentar su velocidad de transmisión **If (cur_MCB_size < MCB_LIMITs && Vz < TH)** **BS (ISVF)**
Cross_AH-AW	// la velocidad de transmisión es cero debido a la desconexión **Vz = Vy = 0**

Cross_AW-AH	// durante el proceso de handover la velocidad de transmisión de la BS y AP es cero debido a la desconexión
	If (handover_process start) Vz = Vy = 0
	// si el proceso de handover no se ha iniciado y el MCB es menor que su límite superior, pedir a la BS Aumenta la Velocidad de Transmisión
	Else If(cur_MCB_size < MCB_LIMITs && Vz < TH)
	BS (ISVF)

Cross_A1-AW	**Vz=Vy=0** // la velocidad de transmisión es cero debido al agujero
Cross_AW-A1	-
Cross_A2-AW	**Vz=Vy=0** // la velocidad de transmisión es cero debido al agujero
Cross_AW-A2	-

7.5.3 El proceso de simulación

El proceso de simulación consiste en varios pasos:

1. Crear objetos de todas las entidades y establecer sus valores iniciales.
2. Obtener valores $\Omega(d_{MC})$ de los APs asociados de los archivos de datos (*RSSI_1.txt* para el primer AP y *RSSI_2.txt* para el segundo AP) usando la función ***read_RSSI***, y establecer el tiempo de simulación a ser igual el tiempo total del RSSI escaneado.
3. Aplicar el filtro Gradiente en estos valores para eliminar los agujeros (con el *Proceso SIM-1: Filtro Gradiente*), en el mismo proceso el filtro llama el Predictor para predecir el próximo estado de MC (*Proceso SIM-2: Predictor Gradiente*).
4. Inicializar las conexiones entre las entidades (BS con VoD, AP con BS, MC con AP).
5. Crear matrices para almacenar $\Omega(d_{MC})$, velocidad de transmisión y los valores de buffer durante el tiempo de simulación.
6. Ejecute los siguientes pasos, mientras que el tiempo total de la simulación no termina:
   - Almacenar $\Omega(d_{MC})$ medido actual de los asociados AP
   - Obtener el estado del MC: función ***getState***.
   - Obtener la transición MC: función ***getTransition***.
   - Obtener acciones asociadas a la transición del MC: función ***getAction***.
   - Llama BSBM: función ***BSBM***.
   - Almacenar el tamaño actual del BSB.
   - llama MCBM: función ***MCBM.***
   - Almacenar el tamaño del MCB.
   - Tenga en cuenta que si BS ha recibido el vídeo completo, entonces $V_z = 0$; Si MC ha recibido el vídeo completo, entonces $V_y = V_z = 0$ y la simulación se dará por terminado

7. Muestra los gráficos de los resultados tomando los datos almacenados

Proceso (SIM-1): Filtro Gradient

```
Variables: x,y,z,w,m,Filtered_value
x = Gradient Predictor (t,RSSI)
m = ( RSSI[t-1] + x ) / 2
y = square root (0.5 * ( RSSI[t-1] - m)^2 + (x - m)^2)
z = signum ( RSSI[t-1] – x )
w = signum ((RSSI[t] * RSSI[t-1])^2)
Filtered_value = (y * z * w) + x
```

Proceso (SIM-2): Predictor Gradient

```
// El predictor comienza a cuando hay 20 valores mínimos de la
muestra, por lo tanto t debe ser mayor de 20
Variables i=0, j=0, predicted, gradient_sum=0, x =0, y=0
Array RSSI_No_Holes[20]
For ( i = t-20, i < t-1, i++){
      If (RSSI[i] ≠ 0){      RSSI_No_Holes [j] = RSSI[i]
                             j++
                     }
}
For( i = 1, i < j, i++)
                   x = x + (RSSI_No_Holes[i] - RSSI_No_Holes[i-1])
gradient_sum = x / 20
predicted = ( gradient_sum *(21))+ RSSI_No_Holes[0]
```

7.5.4 Los resultados de simulación

La simulación demostró que el protocolo simulado proporciona soluciones para tres problemas:

- El control de velocidad de transmisión sea suficiente para gestionar el proceso de buffer que evita la pérdida de transmisión de paquetes durante las desconexiones corto. También, el buffer se mantuvo cerca de su límite superior, y sólo durante las desconexiones que se encontraba bajo este nivel, mientras que la reproducción de vídeo tenia siempre una calidad adecuada (revisa Figura 5.3, 5.4, 5.5, 5.6 y 5.10) podría soportar períodos de desconexión hasta 135s.

- El Predictor degradado podía predecir el siguiente estado del MC que permite los comandos del control de velocidad a ejecutar antes de desconexiones. Como se muestra en todas las gráficas anteriores (capítulo 5), los valores del $\Omega(d_{MC})$ filtrados y predecidas eran muy cercanos a los valores reales, que indican que el rendimiento del predictor es muy buena y precisa, de acuerdo con la prueba sintética en comparación con otros predictores.
- El Filtro Gradiente proporciona una solución muy potente para el problema de los agujeros. Se trata de un filtro eficaz, que se demostró en todos los casos discutidos de agujeros: agujeros cortos (1 s) y los agujeros largos (18 s).

7.6 Conclusiones y líneas de trabajo futuro

Después de 3 años trabajando en mi tesis doctoral se presentan las principales conclusiones y las líneas de trabajo futuro

7.6.1 Conclusiones

Hoy en día, los servicios multimedia están experimentando un rápido desarrollo debido a la creciente popularidad de RTMAs. La mayoría de de estas aplicaciones utilizan la tecnología de streaming para ofrecer servicios a través de Internet, tales como VoIP y VoD. Por lo tanto, las redes inalámbricas WiFi y WiMAX soportan RTMAs y proporcionan al usuario con una variedad de servicios multimedia.

El MC puede solicitar los servicios de streaming de vídeo mientras se está dentro del CA de WiFi AP. Durante el movimiento podría ser desconectado debido a las fluctuaciones de la señal, la cual es causada por los agujeros de cobertura, el handover, o el estado de fuera de cobertura. Los agujeros son posiciones dentro del CA donde la señal fluctúa. Por lo tanto los MCs sufrirán interrupciones en los servicios de video durante las desconexiones mencionadas, causando pérdida en los paquetes de video.

Se han desarrollado trabajos para abordar este problema, algunos de ellos sólo tratan los problemas ocasionados por el handover, otros se centran en la predicción, y otros artículos presentaran técnicas para la gestión del buffer para reducir la pérdida de paquetes de vídeo. Se echa en falta un protocolo efectivo para mitigar los problemas causados por las desconexiones mencionadas aunque sea por los agujeros.

Por lo tanto, hemos desarrollado un protocolo eficaz basado en una nueva especificación matemática del CA, y la identificación de movimiento del MC teniendo en cuenta los agujeros. El protocolo consiste en dos técnicas:

- El Predictor y el filtro del RSSI gradiente se desarrollaron como una técnica de filtrado para mitigar los efectos adversos de los agujeros de cobertura. El filtro se deriva de la degradado promedio de la muestra RSSI establece cuando el MC se mueve con movimientos regulares a velocidad constante. Se utilizó el promedio para calcular el RSSI instantáneo futuro.
- La técnica de la gestión del buffer y el control de velocidad de transmisión para mitigar los paquetes pérdidas en la transmisión de vídeo. Un diagrama de estado para los movimientos de MC se utilizó para generar transiciones en caso de que el MC cruzado diferentes zonas de cobertura. Cada transición genera comandos para controlar la velocidad de transmisión de VoD y BS, lo que efectiva gestiona el BSB y MCB. Esta técnica mantiene a ambos en el límite superior el mayor tiempo posible para proporcionar el MC con los frames de vídeo necesarios durante la duración de la interrupción.

La síntesis y el análisis experimental del Predictor y el filtro del RSSI Gradiente demostrado los mejores resultados en comparación con el filtro de Kalman y el modelo de Grey. Se filtra todos los agujeros existentes de diferentes tamaños en todos los casos y predijo que la próxima cobertura del MC precisa.

Los resultados de la verificación del protocolo y la simulación demostraron su eficiencia. Además, el protocolo es adecuado para todos los tipos de las desconexiones causadas por los agujeros, el handover, o falta de cobertura (zona fuera de cobertura). Las pruebas demostraron que ofrecía la suficiente cantidad de frames de vídeo para ser consumidos durante las desconexiones menciona, incluso para interrupciones de larga duración de alrededor de 135 s.

7.6.2 Líneas de Trabajo Futuro

Proporcionamos el predictor y el filtro que se basan en consideraciones movimientos regulares. Los patrones de movimiento periódico de MC se abordaron pero los patrones no periódicos no pueden ser tratados. Por lo tanto consideramos que es importante desarrollar nuestro trabajo en el futuro a través de mejorar tres líneas importantes:

- El estudio de los patrones no periódica más compleja de modelos de movimiento de MC con el fin de encontrar nuevas matemáticas especificaciones para estos patrones.
- Desarrollar el filtro con la nueva especificación que se adapta a cualquier modelo de movimiento, incluyendo los patrones de los niveles de cobertura de imprevistos.
- Desarrollar el protocolo con el filtro mejorado le proporcionará capacidades de alta para tratar las complejas interrupciones de los casos.

REFERENCES

[1] S. Ing and S. Rudkin, "Simplifying real-time multimedia application development using session descriptions," *Springer Lecture Notes Computer Science*, vol. 1597/1999, pp. 305-314, 1999.

[2] X. Wang and W. Wang, "An efficient negotiation protocol for real-time multimedia applications over wireless networks," *IEEE Wireless Communications and Networking Conf.*, Georgia, 21-25 Mar. 2004, vol. 4, pp. 2533-2538.

[3] N. Sai Shankar and M. van der Schaar, "Performance analysis of video transmission over IEEE 802.11a/e WLANs," *IEEE Trans. on Veh. Technol.*, vol. 56, No. 4, pp. 2346-2362, Jul. 2007.

[4] J.N. Hwang, "Multimedia networking from theory to practice," 1st ed. New York, USA: Cambridge University Press, 2009.

[5] N. Cranley and M. Davis, "An experimental investigation of IEEE 802.11e TXOP facility for real-Time video streaming," presented at the IEEE *Global Telecommunications Conf.*, Washington, 26-30 Nov. 2007, pp. 2075-2080.

[6] U. Varshney, A. Snow, M. McGivern and C. Howard, "Voice over IP," *Commun. ACM Mag*., vol. 45, pp. 89-96, Jan. 2002.

[7] I.F. Akyildiz, J. Xie and SH. Mohanty, "A survey of mobility management in next-generation all-IP-based wireless systems," *IEEE Wireless Commun.*, vol. 11, pp. 16-28, Aug. 2004.

[8] H.R. Sheikh and A.C. Bovik, "Information theoretic approaches to image quality assessment" in *Image and Video Processing,* 2nd ed., Academic Press, New York, 2005, pp. 975-989.

[9] "Supplement to IEEE 802.11a standard for information technology - Telecommunications and information exchange between systems - Local and metropolitan area networks - Specific requirements - Part 11: Wireless LAN

Medium Access Control (MAC) and Physical Layer (PHY) specifications: High-speed Physical Layer in the 5 GHZ Band," IEEE 802.11a, 1999.

[10] "Supplement to IEEE standard for information technology - Telecommunications and information exchange between systems - Local and metropolitan area networks - Specific requirements - Part 11: Wireless LAN Medium Access Control (MAC) and Physical Layer (PHY) specifications: Higher - Speed Physical Layer Extension in the 2.4 GHz Band," IEEE 802.11b, 1999.

[11] "IEEE standard for information technology - Telecommunications and information exchange between systems - Local and metropolitan area networks - Specific requirements - Part 11: Wireless LAN Medium Access Control (MAC) and Physical Layer (PHY) specifications, Amendment 4: Further Higher Data Rate Extension in the 2.4 GHz Band," IEEE 802.11g, 2003.

[12] "IEEE standard for information technology - Telecommunications and information exchange between systems - Local and metropolitan area networks - Specific requirements - Part 11: Wireless LAN Medium Access Control (MAC) and Physical Layer (PHY) Specifications Amendment 5: Enhancements for Higher Throughput," IEEE Std 802.11n, 2009

[13] A. Ksentini, M. Naimi and A. Gueroui, "Toward an improvement of H.264 video transmission over IEEE 802.11e through a cross-layer architecture," *IEEE Commun. Mag.*, vol. 44, pp. 107-114, Jan. 2006.

[14] "IEEE standard for Information technology - Telecommunications and information exchange between systems - Local and metropolitan area networks - Specific requirements - Part 11: Wireless LAN Medium Access Control (MAC) and Physical Layer (PHY) Specifications," IEEE 802.11™, 2007.

[15] H. Zhu, M. Li, I. Chlamtac and B. Prabhakaran, "A survey of quality of service in IEEE 802.11 networks," *IEEE Wireless Commun. Mag.*, vol. 11, pp. 6-14, Aug. 2004.

[16] S. Mangold, S. Choi, G.R. Hiertz, O. Klein and B. Walke, "Analysis of IEEE 802.11e for QoS support in wireless LANs," *IEEE Wireless Commun. Mag.*, vol. 10, pp. 40- 50, Dec. 2003.

[17] R. Corvaja, A. Zanella, M. Dossi, A. Tontoli and P. Zennaro, "Experimental performance of the handover procedure in a WiFi network," in *Proc. 7th Int. Symp. Wireless Personal Multimedia Communications*, Italy, 2004.

[18] G. R. Hiertz, S. Max, R. Zhao, D. Denteneer and L. Berlemann, "Principles of IEEE 802.11s," in *Proc. 16th Int. Conf. Computer Communications and Networks*, Hawaii, 2007, pp. 1002-1007.

[19] D. Deng and H. Yen, "Quality-of-service provisioning system for multimedia transmission in IEEE 802.11 wireless LANs," *IEEE J. on Select. Areas in Commun.*, vol. 23, pp. 1240-1252, June 2005.

[20] L. Berlemann, C. Hoymann, G.R. Hiertz and S. Mangold, "Coexistence and Interworking of IEEE 802.16 and IEEE 802.11(e)," presented at the *IEEE 63rd Vehicular Technology Conf.* (*VTC 2006-Spring*), Melbourne, 7-10 May 2006, vol. 1, pp. 27-31.

[21] M. Sauter, "Beyond 3G- bringing networks, terminals and the web together: LTE, WiMAX, IMS, 4G devices and the mobile web," 1st ed. West Sussex, UK: John Wileys & Sons, 2009.

[22] X. Yang, M. Venkatachalam and S. Mohanty, "Exploiting the MAC layer flexibility of WiMAX to systematically enhance TCP performance," presented at the *IEEE Mobile WiMAX Symp.*, Orlando, 25-29 Mar. 2007, pp. 60-65.

[23] T. Yucek, M.K. Ozdemir, H. Arslan and F.E. Retnasothie, "A comparative study of initial downlink channel estimation algorithms for mobile WiMAX," *IEEE Mobile WiMAX Symp.*, Orlando, 25-29 Mar. 2007, pp. 32-37.

[24] S. Choi, G.H. Hwang, T. Kwon, A.R. Lim and D.H. Cho, “Fast handover scheme for real-time downlink services in IEEE 802.16e BWA system,” presented at the *IEEE 61st Vehicular Technology Conf.*, Stockholm, 30 May-1 June 2005, vol. 3, pp. 2028-2032.

[25] J. Chen and W. Tan, “Predictive dynamic channel allocation scheme for improving power saving and mobility in BWA networks,” *Springer J. Mobile Networks and Applicat.*, vol. 12, no. 1, pp. 15–30, Feb. 2007.

[26] S. Hu, G. Wu, Y.L. Guan, C.L. Law, Y. Yan and S. Li, “Development and performance evaluation of mobile WiMAX testbed,” presented at the *IEEE Mobile WiMAX Symp.*, Orlando, 25-29 Mar. 2007, pp. 104-107.

[27] L. Lee and K. Wang, “A network assisted fast handover scheme for IEEE 802.16e networks,” presented at the *IEEE 18th Int. Symp. Personal, Indoor and Mobile Radio Communications*, Athens, 3-7 Sept. 2007, pp. 1-5.

[28] J. Roy, V. Vaidehi and S.Srikanth, “Always best-connected QoS integration model for the WLAN, WiMAX heterogeneous network,” presented at the *1st Int. Conf. Industrial and Information Systems*, Sri Lanka, 8-11 Aug. 2006, pp. 361-366.

[29] T. Ali-Yahiya, K. Sethom and G. Pujolle, “A Case study: IEEE 802.21 framework design for service continuity across WLAN and WMAN,” presented at the *Int. Conf. Wireless and Optical Communications Networks*, Singapore, 2-4 July 2007, pp. 1–5.

[30] G. Dong and J. Dai, “An improved handover algorithm for scheduling services in IEEE802.16e,” presented at the *IEEE Mobile WiMAX Symp.*, Orlando, 25-29 Mar. 2007, pp. 38-42.

[31] D.J. Wright, “Maintaining QoS during handover among multiple wireless access technologies,” presented at the *Int. Conf. Management of Mobile Business*, Toronto, 9-11 Jul. 2007, pp. 10.

[32] Y. Zhang, X. Jiang, Z. Lin, "A pre-anticipated handover seamless QoS scheme for IEEE 802.16e based on mobile station character pattern," presented at the *Int. Conf. Wireless Communications, Networking and Mobile Computing*, China, 22-24 Sept. 2006, pp. 1-4.

[33] T. Fritsch, H. Ritter and J. Schiller, "Mobile phone gaming (A follow-Up survey of the mobile phone gaming sector and Its users)," *Springer Lecture Notes in Computer Science* - ICEC 2006, vol. 4161, pp. 292-297, Oct. 2006.

[34] F. Zhai, P. Pahalawatta and A. K. Katsaggelos, "Wireless video streaming," in *The Essential Guide to Video Processing*, 2009, London, UK, Elsevier, 2009, ch. 18, pp. 571-618.

[35] M. Hsu and Y. Chen, "Enhanced PCF protocols for real-time multimedia services over 802.11 wireless networks," presented at the *26th IEEE Int. Conf. Distributed Computing Systems Workshops*, Lisboa, 4-7 Jul. 2006, pp. 56.

[36] J.C. Fernandez, T. Talebt, K. Hashimoto, Y. Nemoto and N. Kato, "Multi-path scheduling algorithm for real-time video applications in next-generation wireless networks," presented at the *4th Int. Conf. Innovations in Information Technology*, Dubai, 18-20 Nov. 2007, pp. 73-77.

[37] M. Van Der Schaar and N. Sai Shankar, "Cross-layer wireless multimedia transmission: challenges, principles and new paradigms," *IEEE Wireless Commun. Mag.*, vol. 12, pp. 50-58, Aug. 2005.

[38] G. Kousalya, P. Narayanasamy, J. Park, T. Kim, "Predictive handoff mechanism with real-time mobility tracking in a campus wide wireless network considering ITS," *ACM Comput. Commun.*, vol. 31, pp. 2781-2789, Jul. 2008.

[39] R. El-Marakby and M. Enugula, "Enhanced QoS for real-time multimedia delivery over the wireless link using RFID technology," presented at the *IEEE Int. Symp. Signal Processing and Information Technology*, Vancouver, 27-30 Aug. 2006, pp. 728-734.

[40] M.A. El-Gendy, A. Bose and K.G. Shin, "Evolution of the internet QoS and support for soft real-time applications," in *Proc. of the IEEE*, 2003, vol. 91, pp. 1086-1104.

[41] H. Zhai, X. Chen and Y. Fang, "A call admission and rate control scheme for multimedia support over IEEE 802.11 Wireless LANs," *ACM Wireless Networks*, vol. 12, pp. 451-463, Jul. 2006.

[42] Ahmed A. Kishk, "Fundamentals of Antennas," in *Antennas for Base Stations in Wireless Communications*, ed. Z.N. Chen, K.M. Luk, New York, McGraw Hill Professional, 2009, ch 1, pp. 1-28.

[43] Z. N. Chen, W. K. Toh, S. P. See and X. Qing, "Antennas for WLAN (WiFi) Applications," in *Antennas for Base Stations in Wireless Communications*, New York, McGraw Hill Professional, 2009, ch 7, pp. 241-287.

[44] L. Taylor, R. Titmuss and C. Lebre, "The challenges of seamless handover in future mobile multimedia networks," *IEEE Pers. Commun.*, vol. 6, pp. 32-37, Apr. 1999.

[45] J.H. Li, S. Luo, S. Das, T. McAuley, M. Patel, A. Staikos and M. Gerla, "An integrated framework for seamless soft handoff in Ad Hoc networks," presented at the *Military Communications Conf.*, Washington D.C, 23-25 Oct. 2006, pp. 1-7.

[46] M. Vilas, X.G. Pañeda, D. Melendi, R. García and V.G. García, "Signaling management to reduce roaming effects over streaming services," in *Proc. IEEE 32nd EUROMICRO Conf. Software Engineering and Advanced Applications*, Croatia, 2006.

[47] H.D. Cho, J.K. Park, W.J. Ko, K. Lim and W. Kim, "A study on the MCHO method in hard handover and soft handover between WLAN and CDMA," presented at the *Int. Conf. Consumer Electronics ICCE 2005*, Dig. Tech. Papers, Las Vegas, 8-12 Jan. 2005, pp. 391- 392.

[48] H.H. Choi and D.H. Cho "Takeover: a new vertical handover concept for next-generation heterogeneous networks," presented at the *IEEE 61st Vehicular Technology Conf.*, Stockholm, 30 May-1 June 2005, vol. 4, pp. 2225-2229.

[49] Mo Li, K. Sandrasegaran and T. Tung, "A multi-interface proposal for IEEE 802.21 media independent handover," presented at the *6th Int. Conf. Management of Mobile Business*, Toronto, 9-11 Jul. 2007, pp. 7–7.

[50] Q.B. Mussabbir, W. Yao, Z. Niu and X. Fu, "Optimized FMIPv6 using IEEE802.21 MIH services in vehicular networks," *IEEE Trans. on Veh. Technol.*, vol. 56, pp. 3397 – 3407, Nov. 2007.

[51] Ch. Guo, Z. Guo, Q. Zhang and W. Zhu, "A seamless and proactive end-to-end mobility solution for roaming across heterogeneous wireless networks," *IEEE J. Sel. Areas Commun.*, vol. 22, pp. 834-848, June 2004.

[52] W. Wu, N. Banerjee, K. Basu and S.K. Das, "SIP-based vertical handoff between WWANS and WLANS," *IEEE Wireless Commun.*, vol. 12, pp. 66-72, June 2005.

[53] A.V. Garmonov, S.H. Cheon, D.H. Yim, K.T. Han, Y. S. Park, A.Y. Savinkov, S.A. Filin, S.N. Moiseev and M.S. Kondakov, "QoS-Oriented intersystem handover between IEEE 802.11b and overlay networks," *IEEE Trans. Veh. Technol.*, vol. 57, pp. 1142 – 1154, Mar. 2008.

[54] "IEEE standard for local and metropolitan area networks - Part 16: Air interface for fixed and mobile broadband wireless access systems, Amendment 2: Physical and medium access control layers for combined fixed and mobile operation in licensed bands and corrigendum 1," IEEE 802.16, 2006.

[55] S.C. Oh, C.Y. Lee, Y.S. Shin and J.U. Kim, "A vertical handover based on software communications architectures," presented at the *IEEE 60th Vehicular Technology Conf.*, Los Angeles, 26-29, Sept. 2004, vol. 3, pp. 1973-1977.

[56] L. Dimopoulou, G. Leoleis and L.S. Venieris, “Fast handover support in a WLAN environment: challenges and perspectives,” *IEEE Network Mag.*, vol. 19, pp. 14-20, June 2005.

[57] P. Bellavista, A. Corradi and C. Giannelli, “Mobile proxies for proactive buffering in wireless internet multimedia streaming,” presented at the *Int. Workshop Services and Infrastructure for the Ubiquitous and Mobile Internet* (*SIUMI*), Ohio, 2005.

[58] S.K. Kim, C.G. Kang and K.S. Kim, “A adaptive handover decision algorithm based on the estimating mobility from signal strength measurements,” presented at the *IEEE 60th Vehicular Technology Conf.* (*VTC2004-Fall*), Los Angeles, 26-29 Sept. 2004, vol. 2, pp. 1004-1008,.

[59] “Draft standard for information technology - Telecommunications and information exchange between systems - Local and metropolitan area networks - Specific requirements - Part 11: Wireless LAN Medium Access Control (MAC) and Physical Layer (PHY) specifications Amendment 2: Fast BSS Transition,” IEEE P802.11rTM/D9.0, 2008.

[60] A. Lakas and M. Boulmalf, “Experimental analysis of VOIP over wireless local area networks,” *Academy Publisher J. Commun.* (*JCM*), vol. 2, no. 4, pp. 3-9, June 2007.

[61] Y.H. Kim, S.W. Kim, J.W. Nah and J.T. park, “Extension of Fast Mobile IPv6 with multiple pre-registrations: design and implementation,” presented at the *3rd Int. Conf. Communication Systems Software and Middleware and Workshops*, Bangalore, 6-10 Jan. 2008, pp. 460 – 464,.

[62] P. Iyer, N. Natarajan, M. Venkatachalam, A. Bedekar, E. Gonen, K. Etemad and P. Taaghol, “All-IP network architecture for mobile WiMAX,” presented at the *IEEE Mobile WiMAX Symp.*, Orlando, 25-29 Mar. 2007, pp. 54-59.

[63] P. Bellavista, A. Corradi and C. Giannelli, "Evaluating filtering strategies for decentralized handover," in *Proc. 11th IEEE Symp. Computers and Communications*, Sardinia, 2006, pp. 167-174.

[64] M. Leoni, S.R. Humayoun, M. Mecella and R. Russo, "A bayesian approach for disconnection management in mobile Ad-Hoc networks," Extended version, *Ubiquitous Comput. and Commun.* (*UBICC*) *J. - Special Issue on Coordination of Pervasive Environment*– CPE, Mar. 2008.

[65] G.D. Li, D. Yamaguchi, K. Mizutani and M. Nagai, "New proposal and accuracy evaluation of grey prediction GM," *IEICE Trans. Fundamentals of Electron., Commun. and Comput. Sci.*, vol. E90-A, pp. 1188-1197, June 2007.

[66] C.H. Lee and C.J. Yu, "An Intelligent handoff algorithm for wireless communication systems using grey prediction and fuzzy decision system," presented at the *2004 IEEE Int. Conf. Networking, Sensing and Control*, Taiwan, 21-23 Mar. 2004, vol. 1, pp. 541- 546.

[67] K.R. Anne, K. Kyamakya, F. Erbas, C. Takenga and J.C. Chedjou, "GSM RSSI-based positioning using extended Kalman filter for training artificial neural networks," in *Proc. 60th IEEE Vehicular Technology Conf.*, Los Angeles, 2004, pp. 4141 – 4145.

[68] M. Helén, J. Latvala, H. Ikonen and J. Niittylahti, "Using calibration in RSSI-based location tracking system," Digital and Comput. Syst. Lab., Tampere University of Technol., Tempere, Finland, 2005.

[69] A. Kotanen, M. Hännikäinen, H. Leppäkoski and T.D. Hämäläinen, "Positioning with IEEE 802.11b wireless LAN," presented at the *14th IEEE Int. Symp. Personal, Indoor and Mobile Radio Communications*, Beijing, 7-11 Sept 2003, pp. 2218-2222.

[70] B. Kusy, A. Ledeczi and X. Koutsoukos, "Tracking mobile nodes using RF Doppler shifts," in *Proc. 5th ACM Int. Conf. Embedded Networked Sensor Systems*, Sydney, 2007, pp. 29-42,.

[71] H. Choi and B. Gi Lee, "A TCP agent scheme based on active buffer control to support lossless handover in broadband wireless networks," presented at The *IEEE Global Telecommunications Conf. GLOBECOM '02*, Taiwan, 17-21 Nov. 2002, vol 3, pp.2493 – 2497.

[72] A. Suarez, E. Macías, J. Martín, Y. Gutiérrez and M. Gil, "Light protocol and buffer management for automatically recovering streaming sessions in WiFi mobile telephones," presented at *The 2nd Int. Conf. Mobile Ubiquitous Computing, Systems, Services and Technologies UBICOM08*, Valencia, 29 Sept-4 Oct. 2008, pp. 70 – 76.

[73] H.W. Lin, K.C. Chu, W.T. Lee and J.M. Lin "Seamless handover for multimedia applications between heterogeneous wireless networks," in *Proc. 5th Int. Conf. Intelligent Information Hiding and Multimedia Signal Processing*, Kyoto, Japan, 12-14 Sept. 2009, pp. 985-988.

[74] W.M. Yao and Y.C. Chen, "An enhanced buffer management scheme for fast handover protocol," in *Proc. 24th Int. Conf. Distributed Computing Systems Workshops ICDCSW'04*, Tokyo, 23-24 Mar. 2004, vol. 7, pp. 896 – 901.

[75] M.H. Tsai, J.T. Sung and Y.M. Huang, "Resource management to increase connection capacity of real-time streaming in mobile WiMAX," *IET Comm. J.*, vol. 4, pp. 1108 – 1115, Jun. 2010

[76] N. Yoshihara, H. Tode and K. Murakami, "Buffer management mechanism suitable for TCP streaming in QoS-aware IP router," in *Proc. IEEE 7th Consumer Communications and Networking Conf. (CCNC)*, Las Vegas, NV, 9-12 Jan. 2010, pp. 876-880.

[77] R. Risueño, P. Cuenca, F. Delicado, L. Orozco-Barbosa and A. Garrido, "On the effect of the handover mechanisms in QoS performance in wireless multimedia networks," in *Proc. 24th Int. Conf. Distributed Computing Systems*, Tokyo, 2004, pp. 138–143.

[78] K.H. Lee, H.J. Lee and J.H. Kim, "The active buffer management scheme using virtual transmission delay in the IEEE 802.11e network," presented at *IEEE 7th Consumer Communications and Networking Conf. (CCNC)*, Las Vegas, NV, 9-12 Jan. 2010, pp. 1 - 2

[79] G. Cunningham, P. Perry, J. Murphy and L. Murphy, "Seamless handover of IPTV streams in a wireless LAN network," *IEEE Trans. on Broadcast.*, vol. 55, pp. 796-801, Nov 2009.

[80] G. Cunningham, S. Murphy, L. Murphy and P. Perry, "Seamless handover of streamed video over UDP between wireless LANs," presented at the *2nd IEEE Consumer Communications and Networking Conf.*, Las Vegas, 3-6 Jan. 2005, pp. 284-289.

[81] B. Ciubotaru, G.M. Muntean "Smooth adaptive soft handover algorithm for multimedia streaming over wireless networks," in *Proc. IEEE Wireless Communications and Networking Conf.*, Budapest, 2009, pp. 2174-2179.

[82] S.J. Yoo, D. Cypher and N. Golmie, "Timely effective handover mechanism in heterogeneous wireless networks," *Springer J. in Wireless Pers. Commun.*, vol. 52, No. 3, pp. 449-475, 13 Nov. 2008.

[83] A. Fernandez, R. Perez and J. Alonso, "A method to estimate the horizontal handover decision effect on indoor wireless conversational Video quality," *EURASIP J. Advances in Signal Process.*, vol. 2008.

[84] S. Kashihara and Y. Oie, "Handover management based on the number of retries for VoIP on WLANs," in *Proc. of IEEE 61st Semiannual Vehicular Technology Conf.* (*VTC2005-spring*), Stockholm, 2005 vol. 4, pp. 2201–2206.

[85] A. Suárez, K. Atalah and E. Macías, "Gradient RSSI filter and predictor for wireless network algorithms and protocols," *The online Int. J. Network Protocols and Algorithms*, vol 2, no 2, pp. 1-26, Jun 2010.

[86] K. Atalah Elbatsh, E. Macias Lpez, and A. Surez Sarmiento, "RSSI Gradient: New predictor and filter to support sporadic wireless service interruptions," in *Proc. 7th IASTED Int. Conf. Communication Systems and Networks*, Palma de Mallorca, Spain, 2008, pp. 70-78.

[87] K. Atalah, E. Macías, A. Suárez, "A proactive horizontal handover algorithm based on RSSI supported by a new gradient predictor," *Ubiquitous Computing and Communication J*., vol. 3, no. 3, Jul. 2008.

[88] A. Suárez, K. Elbatsh and E. Macias, "A Proactive horizontal handover algorithm for WiFi-WiMAX Interoperable Networks," presented at the Int. *Conf. Wireless Networks*, London, 2-4 Jul. 2007.

[89] S. Rackley, "Wireless LAN standards," in *Wireless Networking Technology - from Principles to Successful Implementation*, 1st ed. London, UK: Elsevier, 2007, ch. 6, pp. 136-173.

[90] S. Lück, M. Scharf and J. Gil, "An Architecture for acquisition and provision of hotspot coverage information," in *Proc. of the 11th European Wireless Conf. 2005 - Next Generation wireless and Mobile Communications and Services*, Nicosia, 2005, pp. 287-293.

[91] S. D. Hermann, M. Emmelmann, O. Belaifa and A. Wolisz, "Investigation of IEEE 802.11k-based access point coverage area and neighbor discovery," in *Proc. 32nd IEEE Conf. Local Computer Networks*, Dublin, 2007, pp. 949–954,.

[92] C. Schindelhauer, "Mobility in wireless networks," presented at the *32nd Conf. Current Trends in Theory and Practice of Computer Science*, Czech Republic, 21--27 Jan. 2006, LNCS 3831, pp. 110–116.

[93] R.H. Wu, Y.H. Lee, H.W. Tseng, Y.G. Jan and M.H. Chuang, “Study of characteristics of RSSI signal,” presented at the *IEEE Int. Conf. Industrial Technology*, China, 21-24 Apr. 2008, pp. 1-3.

[94] J.W. Floroiu, M. Corici, B.J. Lee, S. Lee, S. Arbanowski and T. Magedanz, “A vertical handover architecture for end-to-end service optimization,” presented at the *16th IST Mobile and Wireless Communications Summit*, Budapest, 1-5 Jul. 2007, pp. 1-5.

[95] R. Trestian, O. Ormond, G.M. Muntean, "Signal strength-based adaptive multimedia delivery mechanism,” presented at the *IEEE 34th Local Computer Networks Conf.* (*LCN*), Zurich, 20-23 Oct. 2009, pp. 297-300.

Web References

[Web-1] “Voice quality in wireless networks,” Octasic SemiConductor, Montreal, Canada, 2002, http://www.vectronics.co.il/_Uploads/137oct6100wp2002.pdf, active page on Oct 2010.

[Web-2] “Wi-Fi CERTIFIED™ 802.11n draft 2.0: longer-range, faster-throughput, multimedia-grade Wi-Fi® networks,” WiFi Alliance, 2007, http://www.wi-fi.org/files/kc/WFA_802_11n_Industry_June07.pdf, active page on Oct 2010.

[Web-3] “Wi-Fi CERTIFIED™ for WMM™ - Support for multimedia applications with quality of service in Wi-Fi® networks,” WiFi Alliance, 2004, http://www.wi-fi.org/files/wp_1_WMM%20QoS%20In%20Wi-Fi_9-1-04.pdf, active page on Oct 2010.

[Web-4] “Mobile WiMAX: The best personal broadband experience,” WiMAX Forum, 2006, http://www.wimaxforum.org/technology/downloads/MobileWiMAX_PersonalBroadband.pdf , active page on Oct 2010.

[Web-5] "Driving the adoption of interoperable wireless broadband worldwide", The WiMAX Forum Certified™ Program, 2008, http://www.wimaxforum.org/files/wimax_forum_2008_certification_white_paper_final.pdf, active page on Oct 2010.

[Web-6] "WiMAX and the IEEE 802.16m Air Interface Standard," WiMAX forum, 2010, http://www.wimaxforum.org/sites/wimaxforum.org/files/document_library/wimax_802.16m.pdf. active page on Oct 2010.

[Web-7] "Mobile WiMAX – Part II: A comparative analysis," WiMAX forum, 2006, http://www.wimaxforum.org/technology/downloads/Mobile_WiMAX_Part2_Comparative_Analysis.pdf, active page on Oct 2010.

[Web-8] "Enabling Mobility in WiMAX Networks," WiMAX.com, 2006, http://www.wimax.com/research/%20whitepapers/WiMAX_07Nov06.pdf, active page on Oct 2008, (available in the CD).

[Web-9] D. Gray, "Mobile WiMAX: A performance and comparative summary," WiMAX Forum, 2006, http://www.wimaxforum.org/technology/downloads/Mobile_WiMAX_Performance_and_Comparative_Summary.pdf, active page on Oct. 2010.

[Web-10] "CDMA2000 International roaming: a status report," CDMA Development Group, CA, USA, 2005. http://www.cdg.org/resources/white_papers/files/Roaming%20Mar%2005%20FINAL2.pdf, active page on Oct. 2010.

[Web-11] J. Bardwell, "Converting signal strength percentage to dBm values," WildPackets Inc., Walnut Creek, CA, 2002. http://www.wildpackets.com/elements/whitepapers/Converting_Signal_Strength.pdf, active page on Oct. 2010.

[Web-12] NetStumbler.com, Marius Milner, www.netstumbler.com, active page on Oct. 2010.

[Web-13] WiFi Explorer/DK2401, Raytac Corporation, http://www.raytac.com/?FID=33&CID=21, active page on Oct. 2010

[Web-14] Wi-Spy overview, Metageek corporation, http://www.metageek.net/products/wi-spy, active page on Oct. 2010.

[Web-15] inSSIDer 2, Metageek corporation, http://www.metageek.net/products/inssider, active page on Oct. 2010.

[Web-16] WirelessMon, PassMark® Software Pty Ltd, http://www.passmark.com/products/wirelessmonitor.htm, active page on Oct. 2010.

[Web-17] More details about Grey Model, Smart Buffer Project (2004-2006), DEIS, University of Bologna, http://lia.deis.unibo.it/research/SOMA/SmartBuffer/Client/htmlDocs/detailsMobPred.html, active page on Oct. 2010.

[Web-18] Cinderella SDL, Cinderella ApS., www.cinderella.dk, active page on Oct. 2010.

[Web-19] Descargar java para windows, Oracle Corporation, http://www.java.com/es/download/index.jsp, active page on Oct. 2010

[Web-20] ChartDirector, Advanced Software Engineering Limited, www.advsofteng.com, active page on Oct. 2010.

APPENDIX

INFORMATION INCLUDED IN THE CD

- **Folder: Software**
  - Network Drawing: *EDraw Network Diagrammer 2.3*
  - Signal Scanning Tool: *NetStumbler 0.4*
  - Specification and Description: *Cinderella SDL 1.3*
  - Programming tool: *JCreator*
  - Programming Language: Java (*Jdk 1.6.0*)
  - External Library: *ChartDirector*

The ChartDirector is a specific library that produce professional charts component. It is necessary to include path of the library in the directories of the java (for .java sources and .jar directories).

All softwares are available in the attached CD or in the web page of each one.

- **Folder: Java Simulator**

It includes the Java classes and the .txt files that contain the RSSI% values for all the cases which were simulated. Also pdf files of all results are available

Simulator Classes:

- MySimulator.java
- BaseStation.java
- MobileClient.java
- AccessPoint.java
- Video_On_Demand.java
- SimulationResults.java
- Splineline1.java
- DemoModule.java

Data files:

- For case1: RSSI_1_case00.txt y RSSI_2_case00.txt
- For case2: RSSI_1_case01.txt y RSSI_2_case01.txt
- For case3: RSSI_1_case02.txt y RSSI_2_case02.txt

- For case4: RSSI_1_case03.txt y RSSI_2_case03.txt
- For case5: RSSI_1_case04.txt y RSSI_2_case04.txt
- For case6: RSSI_1_case05.txt y RSSI_2_case05.txt
- For case7: RSSI_1_case06.txt y RSSI_2_case06.txt
- For case8: RSSI_1_case07.txt y RSSI_2_case07.txt
- For case9: RSSI_1_case08.txt y RSSI_2_case08.txt
- For case10: RSSI_1_case09.txt y RSSI_2_case09.txt
- For case11: RSSI_1_case10.txt y RSSI_2_case10.txt
- For case12: RSSI_1_case11.txt y RSSI_2_case11.txt

Results:

- Case1.pdf
- Case2.pdf
- Case3.pdf
- Case4.pdf
- Case5.pdf
- Case6.pdf
- Case7.pdf
- Case8.pdf
- Case9.pdf
- Case10.pdf
- Case11.pdf

Folder: SDL Specification

This folder includes the SDL Cinderella file and some pdf files for verification results.

Folder: Experiment measurements and results

It contains three appendices:

- Appendix A: for the synthetic test
- Appendix B: for the experimental results.

Folder Thesis: Contains the PhD Thesis in pdf format.

Folder References: Contains all used references in pdf format